New insights from niche theory on plant adaptation and ecosystem functioning

Thomas Koffel

École Doctorale GAIA
Écologie Fonctionnelle et Sciences Agronomiques

Montpellier SupAgro

Thèse de doctorat

Présentée par

Thomas Koffel

en vue de l'obtention du grade de

Docteur de Montpellier Supagro

Spécialité :

Écologie Fonctionnelle et Sciences Agronomiques

Préparée à l'unité mixte de recherche :

Écologie Fonctionnelle et Biogéochimie des Sols et des Agro-écosystèmes
(UMR Eco&Sols, INRA-IRD-Montpellier Supagro-Cirad)

Théorie de la niche : nouvelles perspectives sur l'adaptation des plantes et le fonctionnement des écosystèmes

New insights from niche theory on plant adaptation and ecosystem functioning

Soutenue publiquement le ***19 octobre 2017*** *devant le jury composé de :*

Ophélie Ronce	Présidente
Mathew Leibold	Rapporteur
Elisa Thébault	Rapporteuse
Géza Meszéna	Examinateur
Tanguy Daufresne	Directeur de thèse
Nicolas Loeuille	Co-encadrant

Nous allons chercher bien loin spectacle nouveau pour nos méditations ;
nous l'avons sous les yeux, inépuisable

– Jean-Henri Fabre, *Souvenirs entomologiques VI, 1899*

Remerciements

J'aimerais pour commencer remercier Tanguy Daufresne de m'avoir pris sous son aile, en stage d'abord, puis pendant ces trois années de thèse. Ta passion profonde pour le monde naturel dans toutes ses dimensions, des théories biogéochimiques aux détails d'histoire naturelle, a été pour moi une grande source d'inspiration. Tes nombreuses qualités humaines et scientifiques m'ont été très précieuses. Je te remercie pour ta confiance, l'autonomie que tu m'as laissée, le recul que tu m'as toujours poussé à prendre et bien sûr ces nombreuses sorties nature aux quatre coins de l'Hérault.

I also am deeply grateful to you, Chris Klausmeier, for letting me join KBS as an intern back in 2014, and facilitating all my subsequent visits ; this made my life so much easier. KBS, and particularly the KL Lab, have been a truly stimulating environment for me. Most of what I learned in theoretical ecology comes from you. Thanks for all of our insightful discussions, about science or not, and the pleasant moments spent solving technical problems on the blackboard.

Merci à toi Simon Boudsocq pour l'encadrement informel dont tu m'as fait bénéficier. Merci d'avoir partagé avec moi tes nombreuses connaissances sur les processus fins du système plante-sol. Merci pour tes conseils toujours avisés, ton sens du détail autant sur le fond que sur la forme, ta bonne humeur et ton humour !

Je remercie Nicolas Loeuille pour son regard plus externe sur mon travail de thèse. Merci de m'avoir accueilli quelques jours dans ton groupe à Paris. C'est toujours un vrai plaisir d'interagir avec toi.

Je tiens aussi à remercier Benoît Jaillard d'avoir accepté d'endosser les responsabilités administratives de directeur de thèse. Merci d'avoir rendu possible, et épaulé, mon expérience d'enseignement. Ta vision parfois iconoclaste et ton esprit critique m'ont beaucoup stimulé pendant cette thèse.

Plus largement, j'aimerais remercier tous les membres d'Eco&Sols, et plus particulièrement la direction, qui font de cette unité un environnement vivant et stimulant.

C'est le moment de remercier les membres du jury pour avoir accepté d'évaluer mon travail. Merci donc aux rapporteurs, Mathew Leibold et Elisa Thébaut, ainsi qu'aux examinateurs, Géza Meszéna et Ophélie Ronce.

Je remercie aussi chaleureusement tous les chercheurs avec qui j'ai pu interagir ou collaborer pendant ces trois ans, et plus particulièrement Katherine Bannar-Martin, Sébastien Barot, Colin Kremer, Elena Litchman, François Massol, Alain Rapaport et Tewfik Sari. Un grand merci à Sonia Kéfi et Philippe Hinsinger d'avoir accepté de faire partie de mon comité de thèse.

J'ai une grosse pensée émue pour tous ceux que j'ai pu côtoyer pendant ces trois ans à Eco&Sols : Ade, Rémi (merci pour toutes nos sorties ornitho et le reste !), Mathias, Céline, Camille, Kenji, Yannick, Amandine, Esther, Najet, Rémi, Patoch, Dam's, Lucie, Agnès, Max et Anne. Merci aussi à mes confrères de KBS, Beth, Ghjuvan, Kane, Kirill, Dustin, Sarah, Christine, Ravi, Paul, Danny et Simon. Merci aux éminents membres des JCM et amis du CEFE, à savoir

Anne-Soso, Rémimi et Toto.

Merci enfin à ceux avec qui j'ai eu la chance de partager mon quotidien pendant ces années de thèse : mes colocs Sixtine, Sam et Sylvain, les randonneurs de Montpellier Gautier, Marion, Laure et Juline, les anciens du 22 Paul, à savoir les deux ours Jean-Louis et Alix, Tom, Noémie, Marien l'homme fort de Yaoundé, Simon Feat et le gros D. J'ai aussi une pensée pour mes amis du master d'écologie, Simon, Andy, PA, Aurore, Pierre, Mélodie et Mourad, les barcelonais Amélie, Gianvito et Nicolò, les cachanais MC, Tanguy, Aurélie, Georges, Brice et Cécile, les potes de prépa Boris, Laurent, Yannick, Aurélien, Xi et Jérémie sans oublier les amis d'enfance Xavier, Bérengère, Tis et Serlo.

Un très grand merci à toute ma famille, et plus particulièrement mes parents à qui je dois tant. J'ai aussi une pensée particulière pour ma grand-mère Marie-Louise, qui a su s'occuper avec amour de ses petits-enfants, et qui nous a malheureusement quittés durant la rédaction de cette thèse. Finally, thank you Susan for giving me all I need, and more.

Résumé

Les plantes, comme tous les êtres vivants, entretiennent un rapport double à leur environnement. L'environnement sélectionne quelles stratégies peuvent s'établir, et les stratégies ainsi sélectionnées façonnent en retour cet environnement. Cette boucle de rétroaction environnementale, lorsqu'elle est alimentée par une variabilité de formes, est le moteur de l'évolution, de l'assemblage des communautés et du développement écosystémique, et détermine en fin de compte les propriétés émergentes des écosystèmes. Les approches issues de l'écologie théorique reconnaissent depuis longtemps cette dualité, comme en témoignent les concepts de « niche de besoin » et « niche d'impact » au cœur de la théorie contemporaine de la niche. Similairement, les approches type « théorie des jeux » comme la dynamique adaptative reconnaissent le rôle central joué par la boucle de rétroaction environnementale en tant que moteur des dynamiques éco-évolutives.

Dans cette thèse, j'unifie ces deux perspectives théoriques et les applique à des problèmes écologiques variés, dans le but de comprendre comment les interactions réciproques entre les plantes et leur environnement déterminent les traits adaptatifs des plantes et les propriétés émergentes des écosystèmes.

Dans un premier temps, je propose un cadre mathématique général et rigoureux à la théorie contemporaine de la niche et la méthode graphique qui lui est associée. Après avoir étendu ce cadre à la prise en compte d'un continuum de stratégies en interaction à l'aide d'enveloppes géométriques, je montre comment appliquer la théorie contemporaine de la niche à deux perspectives, à savoir les dynamiques éco-évolutives et l'assemblage de communautés par remplacements successifs de stratégies.

Dans un second temps, j'applique cette approche à l'étude de l'évolution des défenses des plantes contre les herbivores le long de gradients de nutriments, en considérant l'évolution des traits d'acquisition de la ressource, de tolérance et de résistance aux herbivores. Je montre que la prise en compte des transferts trophiques conduit à la sélection de stratégies compétitives mais sans défense dans les environnements pauvres, alors que ce sont toujours des stratégies défendues (résistantes, tolérantes, ou la coexistence des deux) qui dominent dans les environnements riches en nutriments. Mes résultats mettent en évidence le rôle central joué par la rétroaction plante-herbivores dans la détermination des patrons de défense des plantes.

Dans un troisième temps, je montre comment la théorie contemporaine de la niche peut être étendue pour prendre en compte la facilitation. J'utilise ensuite cette approche pour montrer comment la colonisation d'un substrat nu par une communauté de plantes fixatrices d'azote couplée au recyclage des nutriments peut donner naissance à de la succession par facilitation. Contrairement aux modèles habituels de succession, je montre que la succession par facilitation donne lieu à un développement autogène de l'écosystème ainsi qu'un régime de bistabilité entre la végétation et le substrat nu en fin de succession. Enfin, je propose une nouvelle théorie de la succession basée sur les ratios de ressources.

Pris dans leur ensemble, ces nouveaux développements démontrent que la théorie de la niche peut être adaptée à l'étude d'un large champ de situations écologiques, de la facilitation aux dynamiques éco-évolutives et à l'assemblage des communautés. Dans ce cadre conceptuel, mon approche basée sur les enveloppes s'avère être un outil efficace pour passer de l'échelle individuelle à l'échelle de l'écosystème, en assimilant le remplacement adaptatif d'espèces à une plasticité des propriétés écosystémiques. Cette approche permet alors de décrire l'émergence des boucles de régulation qui contrôlent le fonctionnement des écosystèmes, comme l'illustrent mes résultats le long de gradients de nutriments sur la transition entre régimes de succession ou encore l'émergence de culs-de-sac trophiques.

Mots clés : Théorie contemporaine de la niche, fonctionnement des écosystèmes, dynamique adaptative, défenses des plantes, gradients de nutriments, facilitation, succession primaire

Summary

As living organisms, plants present a dual relationship with their biotic and abiotic environment. The environment selects plant strategies that can establish, and selected strategies in turn impact and shape the environment as they spread. This environmental feedback loop – when fueled by variation, through mutation or immigration from a local species pool – drives evolution, community assembly and ecosystem development, and eventually determines the emergent properties of ecosystems.

Theoretical ecology approaches have long recognized this duality, as it is at the core of contemporary niche theory through the concepts of requirement and impact niche. Similarly, game-theoretical approaches such as adaptive dynamics have emphasized the role played by the environmental feedback loop in driving eco-evolutionary dynamics. However, niche theory could benefit from a more individualistic, selection based perspective, while adaptive dynamics could benefit from niche theory's duality and graphical approach.

In my dissertation, I unify these theoretical perspectives and apply them to various ecological situations in an attempt to understand how the reciprocal interaction between plants and their environment determines plant adaptive traits and emergent ecosystem functions.

First, I introduce a general and rigorous mathematical framework to contemporary niche theory and the associated graphical approach. By extending these ideas to a continuum of interacting strategies using geometrical envelopes, I show how contemporary niche theory enables the study of both eco-evolutionary dynamics and community assembly through species sorting. I show how these two perspectives only differ by the range of invaders considered, from infinitesimally similar mutants to any strategy from the species pool. My results also emphasize the fact that selection only acts on the requirement niche, evolution of the impact niche being just an indirect consequence of the former.

Second, I use this approach to study the evolution of plant defenses against herbivores along a nutrient gradient, by considering the joint evolution of resource acquisition, tolerance and resistance to herbivores. I show that trophic transfers lead to the selection of very competitive, undefended strategies in nutrient-poor environments, while defended strategies – either resistant, tolerant or the coexistence of both – always dominate in nutrient-rich environments. My results highlight the central, and often underestimated, role played by plant-environment feedbacks and allocation trade-offs in shaping plant defense patterns.

Third, I extend contemporary niche theory to facilitation originating from positive environmental feedback loops. I use these new tools to show how colonization of a bare substrate by a community of nitrogen-fixing plants coupled with nutrient recycling can lead to facilitative succession. Contrarily to previous competition-based succession models, I point out that facilitative succession leads to autogenic ecosystem development, relatively ordered trajectories and late succession bistability between the vegetated ecosystem and the bare substrate. By showing how facilitative succession can turn into competition-based succession along an increasing

nitrogen gradient, I derive a new resource-ratio theory of succession.

Overall, these new theoretical developments demonstrate that niche theory can be adapted to study a broad range of ecological situations, from facilitation to eco-evolutionary dynamics and community assembly. Within this framework, my envelope-based approach provides a powerful tool to scale from the individual and population levels to the ecosystem level, lumping selection-driven species turnover into plastic ecosystem properties. This, is turn, helps describing the emergence at the ecosystem scale of regulation feedback loops that drive ecosystem dynamics and functioning, as exemplified by my results along increasing resource gradients showing a transition from facilitation- to competition-based succession or the emergence of trophic dead-ends.

Keywords: Contemporary niche theory, ecosystem functioning, adaptive dynamics, plant defenses, nutrient gradients, facilitation, primary succession

Contents

List of Figures

List of Tables

Introduction

For nature is a perpetual circulatory worker,
generating fluids out of solids, & solids out of fluids,
fixed things out of volatile, & volatile out of fixed,
subtle out of gross, & gross out of subtle

– Isaac Newton, *Letter to Oldenbourg, 1675*

Plants, a central component of ecosystems

Plants grow virtually anyywhere on the surface of the planet where liquid water is found, from the surface of the oceans to alpine meadows, deserts and agricultural fields. They present a great diversity of sizes, shapes, specialized organs such as flowers and other adaptations to their specific environments. Yet, they also strike by a unity in term of functioning: the vast majority of them are autotrophs, which means they can use the energy from the sun to combine elements together into complex organic matter, the biomass, to grow and reproduce. In contrast, most of the other life forms on earth rely either directly on plant material to live, either alive — herbivores — or dead — decomposers — or indirectly by eating other organisms that depend on plants — carnivores. Plants thus play a central role as they are at the basis of most food webs. As omnivores, us humans are no exception to the rule, as we depend on plants both for direct food production or indirectly to feed our livestock. Plants also connect the aboveground, where they access light and get exposed to most herbivores and the belowground, where inorganic nutrients lie and organic matter is recycled. As such, they are central components of not only biomass production, but also nutrient acquisition and recycling, connecting the biotic and abiotic worlds. This means plants have an active role in the regulation of biogeochemical cycles, which describe how elements move through the different compartments of the ecosphere. The functioning of these cycles is of central concern for humans, as it underlies their development and determines the sustainability of the planet on the long term.

So, from the plant perspective, what determines one plant form over the other in a particular environment? How can we explain such a diversity of plant forms across the globe? These questions cannot be addressed without taking a step back in the bigger picture, the ecosystem.

How do plant interact with their biotic and abiotic environment and modify it with their activity? What are the consequences of plant traits and diversity on ecosystems? How do plants respond to heterogeneous environmental conditions and anthropogenic perturbations, and how does this cascade onto the rest of the food web?

The plant-environment reciprocal interactions

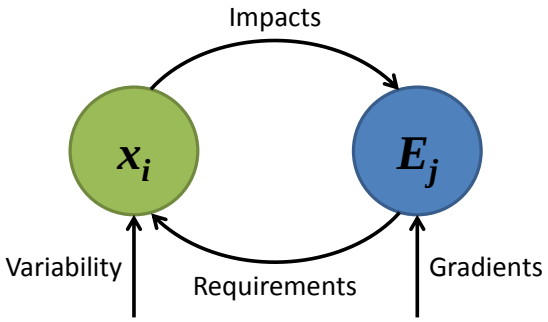

Figure 0.1: Environmental feedback loop between plant strategies i, characterized by their traits x_i, and the components of the environment E_j. The environment E_j selects which plant strategies can establish via their requirement niche. These plant strategies, in turn, collectively modify their environment with their impact niche. The environment E_j is also partially determined by some external conditions along environmental gradients. Potential plant strategies are fueled by trait variability, either internally through mutations or externally via a regional species pool.

To address these questions, we need a conceptual framework accounting for these reciprocal interactions between plants and their environment. In short, plants have to cope with the constraints coming from their environment to establish and persist (through their requirements), but their very existence and activity in turn shapes back their environment (through their impacts). In ecology, this requirement (also sometimes called sensitivity, see Meszéna et al. 2006) and impact duality underlay the early development of niche theory (Grinnell 1917; Elton 1927; Hutchinson 1957) and its modern synthesis from resource competition theory to contemporary niche theory (Levin 1970; MacArthur 1972; Tilman 1982, 1988; Holt et al. 1994; Leibold 1996; Chase and Leibold 2003; Holt 2009a). When put together, the requirement and impact niche components lead to the environmental feedback loop, the core driver of evolution in density- and frequency-dependent approaches such as adaptive dynamics (Hofbauer and Sigmund 1990; Dieckmann and Law 1996; Geritz et al. 1997, 1998; Champagnat et al. 2006), or other approaches from evolutionary game theory (see McNickle and Dybzinski 2013; Brown 2016). This idea that organisms modify their environment via their impacts has received renewed interest recently in

ecology and evolution, through ecosystem engineers (Jones et al. 1994, 1997) and niche construction (Odling-Smee et al. 1996, 2003; Kylafis and Loreau 2011), respectively. Despite the obvious connections between these theories, a general synthetic framework accounting for the previous concepts altogether is still lacking (but see Meszéna et al. 2006; Pásztor et al. 2016): the niche construction literature has not yet used the well-developed tools of eco-evolutionary dynamics (but see Lehmann 2008; Kylafis and Loreau 2008, 2011), an evolutionary theory of the niche has yet to be developed (Holt 2009a) and adaptive dynamics still has to take advantage of the environment perspective, the impact/requirement duality and the graphical approach to contemporary niche theory.

With this unifying purpose in mind, we propose a general framework describing how individual plant strategies interact with their environment (see Fig. 0.1). Only by considering plant-environment interactions simultaneously can we understand how the environment determines life forms and their diversity and how life determines ecosystem structure and functioning. Besides impacts and requirements, two other concepts are necessary to describe plant-environment interactions. On one side, there is a standing diversity of life forms — coupled with the appearance of new morphs generated by de novo mutations — that constitute a pool of potential plant strategies. On the other side, the environment is partially controlled by conditions external to life, such as climate or bedrock nutrient richness, forming what we call environmental gradients as these conditions gradually change through space. When these plant strategies and their environment are put together, the environment selects which plant strategies can grow through their requirements, and selected strategies in turn shape the environment back through their impacts.

We will now detail the different ingredients of the plant-environment feedback loop and link it to the classical ecology and evolution perspectives: plant traits variability and environmental gradients first, population regulation, community, eco-evolutionary and biogeochemical perspectives secondly.

Plant traits and their variability

Plants present such a diversity of forms and functions that one could consider every plant species as being unique and possessing singular properties. But in their common evolutionary history and unicity of environmental functions, they share some measurable characteristics that plant ecologists call traits. These traits are related to the major components of plant fitness, such as growth, survival and reproduction and encode the fundamental ways in which plants interact with their environment (Lavorel and Garnier 2002; McGill et al. 2006; Violle et al. 2007; Litchman and Klausmeier 2008). When quantified, the collection of such trait values fully characterizes a plant strategy and makes the comparison with other strategies possible, whether from the same or a different species. Note that plants are often subdivided into functional groups

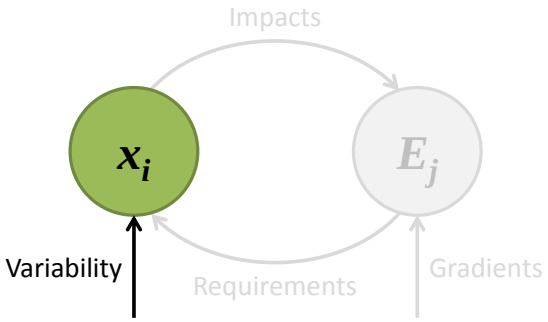

Figure 0.2: Focus on individual plant strategies, defined by their traits, and their variability.

on the basis of some shared functions quantified by singular traits, such as C_4, crassulacean acid metabolism, or nitrogen-fixing plants. For a given problem, focusing on traits relevant to the particular aspect of the environment considered simplifies the problem by reducing the dimension of the strategy space. Flower color matters for the study of plant-pollinators interactions, but can in first approximation be dropped off when one is interested by plant-herbivore interactions. In this thesis, we will focus on the plant's functional traits that mediate basic trophic interactions: acquire basic nutrients such as nitrogen or phosphorus, grow, and be defended, either through tolerance or resistance. Traits are a convenient level of description because they often satisfy constraints at lower levels of organization, such as allometric relationships or allocation trade-offs. Even if they are often debated due to the large dimension of strategy spaces, the existence of these ultimate trade-offs is hard to call into question, as organism only have a limited amount of time, energy ant matter at their disposal.

As motivated in the previous section, selection by the environment of the most adapted plant strategies lies at the core of our approach. Where does this diversity of plant strategies, necessary for selection to act upon, come from? We will consider two perspectives. The first perspective is evolutionary, as it assumes that trait variation appears through random mutations, generating mutant strategies that closely resemble the strategies established in the ecosystem. The second perspective comes from community ecology, and voluntarily sets aside the problem of the creation and maintenance of variability at the regional scale. Instead, this perspective considers our focal ecosystems as being local, embedded in a broader matrix of ecosystems providing a 'hyperdiverse' set of potential strategies, called the regional species pool (Leibold et al. 2004). This approach usually assumes that 'everything is everywhere', namely that there is no dispersal limitation to a species' presence (Baas Becking 1934; De Wit and Bouvier 2006). Such an assumption holds on a human-dominated planet where alien species are moved around the planet at an increasing rate (Seebens et al. 2017). Following the terms of Vellend's (2010) conceptual synthesis of community ecology, this perspective focuses on the selection aspect, and

downplays drift, speciation and dispersal. In any case, variability, wherever it comes from, will go through the complex filter of selection originating from the feedback loop with the environment.

Resources and environmental gradients

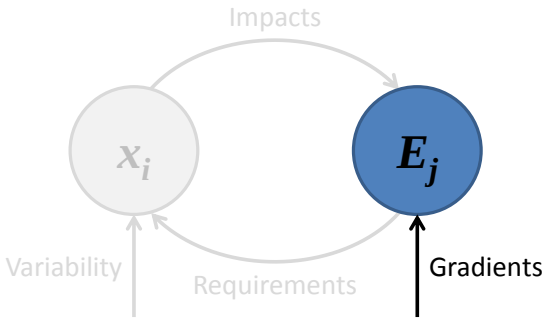

Figure 0.3: Focus on the environmental variables, such as resources, and their gradients in availability.

Plants' growth and reproduction is conditioned by the availability of a variety of environmental factors. Abiotic resources, such as space, light, water, and nutrients, like nitrogen and phosphorous in the soil are essential to plants. The match between the relative abundances of these resources and a plant's requirements determines which of these resources limit plant growth. On the surface of the planet, these resource availabilities can differ drastically due to the combination of heterogeneity in climate, soil characteristics and anthropogenic perturbations. This strongly constrains the plant forms able to grow under given environmental conditions, relatively independently of their precise location on earth or their evolutionary history, through a process called convergent evolution. For example, cactaceae in the Americas and euphorbiaceae in Africa have both evolved short spines and succulent stems as adaptations to desert, water-stressed environment. Environmental conditions, in turn, have major effect on ecosystem functioning and characteristics. The study of these geographical joint patterns in plant forms and ecosystem properties is called biogeography, since their initial description by Von Humbolt and Bonpland (1807) in their Naturgemälde to the modern refinements of Whittaker's (1962) biome diagram. Promising approaches such as functional biogeography are now moving beyond the species concept, historically at the core of biogeography, to a trait-based description, with the potential to better understand and predict worldwide trait-distribution and ecosystem functioning (Violle et al. 2014).

In this thesis, we will be particularly interested in differences in nutrient loads among ecosystems, with an emphasis on nitrogen and phosphorous. These differences can be natural, due to

differences in soil texture and quality, positions along a watershed or landscape use by herbivores. They can also have an anthropogenic origin, associated with human-induced global change. Indeed, run off from agriculture fertilization, and human and livestock waste all increase the availability of both nitrogen and phosphorus in aquatic ecosystems. On terrestrial ecosystems, atmospheric deposition of nitrogen from human emissions of NH_3 and NO_x have global consequences. Such global nutrient enrichment patterns raise the fundamental questions of their effect on plant communities, dominance patterns between species, biomass production and trophic transfers. These can in turn cause serious problems to human societies, as agricultural soil fertility relies on nutrient availability, but pollution originating from excessive nutrient loads can have major impacts on human health, fisheries and recreative activities.

Population regulation and community ecology

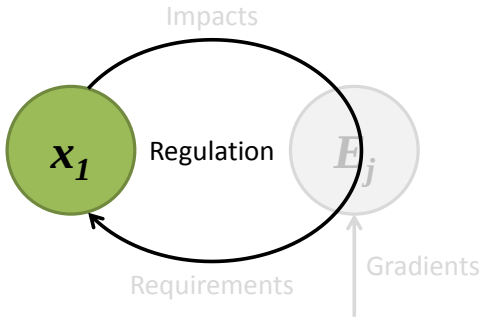

Figure 0.4: With the environment of a given population treated implicitly, impacts and requirements combine into a negative environmental feedback loop that leads to population self-regulation.

When the environmental requirements of a plant strategy are met in a given habitat, this plant thrives and spreads in this habitat. As this population grows, it impacts the environment back, usually depleting the very same resources that it requires, such as nutrients or light as individuals shade each other. In this regard, the shared environment ultimately mediates some negative interactions — competition — between individuals. This negative environmental feedback loop is at the core of population regulation, as it eventually leads to population stabilization on the long term at its carrying capacity, a central principle of population ecology that echoes back to the doctrine of Malthus (Fig. 0.4; Verhulst 1847; Darwin 1859; Turchin 2001; Pásztor et al. 2016). Note that this framework does not negate the existence of positive interactions such as mutualism and facilitation, but recognizes that there is always an ultimate limitation that prevents populations from unlimited growth.

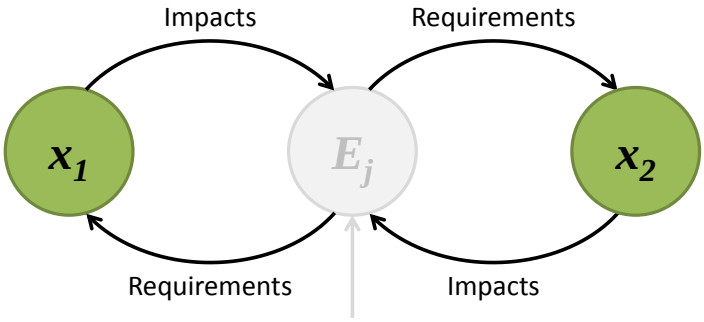

Figure 0.5: The environment

The exact same principle applies when the populations of two different strategies grow together, as the environmental feedback loop leads to differential regulation between the two populations, leading to intraspecific and interspecific competition between individuals. One standard approach in theoretical ecology is to forget about the environment and include it only implicitly. This leads to the classical Lotka-Volterra type systems and their associated competition coefficients (Fig. 0.5; Lotka 1925; Volterra 1926; MacArthur 1970; Chesson 1990). This framework has been used to address a central question of community ecology, i.e. under which conditions do species coexist instead of excluding each other, and is still at the core of modern approaches to the question (Chesson 2000).

Even when the environment has been kept explicit, the emphasis has historically remained centered on the community ecology perspectives. Indeed, including the environment — mostly the shared resource — has long been seen as a mechanistic and testable way to address species coexistence in the resource-ratio theory (MacArthur 1972; León and Tumpson 1975; Tilman 1980, 1982; Miller et al. 2005), and its following extension, the contemporary niche theory (Holt et al. 1994; Leibold 1996; Chase and Leibold 2003). Making the environment explicit leads to important clarifications on the underlying structure of coexistence, such as the concept of limiting similarity (Hutchinson 1959; MacArthur and Levins 1967) and the competitive exclusion principle (Gause 1934; Levin 1970; Meszéna et al. 2006).

Eco-evolutionary dynamics

Within this framework, eco-evolutionary perspectives do not fundamentally differ from the previous community perspective, as it is mostly concerned with competition between alleles or genotypes within a population, rather than between populations, as exemplified by the recent studies on rapid evolution (Thompson 1998; Yoshida et al. 2003; Hairston et al. 2005; Grant and Grant 2006; Stuart et al. 2014; Schreiber et al. 2016). In adaptive dynamics, the main tool is

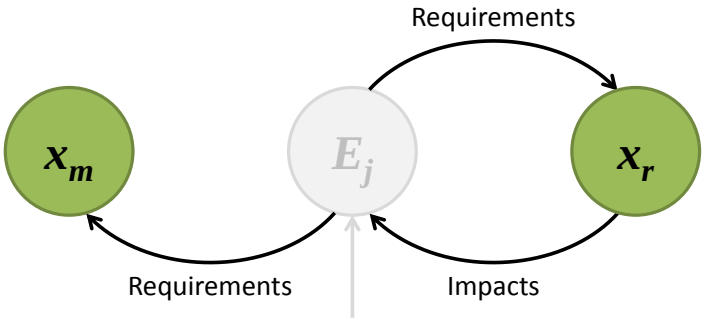

Figure 0.6: Resident-mutant interaction mediated by the environment. The mutant density is at first to low to have any impact on the environment.

the invasion fitness of an individual mutant in a system dominated by a resident population at equilibrium (Hofbauer and Sigmund 1990; Metz et al. 1992; Dieckmann and Law 1996; Geritz et al. 1997, 1998; Champagnat et al. 2006). Again, it is the the shared environment that mediates the mutant-resident interaction, the only difference with the community perspective here being that the mutant does not have any impact on the environment at first, as invasion starts from a very low density. Most of the time, this mutant-resident interaction results in competitive exclusion of one of the two strategies, resulting in either counter-selection of the mutant or the mutant becoming the new resident, the latter corresponding to directional selection. However, other scenarios are possible at the neighborhood of some particular strategies called singular points like stabilizing selection, as well as disruptive selection, also called evolutionary branching (Metz et al., 1996; Geritz et al., 1997, 1998; Dieckmann and Doebeli, 1999), a preclude to diversification.

In fact, most of the models from this eco-evolutionary perspective meet the community ecology agenda, by studying the origin and maintenance of diversity on evolutionary timescales. However, both these community and eco-evolutionary approaches, when explicitly accounting for dynamical environmental components such as nutrient concentrations, make the study of biogeochemical cycles and ecosystem processes possible. To see this, it suffices to flip the feedback loop and make the biotic compartment implicit to now focus on the environmental component. This is the subject of the next section.

Biogeochemical perspective

Biogeochemical cycles describe how elements or chemical compounds move between the different compartments of the ecosphere — the lithosphere, atmosphere, hydrosphere and biosphere — in a cyclical manner. These movements, driven by the laws of physics and chemistry, are

often accompanied by changes in chemical structure while satisfying mass balance. These cycles are essential to the maintenance of life on earth: the carbon cycle regulates Earth's climate, the water cycle continuously injects freshwater in terrestrial ecosystems and the nitrogen and phosphorous cycles are involved in the long-term maintenance of ecosystem fertility. As life is composed of matter, organisms have to spend most of their time acquiring this matter, transforming it, keeping it, and eventually releasing it when it is of no use anymore or when they die. This automatically binds the global faith of inorganic chemical elements with the one of living organisms. This biogeochemical perspective on the environmental feedback loop does not see life abundance and diversity as an end, but rather as a mean through which biogeochemical cycles are set in motion and regulated (Fig. 0.7). As organic molecules present precise elemental

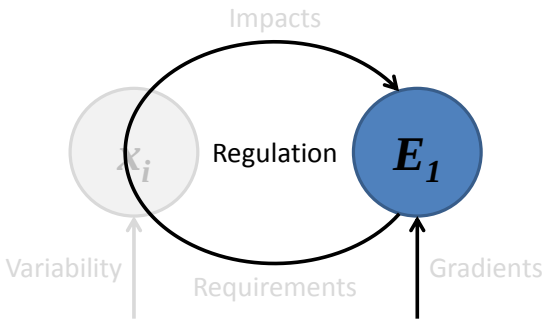

Figure 0.7: Exchanges of matter between two abiotic and biotic compartments lead to the regulation of the abiotic compartment and its biogeochemical cycle.

composition, organisms partially balance their uptake rates to match their requirements (Liebig 1840), mechanically leading to the coupling of biogeochemical cycles (Fig. 0.8; Schlesinger et al. 2011), a central concept of ecological stoichiometry (Redfield 1958; Sterner and Elser 2002).

Taking explicitly into account the contribution of living organisms to biogeochemical cycles is one of the main goals of ecosystem ecology. Theoretically, approaches that aimed at deriving general rules of ecosystem development and functioning have historically been phenomenological, entrenched in an holistic and systemic viewpoint (Clements 1916, 1936; Margalef 1963; Odum 1969, 1971). This is captured by the organismal analogy of Clements (1916) for whom the development of an ecosystem can be compared to the rigid development of an organism, from birth to youth, adulthood and eventually death. Yet a general theory explaining the emergence of ecosystem properties from the underlying ecological mechanisms is still lacking. For example, some intriguing patterns of biogeochemical cycles regulation, such as the fairly constant C:N:P stoichiometric ratio of the deep ocean, are still the subject of ongoing investigations. Due to this lack of general rules, optimality approaches based on performance maximization at the ecosystem level have been used as a rule of thumb, for example to predict optimal allocation

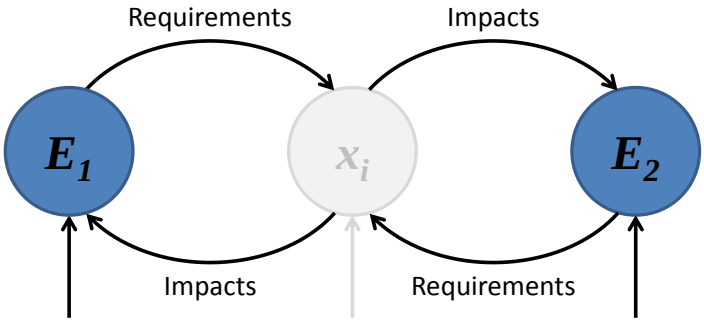

Figure 0.8: Coupling between two biogeochemical cycles through a shared biotic compartment. In this context, requirements and impacts of the biotic compartment correspond to incoming and outgoing fluxes of matter.

patterns between the different organs of a tree in forested ecosystems (Schymanski et al. 2007; Dekker et al. 2012).

Ecosystems as complex adaptive systems

The joint study of plant strategies and their abiotic environment, with the reciprocal interactions, can help in this search of first principles of ecosystem ecology. Plants individuals and other living organisms are subject to natural selection, while the dynamics of abiotic elements obeys the laws of physics and chemistry. Scaling from such an individual-based selection perspective all the way up to the ecosystem level, thus bridging community ecology, evolutionary ecology and ecosystem ecology together, holds the promise of a well-grounded general theory of ecosystems (Levin 1998, 1999; Loreau 2010a,b).

One of the oldest examples of such a general rule of theoretical ecology is Tilman's (1982) R^* rule in community ecology (Hsu et al. 1977; Grover 1997) and it's modern evolutionary equivalent, the pessimization principle (Diekmann 2004; Metz et al. 2008; Boudsocq et al. 2011). This rule states that successive competitive exclusions of different strategies interacting with a single resource lead to the minimization of this resource's availability. This rule, in turn, has been proposed to drive other aspects of ecosystem development, such as higher primary productivity and better cycling efficiency (Loreau 1998b). However, the R^* rule is only valid when a single resource is limiting in a non-fluctuating environment, a situation that rarely occurs within more complex ecosystems. More generally, several studies have recently used natural selection to address the emergence of ecosystem-level patterns: the evolution of nutrient recycling (Loreau 1998b; de Mazancourt et al. 1998; de Mazancourt and Loreau 2000; Boudsocq et al. 2011; Barot et al. 2014), the emergence of food webs (Loeuille and Loreau 2005), oceanic stoichiometry

(Klausmeier et al. 2004; Lenton and Klausmeier 2007), and N-fixation (Menge et al. 2008, 2009b). Such eco-evolutionary perspective on ecosystem functioning is now gaining momentum in more applied fields such as agronomy (Denison et al. 2003; Weiner et al. 2010; Denison 2012; Loeuille et al. 2013; van Loon et al. 2014), forestry (Dybzinski et al. 2015; Weng et al. 2015) or oceanography (Follows et al. 2007; Sauterey et al. 2015).

Main questions and objectives

In this dissertation, we build on the plant-environmental dual perspective to address two essentially linked questions: how does selection by the environmental feedback loop determine plant adaptation and diversification along nutrient gradients? How does plant adaptive strategy turnover control the development, regulation and functioning of ecosystems along nutrient gradients? We will address these two questions with three objectives.

First, we aim at laying down a general mathematical framework of plant-environment reciprocal interactions using contemporary niche theory. Our objective is to extend the associated graphical approach to account for and represent dense strategy turnovers along nutrient gradients. This approach will be illustrated on the example of the evolution of resource specialization.

Second, we aim at applying this framework to the evolution of plant defenses along nutrient gradients inside a three-level food chain. Our objective is to address our main question in the particular context of this example, i.e. to look at plant defensive adaptive patterns along nutrients gradients and how these influence back the functioning of the food chain.

Third, we use our framework to investigate the role of nitrogen-fixing plants and recycling during primary succession. Our objective is to show how N-fixing strategy turnover driven by repeated colonizations of an initially bare substrate can give rise to facilitation-driven succession and ecosystem development. By studying these succession patterns along nutrient gradients, we aim at rejuvenating Tilman's (1985) resource-ratio theory of succession.

Connecting statement

As was motivated in the introduction, a general and rigorous framework describing plant-environment reciprocal interactions is necessary to address the coupling between plant adaptation and ecosystem functioning. In this chapter, we will use contemporary niche theory to lay down such a mathematical framework, and describe a general graphical approach to investigate and represent the outcome of plant-environment interactions along environmental gradients. We will introduce a new tool based on geometrical envelopes to incorporate dense strategy turnover, and see how it makes the study of community assembly and eco-evolutionary dynamics possible within contemporary niche theory. To make this approach more visual, we will illustrate it through the example of the evolution of resource use, where a consumer exploiting two resources can either evolve to be a generalist or completely specialize on one of the two resources.

Chapter 1

Geometrical envelopes: extending graphical contemporary niche theory to communities and eco-evolutionary dynamics

Contents

Abstract

Contemporary niche theory is a powerful structuring framework in theoretical ecology. First developed in the context of resource competition, it has been extended to encompass other types of regulating factors such as shared predators, parasites or inhibitors. A central component of contemporary niche theory is a graphical approach popularized by Tilman that illustrates the different outcomes of competition along environmental gradients, like coexistence and competitive exclusion. These food web modules have been used to address species sorting in community ecology, as well as adaptation and coexistence on eco-evolutionary time scales in adaptive dynamics. Yet, the associated graphical approach has been underused so far in the evolutionary context. In this chapter, we provide a rigorous approach to extend this graphical method to a continuum of interacting strategies, using the geometrical concept of the envelope. Not only does this approach provide community and eco-evolutionary bifurcation diagrams along environmental gradients, it also sheds light on the similarities and differences between those two perspectives. Adaptive dynamics naturally merges with this ecological framework, with a close correspondence between the classification of singular strategies and the geometrical properties of the envelope. Finally, this approach provides an integrative tool to study adaptation between levels of organization, from the individual to the ecosystem.

1.1 Introduction

Competition is a ubiquitous interaction among living organisms, and thus a major driver of community structure and evolution by natural selection. As such, it was at the core of the very first mathematical models of population dynamics and theoretical ecology (Lotka, 1925; Volterra, 1926; Gause, 1934). However, the explicit inclusion of resources for which species compete only came several decades later with the pioneering works of MacArthur and colleagues (MacArthur and Levins, 1964; MacArthur and Wilson, 1967; MacArthur, 1970). Mechanistic competition models, or modules, allow a useful graphical representation introduced by MacArthur and Levins (1964), developed by León and Tumpson (1975) and largely popularized by Tilman (1980, 1982), which summarizes graphically the different outcomes of competition along environmental gradients, delimiting the coexistence regions from competitive exclusion or founder control. This method relies on the combination of three key graphical ingredients: Zero Net Growth Isoclines (ZNGIs), consumption/impact vectors and supply points. These respectively represent a species' minimal requirements, its consumptive impacts, and the externally-driven resource availability in the absence of any consumer. Supported empirically (Miller et al., 2005), the theory also brings strong conceptual results on the conditions for coexistence consistent with the competitive exclusion principle (Levin, 1970).

The concept of resource competition can be generalized to encompass any kind of regulating factors that mediate interspecific interactions. This was done by Chase and Leibold (2003) under the unifying umbrella of "contemporary niche theory", further formalized by recent developments (Meszéna et al., 2006; Barabás et al., 2014b). For example, two prey sharing one predator formally behave as if they were competing for a single resource, a situation referred to as apparent competition by Holt (1977). This allows the use of the graphical representation in this generalized framework, as was done with apparent competition plus resource competition by Holt et al. (1994); Grover (1995); Leibold (1996) and Chase and Leibold (2003). Interference competition through explicit inhibitory product emission also fits in this framework, with the inhibitor playing the role of a regulating factor (Gerla et al., 2009). Recently, several authors further extended this graphical approach to take into account several phenomena: nutrient cycling (Daufresne and Hedin, 2005), cooperation (de Mazancourt and Schwartz, 2010), niche construction (Kylafis and Loreau, 2011) and population structure, either spatial (Ryabov and Blasius, 2011; Haegeman and Loreau, 2015) or demographic (Loreau and Ebenhöh, 1994; Schellekens et al., 2010).

Popularized in the context of a couple of interacting species, these niche theoretic models can be scaled up to investigate community assembly, based on the idea that local environmental conditions are the drivers of species sorting from a large or potentially infinite number of species along a trade-off curve (Leibold et al., 2004). This approach relies on the key assumption that

'everything is everywhere', namely that there is no dispersal limitation to a species' presence (Baas Becking, 1934; De Wit and Bouvier, 2006). The associated generalized graphical methods uses the concept of geometrical envelopes, the boundary of a family of curves, providing a natural way to look graphically at species sorting along an environmental gradient (Armstrong, 1979; Tilman, 1980, 1982; Leibold, 1996; Chase and Leibold, 2003; Schade et al., 2005; Danger et al., 2008). Community composition and levels of regulating factors along the gradient can thus be investigated. These mechanistic models naturally fit into trait-based approaches, which have garnered recent interest in ecology (Lavorel and Garnier, 2002; McGill et al., 2006; Westoby and Wright, 2006; Litchman and Klausmeier, 2008). Traits hold the key to linking trade-offs from the organism level to ecosystem functions and services, in both aquatic and terrestrial ecosystems (Litchman et al., 2007; Lavorel and Grigulis, 2012). Trait-based approaches also are a natural framework to study community responses to climate change (Adler et al., 2012; Thomas et al., 2012; Barabás et al., 2014b).

Simultaneously, it has long been recognized that organisms are the product of their evolutionary history (Dobzhansky, 1973) and there is growing evidence of the interplay between ecology and evolution (Thompson, 1998; Yoshida et al., 2003; Hairston et al., 2005; Grant and Grant, 2006; Stuart et al., 2014). However, the influence of this past or present evolution on food web modules remains understudied. Theoretically, those questions have been addressed during the last decades using Adaptive Dynamics (Hofbauer and Sigmund, 1990; Dieckmann and Law, 1996; Geritz et al., 1997, 1998). This powerful framework allows one to address evolution in arbitrarily complex ecological models. As an evolutionary game theory approach, this is done by including the density- and frequency-dependent selection arising from the feedback loop between the evolving population and its environment (Dieckmann and Metz, 2006). It clarifies the conditions under which evolution acts as an optimizing process (Dieckmann and Ferrière, 2004; Metz et al., 2008) and leads to the concept of evolutionary branching, a potential prelude to diversification (Metz et al., 1996; Geritz et al., 1997, 1998; Dieckmann and Doebeli, 1999). Unlike species sorting, adaptive dynamics considers local invasibility only. Evolution can thus get stuck on local but not global fitness maxima. When applied to food web modules, this enables one to investigate the evolutionary stability of coexistence in various ecological situations (Schreiber and Tobiason, 2003; Klausmeier et al., 2007; Shoresh et al., 2008; Zu et al., 2015). Yet the conditions that allow evolutionarily stable coexistence remain unclear, as ecological coexistence often vanishes on evolutionary time scales through convergent selection. Importantly, the graphical representation is still helpful in those adaptive competition modules to perform invasion analysis when combined with ZNGI geometrical envelopes (Meszéna and Metz, 1999).

The concept of the envelope has a long history in mathematical optimization and its applications. It has for example its own theorem in economics, the Envelope Theorem (Samuelson, 1947),

and is related to the Pareto frontier (Pareto, 1906), a multi-objective optimization concept first introduced in economics and now commonly used in engineer and environmental sciences (Marler and Arora, 2004; Seppelt et al., 2013; Lester et al., 2013). Envelopes of environment-dependent growth rate functions have been used in ecology to identify the optimal species corresponding to given environmental conditions (Eppley, 1972; Norberg, 2013). In resource competition theory, the idea of taking the ZNGI envelope of a continuum of competing strategies can be traced back to Tilman (1982), who applied it heuristically to species sorting from a regional pool or adaptive foraging at the individual scale. It has been used more recently in the context of communities under the names 'community ZNGI' (Schade et al., 2005; Danger et al., 2008) or 'overall ZNGI' (Chase and Leibold, 2003). Meszéna and Metz (1999) introduced the ZNGI envelope in the eco-evolutionary context and called it 'the boundary'. They showed how evolution through the trait substitution process of adaptive dynamics can be pictured by ZNGIs rolling along their envelope, and how this helps identify evolutionary singularities and deduce their properties, both graphically.

The aim of the chapter is to unite the theoretical approaches to community assembly processes and eco-evolutionary dynamics under the common umbrella of a graphical theory of interaction, using geometrical envelopes. This provides a promising tool to investigate adaptation, diversification and functioning along environmental gradients. We first review step-by-step how to apply the graphical method to competition modules with a few species, combining the concepts of invasion analysis and impact map. Then, we show through a rigorous mathematical framework how those ideas can be naturally extended to a continuum of competitors using geometrical envelopes. Building on the intuitions of Meszéna and Metz (1999), we demonstrate for general non-linear ZNGIs how their envelope geometry relates to local invasibility. Moreover, the use of the impact ray map allows us to identify and characterize geometrically the eco-evolutionary singularities associated with a given supply point. This provides both community and eco-evolutionary bifurcation diagrams, predicting a vast range of possible adaptive behaviors along the environmental gradients. Conditions leading to robust coexistence, evolutionary priority effects and branching points can be easily identified, as they present unambiguous graphical signatures. Conceptually, this graphical approach shows how adaptive dynamics naturally combines with mechanistic competition theory. It also emphasizes the similarities and differences between species sorting from a regional pool and evolution through small step mutations, a global versus local picture. The envelope approach provides a unified tool to navigate between scales through adaptation, from the individual to the ecosystem level. Finally, we illustrate the method through the example of a versatile model of competition on two resources (Schreiber and Tobiason, 2003), shedding new light on the conditions leading to the evolution of resource specialization.

1.2 Modeling framework and analysis

1.2.1 Standard graphical construction for n competitors

Let us first introduce the general class of mathematical models treated in this thesis. We consider a community of n species, the abundances of which are denoted $\boldsymbol{N} = (N_1, N_2, ...N_n)$, which interact through p regulating factors $\boldsymbol{R} = (R_1, R_2, ...R_p)$. The dynamics of N_j and R_i obey the following equations:

$$\frac{dN_j}{dt} = w_j(R_1, R_2, ..., R_p)N_j \tag{1.1a}$$

$$\frac{dR_i}{dt} = l_i(S_i - R_i) + \sum_{j=1}^{n} I_{ij}\left(R_1, R_2, ..., R_p\right) N_j \tag{1.1b}$$

where w_j is the net growth rate of population j and I_{ij} its per capita impact on the regulating factor i. No assumptions are made about their expression, except that they both only depend on the regulating factors $\boldsymbol{R}$. We thus follow Meszéna et al. (2006) by considering that interactions between individuals are indirect, only mediated by the regulating factors. As a particular case of Meszéna et al. (2006), eq. (1.1b) assumes that the total impact of a population on a regulating factor is simply proportional to its density. Note that we have chosen the convention that resource consumption corresponds to negative impact I_{ij} but also allowed positive I_{ij}, for example with shared predators. Finally, the supply point $\boldsymbol{S} = (S_1, S_2, ...S_p)$ and the leaching or mortality rates l_i parametrize the semi-chemostat intrinsic dynamics of the regulating factors, which interact only indirectly, through the species $\boldsymbol{N}$. Particularly suited for experimental setups (Novick and Szilard, 1950; Monod, 1950), this framework is classically used to describe abiotic resource dynamics in a wide range of systems (Tilman, 1982; Grover, 1997; Loreau, 1998a). For biotic resources, a well chosen change of variables can be made to map logistic growth into the chemostat dynamics of eq. (1.1b) (see Appendix 1.A). Examples of models following the particular form of eq. (1.1) include resource-consumer modules (Tilman, 1980; Wolkowicz and Lu, 1992; Schreiber and Tobiason, 2003), food webs with keystone predation (Holt et al., 1994; Leibold, 1996), material-cycle models (Loreau, 1998b; Daufresne and Hedin, 2005) and interference competition through inhibitory product emissions (Gerla et al., 2009).

We will restrict our analysis of this system to its equilibria. Setting aside unrealistic fine-tuning between the demographic parameters, this implies that the maximal number of coexisting populations can not be greater than the number p of regulating factors, a classical result known as the Competitive Exclusion Principle (CEP) or Dimension-Diversity Theorem (Levin, 1970; Gyllenberg and Meszéna, 2005; Meszéna et al., 2006). Because of the non-linear feedback loops between the regulating factors and the population densities, it is generally not possible to find analytical expressions for the equilibria of eq. (1.1), except for some particular systems. However,

Table 1.1: Notation

Notation		Definition
		Regulating factor
i		index
p		total number
R_i		density
S_i		external supply
l_i		intrinsic per capita loss rate
Finite case	**Continuous case**	**Interacting population**
j	x	index/trait value
n	$\mathcal{X}$	total number/trait space
N_j	$N(x)$	abundance
w_j	$w(x)$	per capita net growth rate
I_{ij}	$I_i(x)$	impact on regulating factor i
$\tilde{I}_{ij}$	$\tilde{I}_i(x)$	renormalized impact on regulating factor i
	$H(x)$	second derivative of the invasion fitness
	$J(x)$	derivative of the fitness gradient
		Schreiber and Tobiason's model
α		resource interaction shape parameter
m		per capita mortality rate
g_i	$g(x)$	per capita gross growth rate
		Acronyms
ZNGI		Zero Net Growth Isocline
CEP		Competitive Exclusion Principle
ESS		Evolutionarily Stable Strategy
CSS		Convergence Stable Strategy
PIP		Pairwise Invasibility Plot

it is possible to visualize those solutions graphically for up to three regulating factors, following a long tradition in theoretical ecology (León and Tumpson, 1975; Tilman, 1980, 1982; Leibold, 1996; Grover, 1997; Chase and Leibold, 2003). The aim here is to review this graphical construction in the case of the general model of eq (1.1). Doing so, we will introduce the associated basic concepts and notations needed for our generalization of this approach to the community and evolutionary frameworks in the next sections.

The method consists of two steps: invasion analysis and impact map. This decomposes the environmental feedback loop into its sensitivity and impact components following the terminology of Meszéna and colleagues (Meszéna and Metz, 1999; Meszéna et al., 2006), which shares strong similarities with Chase and Leibold's (2003) concepts of requirement and impact niches. To help visualize our method, we will illustrate it by presenting the case of n populations $N_1, N_2, ...N_n$ interacting through two regulating factors R_1 and R_2. While described in general terms in the main text, we will use a flexible resource competition model introduced by Schreiber and Tobiason (2003) as a concrete example (see Box 1 and Figures). The graphical construction of the ecological bifurcation diagram follows two distinct steps, that will naturally be extended later in the eco-evolutionary case.

Invasion analysis Let us first focus our attention on the population equations, eq. (1.1a). At equilibrium, they imply for every population that either $N_i = 0$ (the population is absent) or $w_i = 0$ (its net growth rate is zero). There are thus three possible kind of equilibria: 'empty' or washout state with no population, one non-zero population only, or coexistence of two distinct populations with extinction of the other $n-2$ populations. Coexistence of three or more different populations on two regulating factors is not possible due to the CEP. From equation (1.1a), the presence of a population i in the system restricts R_1 and R_2 to $w_i(R_1, R_2) = 0$. Graphically, this defines the so-called Zero Net Growth Isocline of population i or ZNGI_i (Tilman, 1980). For each competitor i, this curve delimits in the (R_1, R_2) plane the regions where net growth is positive ($w_i > 0$) from the ones where net growth is negative ($w_i < 0$) (see Fig. 1.1). A direct implication is that coexistence between populations at equilibrium is only possible for (R_1, R_2) where their two ZNGIs intersect. On the contrary, the 'empty' equilibrium with no population exists for any set of regulating factors, as none of the populations is imposing its zero net growth constraint on the regulating factors.

More importantly, the ZNGIs also allow one to investigate the stability against invasion of those equilibria through invasion analysis. A necessary condition for any equilibrium involving either 0, 1 or 2 populations to be stable is for the point (R_1, R_2) to be located outside the positive growth regions of all the other potential invaders (Tilman, 1982; Leibold, 1996). Thus, the potentially stable 'empty' equilibria are the ones for which (R_1, R_2) are simultaneously located outside (in the direction of lowered growth rate) the whole set of ZNGIs (shaded regions

in Fig. 1.1). Population i stable equilibria can only be located on the portion of ZNGI_i that is outside all the other ZNGIs, and the same rule extends to stable coexistence points between two populations. The set of points (R_1, R_2) corresponding to non-empty potentially stable equilibria form what we can call the outer envelope of the ZNGIs (thicker border in Fig. 1.1). To conclude, a ZNGI directly represents both the minimum requirements and the competitive ability of its corresponding population.

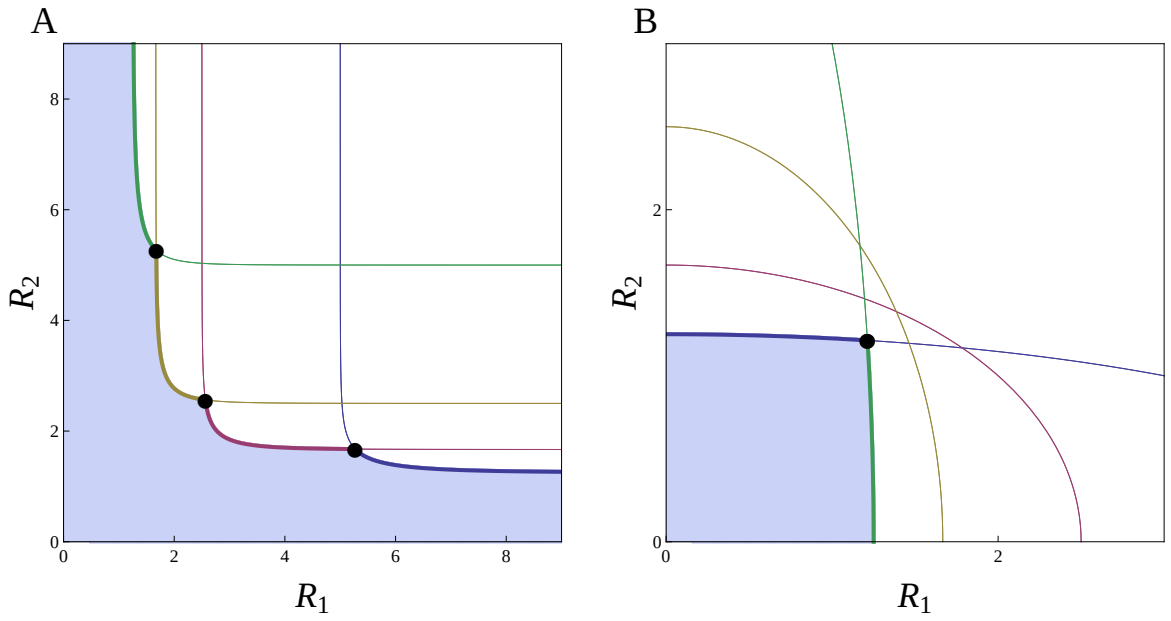

Figure 1.1: Invasion analysis for a set of 4 competing populations consuming two resources R_1 and R_2. Competitors are labeled with i from 1 to 4 (respectively blue, purple, yellow, and green). They follow Schreiber and Tobiason (2003) model described in Box 1 with $x_i = 0.2i$ and $m = 1$. Resources are either A) interactive essential ($\alpha = -5$) or B) antagonistic ($\alpha = 2$). Invasion analysis consists in drawing the set of ZNGIs (thin), selecting its outer envelope corresponding to non-invadable single population equilibria (thick) and potential coexistence points (black dots); the stable 'empty' equilibria are located under the envelope (light blue). In the essential case, each strategy has a range of non-invadable equilibria and can potentially coexist with the neighboring populations. In the antagonistic case, the extreme strategies ($x_1 = 0.2$ and $x_4 = 0.8$) exclude all the other ones but can potentially coexist together.

Supply point mapping We have so far identified the candidate (R_1, R_2) values associated with the different kinds of possible equilibria using eq. (1.1a) only. Yet the solutions (R_1, R_2) also have to satisfy the limiting factor equations eq. (1.1b) set equal to zero. When solved together, this obviously makes them functions of the parameters of the system, including the supply point. To draw a bifurcation diagram, we would like to know for every supply point which are the corresponding (R_1, R_2) at equilibrium and thus deduce its associated characteristics ('empty', one

population or coexistence). In practice, the map is performed using the supplementary constraints emerging from equations (1.1b) taken at equilibrium. First, note that this map is trivial for the regulating factors associated with the 'empty' equilibrium. Indeed, having all the N_i equal to 0 leads to $\boldsymbol{S} = \boldsymbol{R}$. This means that if we now draw the ZNGI envelope in the supply plane, all the supply points situated outside of it will map to the 'empty' equilibrium (White region, Fig. 1.2).

Where are the supply points leading to non-zero populations located? Let us first put aside the coexistence case, and focus on a single population equilibrium with $N_i \neq 0$ and $N_j = 0$ for $i \neq j$. Setting eq. (1.1b) equal to zero leads to

$$\boldsymbol{S} = \boldsymbol{R} + N_i \tilde{\boldsymbol{I}}_{\boldsymbol{i}}(\boldsymbol{R}) \tag{1.2}$$

where $\tilde{\boldsymbol{I}}_{\boldsymbol{i}} = (I_{1i}/l_1, I_{2i}/l_2)$ is the impact vector renormalized to account for different loss rates, N_i is a positive density and $\boldsymbol{R}$ belongs to ZNGI_i stable portion of the envelope. Eq. (1.2) means that for a given regulating factor point on ZNGI_i, the corresponding supply points $\boldsymbol{S}$ are located along the ray that starts from the point (R_1, R_2) when $N_i = 0$ and moves away from it following the direction vector $\tilde{\boldsymbol{I}}_{\boldsymbol{i}}$ as N_i increases. This means that all the supply points along a given ray will map to the same regulating factor at equilibrium, but with different densities. Those 'impact rays', as we suggest to call them, thus allow us to deduce graphically the supply points regions associated with a given single population equilibrium by moving (R_1, R_2) along its corresponding ZNGI portion along the envelope (Fig. 1.2). Let us note the difference between working with the limiting factors $\boldsymbol{R}$ versus their supply $\boldsymbol{S}$. While the invasion analysis takes place in a density-independent framework as we compare the growth rates of the different competitors for given $\boldsymbol{R}$ (Fig. 1.1), including the supply point map and thus the environmental feedback loop for given $\boldsymbol{S}$ fully captures the density and frequency dependence of the model (Fig. 1.2).

In the coexistence case, the method is slightly different. Equations (1.1b) now leads to $\boldsymbol{S} = \boldsymbol{R} + N_i \tilde{\boldsymbol{I}}_{\boldsymbol{i}}(\boldsymbol{R}) + N_j \tilde{\boldsymbol{I}}_{\boldsymbol{j}}(\boldsymbol{R})$ with $\boldsymbol{R}$ at the two ZNGIs' intersection. Thus, all the supply points situated in the cone originating at $\boldsymbol{R}$ and delineated by vectors $\tilde{\boldsymbol{I}}_{\boldsymbol{i}}$ and $\tilde{\boldsymbol{I}}_{\boldsymbol{j}}$ map to this coexistence equilibrium when both densities are positive (Fig. 1.2B). The impact vectors have to be different for this region not to be degenerate. However, this coexistence point is dynamically stable only if (see Appendix 1.B):

$$(I_{1i}I_{2j} - I_{1j}I_{2i}) \left(\frac{\partial w_i}{\partial R_1} \frac{\partial w_j}{\partial R_2} - \frac{\partial w_i}{\partial R_2} \frac{\partial w_j}{\partial R_1} \right) > 0 \tag{1.3}$$

This is known as the mutual invasibility criterion and can be interpreted graphically in terms of relative position between ZNGIs and impact rays (León and Tumpson, 1975; Tilman, 1982; Leibold, 1996). Here, we simply note that it graphically translates for this region as not being

an overlap between the two adjacent non-invadable single population regions (Fig. 1.2B). When those two regions do overlap, coexistence is unstable and replaced by a priority effect between the two single-population equilibria (Fig. 1.2A).

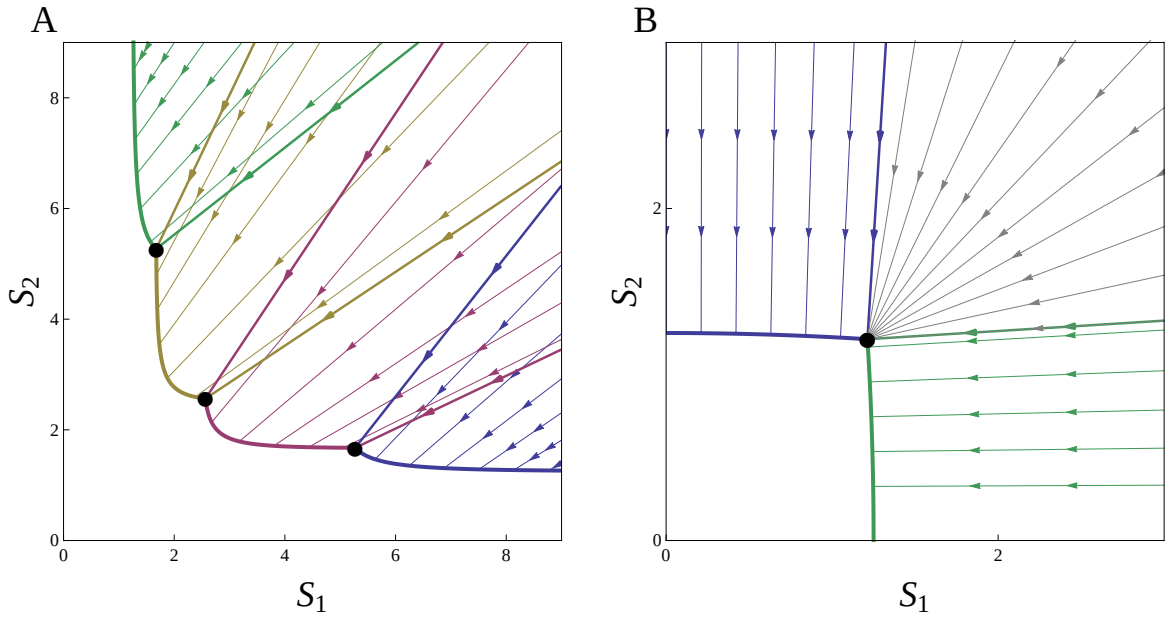

Figure 1.2: Supply point map for a set of 4 competiting populations consuming two resources R_1 and R_2 following the model of Box 1. Same configuration and parameters as Fig. 1.1. The stable ZNGI portions identified in Fig. 1.1 have been directly transposed into the supply point space. Starting from each non-invadable envelope portion (thick, plain), drawing a subset of the corresponding impact rays (thin, arrowed) helps visualizing the map that associates to every supply point its corresponding regulating factors at equilibrium. The boundaries of each portion map (thick, arrowed) combined with its corresponding ZNGI portion delimit zones of similar equilibria of the bifurcation diagram. A: there are four single-population zones (green, yellow, purple and blue) plus an empty one (white). Note that some of the former overlap, accounting for priority effects. B: there are two single-population zones (blue, green) plus an empty one (white) and a coexistence one (gray). Note that all the impact rays map to the same point in the latter case.

To summarize, an ecological bifurcation diagram as a function of the supply points (S_1, S_2) can be obtained by combining ZNGIs and impact rays through the following steps: (1) Draw the ZNGIs of the different populations and identify their outer envelope. (2) Locate the regulating factor points corresponding to the 'empty' solutions (outside the envelope), population i only solutions (on ZNGI$_i$ portions of the envelope) and the coexistence solutions (where the latter portions intersect, typically making a 'kink' in the envelope). (3) Identify the regions of the supply point plane scanned by each population impact rays when its origin moves along its corresponding ZNGI portion (a subset of impact rays can also be represented). (4) Identify potentially stable coexistence 'cones' from the kinks of the envelope.

There are two major advantages of this graphical approach. First, it delimits regions along the supply gradients for which a given species assemblage is present in the system. Historically, this allowed one to identify conditions for coexistence of two consumers (Tilman, 1982) and describe species succession along a nutrient gradient (Tilman, 1982; Leibold, 1996). Secondly, drawing the impact rays also allows one to deduce the equilibrium regulating factor levels and sometimes also population densities directly on the diagram. For consumers growing on essential resources, this is a way to identify which factor will be limiting for a given supply (Tilman, 1982). The direction of the impact vectors also enables one to assess the relative impact of a population on the regulating factors. But using impact rays has other advantages, which have been underused so far. Sometimes, a given supply point can be reached by several impact rays, which means that it maps to several distinct equilibria. In this case, the system presents alternative stable states, which is the basis of the 'founder effect'. There is an interesting diversity of situations that can be encountered depending on the states involved in this bistability. The most well-known case is one single population versus another one (Fig. 1.2A). But it is also possible to have alternative stable states inside a single population as it is often the case for structured populations (Schreiber and Rudolf, 2008; Guill, 2009; Schellekens et al., 2010), or between a community and an 'empty' state as it is common in the presence of a positive feedback loop or an ecosystem engineer (Scheffer et al., 2001; Rietkerk et al., 2004; Kéfi et al., 2010). The graphical method presented here allows one to identify alternative stable states regions in the bifurcation diagram without ambiguity.

With this graphical construction, we have provided only some necessary conditions for the local stability of the different equilibria through invasion analysis, but those are not always sufficient. For example, a single population may have alternative stable states through an Allee effect. These stable states are generally separated by unstable states that would not be identified explicitly as such by the scheme presented above. However, a careful study of the envelope of the impact rays moving along the ZNGI for a single-population equilibrium can supplement this by further restricting an impact ray to its stable portion (see Appendix 1.B). This idea will be used again in the eco-evolutionary case to identify branching points (see supply point mapping in section 1.2.3). Limit cycles and other nonequilibrium attractors are also a possibility, even when criterion (1.3) is satisfied, as the other stability criteria can not always be satisfied. Again, this would not be detectable on the graphical analysis. However, these two situations do not happen for simple systems like the standard two consumers on two resources (Tilman, 1982; Chase and Leibold, 2003; Schreiber and Tobiason, 2003), although they can for three or more resources (Huisman and Weissing, 1999).

Box 1: Schreiber and Tobiason consumer-resource model

Schreiber and Tobiason (2003) studied the evolutionary ecology of n consumer populations feeding on two resources with densities R_1 and R_2. Their model is a particular case of model (1.1) from the main text, with:

$$w_i(R_1, R_2) = g_i(R_1, R_2) - m \tag{1.4}$$

$$g_i(R_1, R_2) = [(x_i R_1)^\alpha + ((1 - x_i)R_2)^\alpha]^{\frac{1}{\alpha}} \tag{1.5}$$

where x_i and $1 - x_i$ account for investment in acquisition of respectively resource 1 and 2 (note this implies a linear trade-off), m is the constant per capita mortality rate and α controls the shape of the interaction between resources. Following Tilman's (1980; 1982) classification of resources relations, $\alpha < 0$ represents interactive essential resources (both necessary and slightly better in balanced proportions), $0 < \alpha < 1$ represents complementary resources (substitutable but better in balanced proportions), $\alpha = 1$ represents perfectly substitutable resources, and $\alpha > 1$ represents antagonistic resources (substitutable but worse in balanced proportions). The limiting cases $\alpha \to -\infty$ and $\alpha \to +\infty$ lead to respectively essential and switching resources (growth is limited by respectively the most limiting and the most abundant resource). The growth rate (1.5) is thus an elegant mathematical way to control the nutritional interaction between the resources. The intrinsic resource dynamics follows chemostat dynamics as in eq. (1.1b) with $l_1 = l_2$. Finally, population N_i influences the resources dynamics in model (1.1) through its impact vector. For $\alpha < 1$, we retain the mass action law used by Schreiber and Tobiason (2003):

$$(I_{i1}, I_{i2}) = -[x_i R_1, (1 - x_i)R_2] \tag{1.6}$$

This describes purely random encounters and removal of both resources, proportionally to their densities through acquisition rates. This consumption process does not satisfy conservation of mass in general, as $I_{i1} + I_{i2} \neq g_i$ for $\alpha \neq 1$. Thus, removal of a certain resource density does not translate into an equivalent consumer growth. In the case of antagonistic resources, this situation would describe nutritional antagonism during the assimilation process, like synergistic effects of toxic compounds (Tilman, 1980). For this reason, we rather used the following impacts in the $\alpha \geq 1$ case:

$$(I_{i1}, I_{i2}) = -g_i^{1-\alpha}[(x_i R_1)^\alpha, ((1 - x_i)R_2)^\alpha] \tag{1.7}$$

Conservation of mass is here satisfied, and antagonism comes from the foraging strategy

of the consumer itself. It describes the behavioral switching of a predator, focusing disproportionately on its most abundant prey (Murdoch, 1969). This situation can emerge when resources are spatially distributed (Murdoch et al., 1975) or through the formation of a search image (Pietrewicz and Kamil, 1979; Dukas and Kamil, 2001).

As explained in the main text, the ZNGI of a given population i is obtained by setting $g_i(R_1, R_2) - m = 0$. Its concavity is controlled by the sign of $\alpha - 1$, as can be visualized in Fig. 1.1: the antagonistic case ($\alpha > 1$) give concave ZNGIs while complementary and interactive essential ($\alpha < 1$) gives convex ones. Moreover, computing the equation of the ZNGIs envelope through eq. (1.11) gives the eco-evolutionary singular points of the system. Solving them in this particular case leads to the following implicit envelope equation:

$$\left(R_1^{\frac{\alpha}{1-\alpha}} + R_2^{\frac{\alpha}{1-\alpha}}\right)^{\frac{1-\alpha}{\alpha}} - m = 0 \tag{1.8}$$

This also gives the expression of the singular trait as a function of the resource level:

$$x(R_1) = \left(\frac{R_1}{m}\right)^{\frac{\alpha}{1-\alpha}} \tag{1.9}$$

When substituted into the impact vector expression, this gives the impact map linking supply points to the corresponding singular points. The resulting ZNGI envelopes and associated impact maps are represented in Fig. 1.3-1.5. In the antagonistic case, the envelope had to be supplemented with the boundary ZNGIs. Those are the horizontal and vertical lines going through the point $(1, 1)$, and correspond to the two specialist strategies $x = 0$ and $x = 1$.

1.2.2 Extension to a continuum of competitors: the ZNGI envelope

We now extend the previous framework from a discrete set of populations to a continuous set of strategies. The evolution of quantitative traits and phenotypic plasticity can be considered as occurring among a continuous set of strategies, as can community assembly (Tilman, 1982, 1988; Chase and Leibold, 2003). Our motivation here is twofold. First, we aim at providing a rigorous framework to address the question of species sorting in communities and integrate this effect at the ecosystem scale. Second, this introduces the basic tools necessary to perform the eco-evolutionary analysis of the next section. This will highlight the similarities and differences between the species sorting and the adaptive dynamics approaches.

Formally, the generalization to a continuum of competitors is straightforward with the re-

sults of the previous section in mind. Omitting time-dependencies to lighten the notation, the dynamics of the system now reads:

$$\frac{\partial N(\boldsymbol{x})}{\partial t} = w(\boldsymbol{R}, \boldsymbol{x}) N(\boldsymbol{x}) \tag{1.10a}$$

$$\frac{dR_i}{dt} = l_i(S_i - R_i) + \int_{\boldsymbol{x} \in \mathcal{X}} I_i\left(\boldsymbol{R}, \boldsymbol{x}\right) N(\boldsymbol{x}) \tag{1.10b}$$

where the subscript j is now replaced by its continuous analog, the trait vector $\boldsymbol{x}$, which contains the functional traits that fully describe the strategy of the population with density $N(\boldsymbol{x})$. The global impact of the competitors on regulating factor i is now obtained by integrating the impact $I_i\left(\boldsymbol{R}, \boldsymbol{x}\right)$ of every strategy $\boldsymbol{x}$ over the whole trait space $\mathcal{X}$. This trait space has to be seen as the collection of all the variable trait combinations that could possibly be present in the system. We assume in practice that $\mathcal{X}$ is a connected subset of a real vector space. Usually, this trait space is constrained by trade-offs inequalities which account for correlations between the traits. This usually excludes 'Hutchinsonian demons' that outcompete all other species (Kneitel and Chase, 2004). In practice, those trade-offs are often taken to be saturated, i.e. as equalities instead of inequalities, in order to reduce the dimensionality of the trait space. When not, they simply add boundaries to the trait space. Note that we work at equilibrium, so the CEP still applies, which means that the $N(\boldsymbol{x})$ can only be a sum of delta functions with a number of peaks lesser or equal to the number of regulating factors p. From now, we will assume the trait space $\mathcal{X}$ to be unidimensional, i.e. an interval, to simplify the analysis and denote the trait as x (but see Appendix 1.C and Discussion).

Global invasion analysis Let us extend the ideas presented in the previous section to a continuum of competitors using geometrical envelopes of ZNGIs. This corresponds to species sorting, as all the strategies from the trait space are considered as potential invaders. Our aim here is to unify the different approaches and terminologies present in the literature (Meszéna and Metz, 1999; Chase and Leibold, 2003; Danger et al., 2008), provide some analytical and geometrical properties of envelopes, and combine them with impact rays to construct community/eco-evolutionary bifurcation diagrams.

The concept of the envelope is easy to understand graphically and allows an extension of the invasion analysis to a continuum of competitors. Let us superimpose a large number of ZNGIs sampled from the trait space $\mathcal{X}$ and identify their discrete outer envelope in the sense of the previous section. When the number of ZNGI sampled tends toward infinity, this discrete envelope tends toward a (generally) smooth curve called the outer geometrical envelope of the ZNGI family (Fig. 1.3A). Note that to every point of this envelope, there is a tangent ZNGI. Mathematically, this condition of tangency formally defines the geometrical envelope. Indeed,

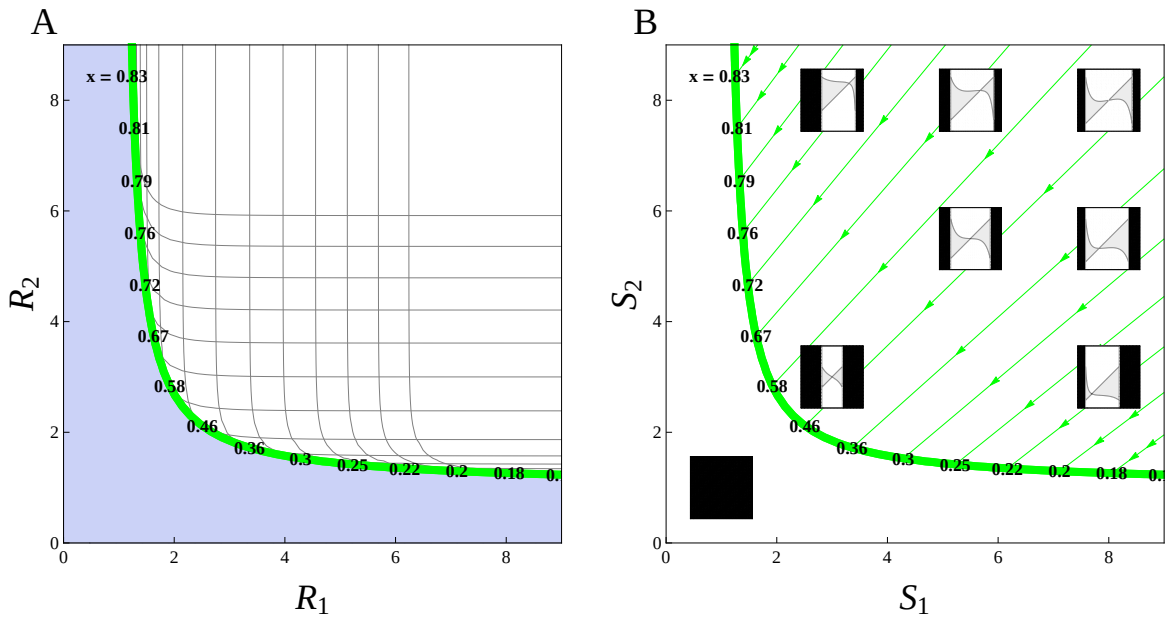

Figure 1.3: Graphical representation of a continuous set of populations consuming two resources R_1 and R_2 following the model of Box 1 in the interactive essential case ($\alpha = -5$). A: the local envelope (thick, green) of the continuum of strategies $0 \leq x \leq 1$ has been displayed. A discrete subsample of strategies had their ZNGIs represented (thin, gray) and the corresponding trait value displayed at the point of contact with the envelope (thick, black). This local envelope appears to be global, as all the ZNGIs are situated above it. B: supply point mapping through the impact rays (arrowed lined). Ecologically, there is a single strategy outcompeting all the other ones when there is enough resources (supply points above the envelope). The optimal strategy tends to be specialized on R_1 as it becomes scarcer compared to R_2, and vice-versa. Contrary to the discrete case (Fig. 1.2A), there is no priority effect zones between neighbor strategies. PIPs (black = resident can't exist, gray = +, white = −) have been displayed for comparison with adaptive dynamics framework (see section 1.2.3 and Fig. 1.5).

the points $\boldsymbol{R}$ belonging to the envelope of a set of ZNGI_x from $\mathcal{X}$ locally satisfy:

$$w(\boldsymbol{R}, x) = 0 \tag{1.11a}$$

$$\partial_x w(\boldsymbol{R}, x) = 0 \tag{1.11b}$$

where equation (1.11a) accounts for the fact that $\boldsymbol{R}$ has to belong to one of the ZNGIs and equation (1.11b) imposes the supplementary condition of tangency. Note that $\boldsymbol{R}$ is a priori considered independently of x in the invasion analysis and thus not targeted by the partial derivative. In practice, an explicit equation of the envelope linking R_2 to R_1 can be obtained by eliminating x from equations (1.11) or implicitly through a parametric equation.

Before moving on, let us emphasize the fact that eq. (1.11b) is a first order, that is, local criterion. As such, this does not insure that the envelope obtained with eq. (1.11b) has the

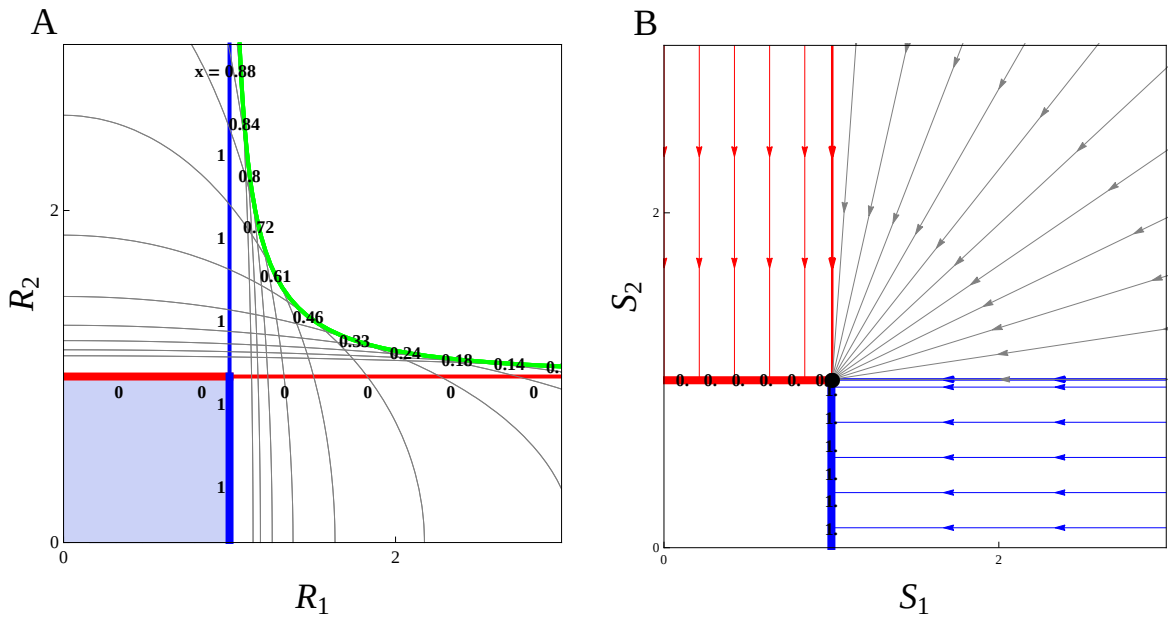

Figure 1.4: A: Local envelope (thick, green) for a continuum of strategies $0 \leq x \leq 1$ in the antagonistic case ($\alpha = 2$). A discrete subsample of strategies has been picked with their ZNGIs represented (thin, gray) and the corresponding trait value displayed at the point of tangency with the envelope (thick, black). The local envelope is an inner one and thus not part of the global one (thick), instead made of two portions of the boundary ZNGIs corresponding to the R_1 and R_2 specialists (resp. blue and red). B: supply point mapping *via* the impact rays (arrowed lined). There is room for coexistence in the 'cone' (gray) originating from the kink (black dot). Those results are very similar to the ones obtained in the discrete case (Fig. 1.2B).

global outer envelope behavior we are looking for. This situation can be understood by analogy with the problem of finding the global maximum of a differentiable function on a closed set. Setting its derivative equal to zero only locates the function's local extrema, which can be either maxima or minima. The same happens with the local envelope obtained through eq. (1.11b). It can coincide with the global outer envelope we are looking for (Fig. 1.3A) and thus have its points $\boldsymbol{R}$ situated outside the whole ZNGI set as they satisfy $w(\boldsymbol{R}, x) \leq 0$ for any x. However, some portions of this envelope could also be local but not global while others could be inner envelopes, i.e. situated inside the whole ZNGI set with $w(\boldsymbol{R}, x) \geq 0$ for any x (green segments in Fig. 1.4A). Those inner envelope portions have to be discarded in the global analysis as they are highly unstable, with every strategy able to invade. There is one last situation to consider. Back to our analogy of maximizing a function, the global maximum could also be situated on the boundaries of its domain and thus not be detected by setting its derivative equal to zero. In our case, it means that the global outer envelope could also be made of ZNGIs whose traits are located on the boundaries of $\mathcal{X}$ (red and blue segments in Fig. 1.4A). To conclude, the global invasion analysis is performed in the continuous case by putting together the local envelope defined by eq. (1.11) and the boundary ZNGIs, and keeping their global outer envelope only

(see Fig. 1.3, 1.4).

When solving eq. (1.11), a singular trait $x^*(\boldsymbol{R})$ is associated with every point $\boldsymbol{R}$ of the envelope (see Box 1 and Fig. 1.3,1.4). This trait corresponds to the ZNGI$_x$ that contributes to the envelope at that point $\boldsymbol{R}$. In the case of a global outer envelope, it means that this strategy x is optimal for those specific regulating factor values $\boldsymbol{R}$, by outcompeting all the other strategies. Note that the global outer envelope can contain kinks where there is a discontinuity of $x^*(\boldsymbol{R})$ as $\boldsymbol{R}$ moves along the envelope. This means that two distinct ZNGIs are tangent to the envelope at that specific point. As an important consequence, those are the only values of the regulating factors where globally stable coexistence is possible. Although kinks are generally plentiful in the discrete case between neighboring strategies (Fig. 1.1), the majority of those kinks usually vanish when the continuous limit is taken (Fig. 1.3). When globally stable coexistence of two different strategies from a continuum does occur, the associated kinks in the global envelope emerge at the self-intersections of the local envelope to which has been added its boundary ZNGIs when needed (Fig. 1.4). This is one of the major differences with the previous discrete approaches (Leibold, 1996; Chase and Leibold, 2003) which we will discuss later. These kinks make globally stable coexistence particularly easy to find and characterize graphically.

Supply point mapping There is virtually no difference with the discrete strategy case. We only have to remember that there is a unique non-invadable strategy $x^*(\boldsymbol{R})$ associated with every point of the global envelope that is not a kink. Plugging this relationship between the traits and the regulating factors into the renormalized impact vector $\tilde{\boldsymbol{I}}(\boldsymbol{R}, x) = \boldsymbol{I}(\boldsymbol{R}, x)/l_i$ allows us to draw the impact rays originating on the envelope points, thus performing the mapping from the ZNGI envelope to the supply point. The envelope thus behaves like a community-wide ZNGI, with its associated impact rays. The functioning of the whole community can indeed be understood as a single entity that behaves like a single population. At a kink, the coexistence cone is obtained by plotting the impact rays associated with the two coexisting strategies, and the stability criterion (1.3) is checked as before.

To summarize, the outcome of species sorting among a continuum of strategies can be seen from the community bifurcation diagram as a function of the supply points (S_1, S_2). It is obtained by combining the envelope and impact rays through the following steps: (1) From the local envelope of the ZNGI continuum and its boundary ZNGIs, keep the global outer envelope. (2) For every point of this envelope, identify the corresponding 'optimal' strategy. (3) Locate the regulating factor points corresponding to the 'empty' solutions (outside the envelope) and the potential coexistence solutions (the kinks). (4) Represent the supply point map by drawing impact rays from the envelope. (5) Identify the potentially globally stable coexistence 'cones' from the kinks.

1.2.3 Eco-evolutionary extension: link with adaptive dynamics

The global invasion analysis presented above considered that all the possible strategies from the trait space can invade the system and compete together. This explains why we have focused on determining the global envelope and discarded local but not global envelope portions. By doing so, we adopted an 'everything is everywhere' approach (Baas Becking, 1934; De Wit and Bouvier, 2006). At the opposite, the strategy space could be explored by evolving a single population through small mutation steps. In the previous section, we have presented a natural way to extend the graphical invasion analysis to a continuum of strategies by introducing the ZNGI envelope concept. As was shown by Meszéna and Metz (1999), this framework naturally allows us to address eco-evolutionary equilibria of adaptive dynamics (Hofbauer and Sigmund, 1990; Geritz et al., 1997, 1998). In fact, the idea of addressing evolution with a graphical mutant invasion analysis can be traced back as far as the early developments of resource competition theory (MacArthur and Levins, 1964; MacArthur and Wilson, 1967). Some methods based on graphical arguments in the trait space have already been developed to analyze evolutionary outcomes (Levins, 1962) and recently extended to fit in the density- and frequency-dependent context of adaptive dynamics (Rueffler et al., 2004; de Mazancourt and Dieckmann, 2004).

Here, we propose to further explore and describe the relationship between the ZNGI envelope and its geometrical properties and the evolutionary singular points and their classification. We will first provide some analytical results to support the intuition of Meszéna and Metz (1999). We will show how those results can be combined with the supply point mapping to provide a complete graphical characterization of the singular points. This approach makes it possible to draw eco-evolutionary bifurcation diagrams along the supply gradients. The whole approach relies on the observation that the growth function $w(\boldsymbol{R}, x)$, represented by ZNGI_x, is actually the invasion fitness of a mutant x in a resident-dominated environment $\boldsymbol{R}(y)$. This means that the local envelope equations (1.11) coupled with the supply point map given by the impact rays directly give the singular points of adaptive dynamics where the fitness gradient is zero. In the particular case of a one-dimensional trait x, we will show how the singular point classification is directly linked with the geometrical properties of the envelopes (but see Appendix 1.C and discussion for the multidimensional case).

Local invasion analysis The local evolutionary stability (in the sense of non-invasibility) of a singular point can be characterized using the second derivative of the invasion fitness (Geritz et al., 1998):

$$H(x) = \left[\frac{\partial^2 w(\boldsymbol{R}(y), x)}{\partial x^2}\right]_{y=x} \equiv \frac{\partial^2 w}{\partial x^2}. \tag{1.12}$$

Following adaptive dynamics terminology, a singular point for which H is negative is said to be a (local) Evolutionarily Stable Strategy (ESS), uninvasible by nearby strategies. This quantity is related to the geometrical properties of the envelope through the following relationship (see Appendix 1.C for demonstration in the multidimensional trait case):

$$H(x) = \frac{\partial w}{\partial R_2}.\left(\left.\frac{\partial^2 R_2}{\partial R_1^2}\right|_{\mathrm{E}} - \left.\frac{\partial^2 R_2}{\partial R_1^2}\right|_{\mathrm{Z}}\right) \Big/ \left(\frac{dx}{dR_1}\right)^2 \tag{1.13}$$

where $\partial^2 R_2/\partial R_1^2|_E$ and $\partial^2 R_2/\partial R_1^2|_Z$ are the second derivatives of respectively the envelope and the tangent ZNGI, and thus quantify their curvature. The difference between the two latter terms describes the relative curvature and thus position between the envelope and the tangent ZNGI: when negative, the envelope is located under the ZNGI set. Conversely, when this difference is positive, the envelope is located above the ZNGI set. The sign of $\partial w/\partial R_2$ translates this relative position along the y axis in terms of relative fitness: when positive (as it is the case within our example, since R_2 is a resource), 'under' means 'outer envelope' ($w(\boldsymbol{R}, x) \leq 0$ for any nearby x) and 'above' means 'inner envelope' ($w(\boldsymbol{R}, x) \geq 0$ for any nearby x); conversely, when $\partial w/\partial R_2 < 0$, 'under' means 'inner' and 'above' means 'outer'. Eq. (1.13) makes the formal link with adaptive dynamics: outer envelope portions always correspond to ESS while the inner ones, which were discarded during the global invasion analysis, are associated with non-ESS. Inner envelope portions play an important role in the eco-evolutionary case as they can be associated with branching points (see below). Eq. (1.13) proves and generalizes the results of Meszéna and Metz (1999) to the case of non-linear ZNGIs, as the curvature of the ZNGI comes into play. As demonstrated for ecological coexistence, evolutionarily stable coexistence can be found at the self-intersections of the local envelope. We showed that its evolutionary stability is directly linked to the ones of its two constituting strategies: coexistence is evolutionarily stable if and only if situated at the intersection of two outer ZNGI envelope portions (see Appendix 1.C for demonstration). In any case, ESS characterization of singular points only depends on ZNGIs.

Supply point mapping It is in fact possible to further characterize the singular points graphically. Let us introduce the Jacobian of the fitness gradient

$$\begin{aligned} J(x) &= \frac{d}{dx}\left[\frac{\partial w(\boldsymbol{R}(y), x)}{\partial x}\right]_{y=x} \\ &\equiv \left(\frac{\partial}{\partial x} + \frac{\partial \boldsymbol{R}}{\partial x}.\frac{\partial}{\partial \boldsymbol{R}}\right)\frac{\partial w}{\partial x} = H(x) + \frac{\partial \boldsymbol{R}}{\partial x}.\frac{\partial}{\partial \boldsymbol{R}}\frac{\partial w}{\partial x} \end{aligned} \tag{1.14}$$

According to the adaptive dynamics classification of singular points, this Jacobian gives information about the singular point's convergence stability, telling if it is an attractor or a repeller for the 1D adaptive dynamics (Eshel, 1983; Geritz et al., 1998). More precisely, the singular point is said to be convergence stable if J is negative. Note that this differs from the previous criterion based on the second derivative H: for example, a singular point can be convergent stable but

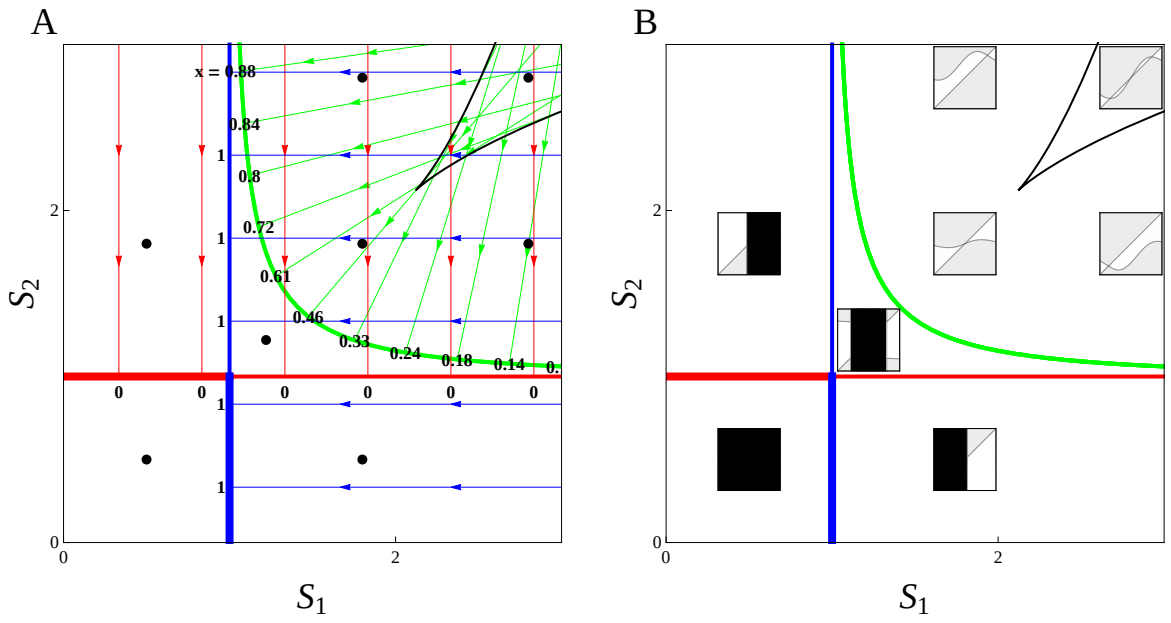

Figure 1.5: Eco-evolutionary bifurcation diagram along the supply gradients for the antagonistic case ($\alpha = 2$). A: full envelope composed of a non-ESS local portion (green) and two boundary ZNGIs (blue, red). The impact ray map (arrows, thin) helps visualizing the number and the properties of the singular points associated with a given supply point of the diagram. For example, every supply point inside the zone delimited by the impact ray envelope (black, thin) gives two boundary CSS, two repellers and one branching point. B: we only kept the global envelope and the skeleton of the impact ray map. Each zone delimited that way shares common properties that can be illustrated with PIPs (gray = +, white = −) being displayed at the exact location of their corresponding supply point (black dot, A). Invasion fitness is not defined for resident traits that do not allow the resident to exist (black).

not evolutionarily stable, which is known as a branching point and can lead a single strategy to diversify into evolutionarily stable coexistence of two different strategies (Eshel, 1983; Metz et al., 1996; Geritz et al., 1997, 1998). It is possible to show the following relationship between J and H (see Appendix 1.C for demonstration in the multidimensional trait case):

$$J = \left(\left. \frac{\partial R_1}{\partial S_1} \right|_{\mathrm{Z}} \Big/ \left. \frac{\partial R_1}{\partial S_1} \right|_{\mathrm{E}} \right) H \tag{1.15}$$

where $\partial R_1/\partial S_1|_Z$ and $\partial R_1/\partial S_1|_E$ describe how R_1 responds to its variation in supply, when R_1 moves along respectively the tangent ZNGI (ecological case, fixed strategy) and the envelope (eco-evolutionary case, adaptive strategy). The same relationship can be obtained for R_2 simply by replacing 1 by 2 from Eq. (1.15). First, note that $\partial R_1/\partial S_1|_Z$ is non-negative for the usual consumer-resource or predator-prey interactions (but see Appendix 1.B and 1.C). This implies that J and H share the same signs when $\partial R_1/\partial S_1|_E > 0$: an ESS is a CSS and a non-ESS is a repeller. Conversely, J and H have opposite signs when $\partial R_1/\partial S_1|_E < 0$: an ESS is then

non-convergent (Garden of Eden strategy) and a non-ESS is a branching point (Geritz et al., 1998). This last situation can be understood as follows: the eco-evolutionary feedback is so strong that the sign of the limiting factor response to supply variation, materialized by $\partial R_1/\partial S_1|_E$, is completely reversed compared to the purely ecological situation.

How can the sign of $\partial R_1/\partial S_1|_E$ be read graphically? To see this, we need to introduce the notion of envelope of impact rays, following the same definition of envelope introduced earlier in the case of ZNGIs. Indeed, the set of impact rays generated by moving the regulating factor point along the ZNGI envelope usually itself possesses an envelope (black curve, Fig. 1.5 and movie S1 in the Supplementary Material). A given impact ray will touch and be tangent to this envelope at a unique contact point. The line portion of the impact ray situated between its origin and this point corresponds to supply points satisfying $\partial R_1/\partial s_1|_E > 0$ while the other part corresponds to $\partial R_1/\partial s_1|_E < 0$. In general, crossing this envelope in the supply point space corresponds to the appearance or the disappearance of a pair of impact rays, i.e. singular points (see Fig. 1.5-1.6). This whole scheme can be understood as a way to use the supply point mapping to explicitly construct how the eco-evolutionary system responds to a local trait perturbation, following the ideas presented by Meszéna and Metz (1999).

We can understand how this works in practice by looking at our example (see also movies S2 and S3 in the Supplementary Material). In the interactive essential resource case, there is no impact ray envelope (see Fig. 1.3). According to the previous section, this means that $\partial R_1/\partial s_1|_E > 0$ and thus all ESS are CSS. The absence of an impact ray envelope also implies that impact rays never cross each other, which explains why there is never more than one singular point per supply point. In the antagonistic resource case, there is always an impact ray envelope (see Fig. 1.5-1.6). Underneath the impact ray envelope, the same reasoning goes as for the interacting resource case. There is thus never more than one non-ESS repeller in that region (Fig. 1.6A,B). In contrast, above the impact ray envelope the impact ray map folds over on itself, leading to three singular points per supply point (Fig. 1.6C,D). Among them, the impact ray in the middle goes through its envelope tangency point before hitting the ZNGI envelope, which means that $\partial R_1/\partial s_1|_E < 0$ and it thus corresponds to a branching point (Fig. 1.6D). The two other singular points are non-ESS repellers. In our example, the impact ray envelope thus delimits the region where non-boundary impact rays intersect. The emergence of alternative stable states as we cross the impact ray envelope is a well-known phenomenon in bifurcation theory, where it is referred to as a 'cusp catastrophe' (Strogatz, 2015).

As in the previous sections, evolutionary stable coexistence is only possible for supply points located between the two impact rays originating from a kink of the ZNGI envelope. Mutual invasibility, obtained by satisfying equation (1.3), is also needed to ensure that this coexistence

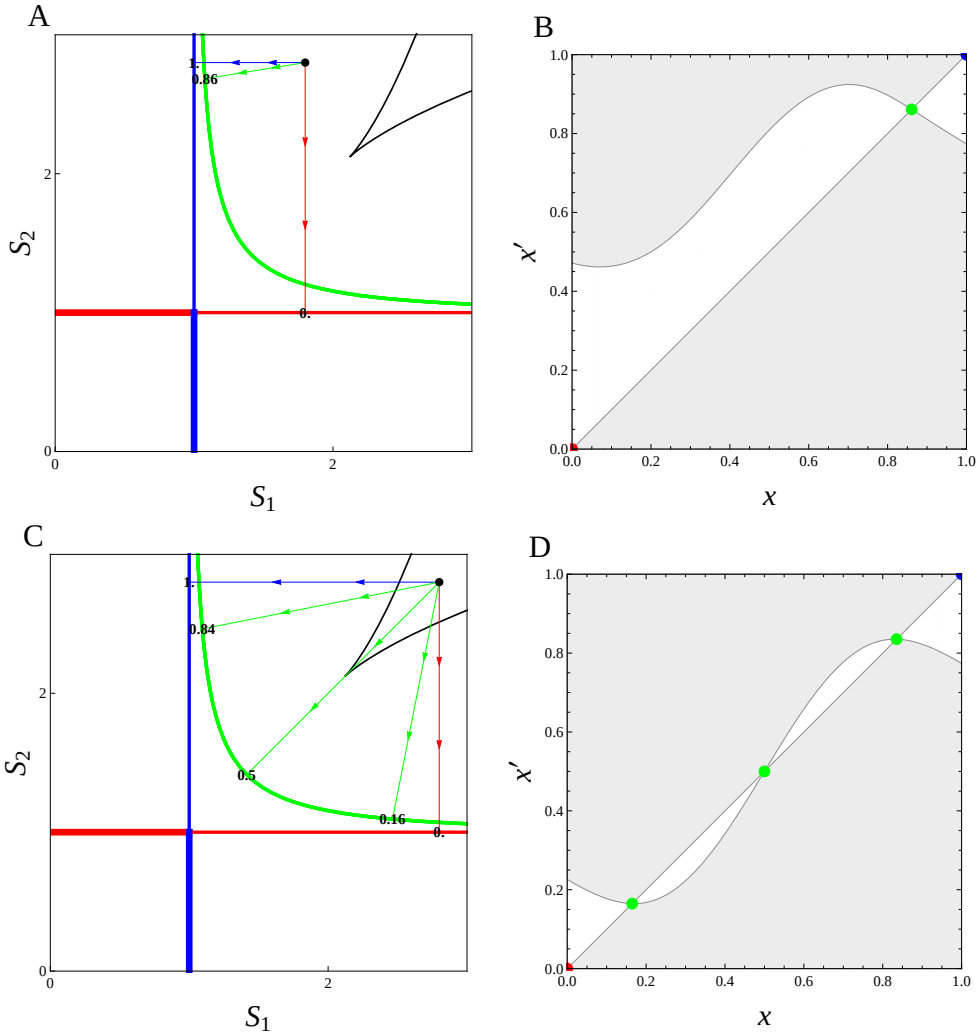

Figure 1.6: Details of the supply point map and its associated Pairwise Invasibility Plot (PIP) in the antagonistic case ($\alpha = 2$) for high but imbalanced (A,B) and balanced (C,D) resource supply, i.e. respectively $\boldsymbol{S} = (1.8, 2.8)$ and $\boldsymbol{S} = (2.8, 2.8)$. A: the impact rays map this supply point to three different eco-evolutionary equilibria on the envelope. The associated singular trait values are also displayed. B: PIP depicting the sign (gray = +, white = −) of the invasion fitness of a mutant with trait x' in a resident population with trait x. For a given resident strategy x, the success of the different invaders can be read along the corresponding vertical line. The limiting curves between the white and the gray regions correspond to invasion fitness equal to zero. Among them, the one-to-one line reminds us that the resident is at equilibrium. The eco-evolutionary fixed points are located at the intersection of this one-to-one line with the other contour or the boundary (colored dots). There are three of them here: one repelling singular point (green) and two boundary CSS $x = 0$ (red) and $x = 1$ (blue). The two latter strategies are locally non-invadable but not globally, as strategies different enough from them can invade. C,D: Contrary to the imbalanced case, this supply points gets mapped to three different points on the non-ESS envelope portion (green). Note that the middle impact ray corresponding to $x = 0.5$ goes through its tangency point on the impact ray envelope (black, thin) before hitting the ZNGI envelope (C). As explained in the main text, this is the signature of this singular point being a branching point, as can be visualized on the PIP (D).

is ecologically stable. Moreover, when polymorphism is saturated (as many distinct strategies as regulating factors) we have $J = H$ for each of the two coexisting strategies (see Appendix 1.C). Thus, evolutionarily stable coexistence is automatically convergence stable coexistence and further evolutionary branching is impossible, in accordance with the CEP (Meszéna and Metz, 1999). This last result is consistent with a recent study of saturated polymorphism (**?**).

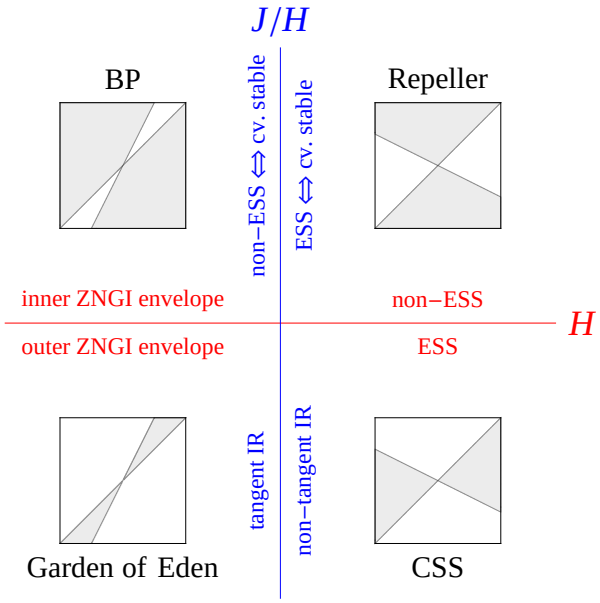

Figure 1.7: Correspondance between the classification of singular strategies and their graphical characterization in the standard consumer-resource or predator-prey case where $I_2.\partial w/\partial R_2 < 0$, e.g. Schreiber and Tobiason's (2003) or Leibold's (1996). The classification has been adapted and simplified from Geritz et al. (1997). 'tangent IR' and 'non-tangent IR' stand for 'impact ray tangent to its envelope' and 'impact ray not tangent to its envelope', while 'cv.' stands for 'convergence'. The case where $I_2.\partial w/\partial R_2 > 0$ (e.g. nitrogen fixing) is obtained by permuting 'tangent IR' and 'non-tangent IR' from the figure.

To summarize, an eco-evolutionary bifurcation diagram along the regulating factors supply can be obtained in the unidimensional trait case through the following steps: (1) Draw the ZNGI envelope. (2) Identify the ESS and non-ESS portions (given by the envelope's relative position with ZNGIs) and add boundary ZNGIs if necessary. (3) Draw the impact ray envelope and a subset of impact rays to represent the supply point map. (4) If there is an evolutionarily stable self-intersection of the ZNGI envelope, draw the coexistence cone. (5) Identify the different regions delimited and the properties of the associated singular points (Fig. 1.7). Note that superimposing a Pairwise Invasibility Plot (PIP) (Geritz et al., 1997) for every region of the diagram helps in visualizing the eco-evolutionary characteristics of the system, like the number and properties of the singular points and mutual invasibility associated with singular dimorphism (Fig. 1.3-1.6). Indeed, those conserved singular point characteristics make PIPs qualitatively similar inside a given region of the diagram.

1.3 Discussion

In this chapter, we show how the graphical approach of contemporary niche theory can be extended to a continuum of strategies to give insights into community assembly processes and eco-evolutionary dynamics along environmental gradients. In section 1.2.1, we reviewed the graphical approach by providing a general step-by-step recipe to create ecological bifurcation diagrams along environmental gradients. In section 1.2.2, we adapted this recipe to the situation of a continuum of competitors using geometrical envelopes, enabling us to study community assembly from a large species pool. Finally, in section 1.2.3 we demonstrated that combining this extension of the graphical approach with the adaptive dynamics framework leads to eco-evolutionary bifurcation diagrams summarizing the various possible evolutionary outcomes of the system.

1.3.1 Extension to structured populations

In this chapter, we have restricted our attention to unstructured populations, demographically and spatially. This was done for the sake of simplicity, as there is no further complication to apply this graphical method to the case of linearly structured populations, that are defined by their dynamics satisfying $d\boldsymbol{N}_i/dt = \boldsymbol{w}_i(R_1, R_2, ..., R_p)\boldsymbol{N}_i$, where the $\boldsymbol{N}_i$ are vectors of abundances at the different states (ages, sizes, or patches, for example) and $\boldsymbol{w}_i$ the net growth matrix (Leslie, 1948; Caswell, 2001). In this case, the ZNGI equation is obtained by setting the largest eigenvalue of the net growth matrix equal to zero (Loreau and Ebenhöh, 1994; Schellekens et al., 2010; Haegeman and Loreau, 2015). The corresponding eigenvector determines the population structure at equilibrium, thus reducing the impact on the regulating factors to a one-dimensional problem similar to the unstructured case. Conversely, there is no such general rule in the case of non-linear population structure, e.g. two-sex models (but see Szilágyi and Meszéna 2009; Barabás et al. 2014a). However, it may still be possible to define a ZNGI, as is the case for the Droop model after a quasi steady state approximation (Klausmeier et al., 2004). Therefore, it is generally possible to apply the envelope method to study the eco-evolution of structured populations.

1.3.2 Extension to higher trait space dimensions

In this chapter, we restricted the presentation of the eco-evolutionary graphical method to the case of a unidimensional trait space. However, it is still possible to define a local envelope in the general case of a trait space with dimension k by replacing the trait derivative of eq. (1.11) by a k-dimensional trait gradient. This k-dimensional trait envelope can be seen as the outcome of a recursive scheme consisting of taking successively k times the envelope along every trait vector component, starting from the ZNGI multidimensional set. In any case, the ZNGI envelope keeps the property of being a unidimensional curve. This has important ecological consequences, as

was pointed out by a more general result of Meszéna and Metz (1999): the singular strategies are necessarily contained in a $p-1$ sub-manifold of the trait space, where p is the number of regulating factors. This means that there is only a specific set of trait combinations that can be evolutionarily stable strategies, all the other ones being automatically discarded whatever the supply point. This introduces correlations between the traits of organisms that could ever be observed. This process can be thought as a pure 'competitive filtering' as it only relies on the invasion analysis. It is thus completely independent of the details of the embedding environment and as such, a very general result. Note that Tilman's (1982) R^* rule is a special case of this result, where a single limiting factor usually leads to a unique singular strategy, or at least a countable number, whatever the supply point. Can a singular point still be characterized locally from the geometry of the envelope in the multidimensional case? Even if the relationships (1.13) and (1.15) can be extended to the k-dimensional case (see Appendix 1.C), they do not give enough information to perform this full characterization.

To conclude, a ZNGI envelope can be obtained for any dimension of the trait space. It selects from the full trait space the strategies that are singular and represents graphically their competitive ability. Their local characteristics can not be deduced from simple graphical properties, but global evolutionary stability remains easy to identify.

1.3.3 From local to global invasibility

The two perspectives presented in sections 1.2.2 and 1.2.3 can be seen as two opposite but complementary pictures. The first, sometimes called the 'everything is everywhere' picture, assumes that all the imaginable strategies from the trait space have a chance to invade the system. The details of the creation and maintenance of this diversity of invaders is simply assumed (Sauterey et al., 2015). This can be seen as the existence of a hyperdiverse regional species pool - the system being embedded in an heterogenous and connected landscape - or with mutations of arbitrary size. By contrast, the second approach focuses on the invasion of a local neighborhood of strategies around the resident, as mutations are small. In this approach, evolution can be 'trapped' at a local-only ESS, and diversification from a monomorphic population only emerges from a branching point. The two approaches can lead to similar bifurcation diagrams, as it is the case for interactive essential resources in the example (Fig. 1.3) where all the local singular points are global CSS. However, the presence of locally non-ESS envelope portions lead to significant differences between the two pictures. In the case of antagonistic resources from our example, the local analysis identifies regions of priority effect between two locally stable specialists and a branching point (Fig. 1.5B, 1.6D). Those details do not matter in the global analysis, replaced by evolutionarily stable coexistence of the two specialists (Fig. 1.4B). The link between the two frameworks can be seen from the PIPs in the second picture, as shown in Fig. 1.5B: evolution under small mutations can be read on the diagonal neighborhood, but

information about invasion of any strategy is also available away from it. Another remark clear in the previous example is that there is no reason for the evolutionarily stable coexistence region and the branching region to coincide. Evolutionarily and convergence stable dimorphism are indeed possible in the absence of branching, thus emerging through invasion or 'macro-mutation' (Geritz et al., 1999) (Fig. 1.5B). An example of this situation was discussed by Wolf et al. (2007); Massol and Crochet (2008); Wolf et al. (2008). Conversely, branching can happen in a region where evolutionary stable coexistence is not possible: one of the two morphs would inevitably experience evolutionary suicide along its eco-evolutionary trajectory (Matsuda and Abrams, 1994; Rankin and López-Sepulcre, 2005; Parvinen, 2005). Local and global approaches are the two extremes of a general invasion analysis picture that can be visualized by combining local and global bifurcation diagrams and associating them with PIPs.

1.3.4 Up- and downscaling with ZNGI envelopes

We have explained in section 1.2.2 how the envelope approach allows one to scale up from the population to the community level to sort out the best competitor from a continuum of strategies. It is also possible to scale down from the population to the individual level in the context of phenotypic plasticity (Tilman, 1982). Indeed, dynamical allocation in response to environmental cues could allow an individual to explore the trait space in search of the optimal strategy, in the sense of competition. The envelope approach gives a practical tool to do so: from all the accessible behaviors represented by the continuous set of ZNGIs, the optimization procedure only retains their envelope, which can be seen as the new integrated ZNGI of the plastic individuals. Adding the family of adaptive impact rays, a direct parallel can be drawn between populations of plastic and non-plastic individuals (Tilman, 1982; Schade et al., 2005). The only difference is that the traits of the former are optimized, thus depending on the limiting factor values. A corollary is that a variety of adaptive ZNGI shapes can arise from simple non-plastic ones. As such, the envelope method provides a practical procedure to navigate through levels of organization by taking into account adaptation and flexibility, from individuals to communities (Smith et al., 2011; Norberg, 2013).

1.3.5 Coevolution from distinct functional groups and discontinuous mutations

The envelope approach is easy to apply to the evolution of n independent guilds, for example from different functional groups. Those guilds must share some regulating factors to be able to interact, but can belong to completely different trait spaces, or be bound by completely distinct trade-offs. Each guild would lead to its own eco-evolutionary envelope, that can then be compared as if they were ZNGIs in the standard discrete invasion analysis (section 1.2.1), as emphasized in the previous subsection. Examples could include plants and decomposers along a material cycle (Loreau, 1998a), nitrogen-fixing and non-nitrogen-fixing phytoplankton (Boushaba and Pascual,

2005; Agawin et al., 2007) or pairs of cooperators (de Mazancourt and Schwartz, 2010). This picture could also allow one to study the global eco-evolutionary outcomes of a strategy composed of a combination of continuous and discrete traits. From the previous point of view, this means allowing a jump from one functional group to another through discontinous mutations. With a unidimensional bounded continuous trait, invasion analysis could still be accurately depicted coupling several PIPs together into a 'meta-PIP'.

1.3.6 From discrete to continuous set of strategies

The continuous approach presented in section 1.2.2 clarifies some results identified in the finite number of strategies context. Indeed, the study of species sorting along environmental gradients has usually been addressed using a large but finite number of competitors. This led some authors to conclude that "coexistence was more likely among the most similar form" (Leibold, 1996). Fig. 1.1A from the interactive essential case contains the signature of this phenomena, as neighboring ZNGIs cross at potential coexistence points. This does not lead to coexistence here because of our choice of impact vectors but the idea is the same. However, we argue that this pattern of coexistence of similar forms is degenerate and corresponds to some kind of nearly 'neutral coexistence', i.e. not ecologically robust sensu Meszéna et al. (2006). This can been seen when looking at the continuous limit in Fig. 1.3. The coexistence points identified earlier have vanished, as neighboring ZNGIs are now infinitely close. In eco-evolutionary terms, this coexistence is not evolutionarily robust as evolution tends to destroy it. Yet, this does not mean that evolutionarily stable coexistence can not happen in the continuous limit, as we have seen in the antagonistic case (Fig. 1.4). It is, however, far less common as it relies on self-intersection of the local envelope, but more robust. Note that those differences depend heavily on the topology of the strategy space: disconnected in the finite case versus connected after the continuous limit. This is in practice related to the question of the existence of infinitely many intermediate forms between different strategies.

If this pattern of coexistence vanishes at the continuous limit, it still leaves a signature on the invasion dynamics. More precisely, whether the potential coexistence points lead to stable coexistence or priority effect influences the shape of the PIPs around the singular points. This can be seen in the interactive essential resource example. For high resource supplies, priority effect between neighboring strategies (Fig. 1.1A) translates into CSS strategies that cannot directly invade their neighborhood and are only attained monotonically through ever-decreasing evolutionary steps (see PIPs on Fig. 1.3B). This is one of the eight singular strategy types identified by the adaptive dynamics classification (Geritz et al., 1997). On the contrary, we predict that coexistence between neighboring strategies in the finite strategy case would lead to CSS strategies able to invade their neighborhood. Giving a mathematical proof of this is out the scope of this chapter. However, those results are intuitive, as priority effects between neighboring

strategies indicate that they are protected from invasion by the other strategies. To conclude, while neighboring coexistence or priority effect vanish when the continuous limit is taken, they leave their signature on the eco-evolutionary characteristics of the singular points.

1.3.7 Importance of the regulating factor space

For a given strategy, the corresponding ZNGI summarizes its competitive ability. This is measured in the regulating factor space, where the competitiveness of different strategies can be compared. In the case of a single regulating factor, the ZNGI reduces to one number, so all the strategies can be ordered and compared without ambiguity. This result is known as Tilman's R^* rule (Hsu et al., 1977; Tilman, 1982; Grover, 1997; Chase and Leibold, 2003) and leads to a pessimization principle in the eco-evolutionary case (Metz et al., 2008). This strict ordering is in general impossible with more regulating factors: invasion analysis with the envelope is the closest equivalent to that rule. Optimization is now multi-objective, so a Pareto front is needed to find the optimal strategies, and this role is played by the envelope. This is why the regulating factor space is so central: it controls species sorting and adaptation through this multi-objective optimization. However, the map between a strategy from the trait space and its ZNGI in the regulating factor space is non-trivial. For example, constraints on organisms encoded by trade-offs are usually inferred at the trait level. Yet, nothing ensures that they efficiently translate into a trade-off in competitive ability of the ZNGI set in the regulating factor space. Another effect of this map is to control the presence of evolutionarily stable coexistence. Indeed, it relates the geometrical characteristics of the ZNGI envelope to the ones of the trait space. For example, some trait space geometries lead to kinked global envelopes and thus potentially to evolutionarily stable coexistence while other do not.

1.3.8 Evolution of resource use

Applying the envelope method to Schreiber and Tobiason's (2003) resource competition model allowed us to confirm and visualize their results. Moreover, we could specify how the number of singular points and their properties depended on the resource supplies through bifurcation diagrams. For $\alpha < 1$, there is always a single generalist CSS, under the condition that there is a sufficient supply of resources (Fig. 1.3). The antagonistic case ($\alpha > 1$) was further characterized with the help of the impact ray map and its envelope (Fig. 1.5). First, there is always a zone of supply points for which evolutionary branching is possible. This is true for both the choice of impact vector expressions used by Schreiber and Tobiason (2003) and the modification we proposed. However, this zone is pushed infinitely far away from the envelope for $\alpha \to \infty$ when using eq. (1.6) while it stays close to it when using eq. (1.7). The former is consistent with Schreiber and Tobiason's (2003) observations. The latter states that branching is still possible on highly antagonistic resources if switching is more abrupt. Note that branching demands a sufficiently large and balanced supply of the two resources to take place. Moreover, this branching point,

when it exists, is always unique and separated from the boundary attracting strategies by two repellers. Also note that it is possible not to have any singular point but still one or two attractive boundaries for low enough resources.

The consumer-resource model of the example also gives some insights in the case of strictly essential ressources. This corresponds to the limit obtained when $\alpha \to -\infty$, leading to a growth rate (1.5) following Liebig's Law of the Minimum and an associated L-shaped ZNGI (León and Tumpson, 1975; Tilman, 1982). It is actually in this context that the use of ZNGI envelopes first appeared (Tilman, 1988) and later spread (Schade et al., 2005; Klausmeier et al., 2007; Danger et al., 2008). The standard approach consists in getting the envelope equation simply by tracking the position of the ZNGI corner. The first order criterion (1.11b) is not only unnecessary in this case, it actually fails to give the envelope equation when applied directly, as the L-shaped ZNGI is non-differentiable at its corner. However, this problem can be worked around by taking the limit when $\alpha \to -\infty$ of the general envelope equation (1.8), leading to a consistent result. Contrary to the standard approach, our method is easy to generalize to a trait space of arbitrary dimension. It could thus be used to further investigate the evolution of consumers feeding on essential resources (Klausmeier et al., 2004; Shoresh et al., 2008).

1.3.9 Conclusion and perspectives

In this chapter, we presented a graphical approach based on geometrical envelopes that can be used to perform invasion analysis and supply point mapping with a continuum of interacting strategies. We showed how relevant this technology is to two biological pictures, namely species sorting and adaptive dynamics, paving the way for an 'evolutionary theory of the niche' (Holt, 2009a). Because of its generality, this approach could be applied to investigate a variety of ecological situations: the evolution in a diamond-shaped food web (Leibold, 1996), cooperation through trading (de Mazancourt and Schwartz, 2010), informed dispersal (Haegeman and Loreau, 2015), nitrogen fixing (Agawin et al., 2007) or niche construction (Kylafis and Loreau, 2011), for example.

Appendices

1.A Transformation toward decoupled chemostat dynamics

We provide here two examples of change of variables that enable one to map more general regulating factors dynamics to a chemostat dynamics form presented in eq. (1.1b). This allows one to apply the graphical method presented in this chapter to those extended situations after the change of variables.

1.A.1 Logistic growth

First, let us consider that a regulating factor R follows a logistic resource dynamics:

$$\frac{dR}{dt} = rR\left(1 - \frac{R}{K}\right) + \sum_{j=1}^{n} I_j(R)N_j \tag{1.16}$$

Introducing the change of variables $\rho = 1/R$, it is straightforward that:

$$\frac{d\rho}{dt} = r(\kappa - \rho) + \sum_{j=1}^{n} \chi_j(\rho)N_j \tag{1.17}$$

with $\kappa = 1/K$ and $\chi_j(\rho) = -I_j(1/\rho)\rho^2$. Thus, this change of variable maps a logistic growth in R toward a chemostat dynamics in ρ. Note that the consumer-resource relationship with N_j is reversed by the change of variable: if a N_j was consuming R, it is now feeding ρ. This can be understood by looking at the dimensions of the new variable: if R is in individual per surface area, ρ is in surface area per individual. Thus, decreasing prey density by consumption conversely increases available surface area per individual.

1.A.2 Linear coupling through diffusion

Our second example considers two diffusion-coupled chemostats, thus following the intrinsic dynamics:

$$\frac{dR_1}{dt} = l_1(S_1 - R_1) - d_{12}R_1 + d_{21}R_2 \tag{1.18}$$

$$\frac{dR_2}{dt} = l_2(S_2 - R_2) + d_{12}R_1 - d_{21}R_2 \tag{1.19}$$

This system being linear, it can be rewritten under the general matrix form in the presence of interacting populations:

$$\frac{d\boldsymbol{R}}{dt} = \boldsymbol{T} - \boldsymbol{M}\boldsymbol{R} + \sum_{j=1}^{n} \boldsymbol{I}_j(\boldsymbol{R})N_j \tag{1.20}$$

with

$$\boldsymbol{T} = \begin{pmatrix} l_1 S_1 \\ l_2 S_2 \end{pmatrix} \quad \text{and} \quad \boldsymbol{M} = \begin{pmatrix} l_1 - d_{12} & d_{21} \\ d_{12} & l_1 - d_{21} \end{pmatrix} \tag{1.21}$$

Then, diagonalization gives $\boldsymbol{M} = \boldsymbol{P}\boldsymbol{D}\boldsymbol{P}^{-1}$ with $\boldsymbol{D} = \mathrm{diag}(\lambda_1, \lambda_2)$ leading to:

$$\frac{d\boldsymbol{\rho}}{dt} = \boldsymbol{D}(\boldsymbol{\sigma} - \boldsymbol{\rho}) + \sum_{j=1}^{n} \boldsymbol{\chi}_j(\boldsymbol{\rho})N_j \tag{1.22}$$

with $\boldsymbol{\rho} = \boldsymbol{P}^{-1}\boldsymbol{R}$, $\boldsymbol{\sigma} = \boldsymbol{D}^{-1}\boldsymbol{P}^{-1}\boldsymbol{T}$ and $\boldsymbol{\chi}_j(\boldsymbol{\rho}) = \boldsymbol{P}^{-1}\boldsymbol{I}_j(\boldsymbol{P}\boldsymbol{\rho})$. As $\boldsymbol{D}$ is a diagonal matrix, the regulating factor vector $\boldsymbol{\rho}$ nows follows decoupled chemostat dynamics.

1.B Analytical study of ecological equilibria for the two consumers on two resources system

1.B.1 Model

In the case of two consumers competing for two resource in a chemostat, model (1.1) can be rewritten:

$$\frac{dN_i}{dt} = w_i(R_1, R_2)N_i \tag{1.23}$$

$$\frac{dR_i}{dt} = l_i(S_i - R_i) + \sum_{j=1}^{2} I_{ij}\left(R_1, R_2\right) N_j \tag{1.24}$$

Let us first classify the different equilibria of the system and characterize their local stability.

1.B.2 Equilibria

Those equations present different kinds of solutions at equilibrium:

Equilibrium (0) corresponds to the case where both populations are absent, i.e. $N_1 = N_2 = 0$. Then $R_1 = S_1$ and $R_2 = S_2$.

Equilibrium (1) corresponds to the case where only population 2 is absent, i.e. $N_1 \neq 0$ and $N_2 = 0$. The system can be rewritten as:

$$\begin{aligned} 0 &= w_1(R_1, R_2) \\ \tilde{I}_{12}(R_1, R_2)(S_1 - R_1) &= \tilde{I}_{11}(R_1, R_2)(S_2 - R_2) \\ N_1 &= \frac{(R_1 - S_1)}{\tilde{I}_{11}(R_1, R_2)} \end{aligned} \tag{1.25}$$

where we have used the simplifying notation $\tilde{I}_{ij} = I_{ij}/l_i$. The regulating factor values at equilibrium (R_1, R_2) are obtained by solving the first two equations together. N_1 is then deduced from the result using the third equation.

Equilibrium (2) corresponds to the case where only population 1 is absent, i.e. $N_2 \neq 0$ and $N_1 = 0$. The equilibrium values can be deduced from the previous paragraph by switching subscripts.

Equilibrium $(1 + 2)$ corresponds to the case where the two populations coexist, i.e. $N_2 \neq 0$ and $N_1 \neq 0$. Then (R_1, R_2) are given after solving:

$$\begin{aligned} 0 &= w_1(R_1, R_2) \\ 0 &= w_2(R_1, R_2) \end{aligned}$$

The densities values at equilibrium follow with:

$$\boldsymbol{N} = \tilde{\boldsymbol{I}}^{-1}(\boldsymbol{S} - \boldsymbol{R}) \tag{1.26}$$

where $\boldsymbol{N} = (N_1, N_2)^T$, $\boldsymbol{S} = (S_1, S_2)^T$, $\boldsymbol{R} = (R_1, R_2)^T$ and $\tilde{\boldsymbol{I}}$ is a 2 by 2 matrix with coefficients $\tilde{I}_{ij} = I_{ij}/l_i$. Note that $\tilde{\boldsymbol{I}}$ is invertible if and only if the renormalized impacts vectors of the two populations are not collinear, which is improbable in the absence of fine-tuning.

1.B.3 Stability

The stability of those different types of equilibria can be assessed introducing the Jacobian of the system:

$$\boldsymbol{J}(N_1, N_2, R_1, R_2) = \begin{pmatrix} w_1 & 0 & \partial_1 w_1 N_1 & \partial_2 w_1 N_1 \\ 0 & w_2 & \partial_1 w_2 N_2 & \partial_2 w_2 N_2 \\ I_{11} & I_{12} & -l_1 + \sum_{j=1}^{2} \partial_1 I_{1j} N_j & \sum_{j=1}^{2} \partial_2 I_{1j} N_j \\ I_{21} & I_{22} & \sum_{j=1}^{2} \partial_1 I_{2j} N_j & -l_2 + \sum_{j=1}^{2} \partial_2 I_{2j} N_j \end{pmatrix} \tag{1.27}$$

where we have omitted the explicit dependencies in (R_1, R_2) and the notation ∂_i stands for $\partial/\partial R_i$. This Jacobian can be evaluated for the different kinds of equilibria we have identified. It is not to be confused with the Jacobian of the fitness gradient J of eq. (1.14).

Equilibrium (0) The Jacobian can be rewritten as:

$$\boldsymbol{J} = \begin{pmatrix} w_1 & 0 & 0 & 0 \\ 0 & w_2 & 0 & 0 \\ I_{11} & I_{12} & -l_1 & 0 \\ I_{21} & I_{22} & 0 & -l_2 \end{pmatrix} \tag{1.28}$$

As $(R_1, R_2) = (S_1, S_2)$, the empty equilibrium is stable if both $w_1(S_1, S_2) < 0$ and $w_2(S_1, S_2) < 0$, which means that none of the two populations can invade. There is no other constraint as the chemostat dynamics are 'intrinsically' stable.

Equilibrium (1) After permutation, the Jacobian can be rewritten as a block-diagonal matrix:

$$\boldsymbol{J} = \begin{pmatrix} w_2 & \mathbf{0} \\ \mathbf{0} & \boldsymbol{K} \end{pmatrix} \tag{1.29}$$

with

$$\boldsymbol{K} = \begin{pmatrix} 0 & \partial_1 w_1 N_1 & \partial_2 w_1 N_1 \\ I_{11} & -l_1 + \partial_1 I_{11} N_1 & \partial_2 I_{11} N_1 \\ I_{21} & \partial_1 I_{21} N_1 & -l_2 + \partial_2 I_{21} N_1 \end{pmatrix} \tag{1.30}$$

Thus, a first necessary condition is non-invasibility by population 2 through $w_2(R_1, R_2) < 0$. Routh-Hurwitz criteria applied on $\boldsymbol{K}$ gives a second necessary condition $\det \boldsymbol{K} < 0$. It is actually possible to show that:

$$\det \boldsymbol{K} = l_2 N_1 I_{11} \frac{\partial w_1}{\partial R_1} \Big/ \frac{\partial R_2}{\partial S_2} \tag{1.31}$$

The object $\partial R_2/\partial S_2$ has an intuitive geometrical interpretation linked to the envelope of the impact rays. The scheme is similar to the one developed in the main text in the eco-evolutionary context (see supply point map in section 1.2.3). Indeed, the family of impact rays associated with

a given ZNGI can possess an envelope. When it is the case, a given impact ray is tangent to its envelope at a particular point. The line portion of the impact ray situated between its origin and this point corresponds to supply points satisfying $\partial R_2/\partial S_2 > 0$ while the other part corresponds to $\partial R_2/\partial S_2 < 0$. In the classical consumer-resource situation where $I_{11}\partial w_1/\partial R_1 < 0$, this means that only the supply points situated before the envelope on the impact ray map to stable equilibria, the other ones being unstable. This graphical criterion shares strong similarities with the eco-evolutionary case presented in the main text. Note that the condition $\det \boldsymbol{K} < 0$ is necessary but not sufficient to ensure stability.

Equilibrium (2) can be deduced from the previous paragraph by switching subscripts. Note that we get the necessary condition $\det \boldsymbol{K'} < 0$ for stability with :

$$\det \boldsymbol{K'} = l_1 N_2 I_{22} \frac{\partial w_2}{\partial R_2} \Big/ \frac{\partial R_1}{\partial S_1} \tag{1.32}$$

Equilibrium $(1+2)$ The Jacobian can be rewritten as:

$$\boldsymbol{J} = \begin{pmatrix} 0 & 0 & \partial_1 w_1 N_1 & \partial_2 w_1 N_1 \\ 0 & 0 & \partial_1 w_2 N_2 & \partial_2 w_2 N_2 \\ I_{11} & I_{12} & -l_1 + \sum_{j=1}^{2} \partial_1 I_{1j} N_j & \sum_{j=1}^{2} \partial_2 I_{1j} N_j \\ I_{21} & I_{22} & \sum_{j=1}^{2} \partial_1 I_{2j} N_j & -l_2 + \sum_{j=1}^{2} \partial_2 I_{2j} N_j \end{pmatrix} \tag{1.33}$$

The necessary condition for stability $\det \boldsymbol{J} > 0$ can be obtained where:

$$\det \boldsymbol{J} = (I_{11} I_{22} - I_{12} I_{21}) \left(\frac{\partial w_1}{\partial R_1} \frac{\partial w_2}{\partial R_2} - \frac{\partial w_1}{\partial R_2} \frac{\partial w_2}{\partial R_1} \right) N_1 N_2 \tag{1.34}$$

this is the mutual invasibility criterion of eq. (1.3) in the main text. We recognize in eq. (1.34) the general decomposition of $\det \boldsymbol{J}$ as the product of the impact and sensitivity map volumes (Meszéna et al., 2006).

1.C Demonstration of the geometrical relationships in the k-dimensional traitspace case

The aim of this section is to link the ZNGI and impact ray envelope properties to the eco-evolutionary properties of the corresponding singular points. We restrict our attention to the case of two regulating factors R_1 and R_2, for a completely general k-dimensional trait $\boldsymbol{x}$.

1.C.1 Monomorphic singular point

When there is only one singular population in the system, the eco-evolutionary invasion analysis of eq. (1.11) can be generalized to the k-dimensional case as:

$$w(\boldsymbol{R}, \boldsymbol{x}) = 0 \tag{1.35}$$

$$\partial_{\boldsymbol{x}} w(\boldsymbol{R}, \boldsymbol{x}) = \boldsymbol{0} \tag{1.36}$$

where we have used the simplifying notation for the fitness gradient:

$$\partial_{\boldsymbol{x}} w(\boldsymbol{R}, \boldsymbol{x}) \equiv \left[\frac{\partial w(\boldsymbol{R}(\boldsymbol{y}), \boldsymbol{x})}{\partial \boldsymbol{x}} \right]_{y=x} \tag{1.37}$$

the notation $\partial/\partial_{\boldsymbol{x}}$ standing for a nabla operator along $\boldsymbol{x}$. Graphically, we recognized in the main text that this set of equations parametrizes the ZNGI envelope. This particular expression of the fitness gradient as a partial derivative along its second coordinate is specific to the fact that mutant and resident only interact indirectly through the regulating factors. This has to be combined with the supply point map:

$$v(\boldsymbol{S}, \boldsymbol{R}, \boldsymbol{x}) = 0 \tag{1.38}$$

with $v(\boldsymbol{S}, \boldsymbol{R}, \boldsymbol{x}) = (S_1 - R_1)\tilde{I}_2(\boldsymbol{R}, \boldsymbol{x}) - (S_2 - R_2)\tilde{I}_1(\boldsymbol{R}, \boldsymbol{x})$. Jointly solving this system gives the singular point trait values.

How can we link the tangent ZNGI and ZNGI envelope relative curvature to the properties of its corresponding singular points? As was done in the main text in the unidimensional case, we need to introduce the Hessian matrix of the invasion fitness $\boldsymbol{H}$:

$$\boldsymbol{H}(\boldsymbol{x}) = \left[\frac{\partial}{\partial \boldsymbol{x}} \frac{\partial}{\partial \boldsymbol{x}^T} w(\boldsymbol{R}(\boldsymbol{y}), \boldsymbol{x}) \right]_{y=x} \equiv \partial_{\boldsymbol{x}} \partial_{\boldsymbol{x}}^T w \tag{1.39}$$

The ZNGI and envelope curvatures at the singular point are both given by second derivatives. The ZNGI curvature can be obtained differentiating $w(R_1, R_2, \boldsymbol{x}) = 0$ twice with respect to R_1, where $R_2 = f(R_1)$:

$$-\partial_{R_2} w. \left. \frac{\partial R_2}{\partial R_1} \right|_{\mathrm{Z}} = \partial_{R_1} w \tag{1.40}$$

$$-\partial_{R_2} w. \left. \frac{\partial^2 R_2}{\partial R_1^2} \right|_{\mathrm{Z}} = \partial_{R_1}^2 w + 2 \frac{\partial R_2}{\partial R_1} \partial_{R_2} \partial_{R_1} w + \left(\frac{\partial R_2}{\partial R_1} \right)^2 \partial_{R_2}^2 w \tag{1.41}$$

where $\boldsymbol{x}$ has been kept fixed for this calculation as we are interested by the properties of the tangent ZNGI. This is not the case for the ZNGI envelope. The envelope curvature is obtained differentiating $w(R_1, R_2, \boldsymbol{x}) = 0$ twice with respect to R_1 and using $\partial_{\boldsymbol{x}} w(R_1, R_2, \boldsymbol{x}) = \boldsymbol{0}$, where

$R_2 = g(R_1)$ and $\boldsymbol{x} = \boldsymbol{h}(R_1)$:

$$-\partial_{R_2} w. \left.\frac{\partial R_2}{\partial R_1}\right|_{\mathrm{E}} = \partial_{R_1} w \tag{1.42}$$

$$\begin{aligned} -\partial_{R_2} w. \left.\frac{\partial^2 R_2}{\partial R_1^2}\right|_{\mathrm{E}} &= \partial^2_{R_1} w + 2\frac{\partial R_2}{\partial R_1}\partial_{R_2}\partial_{R_1} w + \left(\frac{\partial R_2}{\partial R_1}\right)^2 \partial^2_{R_2} w \\ &\quad + \frac{\partial \boldsymbol{x}^T}{\partial R_1}\left(\partial_{R_1}\partial_{\boldsymbol{x}} w + \frac{\partial R_2}{\partial R_1}\partial_{R_2}\partial_{\boldsymbol{x}} w\right) \end{aligned} \tag{1.43}$$

Note that the first order derivatives are the same for the ZNGI and the envelope, which is a result of their tangency and is known in economics as the envelope theorem (Samuelson, 1947). However, the second derivatives differ by a term that accounts for the fact that $\boldsymbol{x}$ also varies along the envelope. Differentiating $\partial_{\boldsymbol{x}} w(R_1, R_2, \boldsymbol{x}) = \boldsymbol{0}$ once with respect to R_1 shows how the last term of (1.43) is actually related to the Hessian:

$$\frac{\partial \boldsymbol{x}^T}{\partial R_1}\left(\partial_{R_1}\partial_{\boldsymbol{x}} w + \frac{\partial R_2}{\partial R_1}\partial_{R_2}\partial_{\boldsymbol{x}} w\right) = -\frac{\partial \boldsymbol{x}^T}{\partial R_1}\boldsymbol{H}\frac{\partial \boldsymbol{x}}{\partial R_1} \tag{1.44}$$

In conclusion, combining all the previous results as the sum $-(1.43)+(1.41)-(1.44)$ and using the fact that $\partial R_2/\partial R_1$ coincides for both ZNGI and envelope leads to the final result:

$$\frac{\partial w}{\partial R_2}\left(\left.\frac{\partial^2 R_2}{\partial R_1^2}\right|_{\mathrm{E}} - \left.\frac{\partial^2 R_2}{\partial R_1^2}\right|_{\mathrm{Z}}\right) = \frac{d\boldsymbol{x}^T}{dR_1}.\boldsymbol{H}.\frac{d\boldsymbol{x}}{dR_1} \tag{1.45}$$

When $\boldsymbol{x}$ is a scalar, the latter expression directly rewrites as eq. (1.13), which concludes the proof.

The second result presented in the main text relates the convergence properties of a singular point to the impact ray envelope. Let us introduce the Jacobian of the fitness gradient $\boldsymbol{J}$:

$$\boldsymbol{J}(\boldsymbol{x}) = \frac{\partial}{\partial \boldsymbol{x}}\left[\frac{\partial}{\partial \boldsymbol{x}^T} w(\boldsymbol{R}(\boldsymbol{y}), \boldsymbol{x})\right]_{y=x} \tag{1.46}$$

$$\equiv \left(\partial_{\boldsymbol{x}} + \partial_{\boldsymbol{x}}\boldsymbol{R}^T.\partial_{\boldsymbol{R}}\right)\partial^T_{\boldsymbol{x}} w \tag{1.47}$$

We thus have:

$$\boldsymbol{J}(\boldsymbol{x}) = \boldsymbol{H}(\boldsymbol{x}) + \partial_{\boldsymbol{x}}\boldsymbol{R}^T.\partial_{\boldsymbol{R}}\partial^T_{\boldsymbol{x}} w \tag{1.48}$$

It is very important to understand that the dependency of $\boldsymbol{R}$ in $\boldsymbol{x}$ depicted by the term $\partial_{\boldsymbol{x}}\boldsymbol{R}^T$ comes from solving completely the ecological system by combining ZNGI and impact ray equations (1.35,1.38) for $\boldsymbol{S}$ fixed. This has to be done for any strategy, singular or not. Note that this object is not directly related to the expression $d\boldsymbol{x}/dR_1$ manipulated above, which tracks how a singular strategy varies along the envelope. Differentiating $w(\boldsymbol{R}, \boldsymbol{x}) = 0$ and $v(\boldsymbol{S}, \boldsymbol{R}, \boldsymbol{x}) = 0$ with

respect to $\boldsymbol{x}$ and evaluating it at a singular point gives the following relationships:

$$\partial_{\boldsymbol{x}} R_1 = -\partial_{\boldsymbol{x}} v \Big/ \left(\partial_{R_1} v + \frac{\partial R_2}{\partial R_1} \partial_{R_2} v \right) \tag{1.49}$$

$$\partial_{\boldsymbol{x}} R_2 = \frac{\partial R_2}{\partial R_1} \partial_{\boldsymbol{x}} R_1 \tag{1.50}$$

Let us first use eq. (1.50) only to rewrite:

$$\boldsymbol{J} - \boldsymbol{H} = \partial_{\boldsymbol{x}} R_1 \left(\partial_{R_1} \partial_{\boldsymbol{x}}^T w + \frac{\partial R_2}{\partial R_1} \partial_{R_2} \partial_{\boldsymbol{x}}^T w \right) \tag{1.51}$$

after multiplying eq. (1.51) on the right by $d\boldsymbol{x}/dR_1$, the RHS reads as the transpose of the LHS of eq. (1.44). When also multiplied by $d\boldsymbol{x}^T/dR_1$ on the left, it leads to:

$$\frac{d\boldsymbol{x}^T}{dR_1} \boldsymbol{J} \frac{d\boldsymbol{x}}{dR_1} = \left(1 - \frac{d\boldsymbol{x}^T}{dR_1} . \partial_{\boldsymbol{x}} R_1 \right) \frac{d\boldsymbol{x}^T}{dR_1} \boldsymbol{H} \frac{d\boldsymbol{x}}{dR_1} \tag{1.52}$$

Finally, coming back to the expression of $\partial_{\boldsymbol{x}} R_1$ given by eq. (1.50):

$$1 - \frac{d\boldsymbol{x}^T}{dR_1} . \partial_{\boldsymbol{x}} R_1 = \left(\partial_{R_1} v + \frac{\partial R_2}{\partial R_1} \partial_{R_2} v + \frac{d\boldsymbol{x}^T}{dR_1} . \partial_{\boldsymbol{x}} v \right) \Big/ \left(\partial_{R_1} v + \frac{\partial R_2}{\partial R_1} \partial_{R_2} v \right) \tag{1.53}$$

$$\equiv \left. \frac{dv}{dR_1} \right|_{\mathrm{E}} \Big/ \left. \frac{dv}{dR_1} \right|_{\mathrm{Z}} \tag{1.54}$$

Now, there is a last step to make the link with the supply point map. Differentiating (1.38) once with respect to S_1, along a ZNGI and the envelope respectively leads to:

$$\left. \frac{\partial R_1}{\partial S_1} \right|_{\mathrm{Z}} = -\tilde{I}_2 \Big/ \left. \frac{dv}{dR_1} \right|_{\mathrm{Z}} \tag{1.55}$$

$$\left. \frac{\partial R_1}{\partial S_1} \right|_{\mathrm{E}} = -\tilde{I}_2 \Big/ \left. \frac{dv}{dR_1} \right|_{\mathrm{E}} \tag{1.56}$$

Putting the pieces together, we finally get the result:

$$\left. \frac{\partial R_1}{\partial s_1} \right|_{\mathrm{E}} \frac{d\boldsymbol{x}^T}{dR_1} \boldsymbol{J} \frac{d\boldsymbol{x}}{dR_1} = \left. \frac{\partial R_1}{\partial s_1} \right|_{\mathrm{Z}} \frac{d\boldsymbol{x}^T}{dR_1} \boldsymbol{H} \frac{d\boldsymbol{x}}{dR_1} \tag{1.57}$$

When $\boldsymbol{x}$ is a scalar and $dx/dR_1 \neq 0$, the latter expression directly rewrites as eq. (1.15), which concludes the proof.

Using the ecological stability criteria (1.32) obtained in the previous section for a single-population, we have:

$$\left. \frac{\partial R_1}{\partial s_1} \right|_{\mathrm{Z}} = -\beta \tilde{I}_2 \frac{\partial w}{\partial R_2} \tag{1.58}$$

where β is a positive function when the ecological equilibrium is stable and the two other terms of the RHS are related to the relationship between the population and the regulating factor R_2. For the usual consumer-resource and predator-prey interactions, this thus leads to $\partial R_1/\partial s_1 > 0$.

Note that the two main relationships obtained here in the case of a general k-dimensional trait $\boldsymbol{x}$ only give information on the Hessian and Jacobian of the eco-evolutionary system along the envelope, i.e. the direction $d\boldsymbol{x}/dR_1$. In the one dimensional case, this is not a problem as soon as this direction exists (is non-zero): it leads to a squared term with thus no effect of its sign for the first result or can be simplified in the second result. For dimensions greater than one, this projection leads to insufficient information on the multiple eigenvalues of both the Hessian and Jacobian matrices, not allowing to conclude on the ESS and convergent properties of the singular points based only on the relative position between the ZNGI and its envelope. Also note that contrary to the one dimensional case, eco-evolutionary stability in the k-dimensional case may also depend on the specific shape of the mutation process (Leimar, 2009).

1.C.2 Dimorphic singular point

When there are two coexisting singular populations in the system with traits $\boldsymbol{x_1} \neq \boldsymbol{x_2}$, the eco-evolutionary invasion analysis reads:

$$w(\boldsymbol{R}, \boldsymbol{x_i}) = 0 \tag{1.59}$$

$$\partial_{\boldsymbol{x}} w(\boldsymbol{R}, \boldsymbol{x_i}) = \boldsymbol{0} \tag{1.60}$$

with $i = 1, 2$. As in the ecological case, this is enough to fully determine the regulating factors at the eco-evolutionary equilibrium, thus the supply point map is not needed here. According to the adaptive dynamics picture, the eco-evolutionary properties of this singular coalition directly emerges from those of its constituents. Thus, we still have:

$$\frac{\partial w}{\partial R_2}\left(\left.\frac{\partial^2 R_2}{\partial R_1^2}\right|_{\mathrm{E}} - \left.\frac{\partial^2 R_2}{\partial R_1^2}\right|_{\mathrm{Z}}\right) = \frac{d\boldsymbol{x_i}^T}{dR_1}.\boldsymbol{H}.\frac{d\boldsymbol{x_i}}{dR_1} \tag{1.61}$$

and thus this coalition is evolutionarily stable if and only if both coexisting strategies satisfy the geometrical condition relatively to their local envelope. The situation is a bit different for the convergence characteristics as $\boldsymbol{R}$ is obtained without the supply point map (and is thus independent of it) in the dimorphic case. Differentiating $w(\boldsymbol{R}, \boldsymbol{x_1}) = 0$ and $w(\boldsymbol{R}, \boldsymbol{x_2}) = 0$ with respect to $\boldsymbol{x_i}$ and evaluating it at the singular point where $R_2 = g(\boldsymbol{x_1}, \boldsymbol{x_2})$ gives the trivial result:

$$\partial_{\boldsymbol{x_i}} R_1 = \partial_{\boldsymbol{x_i}} R_2 = \boldsymbol{0} \tag{1.62}$$

Thus, the regulating factors at equilibrium around a singular coalition are linearly independent from the traits of this coalition. As a result, $\boldsymbol{J} = \boldsymbol{H}$ for each of the two coexisting strategies, so the convergence properties are automatically linked to the invasion one. This means that ESS coalitions are automatically CSS ones and further branching is excluded. This result obtained here in the case of a satured dimorphism (two populations on two regulating factors) strongly echoes to the situation of a single population evolving on a single resource, and can be generalized to any number of regulating factors (Kisdi and Geritz, 2016).

Connecting statement

In Chapter 1, we laid down a general graphical framework for contemporary niche theory and extended it to eco-evolutionary dynamics and community assembly. We showed how such a framework allows one study the adaptive strategy turnover along environmental gradients and its consequences on ecosystem functioning. We will now apply in Chapter 2 this framework to study the evolution of plant strategies along a nutrient gradient in the face of resource limitation and grazing by herbivore. Such a simple food web module encapsulates the functioning of more complex ecosystems, as resources and herbivores are the two most commonly encountered factors limiting plant growth. In this context, we answer the two coupled questions: how does the environmental feedback loop influence patterns of plant adaptive defense along the resource gradient ? How does plant adaptation influence trophic cascading in a three-level food chain along the resource gradient?

Chapter 2

Plant strategies along nutrient gradients

Contents

Abstract

Plants present a variety of defensive strategies against herbivores, broadly classified into tolerance and resistance. Resource availability being another limitation to plant growth, we expect plant allocation between resource acquisition and defense to vary along resource gradients. Yet, the physiological and environmental conditions under which defensive strategy is favored over the other are unclear. Here, we investigate plant adaptive allocation between resource acquisition, tolerance and resistance along a resource gradient in a simple food web module where plants compete for a single nutrient and are grazed upon by a shared herbivore. We implement plant evolution using a recently developed eco-evolutionary graphical tool merging contemporary niche theory with adaptive dynamics. We find that increased nutrient supply could lead to either tolerant or resistant strategies, which potentially coexist, but also intermediate allocation between the two. Whether returns on defense allocations were diminishing or accelerating is central to distinguishing between these different scenarios. We also explore the consequences of this adaptive allocation on species biomasses and trophic transfers. In comparison to previous models of plant allocation strategies along resource gradients, we highlight the role played by the density-dependent environmental feedback loop. As such, this is the first theoretical model to study the joint evolution of plant resistance and tolerance along a resource gradient within a simple food web using an allocation trade-off between three quantitative traits.

2.1 Introduction

Herbivory is a major selective pressure for plants, with dramatic consequences on their growth, survival and reproduction. In response, plants have developed two broad classes of defensive strategies throughout their evolutionary history: resistance and tolerance. Resistance comes from adaptations that reduce the amount of herbivore damage experienced by a plant. Tolerance does not reduce herbivore damage, but mitigates its impact on plant fitness through compensatory growth (Tiffin 2000; Stowe 2013). While dealing with herbivory, plants must also acquire resources such as light, water and nutrients. As availabilities of these resources vary along environmental gradients, they are expected to influence plant defense allocation patterns (Coley et al. 1985; Wise and Abrahamson 2007; Endara and Coley 2011; Hahn and Maron 2016). In this context, a major question is what determines the optimal allocation between resource acquisition, tolerance and resistance.

A diversity of hypotheses and models have been proposed to address the question of plant defense evolution (Stamp 2003). Early theoretical approaches consisted in growth optimization under given, fixed herbivore densities (Coley et al. 1985; Simms and Rausher 1987). However, some evolutionary biologists insisted on the dynamical nature of herbivore population feeding on these defended plants leading to frequency-dependence (Dieckmann and Metz 2006) and its consequences on defense evolution (Augner et al. 1991; Tiffin 2000). By explicitly including resource and herbivore dynamics, food chain and food web approaches are naturally suited for these questions along environmental gradients (Armstrong 1979; Leibold 1996; Loreau and de Mazancourt 1999; Chase et al. 2000). Combined with game theoretical thinking (see McNickle and Dybzinski 2013; Brown 2016 for recent reviews), these models have given rise to eco-evolutionary approaches that have been used over the last decades to investigate plant adaptation and community assembly under joint resource competition and herbivore selection pressure (de Mazancourt et al. 2001; Abrams and Chen 2002; Abrams 2003; Jones and Ellner 2004; Loeuille and Loreau 2004; Våge et al. 2014; Zu et al. 2015).

Yet, all these models to date have concentrated on a one-dimensional problem, the trade-off between resource acquisition and grazer resistance. Empirical evidence suggests that in some scenarios, undefended species can survive under intense herbivory and high resource levels (Moen et al. 1993; Agrawal 1998; Oksanen and Oksanen 2000). How to explain this? To study the evolution of tolerance, it is more realistic to also take into account a third function, intrinsic growth rate. This leads to a 'CRT triangle', a three-way allocation problem between resource affinity (Competition), grazing susceptibility (Resistance) and maximal growth rate (Tolerance). Such three-way allocation models have been influential in ecology (Grime 1974, 1977) and are characterized by an overarching three-way trade-off, which can blur two-way trade-offs when the third covariate is not controlled for (van Noordwijk and de Jong 1986; Mole 1994). There is empirical evidence for such trade-offs (Fineblum and Rausher 1995; Yoshida et al. 2004; Edwards et al. 2011), even though there could also be emergent trade-offs stemming from variation of a

single trait such as stoichiometry or cell size (Litchman et al. 2009; Branco et al. 2010).

In this chapter, we investigate plant adaptive allocation between competitive ability, tolerance and resistance along a resource gradient, using a recently developed extension of the graphical approach from contemporary niche theory (Tilman 1982; Leibold 1996) to eco-evolutionary dynamics and community assembly using geometrical envelopes (Koffel et al. 2016). After describing the ecological model, the plant strategy space and the evolutionary approaches, we answer the following questions: at the functional trait level, which environmental conditions select for tolerance, resistance or both? At the community level, when is evolutionarily stable coexistence of a tolerant and a resistant species favored over a single intermediate one? At the ecosystem level, what are the consequences in terms of transfer efficiency, plant and herbivore biomass of these different scenarios? Finally, what role does the environmental feedback loop, which accounts for density- and frequency-dependence, play in these predictions?

2.2 Ecological analysis

2.2.1 Mathematical model

Let us first introduce the ecological model describing the dynamics of the ecosystem in the absence of evolution. This three-level 'diamond food web' is a classic model of theoretical ecology (e.g. Holt et al. 1994; Leibold 1996; Grover and Holt 1998). It represents a community of n different plant species, whose population densities are denoted P_i ($i = 1, ..., n$), consuming a limiting resource with concentration R and themselves consumed by a single herbivore species with density Z (Fig. 2.1). The dynamics of the food web satisfies the following ordinary differential equations:

$$\frac{dZ}{dt} = I_Z - m_Z Z + \sum_{i=1}^{n} e_i a_i P_i Z \tag{2.1a}$$

$$\frac{dP_i}{dt} = [g_i(R) - a_i Z - m_i] P_i \qquad \forall i = 1, ..., n \tag{2.1b}$$

$$\frac{dR}{dt} = I_R - l_R R - \sum_{i=1}^{n} q_i g_i(R) P_i. \tag{2.1c}$$

All the state variables and parameters, as well as their numerical values and units are summarized in Table 2.1. The abiotic resource is supplied at an input rate I_R and lost at a per capita rate l_R as in a chemostat. Herbivores immigrate into the system at a rate I_Z and die at a per capita rate m_Z. Plants interact with their environment via two distinct trophic transfers. First, plants from species i acquire resource at per capita growth rate $g_i(R)$. Second, plants i are consumed by herbivores through a mass-action law with attack rate a_i. To facilitate the formulation of our evolutionary model later, we can parameterize a_i in terms of resistance, ρ_i, as $a_i = a_0(1 - \rho_i)$, where a_0 is the basal attack rate on an undefended plant. Both trophic transfers

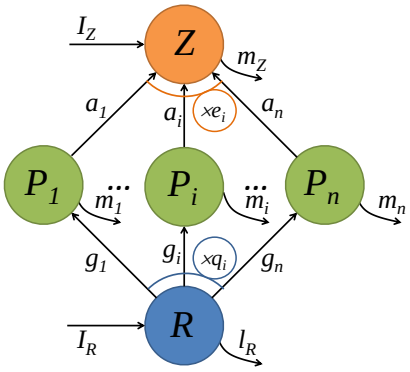

Figure 2.1: Schematic representation of the model, where the shaded boxes represent the state variables of the system and the arrows the fluxes of matter. R represents the abiotic resource, the P_i the different plant species and Z the herbivore. The P_i grow on R at a per capita rate $g_i(R)$, the coefficient q_i converting the biomass gain of plant i in term of nutrient uptake, and die at a constant per capita mortality rate m_i. Similarly, Z grows on each P_i at a per capita rate $a_i P_i$, the coefficient e_i encoding the efficiency of the biomass conversion. Z is subject to constant rates of immigration I_Z and per capita mortality m_Z while R experiences constant rates of external input I_R and per capita losses l_R.

are characterized by constant conversion coefficients, respectively the stoichiometric ratio of the plant q_i and the efficiency of herbivore assimilation e_i. Finally, plants i experience constant, non-grazer-induced mortality at per capita rate m_i.

In contrast to previous models that used type-I functional responses, our model requires a type-II functional response of plants on resources to distinguish between competitive and tolerant strategies:

$$g_i(R) = \frac{\mu_i \alpha_i R}{\mu_i + \alpha_i R} \tag{2.2}$$

When the resource is scarce, the growth rate given by eq. (2.2) is proportional to resource availability R through the resource affinity α_i (resource^{-1}.time^{-1}; Fig. 2.2). Conversely, abundant resources lead to saturation of the functional response towards its maximal value μ_i (time^{-1}). Introducing handling times $h_i = \mu_i^{-1}$ makes the formal link with Holling's (1959) formulations, while $K_i = \mu_i/\alpha_i$ makes the link with Monod's (1950), two standard formulations of the type-II functional response. We chose our formulation because it decouples acquisition and biosynthesis mechanistically, thus facilitating their trade-off in the allocation approach of the 'Eco-evolutionary analysis' section. Note that both α_i and μ_i contribute to growth, with their relative importance driven by resource availability R.

Our analysis of this ecological model will focus on identifying its equilibria and their local

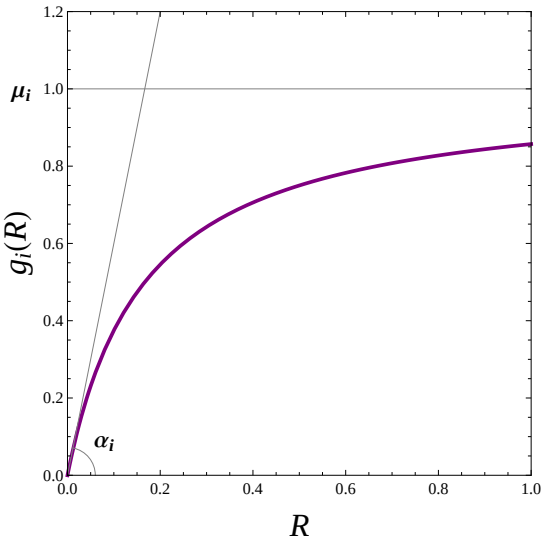

Figure 2.2: Type-II functional response, or Michaelis-Menten kinetics, used to model plant i resource uptake g_i as a function of available resource concentration R. When resource is limiting ($R \ll \mu_i/\alpha_i$), plant uptake is directly proportional to R via the affinity α_i. When resource is not limiting ($R \gg \mu_i/\alpha_i$), plant uptake is no longer controlled by resource availability R and saturates to the plant maximal growth rate μ_i. In this example, $\alpha_i = 6$ and $\mu_i = 1$.

stability along a resource gradient. The particular structure of eq. (2.1) where the per capita growth rates of plants i depend only on two regulating factors, namely the resource concentration R and predator density Z, simplifies its analysis due to the Competitive Exclusion Principle (CEP; Levin 1970; Meszéna et al. 2006). In our model, the CEP implies that no more than two different plant species can stably coexist at equilibrium without parameter fine-tuning. This restricts the analysis to three different cases: absence of plants, one plant species only or two coexisting ones. The details of the calculations can be found in Appendix A.

2.2.2 One species: the graphical ingredients

Following Leibold's (1996) approach, the results of the ecological analysis can be derived and represented graphically as a function of the 'environmental' supplies, namely resource supply and herbivore immigration (Tilman 1980, 1982; Chase and Leibold 2003). This method consists of two steps — invasion analysis and supply point mapping — and is based on three ingredients — Zero Net Growth Isoclines (ZNGIs), impact vectors and supply points.

The invasion analysis separates the environmental (R-Z) plane into regions where plant i can grow from the regions where it cannot (Fig. 2.3A). The boundary between these two regions is obtained where net growth, the right-hand side of eq. (2.1b), equals zero, imposing a necessary link between R and Z when plant i persists at equilibrium. The resulting ZNGI is represented in

Table 2.1: Model notation

Symbol	Meaning	Value used	Units
State variables:			
R	Nutrient concentration		μmol L^{-1}
P_i	Plant species i density		plants L^{-1}
Z	Herbivore density		animals L^{-1}
Parameters:			
g_i	Plant i gross growth rate		day^{-1}
m	Plant death rate	0.07	day^{-1}
a_0	Herbivore basal attack rate on plant	0.1	day^{-1} L animals^{-1}
α_i	Plant i resource affinity	$0-100$	day^{-1} L μmol^{-1}
μ_i	Plant i maximal growth rate	$0-2$	day^{-1}
ρ_i	Plant i degree of resistance	$0-1$	–
$a_i = a_0(1-\rho_i)$	Herbivore attack rate on plant i	$0-0.1$	day^{-1} L animals^{-1}
e	Plant-herbivore conversion efficiency	5.7×10^{-7}	animal plant^{-1}
q	Plant-nutrient conversion efficiency	9.1×10^{-9}	μmol plant^{-1}
m_Z	Herbivore death rate	0.215	day^{-1}
I_Z	Herbivore immigration rate	variable	animals day^{-1}
I_R	Nutrient supply rate	variable	μmol day^{-1}
l_R	Chemostat dilution rate	0.05	day^{-1}
Trade-off:	$(i = \alpha, \mu, d)$		
X_i	Trait i allocation	$0-1$	–
$X_{\rho,\max}$	Necessary ρ allocation for total resistance	0.95	–
ϵ_i	Trait i shape-parameter	variable	–
f_{ϵ_i}	Trait i allocation function	variable	–

Definitions, numerical values and units of the state variables and parameters of the model. The model was parametrized using Grover's (1995) data on a nitrogen-phytoplankton-*Daphnia* food chain in a chemostat.

Fig. 2.3, with positive net growth under the ZNGI and negative above it. Contrary to a type-I functional response (obtained from a type-II by taking μ_i infinite), a typical ZNGI in our model is not linear, but concave (contrast with Leibold 1996; Chase et al. 2000). The ZNGI crosses the R-axis at $R_i^* = 1/\alpha_i \cdot \mu_i m_i/(\mu_i - m_i)$, the minimal resource level species i can tolerate in the absence of herbivore before getting extinct. According to Tilman's R^* theory, this measures this species competitive ability at low resource levels (the smaller the better). Similarly, the ZNGI asymptotically saturates on the Z-axis at $Z_i^* = 1/a_0 \cdot (\mu_i - m_i)/(1-\rho_i)$ for high R values, the maximal predator density a population can tolerate when resources are not limiting (Fig 2.3). This Z^* plays a symmetrical role relative to R^*, as emphasized in the apparent competition framework (Holt 1977; Holt et al. 1994): the most (apparent-)competitive species under high R values is the one with the largest Z^*. The analytical expression of Z_i^* shows that there are two ways to deal with grazers: either with high ρ_i (resistant strategies) or high μ_i (tolerant strategies). Note that a completely resistant strategy with $\rho_i = 1$ has an infinite Z^*, leading to a straight, vertical ZNGI.

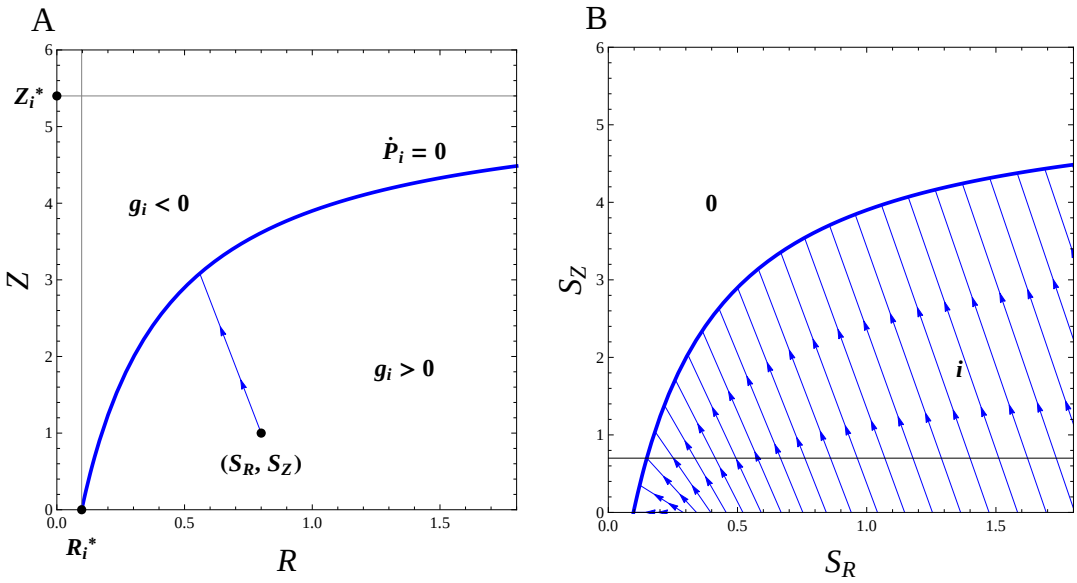

Figure 2.3: A: Illustrative ZNGI (blue, thick), impact vector (blue, thin) and supply point (black dot) for a plant species i. The ZNGI resembles the uptake function $g_i(R)$ of Fig. 2.2, except that it starts on the x-axis at R_i^* and saturates at Z_i^* (gray lines). The impact vector maps this particular supply point to the corresponding equilibrium point on the ZNGI. B: Bifurcation diagram representing the ecological outcome of this plant species i growing on the resource R and being preyed upon by Z, as a function of the external supply (S_R, S_Z). The conditions are too harsh in zone 0 for the plant to survive (above ZNGI_i) whereas they are good enough to enable plant growth in zone i. Note that the plant can never grow when $S_R < R_i^*$ or when $S_Z > Z_i^*$. The impact rays (blue, dashed) map the supply points onto their corresponding limiting factor values (R, Z) at equilibrium, on ZNGI_i. In this example, $\alpha_i = 1$, $\mu_i = 0.25$ and $a_i = 0.033$, the other parameters being from Table 2.1.

The supply point map is obtained by combining impact vectors with supply points. The impact vector of plant i represents how the biomass P_i affects both the resource level and the herbivore density in the system, which corresponds to the factors in front of the P_i terms in eq. (2.1a,2.1c) (Leibold 1996). The supply point (S_R, S_Z) corresponds to the resource and herbivore densities at equilibrium in the absence of plants, given respectively by $S_R = I_R/l_R$ and $S_Z = I_Z/m_Z$. Being proportional to incoming fluxes, the supply point coordinates can easily be tuned in a chemostat. How does the supply point map work in practice? For environmental conditions corresponding to a given supply point, the impact vectors maps this supply point to the corresponding limiting factors values at equilibrium on the ZNGI (Fig 2.3A). Not surprisingly, the presence of a plant decreases resource levels by consuming it and increases herbivore abundance by feeding them. Another way to synthesize these results consists in drawing the ZNGI and the impact vectors directly in the supply point plane. This leads to a bifurcation diagram, as the region spanned by the impact vectors corresponds to conditions leading to plant i's

presence while the other region above the ZNGI corresponds to plant i's absence, noted region 0 (Fig 2.3B).

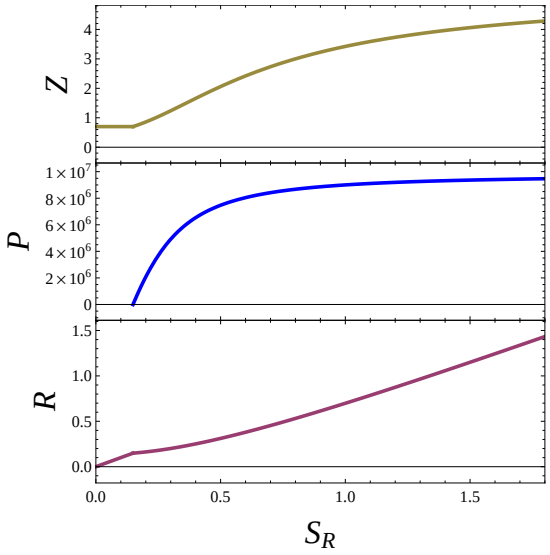

Figure 2.4: Equilibrium nutrient (R), plant (P) and grazer (Z) densities along resource supply gradient (S_R) in the single-species ecological model. The gradient corresponds to a cross-section of the ecological bifurcation diagram (Black line in Fig 2.3B) with increasing nutrient supply and fixed but non-zero grazer supply. The three densities strictly increase along the gradient, with both P and Z saturating at high nutrient supply while R reaches a linear increasing trend. Note that we assume immigration of grazers here, so that they can persist even in the absence of plants.

It is also insightful to represent how resource level, and plant and herbivore densities vary along a resource supply gradient (Fig. 2.4). Several differences with the classic food web patterns (Oksanen et al. 1981; Mittelbach et al. 1988; Leibold 1996) can be identified. If we assume a non-zero herbivore immigration rate, herbivores are always present in the system and their response to plant invasion is not delayed. Moreover, having a saturating plant growth rate μ, combined with top-down control by the herbivores, implies the saturation of both plant and herbivore densities as the resource supply increases. Thus, only the nutrient pool is left to absorb this excess supply. In any case, it is important to note that increasing the nutrient supply indirectly benefits the grazers through trophic transfers from the plant population. This leads the plant to switch from bottom-up to top-down control as nutrient availability increases, explaining why defense is so crucial for the plant at high resource levels, and thus strongly influencing plant defense patterns as we will see later in the 'Eco-evolutionary analysis' section.

2.2.3 Two species competition

The previously described graphical approach is especially useful when two or more different plant species are considered. A multi-species invasion analysis can be performed by superimposing their corresponding ZNGIs: in the two-species case, only the ZNGI portions of species i that are located above the other species' ZNGI correspond to uninvasible species i single species equilibria, the other portion being discarded (Fig. 2.5A). Coexistence only occurs where two ZNGIs intersect. This happens here when there is a trade-off in competitive ability between the two species, with one species being more competitive in the absence of herbivores, i.e. with a smaller R_i^*, and the other one being more apparent-competitive when resources are non-limiting, i.e. with a larger Z_i^*. This trade-off between resource- and apparent-competitive abilities can emerge from an allocation model between plant traits as will be seen in the 'Eco-evolutionary analysis' section. When ZNGIs stable portions are coupled to impact vectors, this leads to multi-species bifurcation diagram. The regions spanned by the impact vectors of species 1 or 2 respectively correspond to species 1 or 2 only (green and blue, Fig. 2.5A), while the cone originating from the ZNGI intersection and delimited by impacts vectors 1 and 2 corresponds to the coexistence region 1&2 (gray, Fig. 2.5A). How equilibrium resource level, plant and herbivore densities vary along the resource gradient can again be represented (Fig. 2.5A), with the major difference with the monospecific case (Fig. 2.4) coming from the coexistence region where R and Z variations are buffered, while P_1 increases and P_2 decreases leading to an overall rapid increase in total plant density.

2.3 Eco-evolutionary analysis

Building on the ecological system of the previous section, we now use a trait-based approach where we consider competition between an arbitrary number of strategies defined by their traits. We focus on finding single strategies or pairs of strategies that render the community uninvasible when they are at their ecological equilibrium. These are called global evolutionarily stable strategies and coalitions (global ESSs and ESCs) respectively. There are at least three possible interpretations of this approach (Abrams 2001; Bonachela et al. 2016): 1) asexual evolution by mutations of arbitrary size (Adaptive Dynamics, but without the assumption of small mutations); 2) coevolution of a number of species that follow quantitative genetics; and 3) community assembly from a large range of extant species in the metacommunity. In all cases, a global ESS or ESC represents an endpoint of evolution or community assembly.

2.3.1 Trait space and trade-off shapes

We focus our attention on the three traits associated with fundamental aspects of the plant's interaction with its environment: the ability to grow when resource is scarce (resource affinity α) or when it is non-limiting (maximal growth rate μ), and the ability to resist herbivory (ρ).

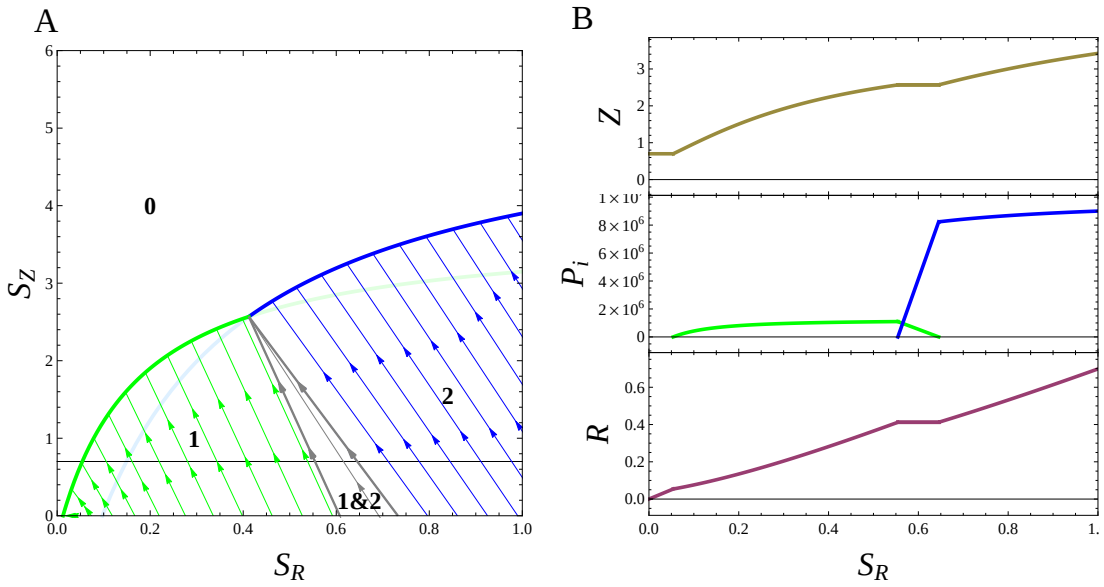

Figure 2.5: A: Bifurcation diagram of two plant species 1 (green, $\alpha_i = 6$, $\mu_i = 1$, $a_i = 0.25$) and 2 (blue, $\alpha_i = 1$, $\mu_i = 0.25$, $a_i = 0.033$) competing for the resource R and sharing the herbivore Z, along resource and herbivore supply gradients. Species 1 and 2 differ in their relative competitive abilities for R and Z. Region 1, spanned by species 1 impact vectors (green) corresponds to species 1 only, while region 2 corresponds to species 2 only (blue). In region 1&2 (grey), the two plant species coexist. Neither of the two species can persist in region 0. B: Equilibrium nutrient (R), plants (P_i) and grazer (Z) densities along the resource gradient (S_R) in the two species model (compare with Fig. 2.3B). When species 1 and 2 coexist, they hold R and Z constant, and species 1 density P_1 increases while species 2 density P_2 decreases along the gradient.

These traits define a three-dimensional strategy space where every point represents a possible allocation strategy (Fig 2.6). Due to the potential complexity of parameterizing a three-way trade-off, we assume an allocation constraint and then specify cost-benefit functions linking each trait to the resources allocated to it. Because every organism faces constraints of finite energy, matter and time, the combinations of plant trait allocation are restricted by a trade-off through the following inequality:

$$X_\rho + X_\alpha + X_\mu \leq 1 \tag{2.3}$$

where the X_i are the allocations to the corresponding trait values $i = \{\alpha, \mu, \rho\}$. Eq. (2.3) ensures that the sum of the three allocations never exceeds the total allocation resources available, chosen to be equal to 1 in the appropriate units. We assume that the trait value $i = 0$ is obtained when $X_i = 0$ and the derivatives of the costs X_i all satisfy $X_i' \geq 0$ as all these three traits positively influence the net growth rate. The maximal possible trait value $i_{\max}$ is obtained when the maximal allocation to that function $X_{i,\max}$ is reached. Contrary to allocation to α and μ for

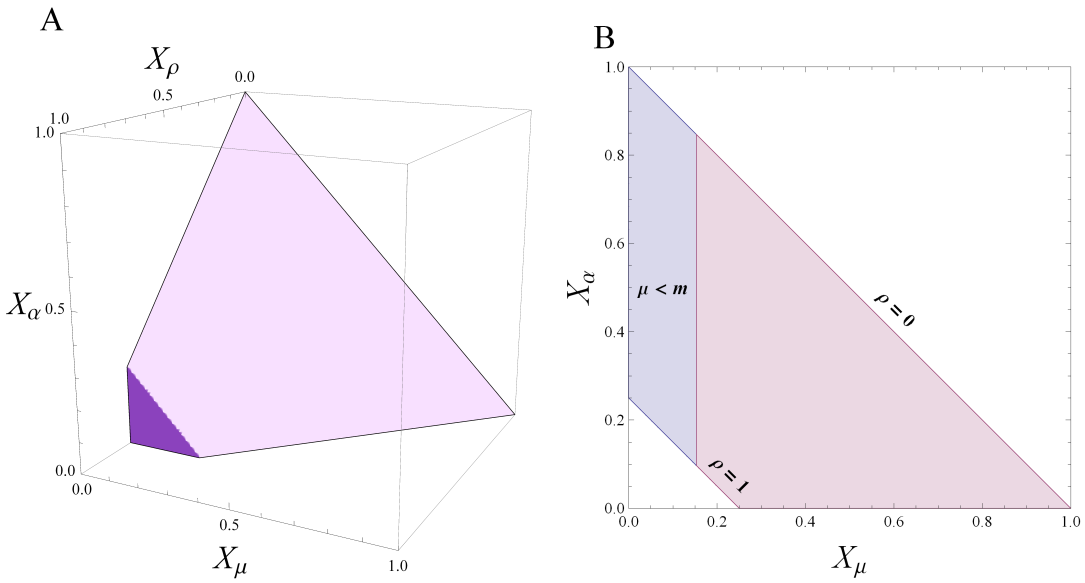

Figure 2.6: Visualization of the trade-off and possible allocation patterns in the allocation space. A) The possible allocations are contained inside a tetrahedron because allocations cannot be negative and their sum cannot exceed one. The truncated corner expresses the fact that total resistance is achieved by the allocation $X_{\rho,\max} < 1$, making further investment in X_d meaningless. B) 2D projection in the (X_μ, X_α) plane of the trapezoid-shaped admissible allocation space. The strategies in the blue region aree discarded as non-viable, because their maximal growth rate does not exceed their mortality rate.

which we allow full allocation, i.e. $X_{\alpha,\max} = 1$ and $X_{\mu,\max} = 1$, we cap the maximal allocation to ρ at a value $X_{\rho,\max} < 1$, sufficient to attain perfect resistance ($\rho_{\max} = 1$). This ensures that a completely inedible strategy still has resources left to allocate to resource uptake and growth. In practice, we took the allocation sum equal to one, as underallocation is strictly dominated. As a result, the trait space dimension can be decreased to 2, which facilitates its visualization (Fig. 2.6B).

There are endless possibilities to relate the allocation costs X_i to their traits i. This must be done carefully, as it is known that trade-off shapes can strongly affect eco-evolutionary results (de Mazancourt and Dieckmann 2004; Kisdi 2015). To facilitate the study of the problem, we chose to introduce the following particular class of allocation functions, for $i = \{\alpha, \mu, \rho\}$:

$$\frac{i}{i_{\max}} = f_{\epsilon_i}\left(\frac{X_i}{X_{i,\max}}\right) \tag{2.4}$$

where we used the one-parameter function f:

$$f_{\epsilon_i}(X_i) = \frac{X_i}{\epsilon_i - (\epsilon_i - 1)X_i} \tag{2.5}$$

This class of functions is fairly flexible, as the parameter ϵ_i enables to control the shape of

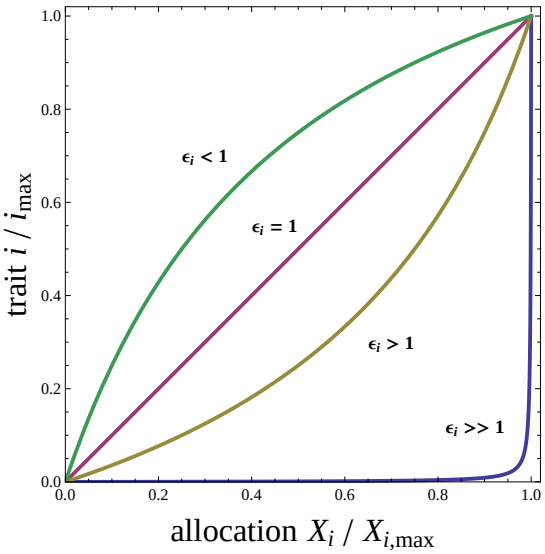

Figure 2.7: Visualization of the flexible allocation function f, linking a given trait allocation level X_i to the obtained trait i value, for various shape-parameters ϵ_i. This relationship is linear when $\epsilon_i = 1$ (purple), concave when $\epsilon_i < 1$ (green) and convex when $\epsilon_i > 1$ (yellow). When ϵ_i is close to 0 or ∞, f tends toward a step function with an abrupt corner (blue).

the allocation function from linear ($\epsilon_i = 1$) to concave ($\epsilon_i < 1$) and convex ($\epsilon_i > 1$) allocation, corresponding to respectively linear, diminishing or accelerating returns (Fig 2.7). This flexibility allows one to span various physiologically-relevant situations. Another convenient feature of these cost functions is that they possess symmetrical, finite derivative at 0 and 1, respectively equal to $1/\epsilon_i$ and ϵ_i. Contrary to a power law function, this avoids singular behaviors at 0, which can lead to strong, pathological consequences on the eco-evolutionary results. Note that accelerating returns on several traits tends to favor all-or-nothing allocations, i.e. specialists, while diminishing returns tend to favor intermediate allocations and thus generalists (Levins 1962). This can be seen in the limiting cases of ϵ_i tending toward plus or minus infinity. Then, the cost function tends towards a step function representing respectively an 'all or nothing' allocation type ($\epsilon_i \to \infty$) or a practically free trait ($\epsilon_i \to 0$).

Following the example of diffusion limitation's effect on affinity (Pasciak and Gavis 1974; Armstrong 2008; Bonachela et al. 2011), we assume that allocations to resource affinity and maximal growth rate satisfy linear or diminishing returns ($\epsilon_\alpha \leq 1$, $\epsilon_\mu \leq 1$). Depending on the details of the plant-herbivore interaction, defensive benefits could however show either diminishing or accelerating returns on investment, as supported by empirical studies (Wetzel et al. 2016), so we consider both $\epsilon_\rho \leq 1$ and $\epsilon_\rho > 1$. Quantitative defenses should show linear or diminishing returns ($\epsilon_\rho \leq 1$), while qualitative defenses should show accelerating returns ($\epsilon_\rho > 1$; Feeny 1976; Stamp 2003).

2.3.2 Adaptive dynamics techniques

Having defined the space of possible plant strategies, we can now couple it with the ecological model (2.1) to investigate how competition leads to the eco-evolutionary response of plant communities along resource gradients. To do so, we define plant fitness following the adaptive dynamics framework (Hofbauer and Sigmund 1990; Dieckmann and Law 1996; Geritz et al. 1997, 1998; Champagnat et al. 2006), the invasion fitness w of an invading strategy with traits $\boldsymbol{x} = (\alpha, \mu, \rho)$ in an environment $\boldsymbol{E} = (R, Z)$ given by:

$$w(\boldsymbol{x}, \boldsymbol{E}) = \frac{1}{P}\frac{dP}{dt} = \frac{\mu\alpha R}{\mu + \alpha R} - a_0(1-\rho)Z - m \tag{2.6}$$

where the environment $\boldsymbol{E}$ is fully determined by the ecological equilibrium of the resident strategy. This feedback loop between the evolving population and its environment leads to density- and frequency-dependent selection, characteristic of game theoretic approaches. Introducing the fitness gradient

$$\boldsymbol{s}(\boldsymbol{x}) = \frac{\partial w}{\partial \boldsymbol{x'}}[\boldsymbol{x'}, \boldsymbol{E}(\boldsymbol{x})]\Big|_{\boldsymbol{x'}=\boldsymbol{x}} \tag{2.7}$$

the evolutionary equilibria, or evolutionarily singular strategies, $\boldsymbol{x}^*$, are obtained by solving $\boldsymbol{s}(\boldsymbol{x}) = \boldsymbol{0}$. Their stability is assessed locally by second order derivatives of the invasion fitness w and globally by evaluation of w across the trait space (Geritz et al. 1998). Among these evolutionary equilibria, Evolutionarily Stable Strategies (ESS) are of particular interest as they correspond to strategies that cannot be invaded by any other one. When they are dynamically convergent, they correspond to the eco-evolutionary endpoints of the system and are called Convergence Stable Strategies (CSS). Note that two coexisting strategies can also be an ESS, which we will refer to an 'Evolutionarily Stable Coalition' (ESC).

In contrast with the standard approaches to adaptive dynamics, we will focus on the global evolutionary stability of these equilibria. Doing so implicitly assumes that all the strategies from the trait space are potential invaders, following a 'everything is everywhere' (Baas Becking 1934; De Wit and Bouvier 2006) picture instead of a small mutations framework. This global framework leads to two formally similar interpretations of the best adapted strategies emerging with our approach: they can be seen as resulting from community assembly, that is, species sorting among a dense regional species pool, or the outcome of evolution by natural selection through mutations of arbitrary magnitude, or the combination of both. This differs from the usual adaptive dynamics approach because we ignore branching point and local but not global ESS and ESC, as these kinds of singular points are invasible by some strategy from the trait space.

2.3.3 Envelope theory

Because we consider three traits linked by a trade-off, our trait space is two-dimensional, so Pairwise Invasibility Plots, the standard graphical approach to find and characterize evolutionary equilibria cannot be used. To overcome this limitation, we used a recently developed extension to eco-evolutionary situations of the graphical approach to competition presented in the 'Ecological analysis' section (Koffel et al. 2016).

This graphical approach works in three steps, mimicking its ecological version. First, a local invasion analysis selects from the whole strategy space the subset of strategies that could potentially be locally singular in the adaptive dynamics sense. Secondly, the resulting envelope in the limiting-factor space enables us to perform a global invasion analysis, discarding the singular points that are not global ESS or ESC. Two-species coexistence appears as a 'kink' in the envelope. Finally, the supply point map uses the impact vectors to associate to each of these strategies the supply points that would lead to it at the eco-evolutionary equilibrium. When inverted, this enables us to plot the ecological (resource levels, plant and herbivore densities) and evolutionary (trait) characteristics of the system along the resource gradient. Tracking the global ESS as a function of environmental parameters can be interpreted as a 'quasistatic process' of species sorting or evolution along a slowly increasing nutrient supply.

2.4 Results

2.4.1 Analytical results on partial two-way trade-offs

Before directly addressing the three-way allocation problem presented in the 'Trade-off shapes' subsection, it is insightful to restrict the analysis to the three partial situations obtained when only two traits can vary, holding the last trait fixed. These three cases can be analyzed for completely general trade-offs, without any supplementary specification on the generic cost functions X_i. In each case, we analytically tracked optimal traits and consequent densities when a single CSS was present along a resource gradient (See Appendix B for the details of the calculations). We did not investigate the conditions that make evolutionarily stable coexistence possible, but when it happens, R, Z and the traits of the ESC remain constant along the resource gradient, as is expected for two evolving populations interacting two limiting factors (Kisdi and Geritz 2016; Koffel et al. 2016). The densities of the ESC vary in a similar fashion to the ecological case, i.e. linearly with one density usually going down and the other one going up. The results for a single CSS are synthesized in Table 2.2.

Our results when μ is fixed can be seen as a generalization of Loeuille and Loreau's (2004) type-I functional response results to the type-II case, i.e. finite μ. Several preliminary conclusions can be drawn from these results. First, concerning densities, both R and Z always increase with the increasing resource supply, thus not differing qualitatively from the purely ecological case. This is a direct consequence of the ecological structure of the food web, i.e. trophic transfers

Table 2.2: Results on partial two-way trade-offs

Case	α	μ	ρ	R	P	Z	Condition
α fixed	0	$-$	$+$	$+$	$+$	$+$	potentially not when S_R large
		$+$	$-$	$+$	$-,+$	$+$	potentially when S_R large
μ fixed	$-$	0	$+$	$+$	$+$	$+$	
ρ fixed	$-$	$+$	0	$+$	$+$	$+$	

Effect of an increase in nutrient supply S_R on plant CSS traits (α, μ and ρ) and equilibrium ecosystem densities (R, P and Z), for each of the three traits kept fixed.

along the food chain coupled with top-down and bottom-up controls of the plant population. This means that the selective pressure coming from herbivore consumption systematically increases along the resource gradient, in stark contrast with non-trophic approaches where herbivore densities are assumed to stay fixed (Coley et al. 1985). Second, concerning traits, α always decreases with resource supply when it is not fixed, confirming that this trait's contribution to fitness automatically decreases as resource availability increases. Conversely, both μ and ρ, i.e. tolerance and resistance, can help the plant cope with increasing herbivore pressure, as shown in the 'Ecological analyses' section. For this reason, μ increases along the gradient when ρ is fixed and ρ increases along the gradient when μ is fixed, coinciding with increasing plant biomass P in both cases. Finally, when α is fixed, these two defense options trade off, their variations thus being mutually exclusive. Resistance, with increasing ρ, is then always the first adaptive response of the plant for low but increasing resource availability. This trend is then either sustained along the gradient, or reversed towards tolerance with increasing μ when tolerance costs are small enough. Interestingly, the latter situation can lead to decreasing plant biomass P, an intuitive population level side-effect of the evolution of tolerance.

2.4.2 Three-way trade-off

With the results of the previous section in mind, we can now explore the full three-way trade-off. As we already emphasized in the 'Trade-off shapes' section, there are various biologically relevant shape parameters ϵ_i to be explored. These exponents deeply affect the eco-evolutionary outcomes of the system along the resource supply gradient. Evolutionarily stable coexistence or not, the presence of an inedible strategy, the evolution of tolerance or resistance under high nutrient supply: all these outcomes depend on the trade-off shape parameters. Examples from closely related models can be found in the literature (Abrams 2003; Jones and Ellner 2004; Zu et al. 2015). Before giving an overview of those outcomes in subsection 'Overview of cases', we first present in detail three particular cases that have been selected for their ecological relevance as well as their representativeness of the model outcomes. Scenarios 1 and 2 investigate the effects of respectively accelerating and diminishing returns on resistance allocation, respectively, coupled with linear returns on the two other traits. Scenario 3 shows how a combination of accelerating

and diminishing returns can lead to a nonmonotonic allocation pattern in resistance along the resource supply gradient.

2.4.3 Scenario 1: Qualitative defenses – accelerating returns on resistance

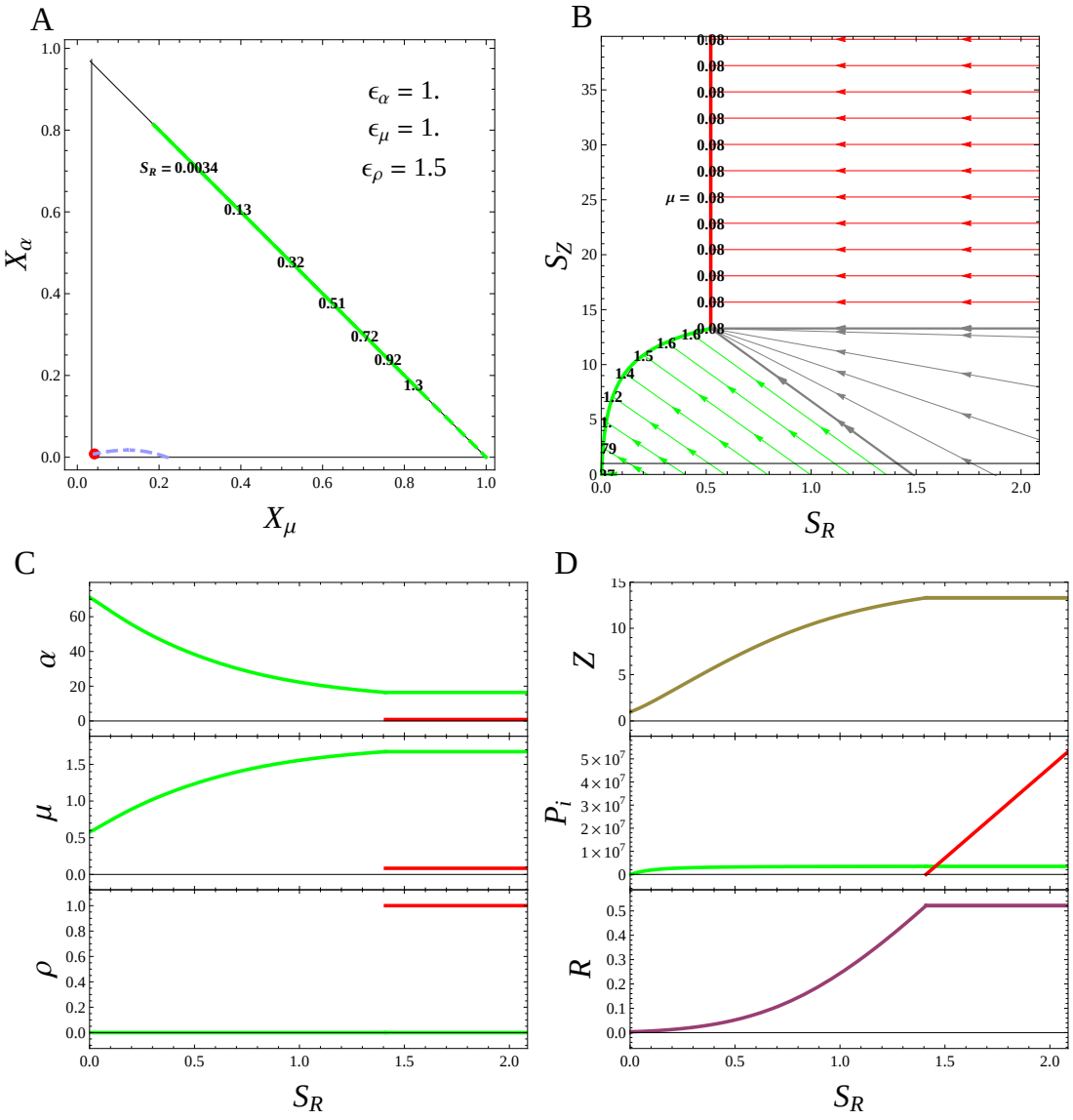

Figure 2.8: Scenario 1: Eco-evolutionary results under accelerating returns on allocation to resistance ($\epsilon_\rho > 1$) and linear returns on allocation to affinity and maximal growth rate ($\epsilon_\alpha = \epsilon_\mu = 1$). A) Adaptive trajectory in the allocation space (X_μ, X_α) along increasing nutrient supply S_R. B) Bifurcation diagram along the supply gradients. C) ESS traits as functions of nutrient supply S_R. A completely non-resistant strategy (green) coexists with the inedible one (red) for high supplies. D) Corresponding ecosystem properties. Parameters from Table 2.1.

This first typical situation arises when there are accelerating returns on resistance allocation ($\epsilon_\rho > 1$, $\epsilon_\alpha = 1$ and $\epsilon_\mu = 1$). This is believed to happen when an herbivore is rather specialized on

the plant and its defense compounds, insensitive to low toxin levels but still affected by high ones (Ali and Agrawal 2012). The succession of ESS traits along the resource gradient is displayed in Fig. 2.8A,C. It starts at very low resource levels with the strategy with the minimal R^*, refered to as R^*-specialist or gleaner (Grover 1997), completely non-resistant ($\rho = 0$) with high allocation in affinity α (green top left corner, Fig. 2.8A; Fig. 2.8B). Then, increasing the nutrient supply leads to reallocation from affinity to maximal growth rate and thus faster growth, though still non-resistant (green line along the triangle edge, Fig. 2.8A; Fig. 2.8B). As a consequence, the herbivore abundance increases, releasing the top-down control of the plant on the resource and thus allowing the resource levels to increase too (Fig. 2.8D). At one point, the resource level in the system is high enough for a completely inedible strategy with $\rho = 1$ to invade (red dot and lines, Fig. 2.8) and coexist with the fast grower it just invaded (green dot, Fig. 2.8A). This particular inedible strategy is the one with the lowest R^* among all inedible strategies, as it excludes all the others. As nutrient supply increases further, these two strategies remain constant and continue to coexist, fixing resource levels and herbivore abundances at a constant level (the 'kink' in Fig. 2.8B) . The population size of the fast growing species also stays constant, whereas the completely inedible population continues to increase as it absorbs all the exceeding resource supply. No intermediately defended strategy appears in this case, being less competitive that the completely defended and undefended ones: accelerating returns in resistance favors plant strategic specialization, which in turn favors coexistence.

2.4.4 Scenario 2: Quantitative defenses – diminishing returns on resistance

This second situation arises when there are diminishing returns on resistance allocation ($\epsilon_\rho < 1$, $\epsilon_\alpha = 1$ and $\epsilon_\mu = 1$) The absence of accelerating returns favors generalist plant strategies, and thus evolutionarily stable coexistence never occurs along the resource supply gradient. We again track the ESS along the resource gradient S_R. Starting with an R^* specialist, increasing nutrient supply again leads to reallocation to maximal growth rate while staying non-resistant (green line along the triangle edge, Fig. 2.9). This happens up to a point where allocation to resistance becomes adaptive. This correlates with a decrease in growth allocation, which leads to a hump shaped maximal growth rate allocation for intermediary supply (Fig. 2.9C). Finally, allocation to resistance keeps increasing while never reaching complete inedibility, even for highly eutrophic conditions. This happens because a completely inedible plant would drive herbivores to very low densities, undermining the competitive advantage brought by resistance. In an ecosystem perspective, evolution towards resistance translates into saturating resource and herbivore densities with increasing plant biomass. As a whole, this situation largely echoes the previous one, the main difference being that coexistence between two specialized strategies is replaced by dominance by a unique generalist.

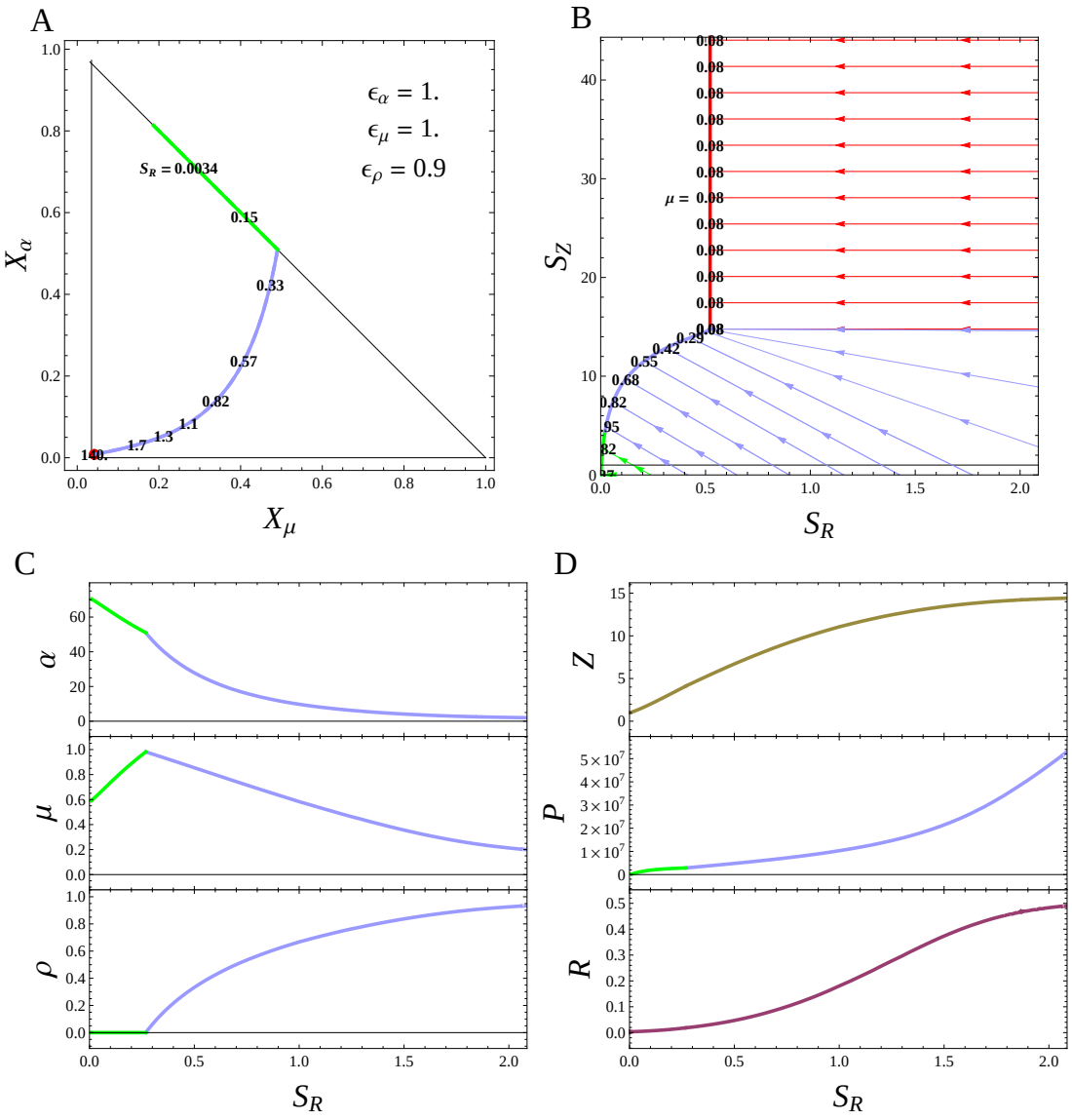

Figure 2.9: Scenario 2: Eco-evolutionary results under diminishing returns on allocation to resistance ($\epsilon_\rho < 1$) and linear returns on allocation to affinity and maximal growth rate ($\epsilon_\alpha = \epsilon_\mu = 1$). A) Adaptive trajectory in the allocation space (X_μ, X_α) along increasing nutrient supply S_R. B) Bifurcation diagram along the supply gradients. C) ESS traits as functions of nutrient supply S_R. D) Corresponding ecosystem properties. Parameters from Table 2.1.

2.4.5 Scenario 3

This third situation occurs for example with diminishing returns on α, linear returns on μ and accelerating returns on ρ ($\epsilon_\alpha < 1$, $\epsilon_\mu = 1$ and $\epsilon_\rho > 1$). The ESS succession along the resource gradient is, again, at first similar to scenario 2: reallocation from R^* specialist to faster grower, then allocation to resistance. However, this allocation to resistance does not tend toward complete inedibility at high supply. Instead, it reaches a maximum for a given supply

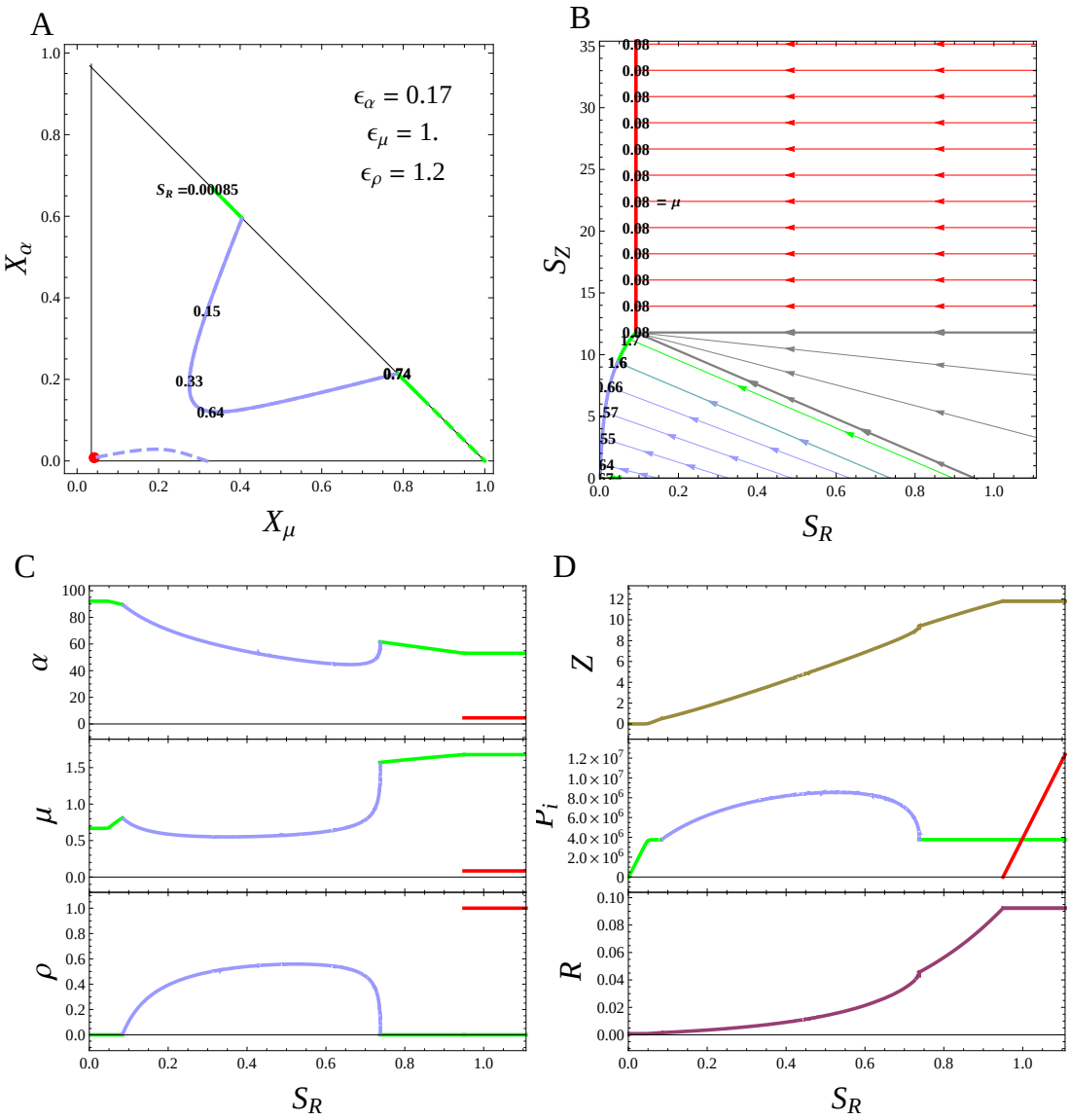

Figure 2.10: Scenario 3: Eco-evolutionary results under diminishing, linear and accelerating returns on allocation to affinity, maximal growth rate and resistance respectively ($\epsilon_\alpha < 1$, $\epsilon_\mu = 1$ and $\epsilon_\rho > 1$). A) Adaptive trajectory in the allocation space (X_μ, X_α) along increasing nutrient supply S_R. B) Bifurcation diagram along the supply gradients. C) ESS traits as functions of nutrient supply S_R. D) Corresponding ecosystem properties. Parameters from Table 2.1.

and decreases again toward a completely un-resistant strategy. This deallocation to resistance leads to reallocation to both affinity and maximal growth rate. This hump-shaped resistance allocation pattern along the resource gradient translates into plant biomass being also hump-shaped (Fig. 2.10D). Then, the inedible strategy invades at one point and brings us back to the same evolutionarily stable coexistence pattern described in Scenario 1. The hump-shape of plant density P is reminiscent of one of the tolerance scenarios in the 'Preliminary results on two-way trade-offs' subsection.

2.4.6 Overview of cases

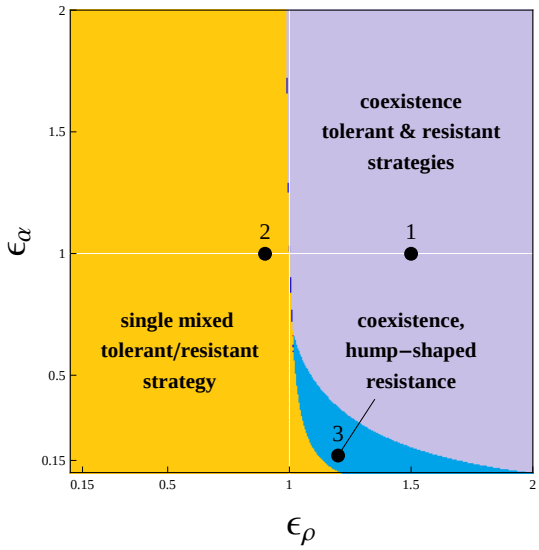

Figure 2.11: Overview of scenarios 1 (mauve), 2 (yellow) and 3 (blue) in the ϵ_ρ-ϵ_α shape parameter plane.

In the previous subsections, we presented different possible adaptive successions patterns along a resource gradient (Fig. 2.8–2.10). Those situations differed by their allocation shape-parameters ϵ_α, ϵ_μ and ϵ_ρ. We assessed the generality of these three patterns by exploring numerically this 3-parameter space and classifying the resulting global envelopes. The results in the ϵ_α and ϵ_ρ plane with $\epsilon_\mu = 1$ are represented in Fig. 2.11 (see Supplemental Fig. 2.16 for more). We see that scenarios 1 and 2 are separated by a decreasing curve going through the point $(\epsilon_\alpha, \epsilon_\rho) = (1, 1)$, with scenario 3 squeezed between them in the bottom-right quadrant. The fact that this boundary goes through $(1, 1)$ means that the scenario with linear returns on allocation on the three traits is mathematically degenerate, as any slight curvature of an allocation function would have sharp consequences by tipping the situation into scenario 1 or 2. This underscores the role played by the shape parameters, a posteriori justifying their introduction. Moreover, the bottom-left corner (diminishing returns on both α and ρ) corresponds to scenario 2 with only a single generalist strategy, while the top-right corner (accelerating returns on both α and ρ) correspond to scenario 1 with evolutionarily stable coexistence of two specialists. The top-left quadrant, even though dominated by scenario 2, can also lead to scenario 3 when ϵ_ρ is close to 1. All three scenarios are possible in the bottom-right quadrant.

In the three scenarios described here, very high resource supplies always lead to the emergence of one very resistant, if not completely inedible, strategy. However, this is not always the case within our model (Appendix E). This happens when ϵ_μ is large enough so that major allocation to μ is needed for a strategy just to be able to grow ($\mu > m$). In this case, there is sometimes not enough allocation left to reach full inedibility. Three new scenarios, $1'$, $2'$ and $3'$ emerge, replacing scenarios 1, 2 and 3 respectively (See Appendix D). In scenario $1'$, no resistant strategy

gets in under high supply, so the tolerant, non-resistant strategy keeps allocating to maximal growth rate. In scenario $2'$, there is also a single tolerant strategy dominating high supplies, while medium supplies show the characteristic hump-shaped allocation to resistance of scenario 2. Finally, scenario $3'$ consists of allocation to resistance under high supply, but this is coupled with a persisting finite allocation to tolerance, so that the asymptotic strategy is truly a mixed resistant/tolerant strategy.

2.5 Comparison with growth rate optimization approach

To compare our results with previous models of plant adaptation to grazing pressure (e.g. Coley et al. 1985), it is instructive to compare the results obtained with our adaptive dynamics approach to the ones that would be given by a fitness optimization procedure without any feedback on resource and herbivore densities. This can be done in our model (2.1) by isolating plant eq. (2.1b) and considering R and Z as external parameters. Doing so, we neglect the ecological feedback of the evolving population on its environment. The optimal strategy for given environmental conditions is then the strategy with the highest per capita growth rate $dP/(Pdt)$.

2.5.1 General results on two-way trade-offs

As in the adaptive dynamics section, it is insightful to first study the three partial problems with one of the traits held constant. Again, these results were obtained without specifying the exact shape of the trade-off functions. See Appendix C for the details of the calculations. The results are synthesized in Table 2.3. Note that coexistence cannot occur in the optimization case, as having two strategies with the exact same growth rate is infinitely unlikely in the absence of any environmental feedback.

Table 2.3: Results on partial two-way trade-offs without feedback loop

Case	α	μ	ρ	Condition
α fixed	0	+	-	
μ fixed	+	0	-	if $\alpha < \frac{\mu}{S_R}$
	-	0	+	if $\alpha > \frac{\mu}{S_R}$
ρ fixed	-	+	0	

Effect of an increase in nutrient supply S_R on plant optimal traits (α, μ and ρ), for each of the three traits kept fixed. Compare with Table 2.2.

It is striking to see the difference with the adaptive dynamics approach (Table 2.2). In the optimization approach, μ appears to be systematically favored with increasing nutrient supply, against both α and ρ. Indeed, in absence of environmental feedback, herbivore pressure does not increase along the resource gradient and resource availability is not made scarcer by consumption, so that the relative importance of herbivory compared to growth potential sharply decreases with

increasing resource availability. When μ is fixed, allocation to α is only favored when the resource is limiting and thus shifts to ρ under high nutrient supplies.

2.5.2 Optimization approach under Scenario 2

The contrasting outcomes of the optimization approach can be further studied using the full three-way allocation problem. Using the exact same parameters as in Scenario 2, with the supplies S_R and S_Z directly playing the roles of R and Z in eq. (2.1b), we assessed strategies maximizing plant growth rate. Note that in absence of trophic transfers, herbivore immigration ($S_Z \neq 0$) is necessary for the herbivore population to be non-zero. The resulting optimal strategy against increasing nutrient supply S_R and constant non-zero herbivore immigration is shown in Fig. 2.12. The main difference when compared to the adaptive dynamics results of Fig. 2.9 is that the optimal strategy consists of a completely non-resistant strategy, with increasing allocation to tolerance along increasing resource supply.

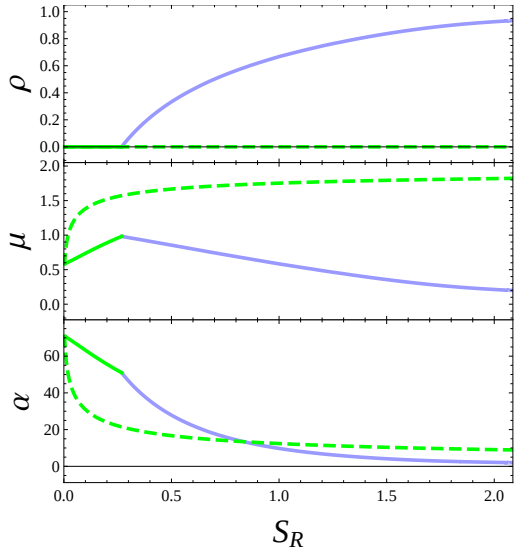

Figure 2.12: Comparison of the adaptive trajectories along the resource gradient between the adaptive dynamics (plain) and optimization (dashed) approaches for scenario 2 (parameters similar to Fig. 2.9). Contrary to the adaptive dynamics case, the plant never allocates to resistance but instead allocates sharply and mostly to tolerance. As the resource is not depleted, allocation to acquisition starts with a steeper decrease.

2.6 Discussion

We studied the adaptive response of plants facing selective pressures from both resource competition and herbivores along a resource gradient. We showed that undefended, competition-specialist strategies are expected to dominate under oligotrophic conditions. Conversely, eu-

trophic conditions, which lead to high herbivore abundance because of trophic transfers, result in the dominance of either a very resistant strategy or evolutionarily stable coexistence between a completely inedible strategy and a fast-growing, tolerant one. Diminishing returns on allocations favor the first scenario, with an intermediate strategy while accelerating returns favors the second one, with coexistence of two extreme strategies. Finally, we compared this food-web, density- and frequency-dependent approach to a more traditional, density-independent optimization approach. We showed that density and frequency-dependence originating from trophic transfers were the cause of this increase in resistance along the resource gradient, as the frequency-independent model rather favored tolerant, fast growing strategies over resistant ones.

2.6.1 Variation in plant defense along the resource gradient

By including three possible strategic archetypes — competitors that specialize in resource acquisition, fast-growing tolerant species and grazing resistance species — our model enabled a realistic exploration of possible plant adaptation to the joint selective pressure of resource acquisition and herbivore grazing. We obtained adaptive trajectories in the strategy space along the resource gradient for various allocation shape-parameters. At low resource levels, the best adapted strategies are always of the competitive type, i.e. low-R^* specialists, as they are the only strategies that can survive in those very nutrient-limited conditions, even if they are very sensitive to herbivory. As these competitor strategies typically subsist at very low densities, this ensures that herbivore populations and thus their damages are low in the absence of immigration. On the contrary, both maximal growth rate and resistance are adaptive under high nutrient supply because high nutrient supply leads to significant herbivore densities and therefore grazing pressure (Armstrong 1979; Leibold 1996; Grover and Holt 1998). However, very resistant strategies, when viable, need either to coexist with a tolerant species or to be slightly edible so that herbivores remain present to maintain their selective advantage (Tiffin 2000). This explains why the fully inedible strategy is never present alone unless there is significant herbivore immigration. Another interesting consequence of working with three traits is that μ and ρ need not be automatically anti-correlated, allowing mixed ESS that are both tolerant and resistant, with their relative weights strongly depending on both the allocation parameters and the nutrient supply. The existence of these mixed defense strategies has been observed empirically (Mauricio et al. 1997; Carmona and Fornoni 2013; Turley et al. 2013).

Strikingly, our results contrast with Coley's Resource Gradient Hypothesis, which used a density-independent optimization model to predict that plant resistance investments should be favored under low resource availability (Coley et al. 1985). We suspect the feedback loop between the plant population and its environment plays a central role in this discrepancy (McNickle and Dybzinski 2013), as underlined by our comparison between the adaptive dynamics and the optimization approaches. Indeed, the results from our optimization approach without feedback are consistent with these early optimization models (Coley et al. 1985). As was already pointed

out by Loreau and de Mazancourt (1999), taking into account the effect of plant growth on the resource availability within a dynamical plant-resource model affected Coley et al.'s (1985) evolutionary predictions and led Loreau and de Mazancourt (1999) to conclude in their fixed herbivore density case that nutrient enrichment does not influence plant strategies. Our approach follows this logic one step further by also including a dynamical herbivore population. In fact, our predictions — selection of defended strategies under high-resource environments — are consistent with previous ecological (Leibold 1996; Chase et al. 2000) or eco-evolutionary approaches (Loeuille and Loreau 2004; Zu et al. 2015), as well as a recent review on intraspecific variation in plant defense (Hahn and Maron 2016). Our study gives a quantitative demonstration of Hahn and Maron's (2016) intuition that the emergence of more defended strategies with increasing resource availability stems from increased herbivore pressure.

Nonetheless, not every plant population so directly controls the population growth of the herbivores that feed on it. We expect the strength of this environmental feedback loop to depend on both plant and herbivore relevant spatial and temporal scales. Among others, plant growth rate, spatial structure and population size, as well as herbivore body size, generation time, dispersal and mobility affect the coupling between plant and herbivore population dynamics and thus the evolution of plant defense (Duffy and Hay 1994; Augner 1995; Underwood 1999; Tiffin et al. 2006). Within the model, this decoupling between plant and herbivore dynamics can be simulated by changing the balance between herbivore immigration and growth through decreased transfer efficiency e. Interestingly, this leads to a decrease in defense allocation for a given resource supply, but does not alter the qualitative allocation patterns along the gradient.

Our model probably overestimates the importance of allocation to resistance by ignoring seasonality, an important driver of plant and herbivore growth in both terrestrial and aquatic ecosystems (Klausmeier and Litchman 2012). During early growth following the start of the good season, the solutions from the density-independent optimization model, i.e. fast growing tolerant strategies, are selected. Including seasonality could thus reconcile the Resource Gradient Hypothesis with our adaptive dynamics approach by creating a balance between early and late season selective forces. This could select for strategies with intermediate characteristics or lead to diversification of seasonal specialists (Kremer and Klausmeier 2013; Miller et al. 2016).

2.6.2 Diversification and coexistence

Our model makes clear the conditions under which diversification of the plant strategies dealing with both resource and herbivore selective pressure is possible. First, the shape of the allocation functions played a crucial role. Accelerating returns on at least one trait appeared to be necessary for evolutionarily stable coexistence to occur, consistent with classical results (Levins 1968). This also supports a recent study on diversification of an intermediate trophic level (Zu et al. 2015), after noting that accelerating returns on resistance ρ is in their model equivalent to diminishing returns on susceptibility $1 - \rho$. The cases of evolutionarily stable coexistence obtained here also

suggest that, when coexistence happens, one of the two coexisting strategies is always completely inedible ($\rho = 1$; but see Appendix for a few exceptions), while the other one is more tolerant. Finally, coexistence only happens under high resource supply, which ensures that both resource availability and herbivore pressure are high enough for both strategies to be advantaged. All in all, our study shines a light on the conditions for initial diversification of nutrient-phytoplankton-zooplankton (NPZ) models (Armstrong 1994; Sauterey et al. 2015) and food web emergence.

Note that contrary to previous models (Chase et al. 2000), priority effects, i.e. dependency of the equilibrium strategy on the timing of arrival, between the tolerant and resistant strategies do not occur here. The reason is that the completely inedible strategy always dominates at high nutrient supply coupled with a horizontal impact vector because it does not feed the herbivore. This prevents the two impact vectors from crossing in the opposite configuration, which is needed to switch from coexistence to priority effects (Tilman 1982; Leibold 1996; Chase and Leibold 2003). However, evolutionary priority effects are still possible between two mixed, partially resistant strategies along the decreasing branch of the hump-shaped investment in resistance of Scenario 3 (not shown here).

2.6.3 Eco-evolutionary response of stocks to nutrient enrichment

Describing plant growth using a type-II functional response allowed some generalizations and refinements compared to previous studies (Oksanen et al. 1981; Leibold 1996; Loeuille and Loreau 2004). First, we mathematically demonstrated in the three two-way trade-off cases that R and Z could only positively respond (or neutrally) to nutrient enrichment in the adaptive case. This seems to hold true in the full three-way case based on our numerical explorations, thus generalizing the previous results. Furthermore, plant biomass P also seems to generally increase along an increasing resource gradient, when ρ is fixed or increasing. However, we found some situations under both two-way and three-way trade-offs where P could, at least under intermediate nutrient supplies, respond negatively to enrichment, which contrasts with previous studies (Leibold 1996; Loeuille and Loreau 2004). This corresponds to a situation in which it is more adaptive for the plant to decrease allocation to resistance and reallocate to maximal growth rate. These shifts from resistance to tolerance, by incurring a sudden increase of attack rate by the herbivore, can negate the positive effect of nutrient increase and thus lead to an overall decrease in plant density along increasing supply (Fig 2.10C). When evolutionarily stable coexistence occurs, R and Z are fixed at the coexistence point, consistent with previous studies (Leibold 1996), while total plant density always responds positively. This is not surprising as the coexistence patterns always involve a density switch from a tolerant to a inedible strategy along increasing supply.

Finally, note that the three scenarios we described all lead to a trophic dead-end within the ecosystem for high nutrient supplies, with saturating nutrient and herbivore densities and increasing inedible plant biomass. This can be related to cyanobacteria blooms, as some species

are believed to be completely inedible by zooplankton, with significant environmental consequences (Lampert 1987; Wilson et al. 2006; but see Perga et al. 2013). However, when total resistance is out of reach, the asymptotic strategies are either completely edible or only partially defended (see scenarios $1'$, $2'$ and $3'$ in Appendix E). In these cases, trophic transfers from plants to herbivores never stop, leading to linear increase in R and saturating P and Z, similarly to the purely ecological case.

To conclude, R, P and Z all respond positively to nutrient enrichment, except when a decrease in resistance allocation occurs leading to P going down for intermediate supplies. On the trade-off parameters bifurcation diagram, this decreasing P situation occurs in scenarios 2 and $2'$ regions.

2.6.4 Generality of the approach

Even though our model necessarily omits many of the details of plant interactions with herbivores, it provides the first theoretical study that considers the joint evolution of plant resistance and tolerance within a simple food web module using an allocation trade-off between three quantitative traits, paving the way towards the study of the evolution of plant defense in more complex ecological situations.

As mentioned earlier, the inclusion of seasonality or environmental fluctuations could alter our results by favoring selection on maximal growth rate. Seasonality could also delay herbivore growth and lead to the succession of more resistant species over the course of a season (Klausmeier and Litchman 2012). Taking into account elemental costs of resistance, generally carbon or nitrogen based (Bryant et al. 1983), and tolerance, demanding in phosphorus-rich ribosomal RNA (Elser 2006), could lead to a more mechanistic implementation of the trade-off linking plant traits. In turn, such a stoichiometrically explicit approach (Meunier et al. 2017), can help addressing large-scale biogeochemical patterns such as Redfield ratios (Redfield 1958; Klausmeier et al. 2004; McGroddy et al. 2004) by predicting plant stoichiometric ratio along a resource gradient (Branco et al. 2010). While we voluntarily used a broad definition of 'plants' throughout this chapter, our model is better suited to phytoplankton communities for which individual growth and population growth coincide. Terrestrial plants, as exemplified by trees, have more complex ontogenies, leading to more complex patterns of tolerance and resistance in the course of their developmental trajectories, or between individual growth and fecundity (Boege et al. 2011). Terrestrial plants also present differentiated organs — roots, stems and leaves — that can be selectively targeted by herbivores (Rasmann and Agrawal 2008), and the combination of size and spatial structure leads to more complex mechanisms of competition, especially for light (Weiner 1990; Dybzinski et al. 2011).

Our results depend on having an herbivore on top of the food chain, inducing a top-down control on the plant population. The addition of a carnivore feeding on the herbivore would drastically change our predictions. Because of top-down control by the carnivore, herbivore

density would not increase with increasing nutrient. This means that the best adapted plant strategy would be the one with the smallest R^*, where mortality includes losses by this constant herbivore pressure, thus not depending on nutrient supply at all, similarly to Loreau and de Mazancourt's (1999) results. This reasoning could be extended to more complex food webs where the responses of the different compartments along a resource gradient have been identified (Wollrab et al. 2012). Another limitation of our approach is that only plants evolve. A variety of different scenarios are possible when accounting for herbivore evolution, as was for example shown by Loeuille and Loreau (2004).

In our model, we have restricted plant resistance to the direct effect on the herbivore attack rate, e.g. through deterring effects or gut passage survival. However, resistance could also affect other herbivore parameters like decreasing conversion efficiency e and increasing herbivore mortality m_Z (Grover 1995). Our model ignores these effects, but it is easy to see that they would only affect the plant impact vectors and thus the supply point map. The invasion analysis being completely independent of e and m_Z, the singular points and their ESS properties would stay the same, leaving the general bifurcation diagrams and the trait responses to increased supply unchanged. Similarly, we suspect that taking into account herbivore handling time h through a type-II functional response instead of a type-I would not qualitatively alter our results as long as h is not too large. Indeed, the previous reasoning with e and m_Z would still hold as the fitness of a mutant would not depend on its own handling time h. If the inclusion of h could potentially destabilize the ecological dynamics (Hastings and Powell 1991,Abrams and Roth 1994), we predict that the main effect at equilibrium would be an increase in plant density and a decrease in both herbivore pressure and nutrient availability, as a direct consequence of decreased herbivore efficiency.

Appendices

2.A Analytical study of ecological equilibria and their stability

In this appendix, we choose to use herbivore attack rate $a_i = a_0(1-\rho_i)$ instead of resistance ρ_i — the latter being implicitly included in the former — to simplify both notations and calculations.

2.A.1 The food chain

Let us first compute the analytical expressions of the different equilibria of the system. There are two cases to consider with the R-P_1-Z food chain: equilibrium (0) and equilibrium (1). We use the notation $\hat{R}$, $\hat{P}_1$ and $\hat{Z}$ for equilibrium densities to distinguish them from R_i^* and Z_i^* defined in the main text.

Equilibrium (0): This is the empty system, $\hat{P}_1 = 0$. It follows from eq. (2.1a) and eq. (2.1c) that $\hat{R} = I_R/l_R = S_R$ and $\hat{Z} = I_Z/m_Z = S_Z$.

Equilibrium (1): Here, $\hat{P}_1 \neq 0$ and thus $g_1(\hat{R}) - a_1\hat{Z} - m_1 = 0$ from eq. (2.1b), meaning that the possible values taken by the limiting factors $(\hat{R}, \hat{Z})$ at equilibrium by definition belong to ZNGI_1. Note that to fulfill the ecological condition $\hat{Z} \geq 0$, it is necessary to have $\hat{R} \geq R_1^*$ with $R_1^* = g_1^{-1}(m_1)$. Setting eq. (2.1a) and eq. (2.1c) equal to zero adds a supplementary constraint. Eliminating $\hat{P}_1$ between these two equations leads to:

$$S_Z - \hat{Z} = \gamma_1(\hat{R}, \hat{Z})(S_R - \hat{R}), \tag{2.8}$$

where γ_1 is the relative impact of the plant on the limiting factors:

$$\gamma_1(\hat{R}, \hat{Z}) = -\frac{e_1}{m_Z}\frac{l_R}{q_1}\frac{a_1\hat{Z}}{g_1(\hat{R})}. \tag{2.9}$$

Note that $\gamma_1(\hat{R}, \hat{Z}) \leq 0$. For a given external supply (S_R, S_Z), the intersection of ZNGI_1 and eq. (2.8) gives the values of the limiting factors $(\hat{R}, \hat{Z})$ at equilibrium. There is generally no analytical solution to this, but it can be represented using the graphical approach. After $(\hat{R}, \hat{Z})$ have

been obtained, the corresponding expression of plant 1's density $\hat{P}_1$ is deduced from eq. (2.1a) or eq. (2.1c):

$$\hat{P}_1 = \frac{l_R}{q_1} \frac{S_R - \hat{R}}{g_1(\hat{R})}. \tag{2.10}$$

This solution is only positive when $S_R > \hat{R}$, which also implies $S_Z < \hat{Z}$ because of eq. (2.8). Geometrically, this means that the supply point (S_R, S_Z) has to be located under ZNGI_1 for this equilibrium to be valid. Note that $\hat{Z} = 0$ is a possibility within Equilibrium (1), and is associated with $\hat{R} = R_1^*$ (following ZNGI_1 equation). As can be seen from eq. (2.1a), this is only possible in the absence of herbivore immigration, i.e. $S_Z = 0$. Conversely, this means that any positive immigration rate ($S_Z > 0$) leads to a positive herbivore population ($\hat{Z} > 0$).

To investigate the stability of equilibria (0) and (1), we first compute the general Jacobian matrix of the model:

$$J(R, P_1, Z) = \begin{pmatrix} -m_Z + e_1 a_1 P_1 & e_1 a_1 Z & 0 \\ -a_1 P_1 & g_1(R) - a_1 Z - m_1 & \frac{dg_1}{dR} P_1 \\ 0 & -q_1 g_1(R) & -l_R - q_1 \frac{dg_1}{dR} P_1 \end{pmatrix} \tag{2.11}$$

and then evaluate it at the various equilbria.

Equilibrium (0): The Jacobian matrix can be written:

$$J(S_R, 0, S_Z) = \begin{pmatrix} -m_Z & e_1 a_1 S_z & 0 \\ 0 & g_1(S_R) - a_1 S_Z - m_1 & 0 \\ 0 & -q_1 g_1(S_R) & -l_R \end{pmatrix} \tag{2.12}$$

The latter matrix being triangularisable, the eigenvalues can be read directly from the diagonal. The stability criterion (all the eigenvalues being negative) is then equivalent to:

$$g_1(S_R) - a_1 S_Z - m_1 < 0 \tag{2.13}$$

Recognizing ZNGI_1 equation, this condition can be interpreted geometrically: the trivial equilibrium is stable if and only if the supply point is located above ZNGI_1, so the plant cannot invade the system.

Equilibrium (1): In this case, the Jacobian matrix reads:

$$J(\hat{R},\hat{P}_1,\hat{Z}) = \begin{pmatrix} -m_Z + e_1 a_1 \hat{P}_1 & e_1 a_1 \hat{Z} & 0 \\ -a_1 \hat{P}_1 & 0 & \frac{dg_1}{dR}\hat{P}_1 \\ 0 & -q_1 g_1(\hat{R}) & -l_R - q_1 \frac{dg_1}{dR}\hat{P}_1 \end{pmatrix} \tag{2.14}$$

We consider two cases: no herbivore population ($\hat{Z} = 0$) and with herbivore population ($\hat{Z} > 0$).

No herbivore population. $\hat{Z} = 0$ is a possibility only when there is no herbivore immigration, so $S_Z = 0$. If $\hat{Z} = 0$, it is easy to deduce relationships involving the three eigenvalues λ_1,λ_+, and λ_-:

$$\lambda_1 = -m_Z + e_1 a_1 \hat{P}_1 \tag{2.15}$$

$$\lambda_+ \lambda_- = q_1 g_1(\hat{R}) \frac{dg_1}{dR}\hat{P}_1 \tag{2.16}$$

$$\lambda_+ + \lambda_- = -l_R - q_1 \frac{dg_1}{dR}\hat{P}_1 \tag{2.17}$$

Because the functional response g_1 is monotonically increasing, $dg_1/dR > 0$ and therefore $\lambda_+ < 0$ and $\lambda_- < 0$. The stability criteria reduces to $\lambda_1 < 0$, which reads $\hat{P}_1 < m_Z/e_1 a_1$. Using eq. (2.10) and the fact that $g_1(\hat{R}) = m_1$, this stability criteria can be written:

$$S_R < R_1^* + R_{Z,1}^* \tag{2.18}$$

with $R_{Z,1}^* = m_1 m_Z q_1/(l_R e_1 a_1)$ and remembering $R_1^* = g_1^{-1}(m_1)$.

Herbivore population. If $\hat{Z} > 0$, it follows from eq. (2.1a) that $-m_Z + e_1 a_1 \hat{P}_1$, the first diagonal term of $J(\hat{R},\hat{P}_1,\hat{Z})$, is equal to $-m_Z S_Z/\hat{Z}$ and thus negative. From there, the sign structure of $J(\hat{R},\hat{P}_1,\hat{Z})$ is such that this equilibrium is always stable when it exists (i.e. when the supply point is under the isocline, as shown in the previous section), as can be checked using the Routh–Hurwitz stability criterion.

To conclude, this stability analysis shows that Equilibrium (1) is always stable when valid, except when $\hat{Z} = 0$ (a possible solution when $S_Z = 0$). In this case, resource supply has to satisfy the supplementary condition $S_R < R_1^* + R_{Z,1}^*$. Otherwise, the $\hat{Z} = 0$ solution is destabilized by the existence of another equilibrium with $\hat{Z} > 0$.

2.A.2 The diamond food web

Again, let us first compute the analytical expressions of the different equilibria of the system. There are now four cases to consider with the full diamond food web: equilibrium (0), equilibrium (1), equilibrium (2) and equilibrium (1&2).

Equilibrium (0): now consists of $\hat{P}_1 = \hat{P}_2 = 0$. It follows from eq. (2.1a) and eq. (2.1c) that $\hat{R} = S_R$ and $\hat{Z} = S_Z$.

Equilibrium (1): consists of $\hat{P}_1 \neq 0$ and $\hat{P}_2 = 0$. Similarly to the food chain, $\hat{R}$ and $\hat{Z}$ are obtained by combining ZNGI_1 and the impact ray map, i.e $g_1(\hat{R}) - a_1\hat{Z} - m_1 = 0$ and $S_Z - \hat{Z} = \gamma_1(\hat{R}, \hat{Z})(S_R - \hat{R})$. P_1 is then deduced from eq. (2.1a), and is positive when the supply point (S_R, S_Z) is located under ZNGI_1.

Equilibrium (2): is identical to Equilibrium (1) after swapping indices 1 and 2.

Equilibrium (1&2): consists of $\hat{P}_1 \neq 0$ and $\hat{P}_2 \neq 0$. This means that $g_i(\hat{R}) - a_i\hat{Z} - m_i = 0$ for $i = 1, 2$: $\hat{R}$ and $\hat{Z}$ are located at the intersection of ZNGI_1 and ZNGI_2, giving a necessary condition for this coexistence equilibrium to be valid (in the positive quadrant). The equilibrium values $\hat{P}_1$ and $\hat{P}_2$ are deduced after inversion of the system made of eq. (2.1a) and eq. (2.1c) set equal to zero. Indeed, this system is linear in P_i^* and can be inverted if $\gamma_1(\hat{R}, \hat{Z}) \neq \gamma_2(\hat{R}, \hat{Z})$, i.e. if the impact vectors of the two species at equilibrium are not colinear. The positivity condition $\hat{P}_1 > 0$ and $\hat{P}_2 > 0$ adds a further constraint, that $(S_Z - \hat{Z})/(S_R - \hat{R})$ must be between $\gamma_1(\hat{R}, \hat{Z})$ and $\gamma_2(\hat{R}, \hat{Z})$. As a geometrically interpretation, this means that the supply point has to be located inside the cone made by species 1 and 2 impact rays and passing through the intersection of the two ZNGIs (Leibold 1996).

To investigate the stability of these equilibria, we compute the Jacobian matrix of the model:

$$J(R, Z, P_1, P_2) = \begin{pmatrix} -m_Z + e_1a_1P_1 + e_2a_2P_2 & e_1a_1Z & e_2a_2Z & 0 \\ -a_1P_1 & g_1(R) - a_1Z - m_1 & 0 & \frac{dg_1}{dR}P_1 \\ -a_2P_2 & 0 & g_2(R) - a_2Z - m_2 & \frac{dg_2}{dR}P_2 \\ 0 & -q_1g_1(R) & -q_2g_2(R) & -l_R - q_1\frac{dg_1}{dR}P_1 - q_2\frac{dg_2}{dR}P_2 \end{pmatrix}$$

Equilibrium (0): As for the case of the food chain, $J(S_R, S_Z, 0, 0)$ can be diagonalized leading to the stability criteria:

$$\begin{cases} g_1(S_R) - a_1S_Z - m_1 < 0 \\ g_2(S_R) - a_2S_Z - m_2 < 0 \end{cases} \tag{2.19}$$

This means that equilibrium (0) is stable if and only if the supply point is simultaneously located above ZNGI_1 and ZNGI_2.

Equilibrium (1): In this case, the Jacobian matrix reads:

$$J(\hat{R},\hat{Z},\hat{P}_1,0) = \begin{pmatrix} -m_Z + e_1 a_1 \hat{P}_1 & e_1 a_1 \hat{Z} & e_2 a_2 \hat{Z} & 0 \\ -a_1 \hat{P}_1 & 0 & 0 & \frac{dg_1}{dR}\hat{P}_1 \\ 0 & 0 & g_2(\hat{R}) - a_2\hat{Z} - m_2 & 0 \\ 0 & -q_1 g_1(\hat{R}) & -q_2 g_2(\hat{R}) & -l_R - q_1 \frac{dg_1}{dR}\hat{P}_1 \end{pmatrix}$$

By expanding $\det(J - \lambda I_4)$ along the third row, it is easy to see that the eigenvalues of J are the same as the ones of equilibrium (1) in the food chain case, plus a fourth one equal to $\lambda_4 = g_2(\hat{R}) - a_2\hat{Z} - m_2$, which is the invasion criterion for species 2. Thus, when it exists, equilibrium (1) is stable only if the limiting factor point $(\hat{R},\hat{Z})$ is located above ZNGI_2. If $\hat{Z} \neq 0$, this condition is sufficient. Otherwise it is also necessary to check that $S_R < R_1^* + R_{Z,1}^*$ (see food chain).

Equilibrium (2): By symmetry, the same conclusions hold in this case after swapping indices 1 and 2.

Equilibrium (1&2): Noting from eq. (2.1a) set equal to zero that $-m_Z + e_1 a_1 \hat{P}_1 + e_2 a_2 \hat{P}_2 = -m_Z s_Z/\hat{Z}$, we have:

$$J(\hat{R},\hat{Z},\hat{P}_1,\hat{P}_2) = \begin{pmatrix} -\frac{m_Z s_Z}{\hat{Z}} & e_1 a_1 \hat{Z} & e_2 a_2 \hat{Z} & 0 \\ -a_1\hat{P}_1 & 0 & 0 & \frac{dg_1}{dR}\hat{P}_1 \\ -a_2\hat{P}_2 & 0 & 0 & \frac{dg_2}{dR}\hat{P}_2 \\ 0 & -q_1 g_1(\hat{R}) & -q_2 g_2(\hat{R}) & -l_R - q_1\frac{dg_1}{dR}\hat{P}_1 - q_2\frac{dg_2}{dR}\hat{P}_2 \end{pmatrix}$$

from this sign structure, it follows that the Routh-Hurwitz criteria can be reduced to $\det J > 0$, a condition that can be rewritten:

$$\left[e_1 a_1 q_2 g_2(\hat{R}) - e_2 a_2 q_1 g_1(\hat{R})\right]\left(a_1\frac{dg_2}{dR} - a_2\frac{dg_1}{dR}\right) > 0 \tag{2.20}$$

$$\iff (\gamma_2 - \gamma_1)\left(\left.\frac{d\hat{Z}}{d\hat{R}}\right|_2 - \left.\frac{d\hat{Z}}{d\hat{R}}\right|_1\right) > 0 \tag{2.21}$$

where $\left.\frac{d\hat{Z}}{d\hat{R}}\right|_i$ denotes the slope of the tangent line to the ZNGI_i. This local stability condition can be interpreted geometrically in terms of relative position of crossing ZNGIs and impact vectors at the coexistence point (León and Tumpson 1975; Leibold 1996; Meszéna et al. 2006; Koffel et al. 2016).

2.B Analytical results on adaptive dynamics with two-way trade-offs

In this appendix, we choose to use herbivore attack rate $a = a_0(1-\rho)$ instead of resistance ρ — the latter being implicitly included in the former — to simplify both notations and calculations. After inversion, this relationship gives $\rho = 1-a/a_0$. Note that ρ and a vary in opposite directions, as $\partial\rho/\partial a < 0$.

2.B.1 Preliminary results

In adaptive dynamics, a singular point is a local ESS if and only if $\partial^2 w/\partial x^2 < 0$, where $\partial^2 w/\partial x^2$ is the second derivative of the invasion fitness with respect to the invader trait, evaluated at the resident trait. In a previous paper (Koffel et al. 2016), we established the following relationship:

$$\frac{\partial w}{\partial Z}\left(\left.\frac{d^2Z}{dR^2}\right|_{\mathrm{E}} - \left.\frac{d^2Z}{dR^2}\right|_{\mathrm{Z}}\right) = \left(\frac{dx}{dR}\right)^2 . \frac{\partial^2 w}{\partial x^2} \tag{2.22}$$

where $d^2Z/dR^2|_{\mathrm{E}}$ and $d^2Z/dR^2|_{\mathrm{Z}}$ are the second derivatives of respectively the envelope and the tangent ZNGI, and thus quantify their curvature. $\partial w/\partial Z$ quantifies how the plant fitness responds to a variation in herbivore density and dx/dR is the total variation of trait x as R varies along the envelope. Expanding on the calculations of Koffel et al. (2016), it is actually possible to show the following general result:

$$\left.\frac{d^2Z}{dR^2}\right|_{\mathrm{E}} - \left.\frac{d^2Z}{dR^2}\right|_{\mathrm{Z}} = \frac{dx}{dR}\frac{\partial}{\partial x}\left(\frac{\partial Z}{\partial R}\right) \tag{2.23}$$

Combining eq. (2.22) and eq. (2.23), we obtain the following useful relationship, linking the variation of the trait along the envelope and the ESS criteria:

$$\frac{dx}{dR}\frac{\partial^2 w}{\partial x^2} = \frac{\partial w}{\partial Z}\frac{\partial}{\partial x}\left(\frac{\partial Z}{\partial R}\right) \tag{2.24}$$

where $\partial Z/\partial R$ is obtained after differentiating the ZNGI equation given by setting eq. (2.1b) equal to zero. In the case of the diamond food web, this is equal to

$$\frac{\partial Z}{\partial R} = \frac{1}{a}\frac{\mu^2\alpha}{(\mu+\alpha R)^2}. \tag{2.25}$$

We'll need to compute the RHS of eq. (2.24) to conclude. This will be done for the three different two-way trade-offs in the next subsections.

A second result from Koffel et al. (2016) can help make the link between the properties of

the singular points and trait variation:

$$\frac{\partial R}{\partial S_R} \cdot \frac{d}{dx}\left(\frac{\partial w}{\partial x}\right) = \delta(x)\frac{\partial^2 w}{\partial x^2} \tag{2.26}$$

where δ is a strictly positive function of the trait x in the particular case of the diamond food web and

$$J(x) = \frac{d}{dx}\left(\frac{\partial w}{\partial x}\right) = \frac{\partial^2 w}{\partial x^2} + \frac{\partial R}{\partial x}\frac{\partial^2 w}{\partial R \partial x} + \frac{\partial Z}{\partial x}\frac{\partial^2 w}{\partial Z \partial x} \tag{2.27}$$

is the Jacobian of the fitness gradient. In adaptive dynamics, a singular point is said to be convergence stable if and only if $J(x) < 0$. This link between ESS and convergence stability properties on one side and eco-evolutionary response of the resource level to an increase of its supply on the other side is striking. It leads to the following result for a singular point x^*:

$$x \text{ is a CSS} \implies \frac{\partial R}{\partial S_R} > 0 \tag{2.28}$$

This relationship will be particularly useful in the examples of the different two-way trade-offs of the next subsections.

2.B.2 Trade-off between α and μ

Let us rewrite this trade-off as a general relationship $\alpha(\mu)$ with $\alpha' < 0$, with a kept constant. Setting the fitness gradient equal to zero, it is then possible to show that singular points satisfy:

$$R = -\alpha'\left(\frac{\mu}{\alpha}\right)^2 \tag{2.29}$$

This gives the parametric equation of the envelope as a function of the trait μ. With $x = \mu$, we can differentiate the expression of $\partial Z/\partial R$ obtained in eq. (2.25) to compute the right hand side of eq. (2.24):

$$\frac{\partial w}{\partial Z}\frac{\partial}{\partial \mu}\left(\frac{\partial Z}{\partial R}\right) = -\frac{\alpha^2 R}{(\mu + \alpha R)^2} \tag{2.30}$$

Where we used eq. (2.29) to get rid of α'. From eq. (2.24), we conclude that for any trade-off between α and μ

$$\frac{d\mu}{dR}\frac{\partial^2 w}{\partial \mu^2} = -\frac{\alpha^2 R}{(\mu + \alpha R)^2} < 0 \tag{2.31}$$

Thus, a singular trait μ corresponding to an ESS, i.e. satisfying $\partial^2 w/\partial \mu^2 < 0$, has to increase when moving along the envelope with increasing R. Because of the trade-off, this means that α conversely decreases. These results are intuitive: plant growth is a balance between resource

acquisition at rate αR and biomass synthesis at rate μ. When R increases, resource acquisition gets faster and it is thus optimal to reallocate from α to μ to keep the two processes balanced. Remember that a is constant in this case, thus the only way to cope with herbivory is to grow faster.

This can be further investigated through the environmental feedback loop. First, let us note that:

$$\frac{\partial \mu}{\partial S_R} = \frac{\partial \mu}{\partial R} \cdot \frac{\partial R}{\partial S_R} \tag{2.32}$$

Combining eq. (2.28) and eq. (2.31) leads to:

$$\mu \text{ is a CSS} \implies \frac{\partial \mu}{\partial S_R} > 0 \tag{2.33}$$

This is a general result true for any trade-off between μ and α satisfying $\partial\alpha/\partial\mu < 0$. This result also does not depend on the details of the plant impact on R and Z, e.g. with e and q functions of μ, as long as the overall impact of the plant on the herbivore remains positive.

2.B.3 Trade-off between α and ρ

Let us rewrite this trade-off as a general relationship $a(\alpha)$ with $a' > 0$, with μ kept constant. Setting the fitness gradient equal to zero, it is then possible to show that singular points satisfy:

$$\frac{a'}{a} = \frac{\mu^2 R}{\mu + \alpha R} \cdot \frac{1}{\mu\alpha R - m(\mu + \alpha R)} \tag{2.34}$$

Applying eq. (2.24) with $x = \alpha$ and using the relationship (2.34) leads to:

$$\frac{d\mu}{dR}\frac{\partial^2 w}{\partial \mu^2} = \frac{a'}{a}\frac{m\mu^2 + (\mu - m)(\alpha R)^2}{R(\mu + \alpha R)^2} > 0 \tag{2.35}$$

As a conclusion, for any trade-off between α and a:

$$\alpha \text{ is an ESS} \implies \frac{\partial \alpha}{\partial R} < 0 \tag{2.36}$$

$$\alpha \text{ is a CSS} \implies \frac{\partial \alpha}{\partial S_R} < 0 \tag{2.37}$$

Thus, a singular trait α corresponding to an CSS has to decrease when moving along the envelope with increasing S_R. Because α and a are traded off, this means that resistance $\rho = 1 - a/a_0$ conversely increases. Again, this is a general result, true for any trade-off between α and ρ, and fairly insensitive to the details of the plant impact on R and Z.

2.B.4 Trade-off between μ and ρ

Let us rewrite this trade-off as a general relationship $a(\mu)$ with $a' > 0$, with α kept constant. To establish a result similar to the one of the previous section, we need to get an explicit expression of R as a function of μ for the singular points. Setting the fitness gradient equal to zero, we get:

$$\left[\frac{a}{a'} - (\mu - m)\right]\left(\frac{\alpha R}{\mu}\right)^2 - (\mu - 2m)\frac{\alpha R}{\mu} + m = 0 \tag{2.38}$$

This equation has solutions if and only if $\Delta = \mu^2 - 4ma/a'$ is positive. Then, there are two solutions:

$$R_\pm = \frac{\mu}{2\alpha}\frac{\mu - 2m \pm \sqrt{\Delta}}{a/a' - (\mu - m)} \tag{2.39}$$

We have the following results on their signs:

$$R_+ > R_- > 0 \iff \frac{a}{a'} > \mu - m > m \tag{2.40}$$

$$R_- > 0 > R_+ \iff \mu - m > \frac{a}{a'} \tag{2.41}$$

When there are singular solutions, positive R_- always exists while positive R_+ only exists under the condition $a/a' > \mu - m > m$. Applying eq. (2.24) with $x = \mu$ and substituting the solution (2.39) leads to:

$$\frac{d\mu}{dR_\pm}\frac{\partial^2 w}{\partial \mu^2} = \mp\frac{a'}{a}\frac{\mu\alpha}{(\mu + \alpha R)^2}\sqrt{\Delta} \tag{2.42}$$

As a conclusion, for any trade-off between μ and a:

$$\mu \text{ is an ESS} \implies \frac{\partial \mu}{\partial R_+} > 0 \text{ and } \frac{\partial \mu}{\partial R_-} < 0 \tag{2.43}$$

$$\mu \text{ is an CSS} \implies \left.\frac{\partial \mu}{\partial S_R}\right|_+ > 0 \text{ and } \left.\frac{\partial \mu}{\partial S_R}\right|_- < 0 \tag{2.44}$$

As the smaller R_- portion always exists, μ of a CSS starts by decreasing along increasing S_R. However, if the larger R_+ portion also exists, μ hits a minimum and then increases with S_R. In this case, the non-monotonic behavior of μ leads some strategies to be CSS twice along the resource gradient (for both low and high S_R).

2.C Analytical results on optimization with two-way trade-offs

In this appendix, we choose to use herbivore attack rate $a = a_0(1 - \rho)$ instead of resistance ρ — the latter being implicitly included in the former — to simplify both notations and calculations.

After inversion, this relationship gives $\rho = 1 - a/a_0$. Note that ρ and a vary in opposite directions, as $\partial\rho/\partial a < 0$.

2.C.1 Preliminary results

Contrary to adaptive dynamics, the approach here consists in maximizing the plant net growth rate $w = g(R) - aZ - m$ without taking into account any environmental feedback loop, i.e. with R and Z fixed. This means for two-way trade-offs that a local Optimal Strategy (OS) with trait x has to satisfy:

$$\frac{\partial w}{\partial x} = 0 \qquad \text{with} \quad \frac{\partial^2 w}{\partial x^2} < 0 \tag{2.45}$$

Solving the previous equation would theoretically give an expression of x as a function of R. Differentiating the previous relationship leads to the useful result:

$$\frac{\partial x}{\partial R}\frac{\partial^2 w}{\partial x^2} = -\frac{\partial^2 w}{\partial x \partial R} \tag{2.46}$$

This relationship is equivalent to eq. (2.24) from the previous section, the difference arising from the absence of partial feedback from the plant zero net growth condition. Indeed, Z does not vary along the resource gradient here because the plant does not feed the herbivores back. As previously, applying eq. (2.46) allows us to conclude on the direction of variation of an OS with trait x along the resource gradient.

Note that in the optimization case, R directly plays the role of S_R as it is the parameter that is determined externally and controls resource availability in the system. To allow more direct comparison with the adaptive dynamics case, let us simply define here $S_R \equiv R$.

2.C.2 Trade-off between α and μ

Let us write this trade-off as a general relationship $\alpha(\mu)$ with $\alpha' < 0$, with a kept constant. Setting the fitness gradient equal to zero, it is then possible to show that a local OS satisfies:

$$\frac{\alpha R}{\mu} = -\frac{\alpha'}{\alpha}\mu \tag{2.47}$$

Applying eq. (2.46) with $x = \mu$ and substituting the expression (2.47) to get rid of α' leads to:

$$\frac{\partial^2 w}{\partial \mu \partial R} = \frac{\alpha^2 R}{(\mu + \alpha R)^2} > 0 \tag{2.48}$$

Because of eq. (2.46), this means:

$$\mu \text{ is an OS} \implies \frac{\partial \mu}{\partial S_R} > 0 \tag{2.49}$$

Thus, a trait μ corresponding to an OS has to increase when moving along the envelope with increasing S_R. Conversely, the trait α decreases. This is a general result true for any trade-off between α and μ. It is actually possible to show that this result still holds with $a(\mu)$ and $m(\mu)$ satisfying $a' > 0$ and $m' > 0$.

2.C.3 Trade-off between α and ρ

Let us write this trade-off as a general relationship $a(\alpha)$ with $a' > 0$, with μ kept constant. To establish a result similar to the one of the previous section, we need to get an explicit expression of R as a function of α for the OS. Setting the fitness gradient equal to zero, we obtain:

$$\left(\frac{\alpha R}{\mu}\right)^2 + \left(2 - \frac{\mu}{\alpha a' Z}\right)\frac{\alpha R}{\mu} + 1 = 0 \tag{2.50}$$

This equation has solutions if and only if $\Delta = b(b-2)$ is positive, with $b = \mu/(2\alpha a' Z)$. Then, there are two of them and they read:

$$R_\pm = \frac{\mu}{\alpha}\left(b - 1 \pm \sqrt{b(b-2)}\right) \tag{2.51}$$

It is moreover easy to show that when they exist, they satisfy:

$$\alpha R_+ \geq \mu \geq \alpha R_- > 0 \tag{2.52}$$

Computing the right hand side of eq. (2.46):

$$\frac{\partial^2 w}{\partial \alpha \partial R} = \mu^2 \frac{\mu - \alpha R}{(\mu + \alpha R)^3} \tag{2.53}$$

Thus, substituting inequality (2.52) in eq. (2.53), we obtain:

$$\frac{\partial^2 w}{\partial \alpha \partial R_-} > 0 \quad \text{and} \quad \frac{\partial^2 w}{\partial \alpha \partial R_+} < 0 \tag{2.54}$$

leading to

$$\alpha \text{ is an OS} \implies \begin{cases} \dfrac{\partial \alpha}{\partial S_R} > 0, & \text{if } \alpha < \dfrac{\mu}{S_R} \\ \dfrac{\partial \alpha}{\partial S_R} < 0, & \text{otherwise} \end{cases} \tag{2.55}$$

The situation can get complicated for a generic trade-off, potentially with multiple local optima. However, the idea from these general results is always the following: if increasing S_R makes a local OS appear, the trait α where this maximum is attained will first increase as S_R keeps increasing. At one point, α will hit the value $\alpha_c = \mu/S_R$ for which it stops increasing. Keeping increasing S_R then leads to a decrease of α either toward 0 or until the OS is destabilized.

This result can be understood by the fact that both αS_R and μ limit plant growth. When both α and S_R are small, resource acquisition is strongly limiting, leading to significant benefits to allocate to α rather than a. However, as S_R becomes large, plant growth saturates to μ and the benefits of a large α vanish, making allocation to ρ more useful again.

2.C.4 Trade-off between μ and ρ

Let us write this trade-off as a general relationship $a(\mu)$ with $a' > 0$ and α kept constant. Then, computing the right hand side of eq. (2.46) reads:

$$\frac{\partial^2 w}{\partial \mu \partial R} = 2\frac{\mu \alpha^2 R}{(\mu + \alpha R)^3} > 0 \tag{2.56}$$

This directly gives the result

$$\mu \text{ is an OS} \implies \frac{\partial \mu}{\partial R} > 0 \tag{2.57}$$

Thus, a trait μ corresponding to an OS has to increase when moving along the envelope with increasing S_R. Conversely, the trait ρ decreases. This is a general result true for any trade-off between μ and ρ.

2.D Scenarios $1'$, $2'$ and $3'$

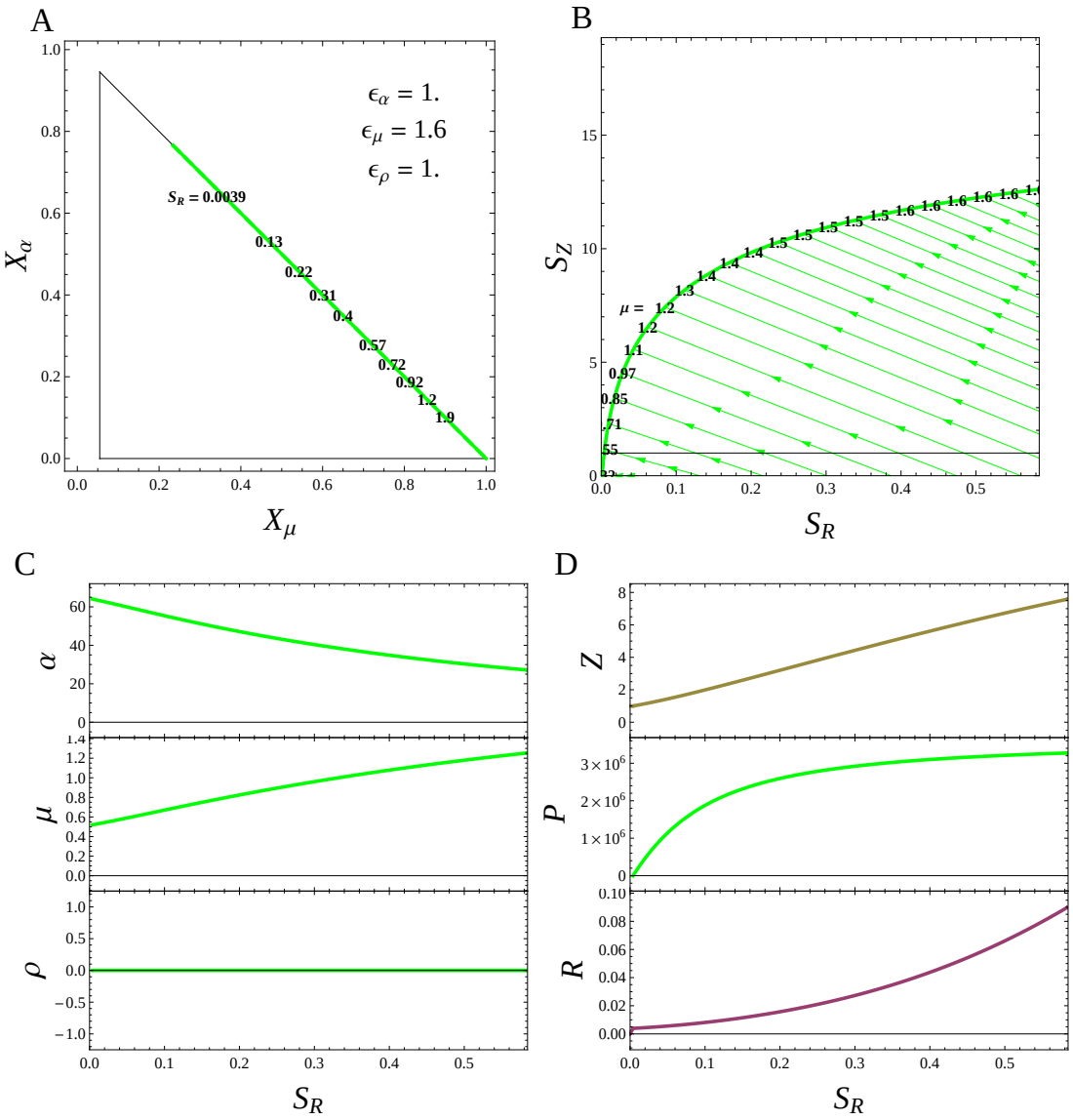

Figure 2.13: Scenario $1'$: Eco-evolutionary results under accelerating returns on allocation to maximal growth rate and linear allocation to affinity and resistance ($\epsilon_\alpha = 1$, $\epsilon_\mu > 1$ and $\epsilon_\rho = 1$). A) Adaptive trajectory in the allocation space (X_μ, X_α) along increasing nutrient supply S_R. B) Bifurcation diagram along the supply gradients. C) ESS traits as functions of nutrient supply S_R. D) Corresponding ecosystem properties. Parameters from Table 2.1.

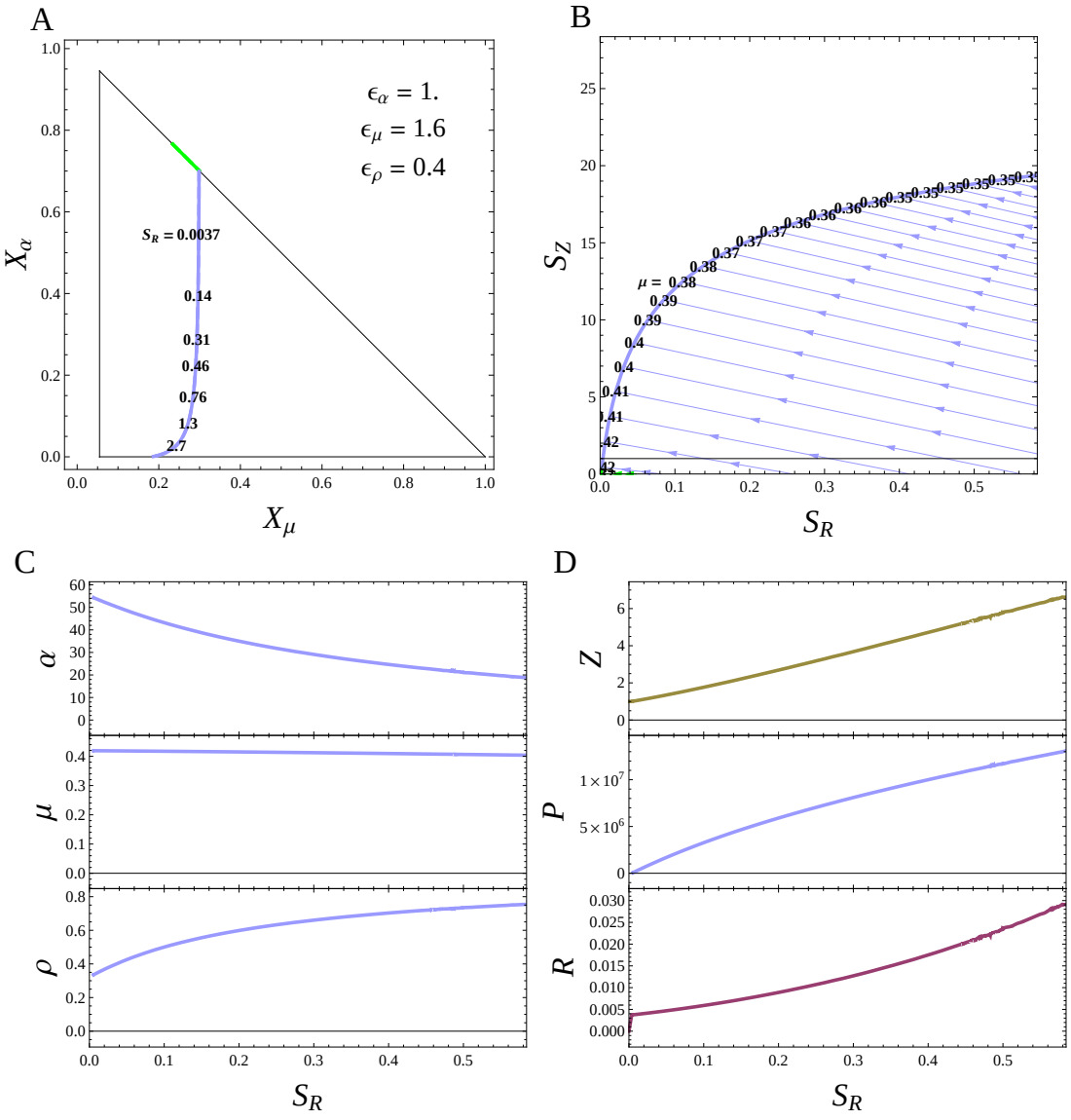

Figure 2.14: Scenario 2′: Eco-evolutionary results under linear, accelerating and diminishing returns on allocation to affinity, maximal growth rate and resistance respectively ($\epsilon_\alpha = 1$, $\epsilon_\mu > 1$ and $\epsilon_\rho < 1$). A) Adaptive trajectory in the allocation space (X_μ, X_α) along increasing nutrient supply S_R. B) Bifurcation diagram along the supply gradients. C) ESS traits as functions of nutrient supply S_R. D) Corresponding ecosystem properties. Parameters from Table 2.1.

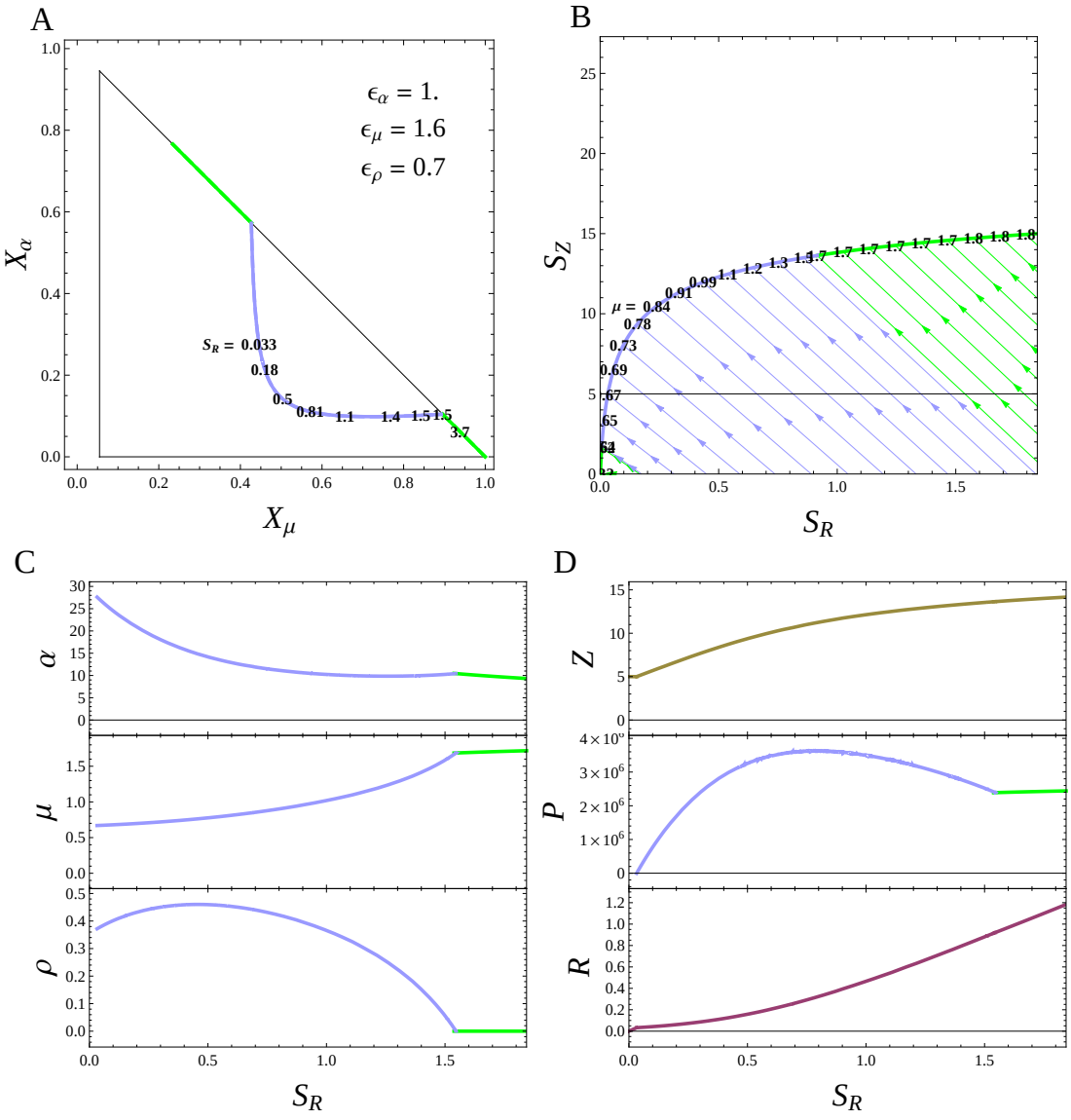

Figure 2.15: Scenario 3′: Eco-evolutionary results under linear, accelerating and diminishing returns on allocation to affinity, maximal growth rate and resistance respectively ($\epsilon_\alpha = 1$, $\epsilon_\mu > 1$ and $\epsilon_\rho < 1$). A) Adaptive trajectory in the allocation space (X_μ, X_α) along increasing nutrient supply S_R. B) Bifurcation diagram along the supply gradients. C) ESS traits as functions of nutrient supply S_R. D) Corresponding ecosystem properties. Parameters from Table 2.1.

2.E Bifurcation diagrams

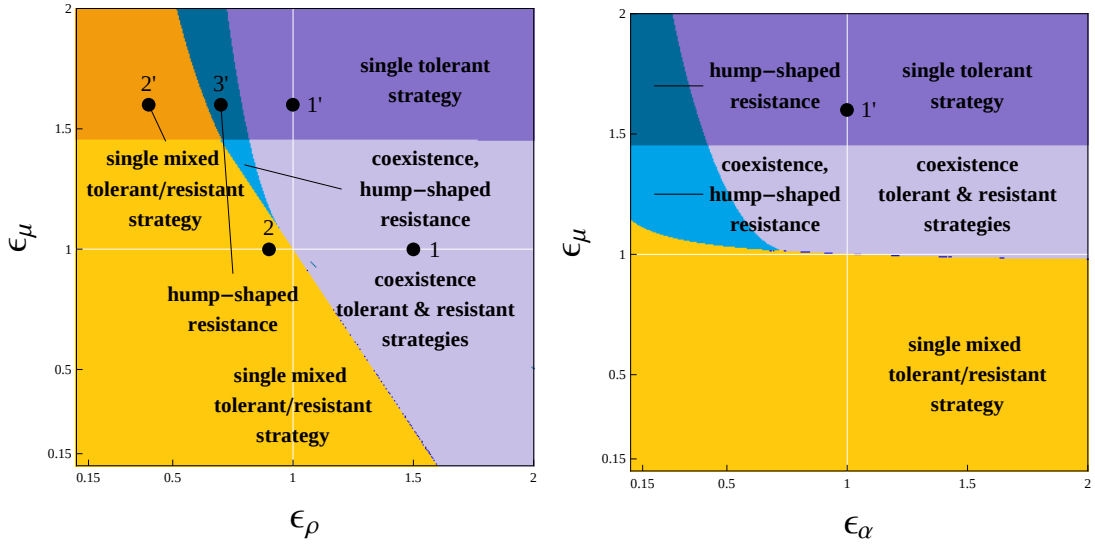

Figure 2.16: Overview of scenarios 1 (mauve), 2 (yellow), 3 (blue), 1' (orange), 2' (dark blue) and 3' (purple) in the ϵ_ρ-ϵ_μ and ϵ_α-ϵ_μ shape parameter planes.

Connecting statement

In Chapter 2, we applied the eco-evolutionary approach to contemporary niche theory laid down in Chapter 1 to the evolution of plant defenses against herbivores along a resource gradient. We showed that high resource availability selects for well-defended strategies, either a single resistant or stable coexistence of both resistant and tolerant, because high resource availability accompanies high herbivore density within the food chain. These adaptive patterns in turn altered the response of the food chain to nutrient enrichment, turning classical trophic cascades into trophic dead-ends. In Chapter 3, we will investigate another major role played by plants in ecosystems, namely N-fixation. Indeed, N-fixation plays a key role in our understanding of ecosystem development and the coupling between the nitrogen and the carbon cycles. We will show how such processes fit in contemporary niche theory and lead to facilitation and catastrophic shifts within a population of N-fixers. Applying Chapter 1's approach to community assembly, we will show how facilitation-driven succession and ecosystem development can emerge from N-fixing species turnover through time following repeated colonization. Finally, we show how this succession scenario and its endpoint, the climax, are drastically altered along an increasing nitrogen gradient.

Chapter 3

Facilitative succession by N-fixers and ecosystem development: a community assembly model

Contents

3.1 Abstract

Symbiotic nitrogen (N)-fixing organisms such as actinorhizal plants and legumes tend to thrive during primary succession, as typical bedrocks lack available N. In turn, fixed N accumulates in soils through biomass turnover and recycling, favoring more nitrophilous organisms. Yet, it is unclear how this facilitation mechanism interacts with competition for other limiting nutrients, e.g. phosphorus (P), and when this leads to succession mostly driven by facilitation. Here, we introduce a resource-explicit, community assembly model of N-fixing species competing for N and P and analyze successional trajectories along resource availability gradients using a recently developed extension of graphical resource competition theory. We show that facilitative succession only occurs under low N availability, and presents three characteristics: autogenic ecosystem development, relatively ordered trajectories and late succession bistability. Put together, these results lead to an enriched version of Tilman's resource-ratio theory of succession.

3.2 Introduction

Primary succession, the sequential replacement of plant species through time following the appearance of a bare substrate, is a central concept in ecology (Walker and del Moral 2003; Shugart 2013), and occurs on virtually any substrate, from sand dunes (Cowles 1901; Olson 1958) to glacial moraines (Chapin et al. 1994). Odum (1969) defines succession through three characteristics: (i) it is a reasonably directional and orderly process, (ii) it results from the reciprocal interaction between the plant community and its physical environment, (iii) it culminates in a climax maximizing biomass and stability. This 'holistic' approach (Walker and del Moral 2003) insists on the deterministic nature of succession at the ecosystem level (Clements 1916, 1936), as opposed to the 'reductionist' approach focusing instead on the site-specificity, stochasticity and idiosyncrasy of species assemblages (Gleason 1939). These two approaches are yet to be unified.

Nitrogen (N)-fixing organisms, such as legumes and actinorhizal plants tend to thrive during primary succession, as typical bedrocks lack available N (Walker and del Moral 2003). In Glacier Bay, Alaska, succession usually includes a broad range of N-fixing species (Walker 1993), from pioneer species like 'black crust'-forming cyanobacteria (Worley 1973; Schmidt et al. 2008) and lichen of the genus *Stereocaulon*, to mid- and late colonists like Drummond's aven (*Dryas drummondii*; Lawrence et al. 1967) and green adler (*Alnus viridis*). Conversely, because of biomass turnover and recycling, fixed N accumulates in the soil, becoming available to the whole community (Crocker and Major 1955; Chapin et al. 1994; Crews et al. 2001; Walker et al. 2003; Kohls et al. 2003). Such facilitation mechanisms (Callaway 1995) are potential drivers of primary succession, as exemplified by the facilitation model of succession, or facilitation-driven succession, in which 'early colonizers modify the environment, thereby making it more suitable for later colonizers to invade and prosper and less suitable for early colonizers to survive' (Connell and Slatyer 1977). This scenario contrasts with most models of succession, usually competition-based, such as models based on the r- and K-selection continuum (Pianka 1970; Huston and Smith 1987) or the colonization-competition trade-off (Tilman 1994) and Connell and Slatyer's (1977) inhibition and tolerance models, where the establishment of early colonists decreases – or at best does not affect – the invasion success or future invaders.

In fact, N-fixing organisms compete for the access to other essential resources such as phosphorus (P). Contrary to N availability, P availability in the pre-succession substrate is usually high, then decreases over time as it gets weathered from the bedrock and immobilized in the biotic compartments (Walker and Syers 1976; Vitousek et al. 1993, 2010). These central yet contrasted roles played by N and P during succession have put them at the center of models of ecosystem development over the last decades (Vitousek and Farrington 1997; Marleau et al. 2011; Laliberté et al. 2012; Menge et al. 2012). Both the absolute and relative richnesses of the abiotic environment in these two nutrients are expected to control succession, as formalized in the 'resource-ratio theory of succession' (Tilman 1985). Yet, it is still unclear how competition for P and facilitation for N interact during succession (Callaway and Walker 1997), and when

this results in facilitation-driven succession.

Models of primary succession have long been limited to verbal and conceptual approaches (Clements 1916; Odum 1969; Connell and Slatyer 1977). Their formalization first led to Markovian models of succession, i.e. based on phenomenological transition probabilities between vegetated states, without specifying any competition mechanisms or expliciting the soil properties that mediates them (Van Hulst 1979; Usher 1981; Siles et al. 2008). On the other hand, population- (Tilman 1985) or individual-based (Huston and Smith 1987) resource competition models rely on the mechanistic plant-soil feedback, an ingredient necessary to describe ecosystem development during succession. In the context of P acquisition and N fixation, recent resource competition models have however been limited to short-scale transient dynamics including only a few different species (Marleau et al. 2011) or a single undifferentiated plant compartment (Menge et al. 2012). On the other end, when dealing with a large number of species in a game theoretical perspective, succession models have yet been unable to capture autogenic N accumulation (Tilman 1985; Loreau 1998b; Sheffer et al. 2015) or have been limited to the analysis of the succession end point rather than the whole developmental trajectory (Menge et al. 2008; Kylafis and Loreau 2008).

In this chapter, we investigate autogenic, facilitation-driven succession by a community of N-fixers, differing in their abilities to fix N and acquire P. First, we use a mechanistic plant-soil model to describe how these species perform in the absence of other competing species, and classify them into three categories accordingly. Second, we embed this ecological model into a community assembly dynamics to answer the following questions: how do competition and facilitation interact, and under what conditions does it lead to facilitation-driven succession? What are the conditions under which succession is reasonably ordered and predictable? How does ecosystem stability change during succession? We conclude by summarizing these results into an enriched version of the 'resource-ratio theory of succession'.

3.3 Ecological model and analysis

3.3.1 Plant-soil model

Consider a plant-soil model from classical resource competition theory (MacArthur 1970; León and Tumpson 1975; Tilman 1982; Grover 1995; Chase and Leibold 2003) adapted to account for N-fixation, where a single species with population biomass B grows on soil nitrogen (N) and phosphorus (P), with concentrations N and P respectively. N and P dynamics are chemostat-like, with nutrients supplied externally at constant influxes I_N and I_P and leaving the system at per capita leaching rates l_N and l_P. Plant's growth is limited by the least available nutrient, following Leibig's law of the minimum:

$$g_{\text{tot}}(P, N) = \min[g_P(P), g_N(N) + F] \tag{3.1}$$

where $g_P(P)$ is the per capita growth rate when N is non-limiting, while the per capita growth rate when P is non-limiting is the sum of $g_N(N)$ and F, growth on soil N and N-fixation from the atmosphere respectively. Assuming constant plant stoichiometric coefficient q_P and q_N, per capita plant growth automatically translates into proportional P uptake rate $q_P.g_{\text{tot}}$. On the N uptake side, soil N is systematically privileged over atmospheric N, with N-fixation only happening when soil N is limiting. This mechanism is justified by the substantial costs associated with N-fixation and implicitly assumes that the plant can freely down-regulate its N-fixing activity. This leads to a soil N uptake rate equal to $q_N.\min[g_P(P), g_N(N)]$. Finally, plant biomass is lost at a constant per capita mortality rate m and partially restituted to P and N through recycling, with efficiency λ. This leads to the following ordinary differential equation system describing the plant-soil population dynamics:

$$\frac{dB}{dt} = [\min[g_P(P), g_N(N) + F] - m]\, B \tag{3.2a}$$

$$\frac{dP}{dt} = I_P - l_P P - q_P \min[g_P(P), g_N(N) + F]B + q_P \lambda m B \tag{3.2b}$$

$$\frac{dN}{dt} = I_N - l_N N - q_N \min[g_P(P), g_N(N)]B + q_N \lambda m B \tag{3.2c}$$

These equations are a simplified version of Menge et al.'s (2009a) model where we have chosen not to explicitly include organic nutrient pools, as they do not influence our results at the ecological equilibrium. In practice, the associated extra parameters can be thought of being lumped in λ. The interplay between N vs. P limitation and N-fixation vs. no fixation, expressed formally by the use of the two different min functions eq. (3.2), leads to three different uptake regimes for the plant: P-limitation without N-fixation, P-limitation with N-fixation and N-limitation (Fig 3.1 and Appendix 3.A).

3.3.2 Regional species pool

To study succession by N-fixers, we consider a pool of plant strategies with different fixation efficiencies F, from plants with low fixing abilities that mostly rely on soil nitrogen to plants that can be completely independent from soil N that we will refer to as "total fixers" (Holter 1984). We assumed that these maximal fixation rates F traded-off against competitive abilities for P through P uptake rate. More precisely, we assumed that $\partial g_P/\partial F < 0$ for fixed P. Indeed, plants present specific adaptations to low-P soil conditions, such as root morphology and architecture (e.g. lateral and cluster roots), root exsudates, rhizosphere acidification and mycorrhizal symbioses which are known to incur substantial costs for the plant (Zhu and Lynch 2004; Lynch and Ho 2005), in turn leading to trade-offs between P-acquisition and other costly functions such as N-fixing ability (Thuynsma et al. 2014).

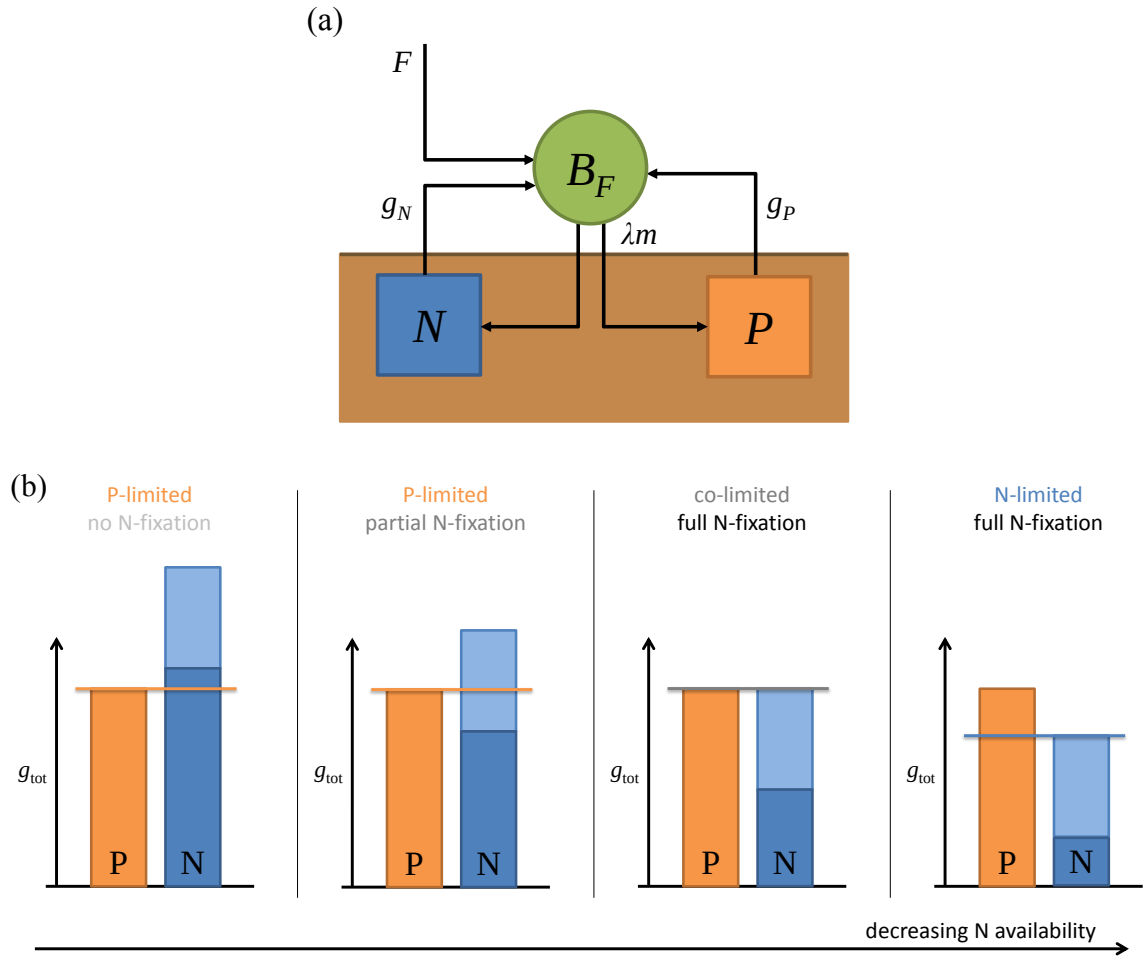

Figure 3.1: (a) Flow diagram of the model. (b) Schematic representation of how soil P availability (orange), soil N availability (dark blue) and N-fixing ability (light blue) combine in Liebig's law to determine plant growth g_{tot} and uptake rates (black arrow) along a N availability gradient. When soil P is more limiting than soil N, plants are P-limited and fixation is unnecessary (far left). When soil N is more limiting than soil P, there are three possibilities. Either maximal fixation rate is large enough for N not to be limiting, leading to P-limitation with partial N-fixation (center left), or maximal fixation is just right to reach colimitation (center right), or fixation is insufficient to overcome N limitation, leading to N-limitation with full N-fixation (far right).

3.3.3 Graphical analysis and classification of N-fixing strategies

A first step consists in visualizing the equilibria reached by an ecosystem dominated by a given plant species with fixation ability F along N and P abiotic gradients. Doing so, we classify N-fixing species from the species pool into three categories -low, high and total N-fixers- according to their qualitative behavior, also shedding light on the different roles the N-fixing species will

play during succession. As previously mentioned, our model is adapted from the essential resource case of competition theory (Tilman 1982; Grover 1997; Chase and Leibold 2003) with the inclusion of nitrogen fixing and nutrient recycling (Daufresne and Hedin 2005). For this reason, it can be analyzed graphically with the help of three ingredients: supply points, Zero Net Growth Isoclines (ZNGI) and impact vectors.

The supply point (S_P, S_N) corresponds to N and P levels at equilibrium in the system in the absence of any plant. It characterizes the baseline fertility of the bare substrate. Setting eq. (3.2b-3.2c) to zero with $B = 0$ gives $S_P = I_P/l_P$ and $S_N = I_N/l_N$. The supply point can be displayed in the resource plane (Black dot, Fig. 3.2b-d).

The ZNGI of a N-fixing species with biomass B can be obtained by setting the growth eq. $(3.2a)$ to zero. It gives the nutrient levels required for the plant to be at equilibrium. The supply points situated above the ZNGI are the bare substrate conditions under which this species can establish itself starting from a very low density. As in the standard essential resource case (Tilman 1982), the ZNGI is a right-angle line whose corner's coordinates are Tilman's R^* for N and P, the minimal resource required for growth (Fig. 3.2). We denote them P^* and N_f^*, the latter subscript f distinguishing N_f^* from the plant's minimal requirements in the absence of fixation N_{nf}^* (See Appendix 3.A for details). As $N_{nf}^* > N_f^*$, N-fixation enables the plant to grow under harsher N-limiting conditions, graphically lowering the position of the ZNGI corner. Because of the trade-off between fixation efficiency F and P acquisition, P^* and N_f^* are anti-correlated. This can be visualized graphically when a large number of species with varying fixation efficiencies are sampled from the species pool and their ZNGIs displayed (Fig. 3.2a): all the ZNGIs' corner form a decreasing curve called the envelope (Klausmeier et al. 2007; Danger et al. 2008; Koffel et al. 2016). This continuum of strategies can be divided into three categories: low, high and total N-fixers (respectively Fig. 3.2b-d). Total N-fixers correspond to strategies with $F > m$, as they have $N_f^* = 0$. They can invade the bare substrate even in the complete absence of N supply, but are the poorest P competitors (Fig 3.2c). To understand the difference between low and high fixers, we need to introduce the impact vectors.

The impact vectors describe the net impact of the plant population on the two nutrients, through consumption and recycling. Their coordinates can be read as the factors in front of B in eq. (3.2b,3.2c). They are displayed on Fig. 3.2 for a few equilibrium points located on the ZNGI. Contrary to the low N-fixer case (Fig. 3.2b), the high and total N-fixer cases (Fig. 3.2c,d) present a soil N threshold denoted N_c^* under which plant presence has a net positive impact on N, with biotic supply by fixation and recycling exceeding soil uptake. This facilitation by and between N-fixing individuals under low N conditions leads to N accumulation and destabilizes the N-limited equilibria (Dashed ZNGI lower branch in Fig. 3.2c, compare with Fig. 3.2b).

In the high N-fixer case, facilitation leads to alternate stable states, namely, the non-zero plant population state and the bare substrate (Purple region in Fig. 3.2b; mathematical details in Appendix 3.A). Indeed, N supply under the ZNGI is too low for N-fixers to invade from

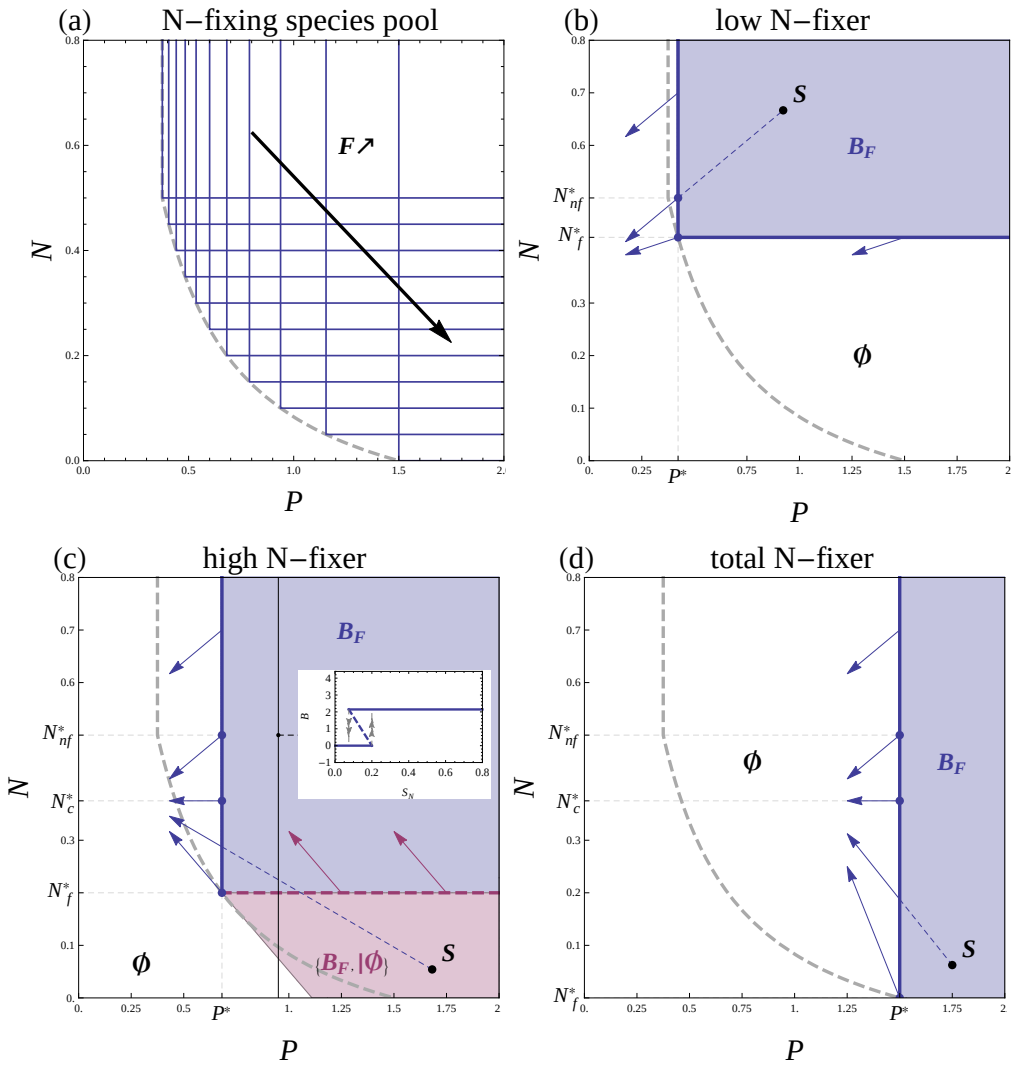

Figure 3.2: (a) ZNGIs (blue, L-shaped) representing the competitive abilities of N-fixers from the species pool with normalized fixation abilities F/m comprised between 0 and 1. The ZNGI corners all line up on a decreasing envelope (dashed grey), which materializes the trade-off between P^* and N^*_{nf}. (b),(c) and (d): Ecological phase diagrams along N and P availabilities for three different N-fixing strategies: low, high and total N-fixer corresponding respectively to $F/m = 0.15$, 0.6 and 1. The ZNGI (thick, L-shaped), a strategy's minimal nutrient requirements for growth, also gives the possible nutrient levels at equilibrium, which can be either stable (blue, plain) or unstable (purple, dashed). The impact vectors (blue and purple vectors) correspond to a strategy's per capita impact on the two nutrients. They point down when this impact is negative, up when it is positive. The blue-shaded region (labeled B_F) gives the external nutrient supplies $S = (S_P, S_N)$ (e.g. black dot) under which the N-fixer can subsist, leading to a vegetated ecosystem. In the white region (labeled $\emptyset$), supplies are too low and the N-fixer goes extinct, leading to the bare substrate. The purple-shaded region (labeled $B_F|\emptyset$) has the vegetated ecosystem and the bare substrate as two alternate stable states. This can be seen in the inset in (c), where the biomasses at equilibrium (blue) of these two stable states (plain) and the unstable state that separates them (dashed) have been plotted against a nutrient gradient with increasing S_N and fixed S_P (black, vertical line). High N-fixer biomass is constant along this N gradient because only P is limiting.

low density, but a population that is large enough can persist under these conditions thanks to facilitation. This alternate stable state regime disappears for total N-fixers, as they can invade for any N availability (Fig. 3.2d). The presence of alternate stable states means that the vegetated ecosystem can undergo a sudden transition to the bare substrate (Scheffer et al. 2001; Kéfi et al. 2008). This sudden transition could be triggered by a slight change in environmental conditions such as a decrease in external phosphorous supply, or happen after a perturbation, e.g. fire or herbivore outbreak, that would be large enough to drive the N-fixing population under its recovery threshold.

Reading Fig. 3.2 as bifurcation diagrams along the nutrient supplies summarizes this analysis, with the white region corresponding to the bare substrate only (the plant can neither invade nor persist), the blue region the plant population only (the plant can invade and persist) and the purple region alternate stable states between the two (the plant can not invade, but can persist).

3.4 Community assembly dynamics

The plant-soil models described in the previous section for species with various fixing abilities F and their classification in three qualitatively different categories are the building blocks of the community assembly dynamics. Indeed, we suppose that these N-fixing species form a regional species pool (Drake 1990; Morton and Law 1997; Chase and Leibold 2003), from which colonization attempts happen at random with the introduction of a few invading individuals into the succession site. To make the problem tractable, we assume a time scale separation between rare colonization attempts from the N-fixing species pool and faster ecosystem relaxation between these invasions. As we are interested in the role played by facilitation during succession, we will also assume for the next two subsections that N availability are low enough for N-fixation to induce a positive feedback loop, i.e. that $S_N < N_c^*$ as was shown in the previous section.

3.4.1 Successional step

Let us describe what happens when a focal invading species is introduced in the successional site formerly at equilibrium. This pre-invasion equilibrium situation corresponds either to the initial bare substrate, or follows the stabilization of a resident vegetated ecosystem after a previous successful colonization, as described in the previous section. In both cases, the pre-invasion soil properties can be described by their equilibrium nutrient concentrations, noted $\tilde{N}$ and $\tilde{P}$, and completely determine the success of the invader. Denoting F' and $B_{F'}$ the fixation ability and biomass of this invader, its success is quantified by the sign of its per capita growth rate when

rare, the invasion fitness ρ (Metz et al. 1992; Geritz et al. 1997, 1998; Hui et al. 2016):

$$\rho(F', \tilde{P}, \tilde{N}) = \frac{1}{B_{F'}} \frac{dB_{F'}}{dt}\bigg|_{\tilde{P},\tilde{N};B_{F'}\to 0^+} = \min[g'_P(\tilde{P}), g_N(\tilde{N}) + F'] - m \tag{3.3}$$

where g'_P denotes phosphorus uptake by the invader and trades off against F'. According to the previous section, if the pre-invasion ecosystem is the bare substrate, $\tilde{N}$ and $\tilde{P}$ are simply equal to the supplies S_N and S_P. Otherwise, $\tilde{N}$ and $\tilde{P}$ are fully determined by the equilibrium of the pre-invasion plant-soil model, i.e. located on the ZNGI of the resident plant species, whose fixing efficiency is denoted F. If $\rho(F', \tilde{P}, \tilde{N})$ is negative, invasion fails as the invader goes extinct and the resident ecosystem stays the same. On the contrary, if $\rho(F', \tilde{P}, \tilde{N})$ is positive, invasion is successful and the invader's population gets large enough to impact the resident equilibrium. From there, several outcomes from this ecological sorting phase are technically possible when invading a resident population: 1) the invader becomes the new resident after excluding the former resident; 2) the invader and the resident reach an equilibrium where they coexist; or 3) invasion by the invader leads to a collapse of the whole ecosystem towards the bare substrate state, a particular case of a phenomenon known as 'the resident strikes back' (Mylius and Diekmann 2001; Geritz et al. 2002). Under the assumption of low N availability ($S_N < N_c^*$), the positive feedback loop ensures that all the possible invaders end up being P-limited at equilibrium, which, in virtue of Tilman's (1982) R^* rule, excludes option 2), i.e. coexistence. As we also checked numerically that option 3), i.e. invasion-driven ecosystem collapse, does not happen, the only outcome here is option 1), i.e. exclusion of the resident by the invader (but see Discussion?). As the invader replaces and becomes the new resident, it sets the nutrient levels at equilibrium on its own ZNGI. Note that this new equilibrium can have the bare substrate as an alternate stable state if strategy F' could not have been able to invade on its own (e.g. situation with high N-fixer depicted in Fig. 3.2c). When this happens, the presence of the resident F facilitated F', by making the invasion of the latter possible (Gerla et al. 2011; Rapaport 2017). We call such an invader-resident replacement a facilitation-driven successional step, as this mechanism . This facilitation-driven successional step is illustrated in Fig. 3.3 with two different strategies from the regional species pool, F_1 and F_2. F_1 is close to total N-fixation but not very competitive for P, whereas F_2 has more balanced N and P competitive abilities while still being a high N-fixer ($F_1 > F_2$). The supply point is such that the initial bare substrate is rich in P but highly N depleted, meaning that only F_1, the pioneer species, can at first invade (S in Fig. 3.3a). However, the establishment of F_1 increases N availability at equilibrium due to positive impact (R_1 in Fig. 3.3). This leads to N level that are above F_2 requirements, making invasion by F_2 now possible. When F_2 invades, it competitively excludes F_1 by pulling P levels down, and further increases N levels in the system (R_2 in Fig. 3.3). As a new resident, F_2 can persist after outcompeting F_1 thanks to the positive feedback loop on N, as S is located in F_2 alternate stable state region.

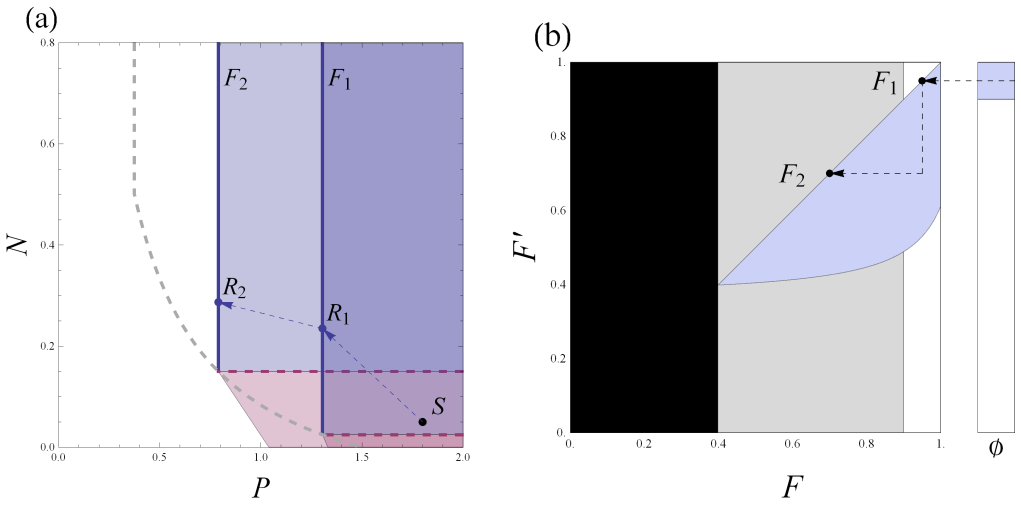

Figure 3.3: Representation of a facilitation-driven successional step in the nutrient (a) and strategy space (b), emerging under low N- and high P-availability, i.e. $S = (S_P, S_N) = (1.8, 0.05)$. (a) The ZNGIs of two high N-fixing strategies F_1 and F_2 are superimposed, following the color code of Fig3.2. F_1 is a better N-fixer than F_2 ($F_1 > F_2$), but worse P-competitor. Only F_1 can invade the bare substrate (S), the supply point (black dot) being located above the invasion N requirements of F_1 (dashed, purple) but below the ones of F_2. As F_1 establishes, it moves the nutrient levels to R_1, where invasion by F_2 is possible. As F_2 establishes, it further moves the nutrient levels to R_2, competitively excluding F_1. As S belongs in F_2 alternate stable state region (purple), F_2 can subsist there even after displacing F_1. (b) Same successional step represented on a PIP, picturing the invasion success of an invader (F') versus a resident state (F and $\emptyset$). The resident state can either be the bare substrate ($\emptyset$), or a previously established strategy with trait F that is globally stable (white, e.g. F_1) or sensitive to catastrophic shift because the bare substrate is an alternate stable state (gray, e.g. F_2). Some strategies F are unable to be resident (black). Positive invasion pairs, by an invader F' in a resident F or $\emptyset$, are pictured in blue. F_1 can invade the bare substrate while F_2 cannot. After F_1 establishes, F_2 can invade F_1 and displace it, leading to a bistable resident state.

In parallel, this successional step can be visualized using an adapted graphical tool from the eco-evolutionary litterature, the Pairwise Invasibility Plot (PIP) (Geritz et al. 1997). It consists in plotting the sign of the invasion growth rate ρ against both the invader trait F' in the y-axis and the pre-invasion state (resident F or bare substrate) in the x-axis (Fig. 3.3b). The figure obtained is divided in two parts: the PIP proper on the left displaying invasion success of an invader F' against a resident F, and an additional bar plot on the right displaying the invader success in the bare substrate ($\rho > 0$ in blue, $\rho < 0$ in white and gray Fig. 3.3b). The strategies with positive invasion on the bar plot correspond to the pioneer species. Information about the resident state status is also reminded on the plot, displaying whether this strategy can not be resident for this supply point (black), or can be resident with (grey) or without an alternate stable state (white). The trajectory on the PIP illustrates the substitution sequence leading to

the successional step. In practice, this means that the community is always dominated by a single species during facilitation-driven succession.

3.4.2 Facilitative succession and ecosystem development

The facilitative step described in the previous section can be iterated by repeated successful colonizations events, leading to facilitation-driven succession. We assume equal probability of introduction for all the N-fixing species, i.e. no colonization-competition trade-off (Tilman 1990). As will be discussed later, we expect facilitation-driven succession to be robust to the release of this assumption. Some general properties of this succession can be read directly on the PIP or deduced from the equilibrium properties of the plant-soil model. We also randomly generated successional trajectories and tracked the three quartiles of the distribution of probability to be in a given succession state through time (Fig. 3.4c-f), using the information contained in the PIP to assess the invasion success of invaders repeatedly chosen at random from the species pool.

In terms of community assembly, succession always starts with a pioneer species, i.e. a plant presenting a high enough fixation rate to invade the bare substrate. The establishment of this plant population can be displaced by another pioneer species, or facilitates its replacement by strategies with lower fixation rates and unable to invade by their own, themselves facilitating species with even lower fixation rates, etc, in an orderly monotonic process. However, as fixing rates decrease, we reach a point where a narrower and narrower range of strategies are able to invade, up to a certain strategy where no further invasion is possible (Fig. 3.4b). This successional end-point is located at the edge of the positive invasion region (blue, Fig. 3.4b), and is called an Evolutionary Stable Strategy (ESS) in game theory. Interestingly, this ESS is never attained but only approached asymptotically as it is unable to invade any other strategy (Geritz et al. 1998), leading to a successional slow down in late succession. As the ESS is located at the end the bistable region (gray, Fig. 3.4b), the late succession ecosystem is never globally stable, as a strong enough perturbation affecting plant biomass, such as fire or a sudden herbivore outbreak, could lead to a collapse back in the bare substrate state.

The succession of above-ground strategies is associated with simultaneous below-ground changes in soil properties, leading to ecosystem development. Soil P starts from S_P and then decreases, asymptotically tending towards a minimal concentration as we get close to the ESS (Fig. 3.4e). Conversely, soil N starts from S_N and increases, asymptotically reaching a plateau (Fig. 3.4f). As the strategies that establish in the course of succession are less and less efficient at N-fixation (Fig. 3.4c), it seems at first contradictory that succession leads to the accumulation of soil N over time. However, plant biomass also increases during succession, as plants better at exploiting P establish in the ecosystem (Fig. 3.4d). As the total fixation flux is proportional to both N-fixer biomass and fixation efficiency, the increase in biomass compensates the decrease in per capita fixation rates, leading to an overall increase in fixation flux, and thus soil N, during succession.

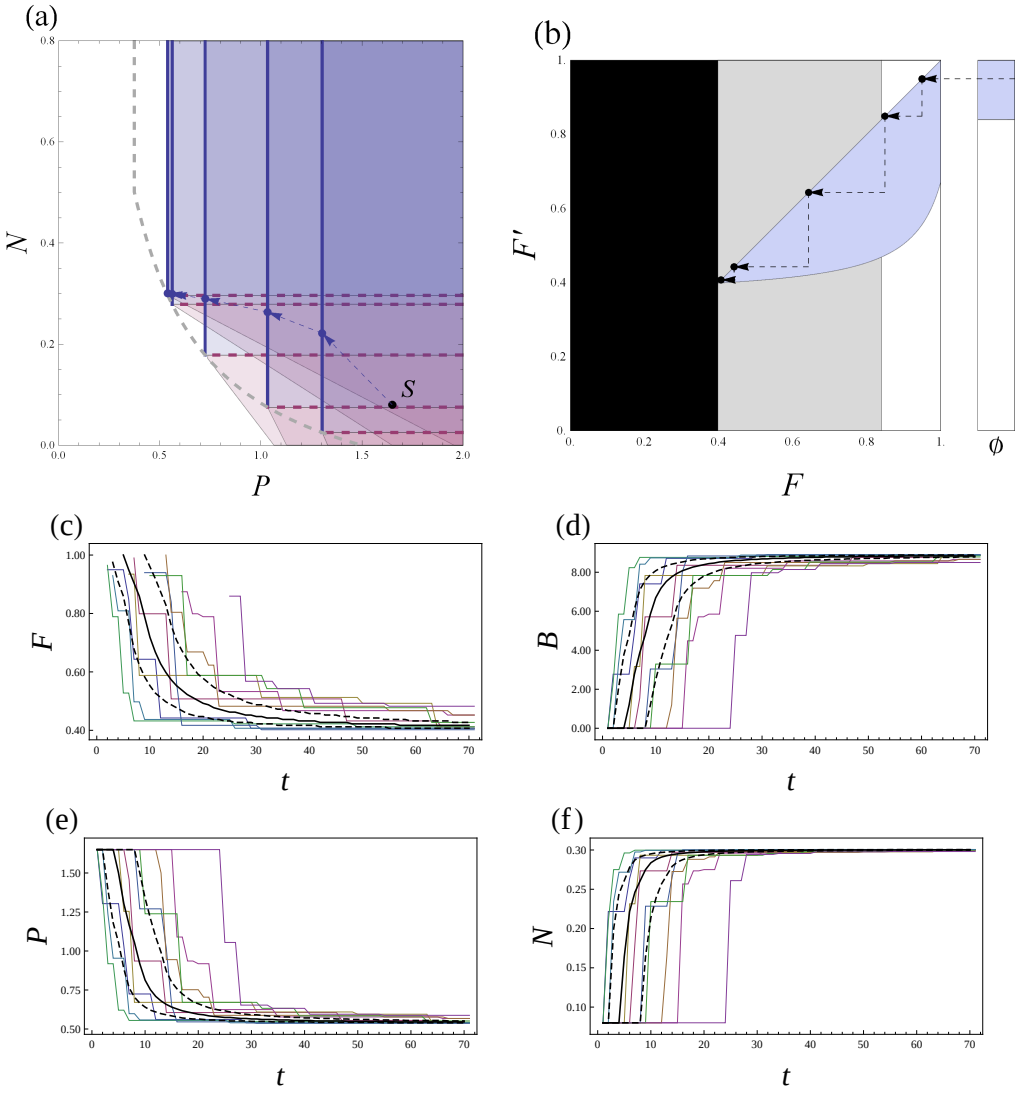

Figure 3.4: Facilitation-driven succession trajectories, under low N and high P supply, i.e. $S = (S_P, S_N) = (1.8, 0.05)$. All the trajectories were the result of 100 iterations of random colonization attempts from the species pool with equal probability followed by an ecological sorting phase resulting in either 1) extinction of the invader; 2) replacement of the resident by the invader. (a) and (b): same situation as Fig. 3.3 iterated 100 times. Rapidly, as the trajectory gets close to the ESS, virtually every colonization attempt fails, which explains why only 5 colonizations succeed out of 100. (c), (d), (e) and (f): ecosystem properties dynamics along succession, respectively per capita fixation efficiency F, biomass B and soil nutrient levels P and N. 10 random trajectories are represented (colored, plain) as well as the three quartiles (black, thick, median plain, 1st and 3rd quartiles dashed) of the full distribution of probability of the succession process, obtained with a Markov chain. F and P decrease during succession, while B and N increase, all of them reaching a climax as we get close to the ESS. Contrary to competition-driven succession (Fig. 3.6), the facilitation mechanism ensures that ecosystem properties are 'channels' during early succession.

Finally, a last characteristic of our facilitation-driven succession model relies in the relative similarity between multiple trajectories despite the intrinsic stochastic nature of the colonization events (Fig. 3.4b-d). An explanation for this comes from the particular shape of the PIP, with the positive invasion region restricted to a relatively narrow band. This means that most of the colonization attempts from this broad species pool get filtered out at every step of succession because environmental conditions are relatively harsh. Interestingly, this combined environmental and competitive filtering can be seen as a moving and narrowing window as succession moves forward, the 'moving' and 'narrowing' effects being respectively the signatures of facilitation and competition.

3.4.3 A resource-ratio theory of succession

In the previous section, we described how repeated colonization from a regional species pool of N-fixers in a P rich, N depleted substrate could lead to facilitative succession. We now want to delimit exactly the supply points leading to facilitative succession, and know if other succession scenarios are possible (Connell and Slatyer 1977). Drawing such a bifurcation diagram along the resource supply gradients can be done easily in this resource competition set-up using the 'envelope approach', a recently developed graphical tool adapting graphical resource competition theory to community assembly dynamics (Koffel et al. 2016). The results are summarized in Fig. 3.5. We identified 4 regions and labeled them with corresponding PIPs. In the bare substrate region (0), both N and P are so low that not a single strategy from the regional species pool can establish or persist. The facilitative succession region (I) is found for low enough N ($S_N < N_c^*$) and high enough P supplies (on the right of the envelope). Interestingly, a small region (II) is located between (0) and (I). There, succession cannot start because no strategy can invade the bare substrate, but the community would go through succession and persist there if a plant population were already present. This can be seen as community-level alternate stable states between the bare substrate and a community that would undergo succession. Finally, region (III) corresponds to high N supplies ($S_N < N_c^*$), where fixation is not high enough for facilitation to happen. This means that succession is purely competition-driven, as can be seen on the corresponding PIP: most of the strategies can invade the initial bare substrate, including the ESS, and the establishment of any strategy can only decrease the chances of further invasion by other strategies. Contrary to the facilitative succession case, trajectories are not monotonous as the trait F can oscillate around the ESS, and early succession is much more impredictable as almost any strategy can establish on the bare substrate (see Fig. 3.6 in Appendix). Ecosystem biomass increases along succession, but both soil P and N levels decrease. This last scenario is close to what Connell and Slatyer (1977) called the tolerance model as it is purely competition-driven.

Abiotic nutrient availabilities not only control succession qualitatively in term of competition scenario, but also influence quantitatively the properties of succession and its endpoint. This can

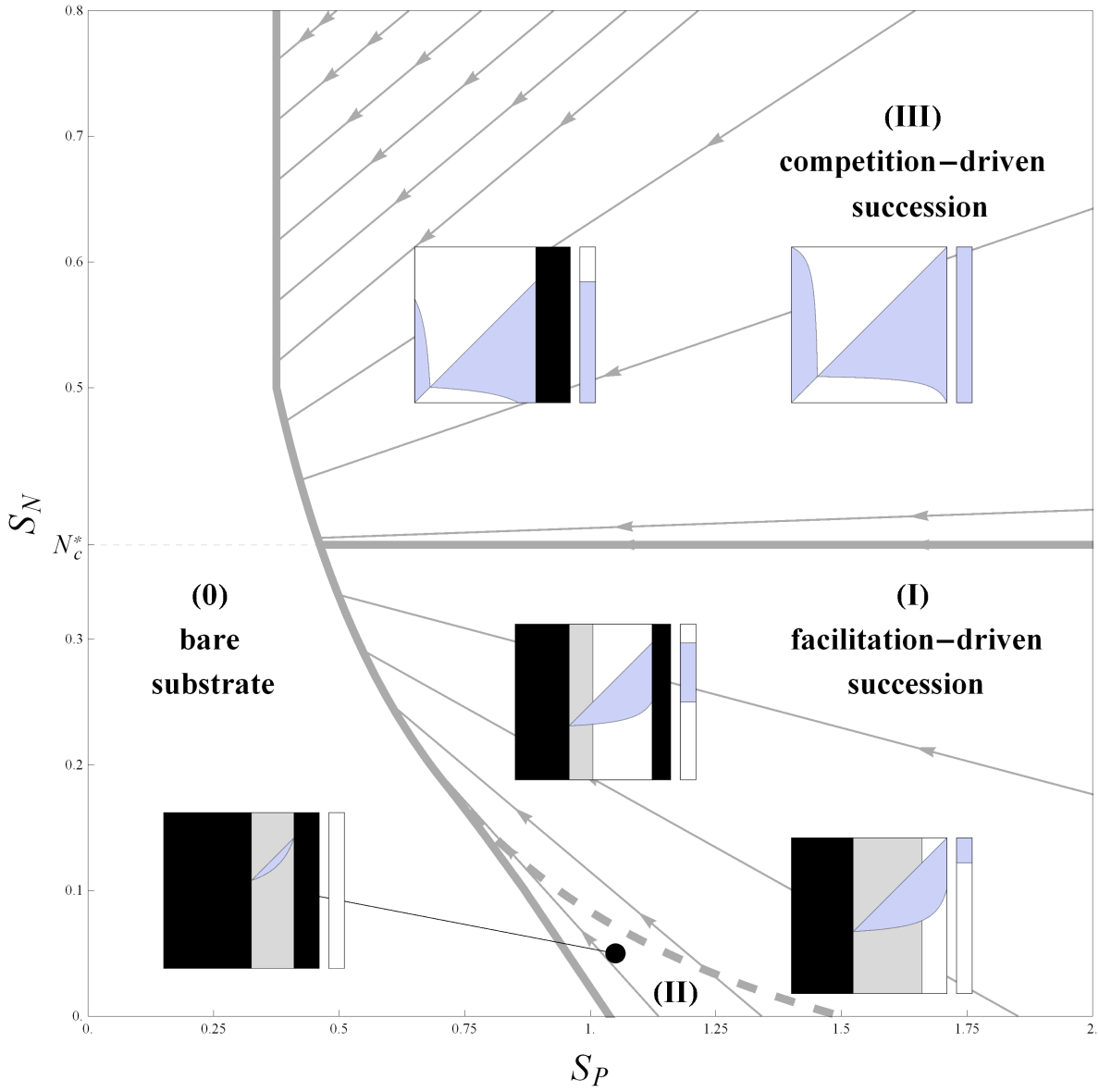

Figure 3.5: Community-level phase diagram summarizing the different succession scenarios along P and N abiotic supplies S_P and S_N. When N and P supplies are too low (white region on the left of the gray curve), not a single strategy can subsist and the ecosystem stays in the bare substrate state (0). Low N supply ($S_N < N_c^*$) favors high N-fixation rates with positive net impact on N, which leads to facilitation-based succession (I). High N supply ($S_N > N_c^*$) favors low N-fixation rate that do not compensate for N uptake, which leads to competition-based succession (III).

be read on Fig. 3.5 with the envelope and the impact vectors, similarly to the standard resource-ratio theory approach. First, because every succession endpoint resource level is located on the envelope, final soil N and P are anti-correlated. For example, the more N is supplied externally in

the system, the higher the N and the lower the P levels at the succession endpoint. The system responds differently to P substrate availability depending on the succession scenario. When competition-based, an increase in S_P leads to an increase in final soil P; the opposite happens in the facilitation case, as a P-richer bedrock will eventually lead to a more P-depleted soil. These non trivial results come from the coupling between the ecological positive feedback loop and the species sorting effects. This also explains why there is a community-level regulation of N-fixation around N_c^*, as the impact rays all tend to converge towards N_c^*. When taken separately, each plant species in the facilitation-based scenario is only P-limited, as an increase in S_N does not lead to an increase in biomass. This contrasts with the community-wide response to N addition, as the community endpoint biomass responds positively both to S_N and S_P increase due to species turnover.

3.5 Discussion

In this chapter, we show how facilitation-driven succession can emerge from successive colonization events by a diversity of N-fixing species in interaction with soil N and P. We characterize the traits, nutrient and biomass changes of the developing ecosystem during facilitation-driven succession and show that late succession presents an increasing sensitivity to catastrophic shifts. Finally, we show how changes in N and P external supplies can affect the succession scenario, shifting from facilitation-driven to competition-driven, and also control succession properties, such as initial variance, average speed and the endpoint characteristics of succession trajectories.

3.5.1 Succession scenarios and link with empirical studies

We have seen how the very basic mechanisms underlying facilitation-driven succession differ from other purely competition-based approaches, namely that the invasion success of non-pioneer species relies on the successful establishment and environment modification of previous strategies before them. This mechanism gives a straightforward way to empirically test for facilitation-driven succession, as was initially proposed by Connell and Slatyer (1977): experimentally remove the pioneer species and look if succession is affected. This gave evidence for facilitation-driven succession with rocky intertidal communities (Farrell 1991), but seemed to rule out this mechanism on old field secondary succession (Hils and Vankat 1982; Armesto and Pickett 1986) and in recent experiments on carrion (Michaud and Moreau 2017). Interestingly, this facilitation effect does not restrict itself to pioneer species, as every species facilitates the invasion of a next strategy after it. This means that every species has a role to play in succession, partially controlling its dynamics, and slowing it down when absent. Indeed, the mean succession time of facilitation-driven succession is expected to be an integrative function of the colonization rates of the whole species pool. This contrasts with competition-driven succession where the mean succession time is, in the absence of inhibition, essentially the inverse of the colonization rate of

the climax strategy and is expected to be much shorter. This gives another empirical way to look for facilitation-driven succession: randomly rarefy the species pool and look if it decreases the mean succession time. If opening a large gap in the species pool is technically possible and could completely block succession at an early stage, redundancy between closely functioning species — as can be estimated by the width of the positive invasion region on the PIPs — ensures a certain robustness of facilitation-driven succession to species loss. This is a sort of 'insurance effect' provided by this diversity of N-fixing strategies during ecosystem development (Yachi and Loreau 1999).

In our approach, we parsimoniously assumed equal colonization probability for every strategy. However, species differ in their dispersal and competitive abilities, as exemplified by the seed size/number trade-off (Turnbull et al. 1999), in turn leading to competition/colonization trade-offs that are at the core of the corresponding succession scenario (Tilman 1994). How would a classical competition/colonization trade-off combine with the facilitation-driven succession scenario? This would depend on how fixation efficiency correlates with dispersal ability. General information on such a correlation is lacking, but we can notice that N-fixing pioneers that can establish directly on the bare substrate tend to be very good dispersers, e.g. microorganisms that travel worldwide attached to dust particules (Gorbushina et al. 2007) or *Dryas drummondii* and its wind-dispersed plumed achenes (Lawrence et al. 1967).

Another classical competition-based succession mechanism is based on the r-K trade-off, where fast growing species first dominate the community before getting displaced by slower growing species (Huston and Smith 1987). In this scenario, there is no timescale separation or dispersal limitation as succession is the single transitory dynamics following initial seeding by all the possible strategies until the best competitor excludes all the others. Mean succession time would again essentially be the inverse of the growth rate of the climax species. By contrast, if we consider facilitation-driven succession in the absence of dispersal limitation, mean succession time would be longer. Indeed, it would resemble a sum of the inverse of the growth rates of the average species involved in the succession. We don't expect any positive correlation between growth rate and N-fixing efficiencies: growth rates of lichens and bacterial crusts, the very first pioneer strategies, are for example notoriously slow (around 50 years; Belnap and Eldridge 2001).

3.5.2 Sensitivity to catastrophic shifts

In our approach, we mentioned the increasing sensitivity to catastrophic shifts of facilitation-driven succession as we slowly converge towards the climax state. This means that if we were to explicitly include small random environmental perturbations in the model on ecological timescales, this would inevitably lead to the collapse of late succession towards the bare substrate. From there, succession would have to start again from scratch, with the initial colonization by a pioneer species. This means that in practice, facilitation-driven succession from our model would look more like a periodic alternation between developmental phase from pioneers

close to a climax and sudden collapses, closely resembling Watt's (1947) autogenic succession cycles. This kind of succession cycles have been observed empirically on simpler systems such as patchy associations between cacti and nursing shrubs (Valiente-Banuet et al. 1991). In contrast, competition-driven succession ends up with a climax strategy that is virtually forever stable unless a major perturbation removes it all at once from the system.

This late succession sensitivity to collapse is partially due to the plant's abrupt switch from N- to P- limitation around the colimitation point, which in turn explains the ESS structural unstability. A smoother transition, such as the one proposed in Schreiber and Tobiason's (2003) consumer-resource model, could override part of this effect. However, late succession alternate stable states are by definition unavoidable in facilitation-driven succession, and are a general consequence of strong positive feedback loops and facilitation (May 1977; Kéfi et al. 2016). Moreover, the increasing sensibility to collapse as we get close to the climax is a direct consequence of the opposition between the private cost of facilitation and its collective benefits, which selects for cheaters, an ecological phenomenon known as the tragedy of the commons (Hardin 1968) or evolutionary suicide (Gyllenberg and Parvinen 2001; Kéfi et al. 2008). Yet, some mechanisms such as spatial aggregation (Kéfi et al. 2016) or 'leakiness' from the recently proposed 'Black Queen Hypothesis' (Morris 2015) could stabilize these positive interactions, and reconcile our predictions with Odum's (1969) viewpoint on maximized stability of the succession climax.

3.5.3 Other mechanisms of facilitation and non-fixers

We focused our approach on nutrient-mediated interactions between plants, namely facilitation for N and competition for P. This is justified as these two resources are known drivers of plant succession (Menge et al. 2012) and the flip from a phosphorus-rich nitrogen-poor to phosphorus-poor nitrogen-rich ecosystem through succession matches empirical data (Vitousek et al. 1997; Richardson et al. 2004; Laliberté et al. 2012). However, the ways through which early colonists, N-fixing or not, can facilitate later invading species are plentiful (Bruno et al. 2003). They can improve soil physical structure and thus water infiltration (Klausmeier 1999; HilleRisLambers et al. 2001), provide shade to light-intolerant species (Gerla et al. 2011), protect from wind, detoxify (Rapaport 2017) or increase some nutrient availability through changes in soil pH (Hinsinger et al. 2011). All these facilitation mechanisms could add up or interfere with our purely N centered approach. Still the general characteristics of facilitation-driven succession highlighted by our study, e.g. in terms of bistability and PIP properties, are expected not to be too sensitive to the details of the facilitation mechanism. Moreover, such a nutrient based facilitation mechanism enabled us to use the graphical tools of contemporary niche theory, i.e. the requirement and impact niches, an efficient way to visualize positive feedback loops and alternate stable states (Koffel et al. 2016).

As soil organic matter accumulation through biomass turnover can lead to better soil properties and nutrient retention, any plant can turn into a facilitator under the right circumstances.

An approach based on decreased leaching rates through soil organic matter build up could thus also explain how N-fixing strategies can get completely excluded by non-fixers in late-succession without leading to ecosystem collapse (Chapin et al. 1994; Menge et al. 2008). This could in turn also lead to decreased nutrient leaching rate during succession instead of increase, a pattern more consistent with empirical observations (Odum 1969).

3.5.4 Long time scale bedrock P depletion

We assumed that P was released from the bedrock at a constant weathering rate, as modeled by the fixed P supply parameter S_P. However, bedrocks eventually become P-depleted on geological timescales, typically from thousand to million years (Vitousek et al. 1997; Menge et al. 2012), so the P supply S_P should decrease accordingly. The consequences of this P depletion on the climax community – here the ESS – is easy to study as this third timescale is much slower than the community assembly timescale (Fortelius et al. 2015), and can be visualized in Fig. 3.5 by moving through the diagram from the right to the left. In the facilitation-driven case, this leads to a decrease in soil N but, paradoxically, an increase in soil P, as was noted in the 'A resource-ratio theory of succession' subsection. Consistent with observations on ecosystem regression (Vitousek et al. 1997; Wardle et al. 2004; Peltzer et al. 2010), P depletion also leads to a decline in ecosystem biomass. If N supplies are low enough, P supply depletion brings the ecosystem in region (II), the community-level alternate stable region, where the climax state can persist but succession could not have initiated, causing a delay in ecosystem regression. On the edge between region (0) and region (II), ecosystem regression ends up abruptly through a sudden transition, or catastrophic shift, to the bare substrate (Scheffer et al. 2001).

3.5.5 Evolutionary interpretation

In our approach, the on-site successive competitive displacements that drive succession were fueled by a standing, regional, inter-specific variability. If, instead, we consider this variability to be intraspecific and generated by small mutations, our results can be read as an eco-evolutionary study of nitrogen fixation with adaptive dynamics (Hofbauer and Sigmund 1990; Dieckmann and Law 1996; Geritz et al. 1997, 1998). Following this perspective, our model predicts that under low N availabilities, evolution would lead high nitrogen-fixing species to systematically decrease their fixation abilities, getting dangerously close to 'evolutionary suicide'. This is consistent with other evolutionary studies on the evolution of facilitation, e.g. in arid ecosystems with high plant dispersal (Kéfi et al. 2008). These results can also be linked to evolutionary niche construction (Odling-Smee et al. 1996, 2003) in the presence of positive plant-soil feedbacks. In this regard, our results are consistent with Kylafis and Loreau's (2008) study, where the evolutionary feedback loop leads to the regulation of nutrient availability by the plant along nutrient gradients.

3.5.6 Insights on niche theory

Our approach brings several insights into contemporary niche theory. In particular, they give a mechanistic example of a model where the establishment or invasion niche and the persistence niche do not coincide — the latter being broader than the former — leading to alternate stables states that can also be seen as a resource-mediated Allee-effect (Holt 2009a). Graphically, this phenomenon can be interpreted in terms of the impact and sensitivity components of the niche, and basically originates from the impact rays overshooting the ZNGI. This is an example of how to use the graphical approach to niche theory to identify alternate stable states, as suggested in one of our former work (Koffel et al. 2016). Moreover, the total N-fixer case is an example of net positive feedback loops not being sufficient to ensure alternate stable states (Kéfi et al. 2016), and can here be understood in terms of necessarily dissimilar invasion and persistence niches.

3.5.7 Conclusion and perspectives

In this chapter, we showed how facilitation-driven succession can emerge from successive colonization events by a diversity of N-fixing species in interaction with soil N and P, using an approach based on contemporary niche theory. We suggest two non-mutually exclusive stimulating directions to complexify this model and address some of the limits of our approach. First, combining a guild of non-fixing plants with a reduced leaching effect from accumulated dead organic matter in the soil could enable to study coexistence between fixers and non-fixers in the course of succession and the possible exclusion of the fixers in late succession. Second, taking space explicitly into account would probably lead to spatial aggregation during succession with interesting consequences on facilitation, and possibly a stabilizing effect during late succession regarding catastrophic shifts.

Appendices

3.A Analytical results of ecological model

3.A.1 Equilibria

There are four cases to consider.
The first equilibrium, called $\emptyset$, is trivial: as $B = 0$, we get from eq. (3.2a) that $N = S_N = I_N/l_N$ and $P = S_P = I_P/l_P$.This equilibrium always exists; we will see in the next subsection when it is stable.
The non-zero biomass equilibrium presents three alternate possibilities. First, let us assume that B is P-limited without fixation, i.e. $g_P(P) < g_N(N)$. We will come back later to the parameter configurations corresponding to this condition. We then get from eq. (3.2a) that $P = P^* = g_P^{-1}(m)$. Then B can be deduced from eq. (3.2b) as being equal to:

$$B = \frac{l_P}{q_P}\frac{S_P - P^*}{(1-\lambda)m} \tag{3.4}$$

and from eq. (3.2c) we get:

$$N = S_N - \frac{q_N}{l_N}(1-\lambda)mB \tag{3.5}$$

Combining these results with the "P-limitation without fixation" condition, this leads to $N > N^*_{nf}$ and thus $\gamma(S_N - N^*_{nf}) > S_P - P^*$ where $N^*_{nf} = g_N^{-1}(m)$ and $\gamma = l_N q_P / l_P / q_N$ with the extra-condition $B > 0$ i.e. $S_P > P^*$.

A second possibility is when the plant is P-limited while fixing, i.e. $g_N(N) < g_P(P) < g_N(N) + F$. In this case, we still get from eq. (3.2a) that $P = P^* = g_P^{-1}(m)$ and the same value for B. However, N is now the solution of the implicit equation:

$$0 = l_N(S_N - N) - q_P[g_N(N) - \lambda m]B \tag{3.6}$$

It is is not possible to come up with a general analytical solution. However, the solutions can be drawn graphically using the supply point map.

Combining these results with the "P-limitation with fixation" condition, this leads to $N^*_{nf} > N > N^*_f$ and thus $\gamma(S_N - N^*_{nf}) > S_P - P^* > \phi\gamma(S_N - N^*_f)$ where $N^*_f = g_N^{-1}(m - F)$ and $\phi = (1 - \lambda m)/(g_N(N^*_f) - \lambda m)$ with the extra-condition $B > 0$ i.e. $S_P > P^*$.

The last possibility is when the plant is N-limited while fixing, i.e. $g_N(N) + F < g_P(P)$. In this case, we now get from eq. (3.2a) that $N = N^*_f$. Then B can be deduced from eq. (3.2b) as being equal to:

$$B = \frac{l_N}{q_N} \frac{S_N - N^*_f}{g_N(N^*_f) - \lambda m} \tag{3.7}$$

and from eq. (3.2c) we get:

$$P = S_P - \frac{q_P}{l_P}(1 - \lambda) m B \tag{3.8}$$

Combining these results with the "N-limitation" condition, this leads to $P > P^*$ and thus $\gamma(S_N - N^*_{nf}) > S_P - P^*$ with the extra-condition $B > 0$ i.e. $S_P > P^*$.

3.A.2 Stability

The general Jacobian of eq. (3.2) writes:

$$\boldsymbol{J}(B, P, N) = \begin{pmatrix} g_{\text{tot}} - m & \partial_P g_{\text{tot}} B & \partial_N g_{\text{tot}} B \\ i_P & -l_P + \partial_P i_P B & \partial_N i_P B \\ i_N & \partial_P i_N B & -l_N + \partial_N i_N B \end{pmatrix} \tag{3.9}$$

where the notations $i_P(P, N) = -q_P[g_{\text{tot}}(P, N) - \lambda m]$ and $i_N(P, N) = -q_N[\min[g_P(P), g_N(N)] - \lambda m]$ designate the per capita net impacts of N-fixers on P and N. In the case of equilibrium $\emptyset$, i.e. for $B = 0$, $N = S_N$ and $P = S_P$, we have:

$$\boldsymbol{J}(\emptyset) = \begin{pmatrix} \min[g_P(S_P), g_N(S_N) + F] - m & 0 & 0 \\ i_P & -l_P & 0 \\ i_N & 0 & -l_N \end{pmatrix} \tag{3.10}$$

the three eigenvalues are located on the diagonal; we conclude from the condition $\min[g_P(S_P), g_N(S_N) + F] - m < 0$ that the empty equilibrium $\emptyset$ is locally stable only when the fixing plant cannot invade, i.e. for supply points located under the L-shaped ZNGI. For the other equilibrium B, we

can simplify:

$$\boldsymbol{J}(B,P,N) = \begin{pmatrix} 0 & \partial_P g_{\text{tot}} B & \partial_N g_{\text{tot}} B \\ i_P & -l_P + \partial_P i_P B & \partial_N i_P B \\ i_N & \partial_P i_N B & -l_N + \partial_N i_N B \end{pmatrix} \tag{3.11}$$

When the plant is P-limited and does not fix, this leads to:

$$\boldsymbol{J}(B,P,N) = \begin{pmatrix} 0 & \partial_P g_P B & 0 \\ -q_P(1-\lambda)m & -l_P - q_P \partial_P g_P B & 0 \\ -q_N(1-\lambda)m & -q_N \partial_P g_P B & -l_N \end{pmatrix} \tag{3.12}$$

which means than $\lambda_N = -l_N$, $\lambda_- \lambda_+ = q_P(1-\lambda)m\partial_P g_P B$ and $\lambda_- + \lambda_+ = -l_P - q_P \partial_P g_P B$; thus, all the eigenvalues are negative and this equilibrium is always locally stable. When the plant is soil N-limited and fixes until limited by P, this leads to:

$$\boldsymbol{J}(B,P,N) = \begin{pmatrix} 0 & \partial_P g_P B & 0 \\ -q_P(1-\lambda)m & -l_P - q_P \partial_P g_P B & 0 \\ -q_N(g_N - \lambda m) & 0 & -l_N - q_N \partial_N g_N B \end{pmatrix} \tag{3.13}$$

which, pretty similarly to the previous case, means than $\lambda_N = -l_N - q_N \partial_N g_N B$, $\lambda_- \lambda_+ = q_P(1-\lambda)m\partial_P g_P B$ and $\lambda_- + \lambda_+ = -l_P - q_P \partial_P g_P B$; thus, all the eigenvalues are negative and this equilibrium is always locally stable. Finally, when the plant is N-limited while fixing:

$$\boldsymbol{J}(B,P,N) = \begin{pmatrix} 0 & 0 & \partial_N g_N B \\ -q_P(1-\lambda)m & -l_P & -q_P \partial_N g_N B \\ -q_N(g_N - \lambda m) & 0 & -l_N - q_N \partial_N g_N B \end{pmatrix} \tag{3.14}$$

which means that $\lambda_P = -l_P$, $\lambda_- \lambda_+ = q_N(g_N - \lambda m)\partial_N g_N B$ and $\lambda_- + \lambda_+ = -l_N - q_N \partial_N g_N B$. Now, the sign of $\lambda_- \lambda_+$ can be positive. This happens if and only if $N_F^* < N_c^*$, i.e. in the high fixing situation.

These analytical results prove what has been displayed in this chapter, i.e. that all non-zero biomass equilibria are locally stable except the N-limited branch in the high fixation situation.

3.B Competition-driven succession

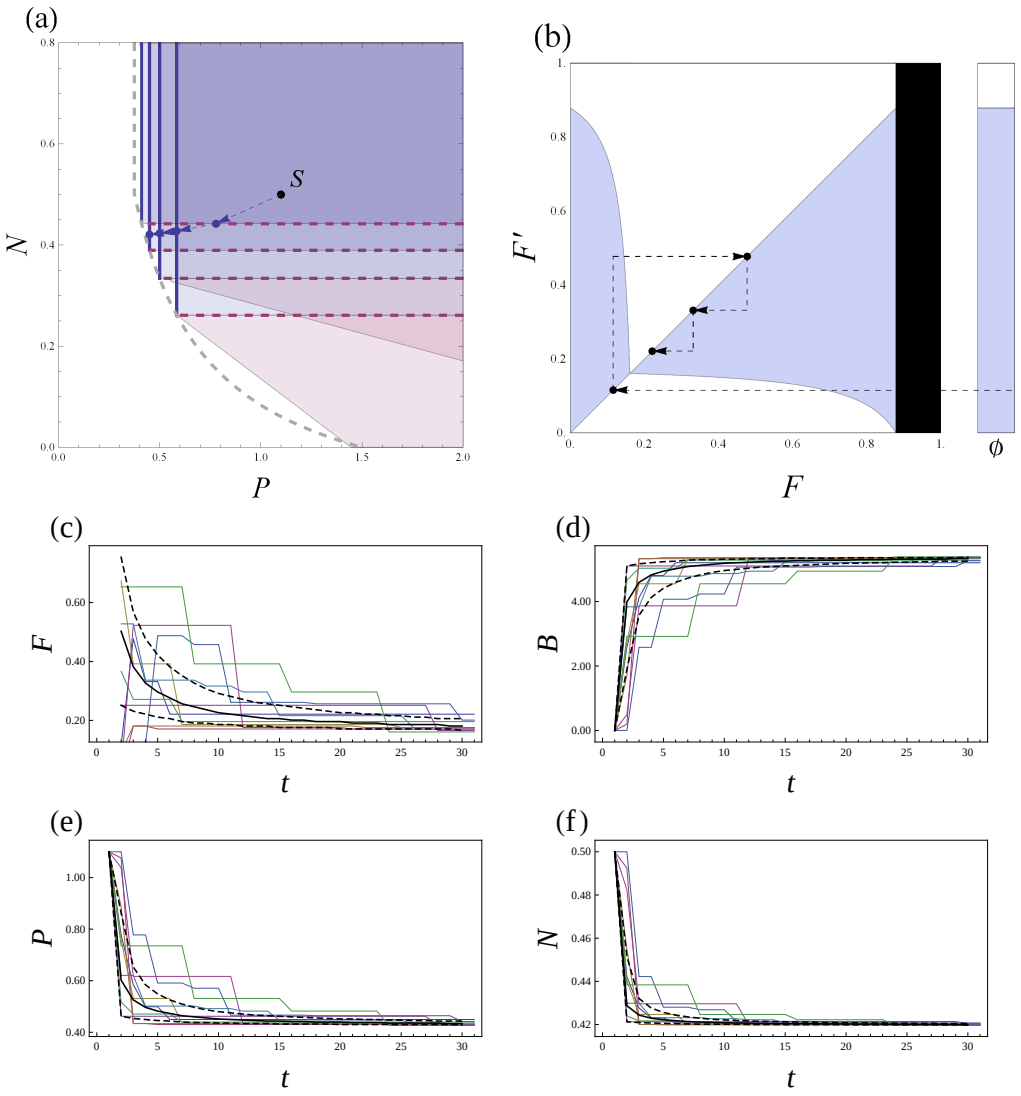

Figure 3.6: Competition-driven succession trajectories, under high N and high P supply, i.e. $S = (S_P, S_N) = (1.1, 0.5)$. Compare with facilitation-driven succession in Fig. 3.4. Contrary to facilitation-driven succession, there is a strong variability in ecosystem properties (c-f) in the early stages of succession. Also note that competition-driven succession relaxes on a faster timescale.

Discussion

Plant-environment interactions are dual in nature: the environment selects the most adapted plants, and selected plant in turn shape their physical and biotic environment. Put together, these reciprocal interactions create a feedback loop that couples plant adaptation and ecosystem regulation. In this thesis, we developed a general framework based on contemporary niche theory to address this coupling between plant adaptation and ecosystem functioning along nutrient gradients, and applied it to two relevant ecological situations, namely the evolution of plant defenses and competitive ability for resources, and the process of succession by nitrogen-fixers.

We showed in Chapter 1 how the general framework of contemporary niche theory could be extended to account for a dense turnover of plant strategies along nutrient gradients, and how this enables the study of eco-evolutionary dynamics and community assembly with the associated graphical approach. We showed that the eco-evolutionary dynamics and community assembly perspectives only differed formally by the range of invaders considered, from closely-resembling mutants to any strategy in the global species pool. Such difference in turn leads to different dynamics and stability properties of their equilibria. We also highlighted the fact that a general fitness function does not depend on the impact niche, which means that impact is never under direct selection.

In Chapter 2, we applied this extended framework to the study of the adaptive response of plants between resource acquisition, tolerance and resistance to herbivores, in a small food web module along a resource gradient. We showed how the high-end of the resource gradient, associated with high herbivore abundance because of trophic transfers, resulted in either the dominance of a very resistant strategy or evolutionarily stable coexistence between a completely inedible strategy and a fast-growing, tolerant one. On the ecosystem properties side, both scenarios lead to a trophic dead-end as nutrients accumulate in the plant compartment.

In Chapter 3, we showed how facilitation can emerge from the presence of nitrogen-fixing plants and nutrient recycling. The successive colonization of an initially bare substrate by such N-fixing strategies with differing fixing efficiencies in turn leads to facilitation-driven succession and ecosystem development. Such a succession scenario was characterized by increasing nitrogen availability through time, relatively ordered sequence of strategy replacement and late succession sensitivity to catastrophic shifts. We also showed that facilitation-driven succession turns into competition-driven succession along an increasing N gradient.

Put together, these results show how selection mediated by the environmental feedback loop jointly determines the traits of the dominant plant strategies and impacts the dynamical and equilibrium properties of ecosystems. As we show using our eco-evolutionary graphical approach, such selection leads to a turnover in plant strategy along nutrient gradients. This turnover, in turn, affects the regulation of ecosystem functions along the gradient: plant adaptation, i.e. trait change, can either add up to, or conversely totally counteract a purely ecological response, i.e. change in density with traits kept fixed.

This complex 'eco-evolutionary' response of the ecosystem along the environmental gradient is illustrated by our results in Chapter 2: both the emergence of a trophic dead-end at the high-end of the gradient, or the hump-shaped plant density pattern associated with tolerance allocation alter the classical top-down-controlled pattern of saturating plant biomass of the purely ecological case. Similarly, the resource-ratio theory of succession presented in Chapter 3 presents an 'abnormal', i.e. decreasing, response of the climax to phosphorous enrichment in the facilitation regime that can only be explained by species turnover. Not only are long-term or climax characteristics of the ecosystem shaped by selection through the environmental feedback loop, but also its developmental trajectory. This is exemplified by Chapter 3, where succession itself is driven by a turnover of strategies and the associated modification of their environment. Let us now discuss a few general perspectives emerging from the different questions addressed in this dissertation.

Regulation of biogeochemical cycles and niche theory

A central question in this thesis was to understand how adaptive strategy turnover along environmental gradients affects the regulation of biogeochemical cycles. Before addressing this aspect, let us first clarify what we mean by regulation and second discuss regulation by the biotic compartment in the absence of strategy turnover, i.e. through their purely demographic response, using the graphical approach.

Regulation can be defined as the mechanism through which a system persists in a given state by buffering or attenuating the effects of external perturbations. As was discussed in the introduction in the context of population regulation, regulation originates from negative feedback loops. There are two principal ways to think about regulation. First, regulation can be thought of as being dynamical, bringing the system back to its equilibrium after a sudden perturbation of a state variable. The strength of regulation is then related to the dynamical stability of this equilibrium, or equivalently to the inverse of its relaxation time (Pásztor et al. 2016). Second, regulation can be thought of as being structural, i.e. buffering the effects on the system of a permanent external perturbation, like a change of parameter value. The strength of regulation is then quantified by the robustness of the equilibrium considered to parameter change, related to sensitivity analysis in ecology (Barabás et al. 2014b). Note that these two measures of regulation

strength or stability are related (Arnoldi et al. 2015; Arnoldi and Haegeman 2016). In this thesis, we implicitly adopt the second, i.e. structural, viewpoint on regulation regarding biogeochemical cycles, as we focus on the response of the ecosystem along environmental gradients. Finally, note that the strength of regulation fundamentally depends on the ecosystem function of interest: ecosystem biomass and nutrient concentrations at equilibrium do not respond the same way to a given perturbation.

Let us now clarify some aspects of ecological regulation by a biotic compartment along environmental gradients and see how they relate to the basic ingredients of contemporary niche theory. From now, we will focus our attention on the regulation of the limiting factors, particularly nutrient concentrations. The first striking result comes from contemporary niche theory and is reminded in Chapter 1: the presence of a single population at equilibrium constrains the limiting factors to this population's ZNGI. That is, the two-dimensional potential variations along environmental gradients are funneled down on a one-dimensional curve, leading to a strong regulating effect. The second aspects of regulation are linked to the impact vectors, because they control how supply points are mapped to the equilibria on the ZNGI. For example, some perturbations are more regulated than others depending on the direction of this perturbation relatively to the direction of the impact vector. Indeed, as all the supply points along a given impact ray map to the same point on the ZNGI, a perturbation along an impact ray leads to total regulation, i.e. no response of the limiting factors at equilibrium. Two other important factors that control regulation strength are the geometry of the impact ray family towards the ZNGI (convergent, parallel or divergent, like for a beam of light) and the distance of the supply point from the ZNGI (a graphical proxy for population biomass). As can be intuited graphically, a convergent family of impact rays strengthens the regulation, even more so with higher distance from the ZNGI. Indeed, this means that a wide range of supplies are concentrated in a small region of limiting factor levels on the ZNGI at equilibrium. This is what happens with both interactive essential and antagonistic resources in Chapter 1 (Fig. 1.2), and with nitrogen fixers in Chapter 3 where the fixation mechanism tends to regulate soil nitrogen around N_c^* (Fig. 3.2). Parallel impact rays are neutral in terms of regulation, and do not interact with distance from the ZNGI. This is the case with the most used model of contemporary niche theory, completely essential resources (Tilman 1982, 1988), and also happens under high nutrient supplies in Chapter 2 (Fig. 2.3). Finally, a divergent family of impact rays leads to a looser regulation, even more so with higher distance from the ZNGI. This happens under low nutrient supplies in Chapter 2 (Fig. 2.3). Such loose regulations usually signal that the equilibrium is getting close from losing stability, with the presence of alternate stable states nearby. Finally, note that coexistence of two species, such as represented in Chapter 1 and 2, leads to perfect regulation of the limiting factors in the coexistence region, as all the supply points converge towards the same coexistence point at the intersection of the two ZNGIs.

Strategy turnover and regulation of biogeochemical cycles

Having introduced the core concepts on regulation in the previous paragraph, we can now address the more complex subject of eco-evolutionary regulation, i.e. the ecosystem response to a perturbation when adaptive strategy turnover is accounted for.

As we have seen in the previous section, ecosystems respond to nutrients gradients by changing the densities of their components at equilibrium, such as plant biomass and nutrient concentrations. However, this also means that the selective forces at play change, leading to changes in the dominant plant traits. This change of dominance cascades back in changes in the environmental components, again modifying the selective forces, etc. Our eco-evolutionary approach to contemporary niche theory graphically solves this complex effect of the adaptive feedback loop along nutrient gradients. The resulting ZNGI envelope, now integrating the adaptive trait turnover, can be used the same way as a regular ZNGI. This means that we can use the same graphical arguments of the previous section to address eco-evolutionary regulation.

Going back to Chapter 1, we can see in the essential resource case that accounting for adaptive turnover does not fundamentally alter the regulation pattern, as the impact rays are loosely convergent (Fig. 1.3B), similarly to the purely ecological case (Fig. 1.2A). In the antagonistic case, however, adaptation completely flips the regulation pattern, as the impact ray family shifts from convergent to divergent (compare Fig. 1.2B and 1.5A). Interestingly, this strong deregulation due to adaptive turnover is associated with branching, an 'eco-evolutionary instability', but eventually leads to perfect regulation through the emergence of two coexisting specialists (Fig. 1.4B).

In Chapter 2, we have seen a good example of how adaptive turnover can affect the regulation pattern. As a reminder, the purely ecological situation leads to a strong regulation of both plant and herbivore densities along the high-end of the increasing nutrient gradient, with the nutrient pool left unregulated. On the contrary, both scenarios 1 and 2 converge towards perfect regulation of the nutrient pool and herbivore density at the high-end of the gradient, as can be seen with the convergence of the impacts rays (Fig. 2.8, 2.9). This is the signature that the food chain evolves towards a trophic dead-end through the inedibility of the plant, reversing the trophic cascade towards top-down control of the resource.

In Chapter 3, the global pattern of nitrogen regulation when accounting for adaptive turnover is similar to the purely ecological case, with a tendency to regulate nitrogen levels around N_c^*. This comes from the way we modeled nitrogen fixation: we assumed that plants could physiologically regulate their fixation ability to fix proportionally to their needs, and that this regulation mechanism was the same for all species (same N_c^*). Other patterns of N-fixation regulation at the individual level (e.g. Menge et al. 2009a) combined with differences in regulation between species could potentially lead to other regulation patterns at the global scale.

Understanding the emergence of such regulation patterns of nitrogen are central to address longstanding questions of biogeochemistry, such as the control of deep ocean stoichiometry

(Lenton and Klausmeier 2007), the effect of raising CO_2 on primary production (Oren et al. 2001; Reich et al. 2006), the maintenance of N-limitation despite the presence of N-fixers (Vitousek and Howarth 1991; Vitousek et al. 2002) and conversely the nitrogen paradox in tropical forests where N is readily available but N-fixation does not seem to be down-regulated (Hedin et al. 2009). Our approach insists on the fact that individual-level regulation patterns cannot be considered independently from the competitive, game-theoretical context in which they live. Only by accounting for selection and the resulting functional turnover can we assess and understand regulation and limitation patterns at the community or ecosystem scale (e.g. Danger et al. 2008).

New developments in contemporary niche theory

As was motivated in the introduction of this manuscript, contemporary niche theory is a well-adapted theoretical and conceptual framework for the study of plant-environment reciprocal interactions. Moreover, the associated graphical approach provides a visual and intuitive tool to analyze and depict the outcome of interactions between an either discrete or dense and unlimited number of strategies along two dimensional environmental gradients. Here, we discuss the clarifications and advances brought by this thesis to contemporary niche theory.

In Chapter 1, we aimed at laying down a general class of models underlying this graphical approach. Even though it was not the case in its early developments, contemporary niche theory is often restricted to its most widespread examples with straight ZNGIs portions, namely the essential and perfectly substitutable resource cases. We would advocate that this viewpoint is too narrow and can lead to imprecise conclusions when taken for a general definition of contemporary niche theory (Kleinhesselink and Adler 2015; Letten et al. 2017). In the formalism of Chapter 1, the net growth rate, and thus the ZNGI shape, have not been imposed any particular shape, as long as growth rate is a continuous function of the limiting factors. The classical assumption of monotony is also unnecessary, as our approach can deal with unstable or alternate stable equilibria. For example, high availability of some resource can lead to an inhibitory effect of growth or increased mortality, such as photoinhibition (Gerla et al. 2011) or toxicity of a nutrient under high concentrations (Haldane 1930; Andrews 1968; Harmand et al. 2017). Following Levin's (1970) extended competition exclusion principle and Holt's (1977) apparent competition framework, our approach does also not restrict itself to resource competition. On the contrary, it can be used to account for any type of limiting factors – also called regulating factors – (Levin 1970; Chase and Leibold 2003; Meszéna et al. 2006; Pásztor et al. 2016) with either positive or negative impacts, as exemplified by Chapter 2 with herbivores, or the facilitation case of Chapter 3 where nitrogen is not regulating *per se* because of the positive feedback loop (See Table 4.1). By accounting for any regulating factors, with any interactions between themselves and within population growth, and any impact of this population back on

the regulating factors, we advocate that the formalism we presented in Chapter 1 provides a satisfying general formal definition of contemporary niche theory on which to build on, in the continuity of previous approaches (Chase and Leibold 2003; Meszéna et al. 2006; Pásztor et al. 2016). To understand how niche theory can deal with non-monotonous growth rates, it is neces-

Table 4.1: The four possible impact niche and requirement niche sign combinations. Two of these combinations lead to positive feedback loops (red). In resource consumption, the plant consumes (− impact) a resource needed for growth (+ requirement). In predation, the plant feeds (+ impact) a predator that harms it (− requirement). In N-fixing + recycling, a plant enriches (+ impact) the soil N that it also needs to grow (+ requirement). Finally in resource inhibition, a plant consumes (− impact) a resource that is toxic (− requirement).

		Requirement	
		−	+
Impact	−	resource inhibition (Andrews 1968; Gerla et al. 2011)	resource consumption (R_i, R and P in Chapters 1, 2 and 3)
	+	predation (Z in Chapter 2)	N-fixing + recycling (N in Chapter 3)

sary to understand how the impact vectors combine with the ZNGI to map a given supply point to its corresponding equilibria, as was done in Chapter 1. We showed that this approach can associate several potential equilibria to some unique environmental conditions, i.e. that a unique supply point can lead to alternate stable states. As discussed in Chapter 1, these alternate stable states can be of diverse natures: between two non-zero equilibria of a single species (e.g. some stage-structured models), between an empty state and a non-zero equilibrium (positive feedback loop, from inhibition or facilitation such as in Chapter 3), between the non-zero equilibria of two species (classical priority effects), between coexistence of two species and a third one, etc. For all these situations, it suffices to identify the uninvadable ZNGI portions and draw the impact rays that originate from them: supply regions where this impact rays overlap then give the supply points for which alternate stable states occur. The characteristics of these alternate states can also be read graphically, such as their resource levels at equilibrium or their stability.

In Chapter 3, we applied this graphical analysis of alternate stable states to a situation that is particularly relevant biologically, facilitation that originates from a positive feedback loop of N-fixers on soil nitrogen. This gave a mechanistic example of how to extend contemporary niche theory to facilitation (Holt 2009b). Interestingly, this also gives an example of a situation where two niche concepts do not overlap: the 'invasion niche' or 'establishment niche', that describes the environmental conditions under which a given strategy can invade from arbitrarily low density, and the 'persistence niche', that describes the environmental conditions under which a population of a given strategy can persist at equilibrium (Holt 2009a). This expresses the fact that a critical density of N-fixing strategies is required for the positive feedback loop to overcome nitrogen leaching out of the system, an example of nutrient-mediated Allee-effect

(Courchamp et al. 1999). This facilitation mechanism, in turn, leads to a niche-theory-based interpretation of how the previous establishment of a pioneer species enables the invasion of such a Allee-effect-prone population, as described in Chapter 3 through the facilitation-driven succession step. This echoes back to the idea that the realized niche of a species can exceed its fundamental niche in the presence of a facilitator (Bruno et al. 2003). When combined, the fundamental vs. realized and establishment vs. persistence niche concepts can lead to a variety of new situations to investigate, with potentially fundamental implications for example in species distribution modeling. Finally, as was advocated by Holt (2009b), one of the strength of such mechanistic models of facilitation is that the shift from facilitation to competition along environmental gradients — a general phenomenon according to the stress gradient hypothesis (Bertness and Callaway 1994) — naturally emerges from the plant-environment interactions without the need to introduce ad hoc ingredients, as exemplified by the shift from facilitation-driven to competition-driven succession in Chapter 3.

Finally, Chapter 1 showed how contemporary niche theory and its graphical approach can be generalized to study a continuum of competing strategies. This generalizes previous approaches with a large number of discrete strategies (Tilman 1982, 1988; Chase and Leibold 2003) or a continuum of strategies competing for essential resources (Klausmeier et al. 2007; Danger et al. 2008). As was discussed in Chapter 1, this continuum of strategies or traits can emerge at different spatial or temporal scales, from individual plasticity, to 'hyperdiverse' regional species pool and long-term evolution through small mutation steps. In all these cases, the envelope approach of Chapter 1 enables to merge the set of individual niches with fixed strategies, materialized by the ZNGI family, into a collective 'meta' niche, the ZNGI envelope. This meta-niche formally behaves like a standard single-strategy niche, excepted that it accounts for trait plasticity that emerges from strategy turnover through selection. This echoes back to Holt's (2009a) evolutionary niche concept, and provides a rigourous, i.e. selection-based, tool to navigate across levels of organization, from individuals to ecosystems (Smith et al. 2011; Norberg 2013; Haegeman et al. 2016).

To conclude this section, we introduced in this thesis a general mathematical framework for contemporary niche theory. This framework, by its generality, enables us to address and combine a variety of ecological situations using contemporary niche theory tools, such as alternate stable states, facilitation, eco-evolutionary dynamics and ecosystem functioning. These contemporary niche theory modules can in turn serve as building blocks to feed more detailed and predictive ecological models along environmental gradients, such as species ranges in biogeography (Godsoe et al. 2017) or the coupled response of the biotic and abiotic oceanic compartments to global change (Follows et al. 2007; Thomas et al. 2012; Litchman et al. 2015).

Selection on the impact niche and niche construction

An important result, although seemingly tautological, of Chapter 1 is that the fitness of an invader is only determined by its requirement niche, materialized by the ZNGI. Indeed, the invasion fitness *is* the requirement of the invader to the conditions imposed by the resident population. Conversely, this means that the impact niche does not contribute to the invasion fitness. Even though obvious, this result is made more clear in our framework where the environment mediating the mutant-resident interaction is kept explicit, and the environmental feedback loop is split between its requirement and impact components. A strong consequence of this results is that the impact niche is never under direct selection. Indeed, invading rare mutants are at first not numerous enough to affect the environment — its properties being only determined by the dominating resident —, so their impact on the environment can not be the target of selection. This appears as a fundamental conundrum when trying to understand adaptive niche construction, i.e. how can evolution lead species to modify their environment, especially positively, if natural selection does not see this impact? The following section proposes some ways to move forward this apparent contradiction.

A first way out is to notice that requirements and impacts are not independent, because multiple constraints such as mass balance link the two processes. This is obvious when looking at the simple consumer-resource models used in this manuscript, where a given nutrient uptake translates into an equivalent biomass growth multiplied by some fixed stoichiometric coefficent. Even when this relationship is lose, such as in the case of luxurious consumption (van den Driessche 1974; Chapin 1980; van Wijk et al. 2003) or in the Droop model (Droop 1968; Oyarzun and Lange 1994; Klausmeier et al. 2007; Lemesle and Mailleret 2008), acquisition and growth are never totally uncorrelated. Indeed, mass balance again constraints uptake and growth at equilibrium as internal nutrients can not accumulate indefinitely. This means that direct selection on traits affecting plant growth indirectly cascades onto its impact on the resource through mass balance. Finally, an ecological or allocation trade-off could link the trait under selection with traits that influence the impact. Chapter 3 gives an example of how sensitivity and impact can be linked, with both fixation efficiency and phosphorous acquisition being under selection and affecting back the plant impact on the resources as they evolve. As a consequence, we have seen that this leads the positive impact, and thus facilitation, to decrease throughout the eco-evolutionary trajectory. This effect is compensated by increased phosphorus efficiency leading to increased total plant biomass and maintained fixation flux, but ends up in extreme sensitivity to catastrophic shift as the climax or ESS is reached, i.e evolutionary suicide. This, again, is a proof that the positive impact leading to facilitation is not directly under selection, but only evolves indirectly.

So, is genuine selection on impact possible, i.e. can evolving species really be selected on their ability to modify, especially positively, their environment? There is ample evidence for that in the niche construction, altruism and cooperation literature. So, what are the missing

ingredients in our niche-based approach? The main issue here comes from the tragedy of the commons (Hardin 1968; Rankin et al. 2007). Indeed, our modeling framework implicitly assumes well-mixed populations, which, in the case of resource-mediated interaction, translates into a completely public, i.e. shared by all the individuals, resource pool. This means that if positive impacts are costly, a selfish strategy can just cheat by not paying this cost while still benefiting from the collective improvement by the other strategies. The long-term outcome is population collapse and has been coined 'evolutionary suicide' in the eco-evolutionary literature, and can happen either suddenly with a catastrophic shift (Gyllenberg and Parvinen 2001; Kéfi et al. 2008) or asymptotically (Boudsocq et al. 2011). Similarly to human systems, a solution to avoid the tragedy of the commons consists in introducing some sort of privatization of the common good. This can be achieved by breaking the homogeneity of the resource, recognizing that individuals have a privileged access and influence on nearby resources. The role played by spatial heterogeneity at different scales is particularly obvious with terrestrial plants: soil properties vary greatly with substrate characteristics, plants movements are fundamentally restricted, interactions between plants preferentially occur between neighbors through shading and root proximity and reproduction is often also relatively local through vegetative growth or seed dispersal (Hutchings 1986; Huston and DeAngelis 1994; Stoll and Weiner 2000; Casper et al. 2003).

This naturally leads us outside the modeling scope of this manuscript, with the consideration of space-explicit models. Indeed, we suspect that including space is an unavoidable ingredient to explain selection on impact and, more generally, the emergence and stabilization of positive interactions within ecosystems. For example, building on standard mean-field plant-soil modules (Boudsocq et al. 2011; Loeuille et al. 2017), the inclusion of space enabled to avoid the pessimization principle, or Tilman's R^* rule, a clear signature of the absence of selection on impact (Barot et al. 2014, 2015). More generally, spatially explicit setups with limited dispersal are known for enabling spatial self-clustering and mutant-mutant interactions, which in turn can stabilize positive interactions between neighbors on evolutionary timescales (Lion and van Baalen 2008; Kéfi et al. 2008). Such spatializied systems in turn have interesting ramifications with cooperation, kin selection, inclusive fitness or group selection and multilevel selection (Lehmann 2008; Lion and van Baalen 2008). To conclude, space probably plays a central role in balancing selection from the individual to the ecosystem scale, in turn strongly affecting the evolution of niche-constructing strategies and the emergence of ecosystem properties and functioning (de Mazancourt and Loreau 2000; Loreau 2010a).

The last approach to understand how resource privatization can help explain the evolution of the impact niche comes from the 'Black Queen Hypothesis', developed recently in the context of adaptive gene loss in in well-mixed microbial communities (Morris et al. 2012; Morris 2015). This hypothesis relies on the idea that 'helpers' and 'beneficiaries' can stably coexist if the beneficial function performed by 'helpers' benefits the 'beneficiaries' as it leaks into the shared

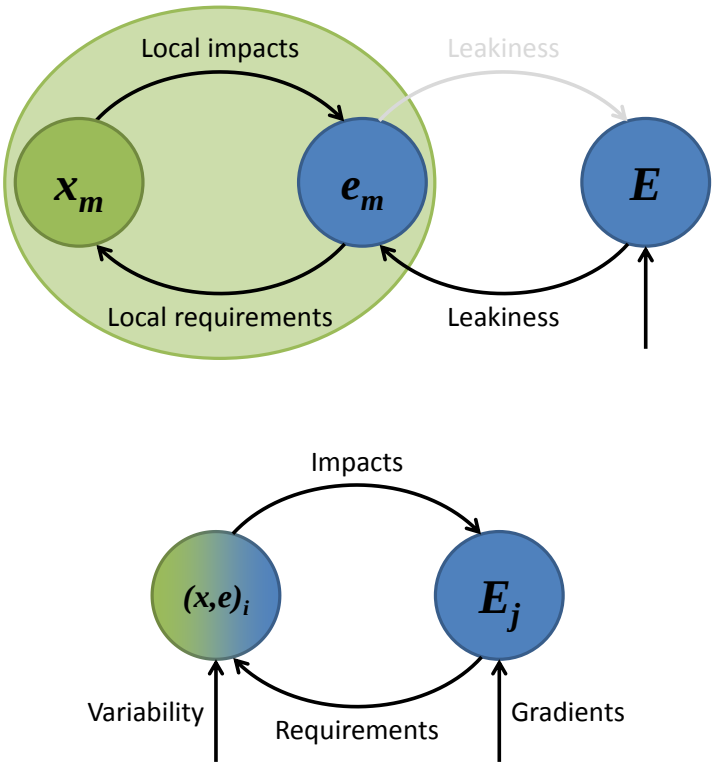

Figure 4.1: Schematic of how accounting for the local environmental sphere of influence e_m of a rare strategy x_m can lead to direct selection on local impacts, which can in turn lead to positive niche construction (top). When combined, the strategy and its local environment form a single hybrid strategy that can be studied and represented using all the contemporary niche theory tools described in this thesis.

environment, while still leading to a stronger direct benefit for the 'helper'. Biologically relevant situations can be organized along a leakiness spectrum, where completely public or completely private goods correspond to the to two extreme cases (Morris 2015). We suggest that this framework can be transposed to Huston and DeAngelis's (1994) ideas, where individual plants comes with a local sphere of influence, and that these spheres of influence buffer plants interactions with their shared environment. In these context, plants can benefit from local, niche-constructing impacts, but these impacts also leak back onto the shared-environment, contributing to global ecosystem properties. Such an idea is easily implemented in our niche framework at a low technical cost with a slight modification of the consumer-resource module. Indeed, it is formally equivalent to the Droop Model developed in the context of unicellular organisms, where every individual cell is given an internal state, the quota, that quantifies the internal accumulation of resources available to cell growth (Droop 1968; Oyarzun and Lange 1994; Klausmeier et al. 2007; Lemesle and Mailleret 2008). The rigourous treatment of such a quota-structured model could

require tracking the full distribution of quota in the population (Pascual and Caswell 1997), but in the absence of spatial structure, i.e. in a well-mixed environment, it usually suffices to assume that all the cells are in the same internal state. Back to the plant-soil model, this means that three state variables suffice to describe such a system: shared resource pool concentration, total plant biomass, and their local resource pool concentration. Formally, this is equivalent to giving the plant an extra degree of freedom, and can be interpreted biologically in terms of the plant's extended phenotype. From there, computing the invasion fitness of an invader after relaxation of its internal degree of freedom, maps the problem back to a classical consumer-resource system. However, the plant's R^* quantifying its competitive ability is now a hybrid between the plant requirement traits, its local impact traits and local abiotic processes such as nutrient diffusion. In terms of niche components, this means that the requirement niche is now a function of the local impact. This, in turn, implies that the local impact, and thus local niche construction, are under selection.

To conclude, we have seen how our niche-based approach could be adapted to investigate selection on impact, facilitation and niche construction. This, in turn, is fundamental to understand how ecosystem functions emerge, and could yield significant applications if coupled with recent eco-evolutionary perspectives, for example in microbiology and agriculture (Weiner et al. 2010; Hinsinger et al. 2011; Denison 2012; Brooker et al. 2016).

Evolutionary stable coexistence and the evolution of specialization

Historically, early niche and resource competition models have been used as mechanistic tools to investigate the conditions under which two species could coexist on two resources — or limiting factors more generally (MacArthur 1972; Tilman 1982, 1988; Leibold 1996). The resulting necessary conditions can be interpreted graphically in terms of ZNGI crossing and impact vectors relative positions, as reviewed in the first subsection of Chapter 1. The needs for the two ZNGIs to cross is a relatively intuitive condition for coexistence, as it basically translates the fact that a trade-off in competitive ability is needed for two species to coexist. Indeed, as ZNGIs are usually continuous, the absence of intersection would mean that one ZNGI is entirely 'contained' inside the other one, which in turn means that one species completely dominates the other one, i.e. systematically excludes it competitively whatever the environmental conditions.

As showed and discussed in Chapter 1, evolutionarily stable coexistence, i.e. coexistence in the context of a continuum of interacting strategies, relies on a different kind of condition. The subtlety comes from the fact that between two intersecting ZNGIs sampled out of the continuum, there will always exist intermediate strategies which are usually able to displace one of the original two strategies and replace it. When iterated, these successive replacements lead to convergent evolution of the two coexisting strategies, until there is just one uninvadable strategy

left. We called such a single well-adapted strategy a generalist. We have seen in Chapter 1 that a way out of this conundrum relies on self-intersections of the local ZNGI envelope, which results in kinks in the global envelope. This expresses the need for some intermediate generalists strategies to perform less well than the pairs of more specialized strategies they are the intermediate of. In these terms, evolutionary stable coexistence basically happens when a pair of two coexisting specialized strategies outcompetes their intermediate generalists. So, when does evolution favor specialists over generalists? Chapter 1 and 2 give two different but complementary perspectives on the emergence of evolutionarily stable coexistence, respectively on the regulating factor side and on the trait and trade-off side.

In Chapter 1, the trade-off between the acquisition rates for the two resources was assumed to be fixed, and linear for parsimony. Conversely, the response of population growth to the two resources — the interaction between the two resources — could be tuned at will through a shape parameter α. Antagonistic resources with a concave ZNGI were obtained with $\alpha > 1$ and synergistic resources, either essential or complementary, with a convex ZNGI were obtained with $\alpha < 1$. With this in mind, Chapter 1 revisits and interprets Schreiber and Tobiason's (2003) results on the evolution of resource use. Evolutionarily stable coexistence is only possible in the antagonistic case, i.e. when ZNGIs are concave ($\alpha > 1$). Graphically, this corresponds to the ZNGI envelope being an inner envelope, i.e. located outside the ZNGI set, with the envelope being less concave than its ZNGIs. This is intuitive, as the antagonism makes it easier to select specialists on one resource or the other, as a mixed diet is not beneficial by any means.

In Chapter 2, we investigated the effect of the trade-off and trait allocation shape parameters on evolutionarily stable coexistence, while the ZNGI shape — hyperbolic — was kept fixed. From the previous paragraph perspective, such a hyperbolic ZNGI shape in the resource-herbivore plane translates into interacting essential resources — the plant having to deal with *both* the resource and the herbivore to be able to grow —, i.e. a 'convex' ZNGI and should thus favor a single generalist strategy. However, we found that this trend could be reversed by a convex trade-off caused by accelerating returns on allocation towards at least one of the three traits, making evolutionary stable coexistence possible.

To conclude, we showed how both resource antagonism — concave ZNGI — and trait antagonism — convex trade-off — tend to favor specialization, as a combination of the two determines evolutionarily stable coexistence. Our envelope-based graphical approach enables a quick visualization of this outcome in terms of relative position between the ZNGI set and their envelope. Back to the strategy-environment dichotomy, our approach looks at the problem from the environmental perspective, i.e. in the resource plane, where resource interactions are directly represented with the ZNGIs, but the trade-off only implicitly contributes to the envelope shape. Following Levins's (1962) work, Rueffler et al. (2004) and de Mazancourt and Dieckmann (2004) developed the complementary approach from the trait perspective, i.e. in the trait space, with this time the trade-off being explicitly represented, while resource interactions contribute only

implicitly through the shape of the invasion boundary.

Note that we have so far not discussed the emergence of diversity on evolutionary time, only its maintenance. Yet, chapter 1 gives some insights on diversification too. The main message in the antagonistic case is that the existence of an evolutionary stable coexistence equilibrium does not systematically ensure that it can be reached through infinitesimal mutation steps by a monomorphic strategy, as it is not necessarily associated with a branching point. We showed that only large enough and balanced enough resource supplies could lead to branching. The reason is that a large consumer density is needed to get a strong enough eco-evolutionary feedback, i.e. joint trait and density response, to overturn the ecological-only feedback, i.e. density-only response.

As we have seen in this dissertation, most of our eco-evolutionary results, like the evolution of specialization, strongly depend on the existence and shape of the trade-off or allocation functions. These shapes in turn depend on the laws of physics, the physiology of the organisms, and the ecological context they live in. Despite the central role they play, these trade-offs are largely unknown. This should encourage further studies to describe them within and across taxa and get a better understanding of the mechanisms that underlie them.

Towards complex food web assembly

In this thesis, we focused on the analysis of what we called small food web modules, as they can easily be represented graphically, are analytically tractable and provide a good grasp on the mechanisms at play. Most of the complexity there comes from considering a highly diverse continuum of competing strategies, but having a two-dimensional niche space ensures that the realized diversity never exceeds two, thanks to the Competitive Exclusion Principle (CEP). Yet, most food webs encountered in the natural world are of much greater complexity, both horizontally — in number of coexisting competing species — and vertically — in number of trophic levels. Their analysis has given rise to its own sub-discipline, with specific tools and approaches — such as random matrix theory — and an emphasis on stability (May 1973; Bascompte et al. 2003; Thébault and Fontaine 2010; Allesina and Tang 2012). Still, we will argue that despite their simplicity, small food web modules can provide some fundamental insight on the mechanisms at play in the emergence of their more complex relatives, as well as some generalizable principles on the mechanisms structuring and stabilizing these food webs at equilibrium.

Firstly, this thesis illustrates and analyses three mechanisms by which complex food webs can assemble and undergo irreversible changes through time as species invade and establish: vertical and horizontal assembly on one side, and facilitative replacement on the other. Vertical assembly consists in the establishment of a new trophic level, provided that the resources or preys of this new consumer species are present and available at high enough density. This happens in Chapter 3 with the initial colonization of the bare substrate by a pioneer species. In Chapter

2, we did not simulate assembly through time *per se*, but the first stages of the response of the food chain structure to an increasing nutrient gradient mimicked this vertical assembly. Horizontal assembly happens when the niche space of a guild of competitors is not saturated, or follows the apparition of a new niche dimension. This is what happens in Chapter 2: according to the apparent-competition framework (Holt 1977; Holt et al. 1994; Grover 1995; Leibold 1996), the establishment of herbivores opens a new niche for plants to specialize on, leading to the coexistence of both tolerant and resistant plant species in the diamond module. This diamond module, in turn, is the first step towards a joint plant-herbivore horizontal diversification on a single resource: the appearance of the defended plant can allow the invasion of a new herbivore species, itself allowing invasion of another plant, and so on (Armstrong 1994; Sauterey et al. 2017). This is consistent with the CEP: n plant species are necessary for n herbivores to coexist, and n herbivores plus 1 resource are more than what is necessary to enable n plants to coexist. Of course, vertical assembly is also possible, with the further establishment of carnivores and their diversification.

Facilitative replacement, as described in Chapter 3, gives another potentially general niche-based mechanism that could drive community assembly. It happens when the establishment of a first species relies on the previous establishment of a second, facilitating species. It reminds of vertical assembly, where predator's establishment relies on prey's previous establishment. However, it differs from it by its horizontal and indirect nature — a plant facilitating another plant by modifications of the environment — and the fact that the first species ends up completely replacing the second one. In our model, positive feedback loops indeed enable the first species to persist even after excluding its facilitator, at the cost of sensitivity to catastrophic shifts. The iteration of such facilitative replacements lead to irreversible succession and ecosystem development, without any diversification of the food web. Facilitative replacement, and more generally facilitation and positive feedback loops, could thus be combined with the more classical mechanisms of horizontal and vertical assembly to give rise to unexplored patterns of food web assembly (Bruno et al. 2003; Kéfi et al. 2012; Pantel et al. 2017), such as alternative stable states or alternative transient states at the food-web level (Fukami 2015).

Note that we presented horizontal and vertical assembly as two clearly distinct processes for simplicity. When omnivory and cannibalism are accounted for, which is very common in some food webs such as aquatic systems or decomposer networks, it becomes much harder to draw a clear line between these two processes. Still, chain-like trophic structure can emerge from food web assembly models with very simple rules of omnivory (Loeuille and Loreau 2005).

Finally, some concepts of contemporary niche theory developed on small modules are helpful in understanding what allows and stabilizes coexistence within more complex food webs. Levin's (1970) general formulation of the competitive exclusion principle, which includes the apparent competition framework (Holt 1977), is one example of such structural constraints a food web has to satisfy if its competitors were to coexist. Such a constraint is connected to the

concept of 'niche overlap' (MacArthur and Levins 1964), a metric that measures the difference in resource use of two competitors and quantifies how probable their coexistence is. Niche overlap has a very simple geometrical interpretation in contemporary niche theory (Petraitis 1989; Meszéna et al. 2006), and can also be extended to account for apparent competition (Chesson and Kuang 2008). Recently, this concept was extended to any number of coexisting species within a general Lotka-Volterra model, shedding new lights on how indirect interactions contribute to coexistence (Saavedra et al. 2017).

Bibliography

Abrams, P. A. (2001). Modelling the adaptive dynamics of traits involved in inter- and intarspecific interactions: an assesment of three methods. *Ecology Letters*, 4(2):166–175.

Abrams, P. A. (2003). Can adaptive evolution or behaviour lead to diversification of traits determining a trade-off between foraging gain and predation risk? *Evolutionary Ecology Research*, 5(5):653–670.

Abrams, P. A. and Chen, X. (2002). The evolution of traits affecting resource acquisition and predator vulnerability: character displacement under real and apparent competition. *The American Naturalist*, 160(5):692–704.

Abrams, P. A. and Roth, J. D. (1994). The effects of enrichment of three-species food chains with nonlinear functional responses. *Ecology*, 75(4):1118–1130.

Adler, P. B., Dalgleish, H. J., and Ellner, S. P. (2012). Forecasting plant community impacts of climate variability and change: when do competitive interactions matter? *Journal of Ecology*, 100(2):478–487.

Agawin, N. S. R., Rabouille, S., Veldhuis, M. J. W., Servatius, L., Hol, S., van Overzee, H. M. J., and Huisman, J. (2007). Competition and facilitation between unicellular nitrogen-fixing cyanobacteria and non-nitrogen-fixing phytoplankton species. *Limnology and Oceanography*, 52(5):2233–2248.

Agrawal, A. A. (1998). Algal defense, grazers, and their interactions in aquatic trophic cascades. *Acta Oecologica*, 19(4):331–337.

Ali, J. G. and Agrawal, A. A. (2012). Specialist versus generalist insect herbivores and plant defense. *Trends in Plant Science*, 17(5):293–302.

Allesina, S. and Tang, S. (2012). Stability criteria for complex ecosystems. *Nature*, 483(7388):205–208.

Andrews, J. F. (1968). A mathematical model for the continuous culture of microorganisms utilizing inhibitory substrates. *Biotechnology and Bioengineering*, 10(6):707–723.

Armesto, J. J. and Pickett, S. T. A. (1986). Removal experiments to test mechanisms of plant succession in oldfields. *Vegetatio*, 66(2):85–93.

Armstrong, R. A. (1979). Prey species replacement along a gradient of nutrient enrichment: a graphical approach. *Ecology*, 60(1):76–84.

Armstrong, R. A. (1994). Grazing limitation and nutrient limitation in marine ecosystems: steady state solutions of an ecosystem model with multiple food chains. *Limnology and Oceanography*, 39(3):597–608.

Armstrong, R. A. (2008). Nutrient uptake rate as a function of cell size and surface transporter density: a Michaelis-like approximation to the model of Pasciak and Gavis. *Deep-Sea Research Part I: Oceanographic Research Papers*, 55(10):1311–1317.

Arnoldi, J.-F. and Haegeman, B. (2016). Unifying dynamical and structural stability of equilibriums. *Proceedings of the Royal Society A*, 472:20150874.

Arnoldi, J.-F., Loreau, M., and Haegeman, B. (2015). Resilience, reactivity and variability: a mathematical comparison of ecological stability measures. pages 1–35.

Augner, M. (1995). Low nutritive quality as a plant defence: effects of herbivore-mediated interactions. *Evolutionary Ecology*, 9(6):605–616.

Augner, M., Fagerström, T., and Tuomi, J. (1991). Competition, defense and games between plants. *Behavioral Ecology and Sociobiology*, 29(4):231–234.

Baas Becking, L. G. M. (1934). *Geobiologie of Inleiding Tot de Milieukunde*. Van Stockum, Den Haag.

Barabás, G., Meszéna, G., and Ostling, A. (2014a). Fixed point sensitivity analysis of interacting structured populations. *Theoretical Population Biology*, 92:97–106.

Barabás, G., Pásztor, L., Meszéna, G., and Ostling, A. (2014b). Sensitivity analysis of coexistence in ecological communities: theory and application. *Ecology Letters*, 17(12):1479–1494.

Barot, S., Abbadie, L., Couvet, D., Hobbs, R. J., Lavorel, S., Mace, G. M., and Le Roux, X. (2015). Evolving away from the linear model of research: a response to Courchamp et al. *Trends in Ecology & Evolution*, pages 1–2.

Barot, S., Bornhofen, S., Loeuille, N., Perveen, N., Shahzad, T., and Fontaine, S. (2014). Nutrient enrichment and local competition influence the evolution of plant mineralization strategy: a modelling approach. *Journal of Ecology*, 102:357–366.

Bascompte, J., Jordano, P., Melián, C. J., and Olesen, J. M. (2003). The nested assembly of plant-animal mutualistic networks. *Proceedings of the National Academy of Sciences of the United States of America*, 100(16):9383–7.

Belnap, J. and Eldridge, D. (2001). Disturbance and recovery of biological soil crusts. In Belnap, J. and Lange, O. L., editors, *Biological Soil Crusts: Structure, Function, and Management*. Springer-Verlag, Berlin Heidelberg.

Bertness, M. D. and Callaway, R. (1994). Positive interactions in communities. *Trends in Ecology & Evolution*, 9(5):191–193.

Boege, K., Barton, K. E., and Dirzo, R. (2011). Influence of tree ontogeny on plant-herbivore interactions. In Meinzer, F. C., Lachenbruch, B., and Dawson, T. E., editors, *Size-and Age-Related Changes in Tree Structure and Function*, volume 4, pages 193–214. Springer Netherlands.

Bonachela, J. A., Klausmeier, C. A., Edwards, K. F., Litchman, E., and Levin, S. A. (2016). The role of phytoplankton diversity in the emergent oceanic stoichiometry. *Journal of Plankton Research*, 38(4):1021–1035.

Bonachela, J. A., Raghib, M., and Levin, S. A. (2011). Dynamic model of flexible phytoplankton nutrient uptake. *Proceedings of the National Academy of Sciences of the United States of America*, 108(51):20633–20638.

Boudsocq, S., Barot, S., and Loeuille, N. (2011). Evolution of nutrient acquisition: when adaptation fills the gap between contrasting ecological theories. *Proceedings of the Royal Society of London B: Biological Sciences*, 278(1704):449–457.

Boushaba, K. and Pascual, M. (2005). Dynamics of the 'echo' effect in a phytoplankton system with nitrogen fixation. *Bulletin of Mathematical Biology*, 67(3):487–507.

Branco, P., Stomp, M., Egas, M., and Huisman, J. (2010). Evolution of nutrient uptake reveals a trade-off in the ecological stoichiometry of plant- herbivore interactions. *The American Naturalist*, 176(6):162–176.

Brooker, R. W., Karley, A. J., Newton, A. C., Pakeman, R. J., and Schöb, C. (2016). Facilitation and sustainable agriculture: a mechanistic approach to reconciling crop production and conservation. *Functional Ecology*, 30(1):98–107.

Brown, J. S. (2016). Why Darwin would have loved evolutionary game theory. *Proceedings of the Royal Society of London B: Biological Sciences*, 283:20160847.

Bruno, J. F., Stachowicz, J. J., and Bertness, M. D. (2003). Inclusion of facilitation into ecological theory. *Trends in Ecology & Evolution*, 18(3):119–125.

Bryant, J. P., Chapin, F. S., Klein, D. R., Bryant, J. P., Chapin, F. S., and Klein, D. R. (1983). Carbon/nutrient balance of boreal plants in relation to vertebrate herbivory. *Oikos*, 40(3):357–368.

Callaway, R. M. (1995). Positive interactions among plants. *The Botanical Review*, 61(4):306–349.

Callaway, R. M. and Walker, L. R. (1997). Competition and facilitation: a synthetic approach to interactions in plant communities. *Ecology*, 78(7):1958–1965.

Carmona, D. and Fornoni, J. (2013). Herbivores can select for mixed defensive strategies in plants. *New Phytologist*, 197(2):576–585.

Casper, B. B., Schenk, H. J., and Jackson, R. B. (2003). Defining a plant's belowground zone of influence. *Ecology*, 84(9):2313–2321.

Caswell, H. (2001). *Matrix Population Models: Construction, Analysis, and Interpretation*. Sinauer Associates, Sunderland, MA.

Champagnat, N., Ferrière, R., and Méléard, S. (2006). Unifying evolutionary dynamics: from individual stochastic processes to macroscopic models. *Theoretical Population Biology*, 69(3):297–321.

Chapin, F. S. (1980). The mineral nutrition of wild plants. *Annual Review of Ecology and Systematics*, 11(1980):233–260.

Chapin, F. S., Walker, L. R., Fastie, C. L., and Sharman, L. C. (1994). Mechanisms of primary succession following deglaciation at Glacier Bay, Alaska. *Ecological Monographs*, 64(2):149–175.

Chase, J. M. and Leibold, M. A. (2003). *Ecological Niches: Linking Classical and Contemporary Approaches*. University of Chicago Press, Chicago.

Chase, J. M., Leibold, M. A., and Simms, E. (2000). Plant tolerance and resistance in food webs: community-level predictions and evolutionary implications. *Evolutionary Ecology*, 14:289–314.

Chesson, P. (1990). MacArthur's consumer-resource model. *Theoretical Population Biology*, 37:26–38.

Chesson, P. (2000). Mechanisms of maintenance of species diversity. *Annual Review of Ecology and Systematics*, 31(1):343–366.

Chesson, P. and Kuang, J. J. (2008). The interaction between predation and competition. *Nature*, 456(7219):235–8.

Clements, F. E. (1916). *Plant Succession. An Analysis of the Development of Vegetation*.

Clements, F. E. (1936). Nature and structure of the climax. *Journal of Ecology*, 24(1):252–284.

Coley, P. D., Bryant, J. P., and Chapin, F. S. (1985). Resource availability and plant antiherbivore defense. *Science*, 230(4728):895–899.

Connell, J. H. and Slatyer, R. O. (1977). Mechanisms of succession in natural communities and their role in community stability and organization. *The American Naturalist*, 111(982):1119–1144.

Courchamp, F., Clutton-Brock, T., and Grenfell, B. (1999). Inverse density dependence and the Allee effect.

Cowles, H. C. (1901). The physiographic ecology of Chicago and vicinity: a study of the origin, development, and classification of plant societies. *Botanical Gazette*, 31(3):73–108, 145–182.

Crews, T. E., Kurina, L. M., and Vitousek, P. M. (2001). Organic matter and nitrogen accumulation and nitrogen fixation during early ecosystem development in Hawaii. *Biogeochemistry*, 52(3):259–279.

Crocker, R. L. and Major, J. (1955). Soil development in relation to vegetation surface age at Glacier Bay, Alaska. *Journal of Ecology*, 43:427–448.

Danger, M., Daufresne, T., Lucas, F., Pissard, S., and Lacroix, G. (2008). Does Liebig's law of the minimum scale up from species to communities? *Oikos*, 117(11):1741–1751.

Darwin, C. (1859). *On the Origin of Species by Means of Natural Selection, or the Preservation of Favoured Races in the Struggle for Life*. John Murray, London.

Daufresne, T. and Hedin, L. O. (2005). Plant coexistence depends on ecosystem nutrient cycles: extension of the resource-ratio theory. *Proceedings of the National Academy of Sciences of the United States of America*, 102(26):9212–9217.

de Mazancourt, C. and Dieckmann, U. (2004). Trade-off geometries and frequency-dependent selection. *The American Naturalist*, 164(6):765–778.

de Mazancourt, C. and Loreau, M. (2000). Grazing optimization, nutrient cycling, and spatial heterogeneity of plant-herbivore interactions: should a palatable plant evolve? *Evolution*, 54(1):81–92.

de Mazancourt, C., Loreau, M., and Abbadie, L. (1998). Grazing optimization and nutrient cycling: when do herbivores enhance plant production? *Ecology*, 79(7):2242–2252.

de Mazancourt, C., Loreau, M., and Dieckmann, U. (2001). Can the evolution of plant defense lead to plant-herbivore mutualism? *The American Naturalist*, 158(2):109–23.

de Mazancourt, C. and Schwartz, M. W. (2010). A resource ratio theory of cooperation. *Ecology Letters*, 13(3):349–59.

De Wit, R. and Bouvier, T. (2006). 'Everything is everywhere, but, the environment selects'; what did Baas Becking and Beijerinck really say? *Environmental Microbiology*, 8(4):755–758.

Dekker, S. C., Vrugt, J. A., and Elkington, R. J. (2012). Significant variation in vegetation characteristics and dynamics from ecohydrological optimality of net carbon profit. *Ecohydrology*, 5:1–18.

Denison, R. F. (2012). *Darwinian agriculture: how understanding evolution can improve agriculture*.

Denison, R. F., Kiers, E. T., and West, S. A. (2003). Darwinian agriculture: when can humans find solutions beyond the reach of natural selection? *The Quarterly Review of Biology*, 78(2):145–168.

Dieckmann, U. and Doebeli, M. (1999). On the origin of species by sympatric speciation. *Nature*, 400(6742):354–357.

Dieckmann, U. and Ferrière, R. (2004). Adaptive dynamics and evolving biodiversity. In *Evolutionary Conservation Biology*, pages 188–224. Cambridge University Press, Cambridge, UK.

Dieckmann, U. and Law, R. (1996). The dynamical theory of coevolution: a derivation from stochastic ecological processes. *Journal of Mathematical Biology*, 34(5-6):579–612.

Dieckmann, U. and Metz, J. A. J. (2006). Surprising evolutionary predictions from enhanced ecological realism. *Theoretical Population Biology*, 69(3):263–281.

Diekmann, O. (2004). A beginner's guide to adaptive dynamics. *Banach Center publications*, 63:47–86.

Dobzhansky, T. (1973). Nothing in biology makes sense except in the light of evolution. *The American Biology Teacher*, 35(3):125–129.

Drake, J. A. (1990). The mechanics of community assembly and succession. *Journal of Theoretical Biology*, 147:213–233.

Droop, M. R. (1968). Vitamin B12 and marine ecology. IV. The kinetics of uptake, growth and inhibition in Monochrysis lutheri. *Journal of the Marine Biological Association of the United Kingdom*, 48(03):689–733.

Duffy, J. E. and Hay, M. E. (1994). Herbivore resistance to sea weed chemical defense: the roles of mobility and predation risk. *Ecology*, 75(5):1304–1319.

Dukas, R. and Kamil, A. C. (2001). Limited attention: the constraint underlying search image. *Behavioral Ecology*, 12(2):192–199.

Dybzinski, R., Farrior, C., Wolf, A., Reich, P. B., and Pacala, S. W. (2011). Evolutionarily stable strategy carbon allocation to foliage, wood, and fine roots in trees competing for light and nitrogen: an analytically tractable, individual-based model and quantitative comparisons to data. *The American Naturalist*, 177(2):153–166.

Dybzinski, R., Farrior, C. E., and Pacala, S. W. (2015). Increased forest carbon storage with increased atmospheric CO2 despite nitrogen limitation: a game-theoretic allocation model for trees in competition for nitrogen and light. *Global Change Biology*, 21(3):1182–1196.

Edwards, K. F., Klausmeier, C. a., and Litchman, E. (2011). Evidence for a three-way trade-off between nitrogen and phosphorus competitive abilities and cell size in phytoplankton. *Ecology*, 92(11):2085–95.

Elser, J. (2006). Biological stoichiometry: a chemical bridge between ecosystem ecology and evolutionary biology. *The American Naturalist*, 168(S6):S25–S35.

Elton, C. (1927). *Animal Ecology*. Sidgwick & Jackson, London.

Endara, M.-J. and Coley, P. D. (2011). The resource availability hypothesis revisited: a meta-analysis. *Functional Ecology*, 25(2):389–398.

Eppley, R. W. (1972). Temperature and phytoplankton growth in the sea. *Fishery Bulletin*, 70(4):1063–1085.

Eshel, I. (1983). Evolutionary and continuous stability. *Journal of Theoretical Biology*, 103:99–111.

Farrell, T. M. (1991). Models and mechanisms of succession: an example from a rocky intertidal community. *Ecological Monographs*, 61(1):95–113.

Feeny, P. (1976). Plant apparency and chemical defense. In *Biochemical Interaction Between Plants and Insects*, pages 1–40.

Fineblum, W. L. and Rausher, M. D. (1995). Tradeoff between resistance and tolerance to herbivore damage in a morning glory. *Nature*, 377:517–520.

Follows, M. J., Dutkiewicz, S., Grant, S., and Chisholm, S. W. (2007). Emergent biogeography of microbial communities in a model ocean. *Science*, 315(5820):1843–1846.

Fortelius, M., Geritz, S., Gyllenberg, M., and Toivonen, J. (2015). Adaptive dynamics on an environmental gradient that changes over a geological time-scale. *Journal of Theoretical Biology*, 376:91–104.

Fukami, T. (2015). Historical contingency in community assembly: integrating niches, species pools, and priority effects. *Annual Review of Ecology Evolution and Systematics*, 46:1–23.

Gause, G. F. (1934). *The Struggle for Existence*. Williams & Wilkins Company, Baltimore, MD.

Geritz, H., Gyllenberg, M., Jacobs, A., and Parvinen, K. (2002). Invasion dynamics and attractor inheritance. *Journal of Mathematical Biology*, 44(6):548–560.

Geritz, S., Metz, J. A. J., Kisdi, É., and Meszéna, G. (1997). Dynamics of adaptation and evolutionary branching. *Physical Review Letters*, 78(10):2024–2027.

Geritz, S. A., van der Meijden, E., and Metz, J. A. (1999). Evolutionary dynamics of seed size and seedling competitive ability. *Theoretical Population Biology*, 55(3):324–343.

Geritz, S. A. H., Kisdi, É., Meszéna, G., and Metz, J. A. J. (1998). Evolutionarily singular strategies and the adaptive growth and branching of the evolutionary tree. *Evolutionary Ecology*, 12(1):35–57.

Gerla, D. J., Mooij, W. M., and Huisman, J. (2011). Photoinhibition and the assembly of light-limited phytoplankton communities. *Oikos*, 120:359–368.

Gerla, D. J., Vos, M., Kooi, B. W., and Mooij, W. M. (2009). Effects of resources and predation on the predictability of community composition. *Oikos*, 118(7):1044–1052.

Gleason, H. A. (1939). The individualistic concept of the plant association. *The American Midland Naturalist*, 21(1):92–110.

Godsoe, W., Jankowski, J., Holt, R. D., and Gravel, D. (2017). Integrating biogeography with contemporary niche theory. *Trends in Ecology & Evolution*, xx:1–12.

Gorbushina, A. A., Kort, R., Schulte, A., Lazarus, D., Schnetger, B., Brumsack, H.-j., Broughton, W. J., and Favet, J. (2007). Life in Darwin's dust: intercontinental transport and survival of microbes in the nineteenth century. *Environmental Microbiology*, 9(12):2911–2922.

Grant, P. R. and Grant, B. R. (2006). Evolution of character displacement in Darwin's finches. *Science*, 313(5784):224–226.

Grime, J. P. (1974). Vegetation classification by reference to strategies. *Nature*, 250(5461):26–31.

Grime, J. P. (1977). Evidence for the existence of three primary strategies in plants and its relevance to ecological and evolutionary theory. *The American Naturalist*, 111(982):1169–1194.

Grinnell, J. (1917). The niche-relationships of the California thrasher. *American Ornithologists' Union*, 34(4):427–433.

Grover, J. P. (1995). Competition, herbivory and enrichment: nutrient-based models for edible and inedible plants. *The American Naturalist*, 145(5):746–774.

Grover, J. P. (1997). *Resource Competition*. Chapman & Hall, London.

Grover, J. P. and Holt, R. D. (1998). Disentangling resource and apparent competition: realistic models for plant-herbivore communities. *Journal of Theoretical Biology*, 191(4):353–376.

Guill, C. (2009). Alternative dynamical states in stage-structured consumer populations. *Theoretical Population Biology*, 76(3):168–78.

Gyllenberg, M. and Meszéna, G. (2005). On the impossibility of coexistence of infinitely many strategies. *Journal of Mathematical Biology*, 50:133–160.

Gyllenberg, M. and Parvinen, K. (2001). Necessary and sufficient conditions for evolutionary suicide. *Bulletin of Mathematical Biology*, 63(5):981–993.

Haegeman, B., Arnoldi, J.-F., Wang, S., de Mazancourt, C., Montoya, J. M., and Loreau, M. (2016). Resilience, invariability, and ecological stability across levels of organization. pages 1–15.

Haegeman, B. and Loreau, M. (2015). A graphical-mechanistic approach to spatial resource competition. *The American Naturalist*, 185(1):1–13.

Hahn, P. G. and Maron, J. L. (2016). A framework for predicting intraspecific variation in plant defense. *Trends in Ecology & Evolution*, 31(8):646–656.

Hairston, N. G., Ellner, S. P., Geber, M. A., Yoshida, T., and Fox, J. A. (2005). Rapid evolution and the convergence of ecological and evolutionary time. *Ecology Letters*, 8(10):1114–1127.

Haldane, J. S. H. (1930). *Enzymes*. Longmans Green and Co, London.

Hardin, G. (1968). The tragedy of the commons. *Science*, 162:1243–1248.

Harmand, J., Lobry, C., Rapaport, A., and Sari, T. (2017). *Le Chemostat, Théorie Mathématique des Cultures de Micro-organismes*.

Hastings, A. and Powell, T. (1991). Chaos in a three-species food chain. *Ecology*, 72(3):896–903.

Hedin, L. O., Brookshire, E. N. J., Menge, D. N. L., and Barron, A. R. (2009). The nitrogen paradox in tropical forest ecosystems. *Annual Review of Ecology, Evolution, and Systematics*, 40:613–635.

HilleRisLambers, R., Rietkerk, M., van den Bosch, F., Prins, H. H. T., and De Kroon, H. (2001). Vegetation pattern formation in semi-arid grazing systems. *Ecology*, 82(1):50–61.

Hils, M. H. and Vankat, J. L. (1982). Species removals from a first-year old-field plant community. *Ecology*, 63(3):705–711.

Hinsinger, P., Betencourt, E., Bernard, L., Brauman, A., Plassard, C., Shen, J., Tang, X., and Zhang, F. (2011). P for two, sharing a scarce resource: soil phosphorus acquisition in the rhizosphere of intercropped species. *Plant physiology*, 156(3):1078–86.

Hofbauer, J. and Sigmund, K. (1990). Adaptive dynamics and evolutionary stability. *Applied Mathematics Letters*, 3(4):75–79.

Holling, C. S. (1959). Some characteristics of simple types of predation and parasitism. *The Canadian Entomologist*, 91(7):385–398.

Holt, R. D. (1977). Predation, apparent competition, and the structure of prey communities. *Theoretical Population Biology*, 12(2):197–229.

Holt, R. D. (2009a). Bringing the Hutchinsonian niche into the 21st century: ecological and evolutionary perspectives. *Proceedings of the National Academy of Sciences of the United States of America*, 106:19659–19665.

Holt, R. D. (2009b). IJEE Soapbox: Prince Kropotkin meets the Hutchinsonian niche. *Israel Journal of Ecology & Evolution*, 55(1):1–10.

Holt, R. D., Grover, J. P., and Tilman, D. (1994). Simple rules for interspecific dominance in systems with exploitative and apparent competition. *The American Naturalist*, 144(5):741–771.

Holter, V. (1984). N2(C2H2)-fixation in early stages of a primary succession on a reclaimed salt marsh. *Holarctic Ecology*, 7:165–170.

Hsu, S. B., Hubbell, S., and Waltman, P. (1977). A mathematical theory for single-nutrient competition in continuous cultures of micro-organisms. *SIAM Journal on Applied Mathematics*, 32(2):366–383.

Hui, C., Richardson, D. M., Landi, P., Minoarivelo, H. O., Garnas, J., and Roy, H. E. (2016). Defining invasiveness and invasibility in ecological networks. *Biological Invasions*, 18(4):971–983.

Huisman, J. and Weissing, F. J. (1999). Biodiversity of plankton by species oscillations and chaos. *Nature*, 402(6760):407–410.

Huston, M. and Smith, T. (1987). Plant succession: life history and competition. *The American Naturalist*, 130(2):168–198.

Huston, M. A. and DeAngelis, D. L. (1994). Competition and coexistence: the effects of resource transport and supply rates. *The American Naturalist*, 144(6):954–977.

Hutchings, M. J. (1986). The structure of plant populations. In Crawley, M. J., editor, *Plant Ecology*, pages 97–136. Blackwell, Oxford, UK.

Hutchinson, G. E. (1957). Concluding remarks. *Cold Spring Harbor Symposia on Quantitative Biology*, 22:415–427.

Hutchinson, G. E. (1959). Homage to Santa Rosalia or why are there so many kinds of animals? *The American Naturalist*, 93(870):145–159.

Jones, C. G., Lawton, J. H., and Shachak, M. (1994). Organisms as ecosystem engineers. *Oikos*, 69(3):373–386.

Jones, C. G., Lawton, J. H., and Shachak, M. (1997). Positive and negative effects of organisms as physical ecosystem engineers. *Ecology*, 78(7):1946–1957.

Jones, L. E. and Ellner, S. P. (2004). Evolutionary tradeoff and equilibrium in an aquatic predator-prey system. *Bulletin of Mathematical Biology*, 66(6):1547–1573.

Kéfi, S., Berlow, E. L., Wieters, E. A., Navarrete, S. A., Petchey, O. L., Wood, S. A., Boit, A., Joppa, L. N., Lafferty, K. D., Williams, R. J., Martinez, N. D., Menge, B. A., Blanchette, C. A., Iles, A. C., and Brose, U. (2012). More than a meal ... integrating non-feeding interactions into food webs. *Ecology Letters*, pages 291–300.

Kéfi, S., Eppinga, M. B., de Ruiter, P. C., and Rietkerk, M. (2010). Bistability and regular spatial patterns in arid ecosystems. *Theoretical Ecology*, 3(4):257–269.

Kéfi, S., Holmgren, M., and Scheffer, M. (2016). When can positive interactions cause alternative stable states in ecosystems? *Functional Ecology*, 30:88–97.

Kéfi, S., van Baalen, M., Rietkerk, M., and Loreau, M. (2008). Evolution of local facilitation in arid ecosystems. *The American Naturalist*, 172(1):E1–E17.

Kisdi, É. (2015). Construction of multiple trade-offs to obtain arbitrary singularities of adaptive dynamics. *Journal of Mathematical Biology*, 70(5):1093–1117.

Kisdi, É. and Geritz, S. A. H. (2016). Adaptive dynamics of saturated polymorphisms. *Journal of Mathematical Biology*, 72(4):1039–1079.

Klausmeier, C. A. (1999). Regular and irregular patterns in semiarid vegetation. *Science*, 284(5421):1826–8.

Klausmeier, C. A. and Litchman, E. (2012). Successional dynamics in the seasonally forced diamond food web. *The American Naturalist*, 180(1):1–16.

Klausmeier, C. A., Litchman, E., Daufresne, T., and Levin, S. A. (2004). Optimal nitrogen-to-phosphorus stoichiometry of phytoplankton. *Nature*, 429(6988):171–174.

Klausmeier, C. A., Litchman, E., and Levin, S. A. (2007). A model of flexible uptake of two essential resources. *Journal of Theoretical Biology*, 246(2):278–89.

Kleinhesselink, A. R. and Adler, P. B. (2015). Indirect effects of environmental change in resource competition models. *The American Naturalist*, pages 1–44.

Kneitel, J. M. and Chase, J. M. (2004). Trade-offs in community ecology: linking spatial scales and species coexistence. *Ecology Letters*, 7(1):69–80.

Koffel, T., Daufresne, T., Massol, F., and Klausmeier, C. A. (2016). Geometrical envelopes: extending graphical contemporary niche theory to communities and eco-evolutionary dynamics. *Journal of Theoretical Biology*, 407:271–289.

Kohls, S. J., Baker, D. D., Van Kessel, C., and Dawson, J. O. (2003). An assessment of soil enrichment by actinorhizal N2 fixation using d15N values in a chronosequence of deglaciation at Glacier Bay, Alaska. *Plant and Soil*, 254(1):11–17.

Kremer, C. T. and Klausmeier, C. A. (2013). Coexistence in a variable environment: eco-evolutionary perspectives. *Journal of Theoretical Biology*, 339:14–25.

Kylafis, G. and Loreau, M. (2008). Ecological and evolutionary consequences of niche construction for its agent. *Ecology Letters*, 11(10):1072–81.

Kylafis, G. and Loreau, M. (2011). Niche construction in the light of niche theory. *Ecology Letters*, 14(2):82–90.

Laliberté, E., Turner, B. L., Costes, T., Pearse, S. J., Wyrwoll, K. H., Zemunik, G., and Lambers, H. (2012). Experimental assessment of nutrient limitation along a 2-million-year dune chronosequence in the south-western Australia biodiversity hotspot. *Journal of Ecology*, 100(3):631–642.

Lampert, W. (1987). Laboratory studies on zooplankton-cyanobacteria interactions. *New Zealand Journal of Marine and Freshwater Research*, 21:483–490.

Lavorel, S. and Garnier, E. (2002). Predicting changes in community composition and ecosystem functioning from plant traits: revisting the Holy Grail. *Functional Ecology*, 16(5):545–556.

Lavorel, S. and Grigulis, K. (2012). How fundamental plant functional trait relationships scale-up to trade-offs and synergies in ecosystem services. *Journal of Ecology*, 100(1):128–140.

Lawrence, D. B., Schoenike, R. E., Quispel, A., and Bond, G. (1967). The role of Dryas drummondii in vegetation development following ice recession at Glacier Bay, Alaska, with special reference to its nitrogen fixation by root nodules. *Journal of Ecology*, 55(3):793–813.

Lehmann, L. (2008). The adaptive dynamics of niche constructing traits in spatially subdivided populations: evolving posthumous extended phenotypes. *Evolution*, 62(3):549–566.

Leibold, M. A. (1996). A graphical model of keystone predators in food webs: trophic regulation of abundance, incidence, and diversity patterns in communities. *The American Naturalist*, 147(5):784–812.

Leibold, M. A., Holyoak, M., Mouquet, N., Amarasekare, P., Chase, J. M., Hoopes, M. F., Holt, R. D., Shurin, J. B., Law, R., Tilman, D., Loreau, M., and Gonzalez, A. (2004). The metacommunity concept: a framework for multi-scale community ecology. *Ecology Letters*, 7(7):601–613.

Leimar, O. (2009). Multidimensional convergence stability. *Evolutionary Ecology Research*, 11(2):191–208.

Lemesle, V. and Mailleret, L. (2008). A mechanistic investigation of the algae growth "droop" model. *Acta Biotheoretica*, 56(1-2):87–102.

Lenton, T. M. and Klausmeier, C. A. (2007). Biotic stoichiometric controls on the deep ocean N:P ratio. *Biogeosciences*, 4(3):353–367.

León, J. A. and Tumpson, D. B. (1975). Competition between two species for two complementary or substitutable resources. *Journal of Theoretical Biology*, 50(1):185–201.

Leslie, P. H. (1948). Further notes on the use of matrices in population mathematics. *Biometrika*, 35:213–245.

Lester, S. E., Costello, C., Halpern, B. S., Gaines, S. D., White, C., and Barth, J. A. (2013). Evaluating tradeoffs among ecosystem services to inform marine spatial planning. *Marine Policy*, 38:80–89.

Letten, A. D., Ke, P. J., and Fukami, T. (2017). Linking modern coexistence theory and contemporary niche theory. *Ecological Monographs*, 87(2):161–177.

Levin, S. A. (1970). Community equilibria and stability, and an extension of the competitive exclusion principle. *The American Naturalist*, 104(939):413–423.

Levin, S. A. (1998). Ecosystems and the biosphere as complex adaptive systems. *Ecosystems*, 1(5):431–436.

Levin, S. A. (1999). *Fragile Dominion: Complexity and the Commons*.

Levins, R. (1962). Theory of fitness in a heterogeneous environment. I. The fitness set and adaptive function. *The American Naturalist*, 96(891):361–373.

Levins, R. (1968). *Evolution in Changing Environments: Some Theoretical Explorations*. Princeton University Press, Princeton, N.J.

Liebig, J. F. (1840). *Die organische Chemie in ihrer Anwendung auf Agricultur und Physiologie*. Braunschweig.

Lion, S. and van Baalen, M. (2008). Self-structuring in spatial evolutionary ecology. *Ecology Letters*, 11(3):277–295.

Litchman, E., Edwards, K. F., and Klausmeier, C. A. (2015). Microbial resource utilization traits and trade-offs: implications for community structure, functioning, and biogeochemical impacts at present and in the future. *Frontiers in Microbiology*, 06(April):1–10.

Litchman, E. and Klausmeier, C. A. (2008). Trait-based community ecology of phytoplankton. *Annual Review of Ecology, Evolution, and Systematics*, 39(1):615–639.

Litchman, E., Klausmeier, C. A., Schofield, O. M., and Falkowski, P. G. (2007). The role of functional traits and trade-offs in structuring phytoplankton communities: scaling from cellular to ecosystem level. *Ecology Letters*, 10(12):1170–1181.

Litchman, E., Klausmeier, C. A., and Yoshiyama, K. (2009). Contrasting size evolution in marine and freshwater diatoms. *Proceedings of the National Academy of Sciences of the United States of America*, 106(8):2665–2670.

Loeuille, N., Barot, S., Georgelin, E., Kylafis, G., and Lavigne, C. (2013). Eco-evolutionary dynamics of agricultural networks: implications for sustainable management. *Advances in Ecological Research*, 49:339–434.

Loeuille, N., Le Mao, T., and Barot, S. (2017). Effects of plant evolution on nutrient cycling couple aboveground and belowground processes. *Theoretical Ecology*, 10(1):117–127.

Loeuille, N. and Loreau, M. (2004). Nutrient enrichment and food chains: can evolution buffer top-down control? *Theoretical Population Biology*, 65(3):285–98.

Loeuille, N. and Loreau, M. (2005). Evolutionary emergence of size-structured food webs. *Proceedings of the National Academy of Sciences of the United States of America*, 102(16):5761–6.

Loreau, M. (1998a). Biodiversity and ecosystem functioning: a mechanistic model. *Proceedings of the National Academy of Sciences of the United States of America*, 95(10):5632–5636.

Loreau, M. (1998b). Ecosystem development explained by competition within and between material cycles. *Proceedings of the Royal Society of London B: Biological Sciences*, 265(1390):33–38.

Loreau, M. (2010a). *From Populations to Ecosystems: Theoretical Foundations for a New Ecological Synthesis*. Princeto, Princeton and Oxford.

Loreau, M. (2010b). Linking biodiversity and ecosystems: towards a unifying ecological theory. *Philosophical Transactions of the Royal Society B: Biological Sciences*, 365:49–60.

Loreau, M. and de Mazancourt, C. (1999). Should plants in resource-poor environments invest more in antiherbivore defence? *Oikos*, 87:195–200.

Loreau, M. and Ebenhöh, W. (1994). Competitive exclusion and coexistence of species with complex life cycles. *Theoretical Population Biology*, 46(1):58–77.

Lotka, A. J. (1925). *Elements of Physical Biology*. Williams & Wilkins, Baltimore.

Lynch, J. P. and Ho, M. D. (2005). Rhizoeconomics: Carbon costs of phosphorus acquisition. *Plant and Soil*, 269(1-2):45–56.

MacArthur, R. and Levins, R. (1967). The limiting similarity, convergence, and divergence of coexisting species. *The American Naturalist*, 101(921):377.

MacArthur, R. H. (1970). Species packing and competitive equilibrium for many species. *Theoretical Population Biology*, 1:1–11.

MacArthur, R. H. (1972). *Geographical Ecology: Patterns in the Distribution of Species*. Harper & Row, New York.

MacArthur, R. H. and Levins, R. (1964). Competition, habitat selection and character displacement in a patchy environment. *Proceedings of the National Academy of Sciences of the United States of America*, 51(6):1207–1210.

MacArthur, R. H. and Wilson, E. O. (1967). *The Theory of Island Biogeography*. Princeton University Press, Princeton, NJ.

Margalef, R. (1963). On certain unifying principles in ecology. *The American Naturalist*, 97(897):357.

Marleau, J. N., Jin, Y., Bishop, J. G., Fagan, W. F., and Lewis, M. A. (2011). A stoichiometric model of early plant primary succession. *The American Naturalist*, 177(2):233–245.

Marler, R. T. and Arora, J. S. (2004). Survey of multi-objective optimization methods for engineering. *Structural and Multidisciplinary Optimization*, 26(6):369–395.

Massol, F. and Crochet, P.-A. (2008). Do animal personalities emerge? *Nature*, 451(7182):E8–E9.

Matsuda, H. and Abrams, P. A. (1994). Runaway evolution to self-extinction under asymmetrical competition. *Evolution*, 48(6):1764–1772.

Mauricio, R., Rausher, M., and Burdick, D. (1997). Variation in the defense strategies of plants: are resistance and tolerance mutually exclusive? *Ecology*, 78(5):1301–1311.

May, R. M. (1973). Stability and complexity in model ecosystems.

May, R. M. (1977). Thresholds and breakpoints in ecosystems with a multiplicity of stable states. *Nature*, 269:471–477.

McGill, B. J., Enquist, B. J., Weiher, E., and Westoby, M. (2006). Rebuilding community ecology from functional traits. *Trends in Ecology & Evolution*, 21(4):178–185.

McGroddy, M. E., Daufresne, T., and Hedin, L. O. (2004). Scaling of C:N:P stoichiometry in forests worldwide: implications of terrestrial redfield-type ratios. *Ecology*, 85(9):2390–2401.

McNickle, G. G. and Dybzinski, R. (2013). Game theory and plant ecology. *Ecology Letters*, 16:545–555.

Menge, D. N. L., Hedin, L. O., and Pacala, S. W. (2012). Nitrogen and phosphorus limitation over long-term ecosystem development in terrestrial ecosystems. *PLoS ONE*, 7(8):e42045.

Menge, D. N. L., Levin, S. A., and Hedin, L. O. (2008). Evolutionary tradeoffs can select against nitrogen fixation and thereby maintain nitrogen limitation. *Proceedings of the National Academy of Sciences of the United States of America*, 105(5):1573–1578.

Menge, D. N. L., Levin, S. A., and Hedin, L. O. (2009a). Facultative versus obligate nitrogen fixation strategies and their ecosystem consequences. *The American Naturalist*, 174(4):465–477.

Menge, D. N. L., Pacala, S. W., and Hedin, L. O. (2009b). Emergence and maintenance of nutrient limitation over multiple timescales in terrestrial ecosystems. *The American Naturalist*, 173(2):164–75.

Meszéna, G., Gyllenberg, M., Pásztor, L., and Metz, J. A. J. (2006). Competitive exclusion and limiting similarity: a unified theory. *Theoretical Population Biology*, 69(1):68–87.

Meszéna, G. and Metz, J. A. J. (1999). Species diversity and population regulation: the importance of environmental feedback dimensionality. *IIASA Working Paper WP-99-045*.

Metz, J. A. J., Geritz, S. A. H., Meszéna, G., Jacobs, F. J. A., and van Heerwaarden, J. S. (1996). Adaptive dynamics, a geometrical study of the consequences of nearly faithful reproduction. In *Stochastic and Spatial Structures of Dynamical Systems. Proceedings of the Royal Dutch Academy of Science*, pages 183–231.

Metz, J. A. J., Mylius, S. D., and Diekmann, O. (2008). When does evolution optimize? *Evolutionary Ecology Research*, 10:629–654.

Metz, J. A. J., Nisbet, R. M., and Geritz, S. A. (1992). How should we define 'fitness' for general ecological scenarios? *Trends in Ecology & Evolution*, 7(6):198–202.

Meunier, C. L., Boersma, M., El-Sabaawi, R., Halvorson, H. M., Herstoff, E. M., Van de Waal, D. B., Vogt, R. J., and Litchman, E. (2017). From elements to function: toward unifying ecological stoichiometry and trait-based ecology. *Frontiers in Environmental Science*, 5(May):1–10.

Michaud, J. P. and Moreau, G. (2017). Facilitation may not be an adequate mechanism of community succession on carrion. *Oecologia*, 183(4):1143–1153.

Miller, G. H., Magee, J., Smith, M., Spooner, N., Baynes, A., Lehman, S., Fogel, M., Johnston, H., Williams, D., Clark, P., Florian, C., Holst, R., and DeVogel, S. (2016). Human predation contributed to the extinction of the Australian megafaunal bird Genyornis newtoni ˜47 ka. *Nature Communications*, 7:1–7.

Miller, T. E., Burns, J. H., Munguia, P., Walters, E. L., Kneitel, J. M., Richards, P. M., Mouquet, N., and Buckley, H. L. (2005). A critical review of twenty years' use of the resource-ratio theory. *The American Naturalist*, 165(4):439–48.

Mittelbach, G. G., Osenberg, C. W., and Leibold, M. A. (1988). Trophic relations and ontogenetic niche shifts in aquatic ecosystems. In *Size-Structured Populations*, pages 219–235.

Moen, J., Gardfjell, H., Oksanen, L., Ericson, L., and Ekerholm, P. (1993). Grazing by food-limited microtine rodents on a productive experimental plant community: does the green desert exist? *Oikos*, 68(3):401–413.

Mole, S. (1994). Trade-offs and constraints in plant-herbivore defense theory: a life-history perspective. *Oikos*, 71(1):3–12.

Monod, J. (1950). Theory and application of the technique of continuous culture. *Annals of the Pasteur Institute*, 79:590–410.

Morris, J. J. (2015). Black Queen evolution: the role of leakiness in structuring microbial communities. *Trends in Genetics*, 31(8):475–482.

Morris, J. J., Lenski, R. E., and Zinser, E. R. (2012). The Black Queen hypothesis: evolution of dependencies through adaptive gene loss. *mBio*, 3(2):1–7.

Morton, R. D. and Law, R. (1997). Regional species pools and the assembly of local ecological communities. *Journal of Theoretical Biology*, 187(3):321–331.

Murdoch, W. W. (1969). Switching in general predators: experiments on predator specificity and stability of prey populations. *Ecological Monographs*, 39(4):335–354.

Murdoch, W. W., Avery, S., and Smyth, M. E. B. (1975). Switching in predatory fish. *Ecology*, 56(5):1094–1105.

Mylius, S. D. and Diekmann, O. (2001). The resident strikes back: invader-induced switching of resident attractor. *Journal of Theoretical Biology*, 211:297–311.

Norberg, J. (2013). Biodiversity and ecosystem functioning: a complex adaptive systems approach. *Limnology and Oceanography*, 49(4):1269–1277.

Novick, A. and Szilard, L. (1950). Description of the chemostat. *Science*, 112:715–716.

Odling-Smee, J., Laland, K. N., and Feldman, M. W. (1996). Niche construction. *The American Naturalist*, 147(4):641–648.

Odling-Smee, J., Laland, K. N., and Feldman, M. W. (2003). *Niche Construction: The Neglected Process in Evolution*. Princeton University Press.

Odum, E. P. (1969). The strategy of ecosystem development. *Science*, 164(3877):262–270.

Odum, H. T. (1971). *Environment, Power and Society*. Wiley-Interscience, New York, USA.

Oksanen, L., Fretwell, S. D., Arruda, J., and Niemela, P. (1981). Exploitation ecosystems in gradients of primary productivity. *The American Naturalist*, 118(2):240–261.

Oksanen, L. and Oksanen, T. (2000). The logic and realism of the hypothesis of exploitation ecosystems. *The American Naturalist*, 155(6):703–723.

Olson, J. S. (1958). Rates of succession and soil changes on southern Lake Michigan sand dunes. *Botanical Gazette*, 119(3):125–170.

Oren, R., Ellsworth, D. S., Johnsen, K. H., Phillips, N., Mccarthy, H., Ewers, B. E., Maier, C., Schäfer, K. V. R., Hendrey, G., Mcnulty, S. G., and Katul, G. G. (2001). Soil fertility limits carbon sequestration by forest ecosystems in a CO2-enriched atmosphere. *Nature*, 411(6836):469–472.

Oyarzun, F. J. and Lange, K. (1994). The attractiveness of the Droop equations II. Generic uptake and growth functions. *Mathematical Biosciences*, 121(2):127–139.

Pantel, J. H., Bohan, D. A., Calcagno, V., David, P., Duyck, P.-F., Kamenova, S., Loeuille, N., Mollot, G., Romanuk, T. N., Thébault, E., Tixier, P., and Massol, F. (2017). 14 Questions for Invasion in Ecological Networks. In *Networks of Invasions in Advances in Ecological Research*, page 318.

Pareto, V. (1906). *Manuale di Economia Politica con una Introduzione alla Scienza Sociale*. Societa Editrice Libraria, Milano.

Parvinen, K. (2005). Evolutionary suicide. *Acta Biotheoretica*, 53(3):241–264.

Pasciak, W. J. and Gavis, J. (1974). Transport limitation of nutrient uptake in phytoplankton. *Limnology and Oceanography*, 19(6):881–888.

Pascual, M. and Caswell, H. (1997). From the cell cycle to population cycles in phytoplankton-nutrient interactions. *Ecology*, 78(3):897–912.

Pásztor, L., Botta-Dukát, Z., Magyar, G., Czárán, T., and Meszéna, G. (2016). *Theory-Based Ecology: A Darwnian Approach*. Oxford University Press.

Peltzer, D. A., Wardle, D. A., Allison, V. J., Baisden, W. T., Bardgett, R. D., Chadwick, O. A., Condron, L. M., Parfitt, R. L., Porder, S., Richardson, S. J., Turner, B. L., Vitousek, P. M., Walker, J., and Walker, L. R. (2010). Understanding ecosystem retrogression. *Ecological Monographs*, 80(4):509–529.

Perga, M. E., Domaizon, I., Guillard, J., Hamelet, V., and Anneville, O. (2013). Are cyanobacterial blooms trophic dead ends? *Oecologia*, 172(2):551–562.

Petraitis, P. S. (1989). The representation of niche breadth and overlap on Tilman's consumer-resource graphs. *Oikos*, 56(3):289–292.

Pianka, E. R. (1970). On r- and K- selection. *The American Naturalist*, 104(940):592–597.

Pietrewicz, A. T. and Kamil, A. C. (1979). Search image formation in the blue jay (Cyanocitta cristata). *Science*, 204(4399):1332–1333.

Rankin, D. J., Bargum, K., and Kokko, H. (2007). The tragedy of the commons in evolutionary biology. *Trends in Ecology and Evolution*, 22(12):643–651.

Rankin, D. J. and López-Sepulcre, A. (2005). Can adaptation lead to extinction? *Oikos*, 111(3):616–619.

Rapaport, A. (2017). Some non-intuitive properties of simple extensions of the chemostat model. *Ecological Complexity*, page https://doi.org/10.1016/j.ecocom.2017.02.003.

Rasmann, S. and Agrawal, A. A. (2008). In defense of roots: a research agenda for studying plant resistance to belowground herbivory. *Plant Physiology*, 146(3):875–880.

Redfield, A. C. (1958). The biological control of chemical factors in the environment. *American Scientist*, 46(3):205–221.

Reich, P. B., Hobbie, S. E., Lee, T., Ellsworth, D. S., West, J. B., Tilman, D., Knops, J. M. H., Naeem, S., and Trost, J. (2006). Nitrogen limitation constrains sustainability of ecosystem response to CO2. *Nature*, 440(7086):922–5.

Richardson, S. J., Peltzer, D. A., Allen, R. B., McGlone, M. S., and Parfitt, R. L. (2004). Rapid development of phosphorus limitation in temperate rainforest along the Franz Josef soil chronosequence. *Oecologia*, 139(2):267–76.

Rietkerk, M., Dekker, S. C., de Ruiter, P. C., and van de Koppel, J. (2004). Self-organized patchiness and catastrophic shifts in ecosystems. *Science*, 305(5692):1926–9.

Rueffler, C., Van Dooren, T. J. M., and Metz, J. A. J. (2004). Adaptive walks on changing landscapes: Levins' approach extended. *Theoretical Population Biology*, 65(2):165–178.

Ryabov, A. B. and Blasius, B. (2011). A graphical theory of competition on spatial resource gradients. *Ecology Letters*, 14(3):220–228.

Saavedra, S., Rohr, R. P., Bascompte, J., Godoy, O., Kraft, N. J. B., and Levine, J. M. (2017). A structural approach for understanding multispecies coexistence. *Ecological Monographs*, 87(3):470–486.

Samuelson, P. A. (1947). *Foundations of Economic Analysis*. Harvard University Press, Cambridge.

Sauterey, B., Ward, B., Rault, J., Bowler, C., and Claessen, D. (2017). The implications of eco-evolutionary processes for the emergence of marine plankton community biogeography. *The American Naturalist*, 190(1):000–000.

Sauterey, B., Ward, B. A., Follows, M. J., Bowler, C., and Claessen, D. (2015). When everything is not everywhere but species evolve: an alternative method to model adaptive properties of marine ecosystems. *Journal of Plankton Research*, 37(1):28–47.

Schade, J. D., Espeleta, J. F., Klausmeier, C. A., McGroddy, M. E., Thomas, S. A., and Zhang, L. (2005). A conceptual framework for ecosystem stoichiometry: balancing resource supply and demand. *Oikos*, 109(1):40–51.

Scheffer, M., Carpenter, S., Foley, J. A., Folke, C., and Walker, B. (2001). Catastrophic shifts in ecosystems. *Nature*, 413:591–596.

Schellekens, T., de Roos, A. M., and Persson, L. (2010). Ontogenetic diet shifts result in niche partitioning between two consumer species irrespective of competitive abilities. *The American Naturalist*, 176(5):625–637.

Schlesinger, W. H., Cole, J. J., Finzi, A. C., and Holland, E. A. (2011). Introduction to coupled biogeochemical cycles. *Frontiers in Ecology and the Environment*, 9(1):5–8.

Schmidt, S. K., Reed, S. C., Nemergut, D. R., Grandy, A. S., Cleveland, C. C., Weintraub, M. N., Hill, A. W., Costello, E. K., Meyer, A. F., Neff, J. C., and Martin, A. M. (2008).

The earliest stages of ecosystem succession in high-elevation (5000 metres above sea level), recently deglaciated soils. *Proceedings of the Royal Society of London B: Biological Sciences*, 275(1653):2793–2802.

Schreiber, S. J., Patel, S., and TerHorst, C. (2016). Evolution as a coexistence mechanism: does genetic architecture matter? page arXiv:1609.05571.

Schreiber, S. J. and Rudolf, V. H. W. (2008). Crossing habitat boundaries: coupling dynamics of ecosystems through complex life cycles. *Ecology Letters*, 11(6):576–87.

Schreiber, S. J. and Tobiason, G. A. (2003). The evolution of resource use. *Journal of Mathematical Biology*, 47:56–78.

Schymanski, S. J., Roderick, M. L., Sivapalan, M., Hutley, L. B., and Beringer, J. (2007). A test of the optimality approach to modelling canopy properties and CO2 uptake by natural vegetation. *Plant, Cell and Environment*, 30(12):1586–1598.

Seebens, H., Blackburn, T. M., Dyer, E., Genovesi, P., Hulme, P. E., Jeschke, J. M., Pagad, S., Pyšek, P., Winter, M., Arianoutsou, M., Bacher, S., Blasius, B., Brundu, G., Capinha, C., Celesti-Grapow, L., Dawson, W., Dullinger, S., Fuentes, N., Jäger, H., Kartesz, J., Kenis, M., Kreft, H., Kühn, I., Lenzner, B., Liebhold, A., Mosena, A., Moser, D., Nishino, M., Pearman, D., Pergl, J., Rabitsch, W., Rojas-Sandoval, J., Roques, A., Rorke, S., Rossinelli, S., Roy, H. E., Scalera, R., Schindler, S., Štajerová, K., Tokarska-Guzik, B., van Kleunen, M., Walker, K., Weigelt, P., Yamanaka, T., and Essl, F. (2017). No saturation in the accumulation of alien species worldwide. *Nature Communications*, pages 1–9.

Seppelt, R., Lautenbach, S., and Volk, M. (2013). Identifying trade-offs between ecosystem services, land use, and biodiversity: a plea for combining scenario analysis and optimization on different spatial scales. *Current Opinion in Environmental Sustainability*, 5(5):458–463.

Sheffer, E., Batterman, S. A., Levin, S. A., and Hedin, L. O. (2015). Biome-scale nitrogen fixation strategies selected by climatic constraints on nitrogen cycle. *Nature Plants*, 1(12):15182.

Shoresh, N., Hegreness, M., and Kishony, R. (2008). Evolution exacerbates the paradox of the plankton. *Proceedings of the National Academy of Sciences of the United States of America*, 105(34):12365–12369.

Shugart, H. H. (2013). Ecological succession and community dynamics. In Leemans, R., editor, *Ecological Systems: Selected Entries from the Encyclopedia of Sustainability Science and Technology*, pages 31–57. Springer Science.

Siles, G., Rey, P. J., Alcántara, J. M., and Ramírez, J. M. (2008). Assessing the long-term contribution of nurse plants to restoration of Mediterranean forests through Markovian models. *Journal of Applied Ecology*, 45(6):1790–1798.

Simms, E. L. and Rausher, M. D. (1987). Costs and benefits of plant resistance to herbivory. *The American Naturalist*, 130(4):570–581.

Smith, S. L., Pahlow, M., Merico, A., and Wirtz, K. W. (2011). Optimality-based modeling of planktonic organisms. *Limnology and Oceanography*, 56(6):2080–2094.

Stamp, N. (2003). Out of the quagmire of plant defense hypotheses. *The Quarterly Review of Biology*, 78(1):23–55.

Sterner, R. W. and Elser, J. J. (2002). *Ecological stoichiometry: the biology of elements from molecules to the biosphere*. Princeton University Press.

Stoll, P. and Weiner, J. (2000). A neighborhood view of interactions among individual plants. In *The Geometry of Ecological Interactions: Simplifying Spatial Complexity*, pages 11–27.

Stowe, K. A. (2013). Defense and tolerance: is the distinction between these two plant strategies useful? *International Journal of Modern Botany*, 3:1–4.

Strogatz, S. H. (2015). *Nonlinear Dynamics and Chaos: With Applications to Physics, Biology, Chemistry, and Engineering*. Westview Press, Boulder, CO.

Stuart, Y. E., Campbell, T. S., Hohenlohe, P. A., Reynolds, R. G., Revell, L. J., and Losos, J. B. (2014). Rapid evolution of a native species following invasion by a congener. *Science*, 346(6208):463–466.

Szilágyi, A. and Meszéna, G. (2009). Limiting similarity and niche theory for structured populations. *Journal of Theoretical Biology*, 258:27–37.

Thébault, E. and Fontaine, C. (2010). Stability of ecological communities and the architecture of mutualistic and trophic networks. *Science*, 329(5993):853–6.

Thomas, M. K., Kremer, C. T., Klausmeier, C. A., and Litchman, E. (2012). A global pattern of thermal adaptation in marine phytoplankton. *Science*, 338:1085–1089.

Thompson, J. N. (1998). Rapid evolution as an ecological process. *Trends in Ecology & Evolution*, 13(8):329–32.

Thuynsma, R., Valentine, A., and Kleinert, A. (2014). Phosphorus deficiency affects the allocation of below-ground resources to combined cluster roots and nodules in Lupinus albus. *Journal of Plant Physiology*, 171(3-4):285–291.

Tiffin, P. (2000). Are Tolerance, avoidance, and antibiosis evolutionarily and ecologically equivalent responses of plants to herbivores? *The American Naturalist*, 155(1):128–138.

Tiffin, P., Inouye, B. D., and Underwood, N. (2006). Induction and herbivore mobility affect the evolutionary escalation of plant defence. *Evolutionary Ecology Research*, 8(2):265–277.

Tilman, D. (1980). Resources: a graphical-mechanistic approach to competition and predation. *The American Naturalist*, 116(3):362–393.

Tilman, D. (1982). *Resource Competition and Community Structure*. Princeton University Press, Princeton, NJ.

Tilman, D. (1985). The resource-ratio hypothesis of plant succession. *The American Naturalist*, 125(6):827–852.

Tilman, D. (1988). *Plant Strategies and the Dynamics and Structure of Plant Communities*. Princeton University Press, Princeton, NJ.

Tilman, D. (1990). Constraints and tradeoffs: toward a predictive theory of competition and succession. *Oikos*, 58(1):3–15.

Tilman, D. (1994). Competition and biodiversity in spatially structured habitats. *Ecology*, 75(1):2–16.

Turchin, P. (2001). Does population ecology have general laws? *Oikos*, 94(1):17–26.

Turley, N. E., Godfrey, R. M., and Johnson, M. T. J. (2013). Evolution of mixed strategies of plant defense against herbivores. *New Phytologist*, 197(2):359–361.

Turnbull, L. A., Rees, M., and Crawley, M. J. (1999). Seed mass and the competition/colonization trade-off: a sowing experiment. *Journal of Ecology*, 87:899–912.

Underwood, N. (1999). The influence of plant and herbivore characteristics on the interaction between induced resistance and herbivore population dynamics. *The American Naturalist*, 153(3):282–294.

Usher, M. B. (1981). Modelling ecological succession, with particular reference to Markovian models. *Vegetatio*, 46:11–18.

Våge, S., Storesund, J. E., Giske, J., and Thingstad, T. F. (2014). Optimal defense strategies in an idealized microbial food web under trade-off between competition and defense. *PLoS ONE*, 9(7).

Valiente-Banuet, A., Vite, F., and Zavala-Hurtado, J. A. (1991). Interaction between the cactus Neobuxbaumia tetetzo and the nurse shrub Mimosa luisana. *Journal of Vegetation Science*, 2(1978):11–14.

van den Driessche, R. (1974). Prediction of mineral nutrient status of trees by foliar analysis. *The Botanical Review*, 40(3):347–94.

Van Hulst, R. (1979). On the dynamics of vegetation: Markov chains as models of succession. *Vegetatio*, 40(1):3–14.

van Loon, M. P., Schieving, F., Rietkerk, M., Dekker, S. C., Sterck, F., and Anten, N. P. R. (2014). How light competition between plants affects their response to climate change. *New Phytologist*, 203(4):1253–1265.

van Noordwijk, A. T. and de Jong, G. (1986). Acquisition and allocation of resources: their influence on variation in life history tactics. *The American Naturalist*, 128(1):137–142.

van Wijk, M. T., Williams, M., Gough, L., Hobbie, S. E., and Shaver, G. R. (2003). Luxury consumption of soil nutrients: a possible competitive strategy in above-ground and below-ground biomass allocation and root morphology for slow-growing arctic vegetation? *Journal of Ecology*, 91:664–676.

Vellend, M. (2010). Conceptual synthesis in community ecology. *The Quarterly review of biology*, 85(2):183–206.

Verhulst, P. F. (1847). Deuxième mémoire sur la loi d'accroissement de la population. *Mém. de l'Academie Royale des Sci., des Lettres et des Beaux-Arts de Belgique*, 18:1—-32.

Violle, C., Navas, M.-L., Vile, D., Kazakou, E., Fortunel, C., Hummel, I., and Garnier, E. (2007). Let the concept of trait be functional! *Oikos*, 116(5):882–892.

Violle, C., Reich, P. B., Pacala, S. W., Enquist, B. J., and Kattge, J. (2014). The emergence and promise of functional biogeography. *Proceedings of the National Academy of Sciences of the United States of America*, 111(38).

Vitousek, P. M., Cassman, K. E. N., Cleveland, C., Field, C. B., Grimm, N. B., and Hole, W. (2002). Towards an ecological understanding of biological nitrogen fixation. *Biogeochemistry*, 57(1):1–45.

Vitousek, P. M. and Farrington, H. (1997). Nutrient limitation and soil development: experimental test of a biogeochemical theory. *Biogeochemistry*, 37:63–75.

Vitousek, P. M. and Howarth, R. W. (1991). Nitrogen limitation on land and in the sea: how can it occurs? *Biochemistry*, 13(2):87–115.

Vitousek, P. M., Mooney, H. A., Lubchenco, J., and Melillo, J. M. (1997). Human Domination of Earth's Ecosystems. *Science*, 277(5325):494–499.

Vitousek, P. M., Porder, S., Houlton, B. Z., and Chadwick, O. A. (2010). Terrestrial phosphorus limitation: mechanisms, implications, and nitrogen-phosphorus interactions. *Ecological Applications*, 20(1):5–15.

Vitousek, P. M., Walker, L. R., Whiteaker, L. D., and Matson, P. A. (1993). Nutrient limitations to plant growth during primary succession in Hawaii Volcanoes National Park. *Biogeochemistry*, 23(3):197–215.

Volterra, V. (1926). Fluctuations in the abundance of a species considered mathematically. *Nature*, 118(2972):558–560.

Von Humbolt, A. and Bonpland, A. (1807). *Essai sur la géographie des plantes*.

Walker, L. R. (1993). Nitrogen fixers and species replacements in primary succession. In Miles, J. and Walton, D. W. H., editors, *Primary Succession on Land*, pages 249–272.

Walker, L. R., Clarkson, B. D., Silvester, W. B., and Clarkson, B. R. (2003). Colonization dynamics and facilitative impacts of a nitrogen-fixing shrub in primary succession. *Journal of Vegetation Science*, 14(2):277–290.

Walker, L. R. and del Moral, R. (2003). *Primary Succession and Ecosystem Rehabilitation*. Cambridge University Press, Cambridge, UK.

Walker, T. W. and Syers, J. K. (1976). The fate of phosphorus during pedogenesis. *Geoderma*, 15:1–19.

Wardle, D. A., Walker, L. R., and Bardgett, R. D. (2004). Ecosystem properties and forest decline in contrasting long-term chronosequences. *Science*, 305(5683):509–513.

Watt, A. S. (1947). Pattern and process in the plant community. *Journal of Ecology*, 35(1/2):1–22.

Weiner, J. (1990). Asymmetric competition in plant populations. *Trends in Ecology and Evolution*, 5(11):360–364.

Weiner, J., Andersen, S. B., Wille, W. K., Griepentrog, H. W., and Olsen, J. M. (2010). Evolutionary agroecology: the potential for cooperative, high density, weed-suppressing cereals. *Evolutionary Applications*, 3:473–479.

Weng, E. S., Malyshev, S., Lichstein, J. W., Farrior, C. E., Dybzinski, R., Zhang, T., Shevliakova, E., and Pacala, S. W. (2015). Scaling from individual trees to forests in an Earth system modeling framework using a mathematically tractable model of height-structured competition. *Biogeosciences*, 12(9):2655–2694.

Westoby, M. and Wright, I. J. (2006). Land-plant ecology on the basis of functional traits. *Trends in Ecology & Evolution*, 21(5):261–268.

Wetzel, W. C., Kharouba, H. M., Robinson, M., Holyoak, M., and Karban, R. (2016). Variability in plant nutrients reduces insect herbivore performance. *Nature*, 539(7629):425–427.

Whittaker, R. H. (1962). Classification of natural communities. *Botanical Review*, 28(1):1–239.

Wilson, A. E., Sarnelle, O., and Tillmanns, A. R. (2006). Effects of cyanobacterial toxicity and morphology on the population growth of freshwater zooplankton: meta-analyses of laboratory experiments. *Limnology and Oceanography*, 51(4):1915–1924.

Wise, M. J. and Abrahamson, W. G. (2007). Effects of resource availability on tolerance of herbivory: a review and assessment of three opposing models. *The American Naturalist*, 169(4):443–454.

Wolf, M., van Doorn, G. S., Leimar, O., and Weissing, F. J. (2007). Life-history trade-offs favour the evolution of animal personalities. *Nature*, 447(7144):581–584.

Wolf, M., van Doorn, G. S., Leimar, O., and Weissing, F. J. (2008). Wolf et al. reply. *Nature*, 451(7182):E9–E10.

Wolkowicz, G. S. K. and Lu, Z. (1992). Global dynamics of a mathematical model of competition in the chemostat: general response functions and differential death rates. *SIAM Journal on Applied Mathematics*, 52(1):222–233.

Wollrab, S., Diehl, S., and De Roos, A. M. (2012). Simple rules describe bottom-up and top-down control in food webs with alternative energy pathways. *Ecology Letters*, 15(9):935–46.

Worley, I. A. (1973). The "black crust" phenomenon in Upper Glacier Bay, Alaska. *Northwest Science*, 47:20–29.

Yachi, S. and Loreau, M. (1999). Biodiversity and ecosystem productivity in a fluctuating environment: The insurance hypothesis. *Proceedings of the National Academy of Sciences of the United States of America*, 96:1463–1468.

Yoshida, T., Hairston, N. G., and Ellner, S. P. (2004). Evolutionary trade-off between defence against grazing and competitive ability in a simple unicellular alga, Chlorella vulgaris. *Proceedings of the Royal Society of London B: Biological Sciences*, 271(1551):1947–1953.

Yoshida, T., Jones, L. E., Ellner, S. P., Fussmann, G. F., and Hairston, N. G. (2003). Rapid evolution drives ecological dynamics in a predator-prey system. *Nature*, 424(6946):303–306.

Zhu, J. and Lynch, J. P. (2004). The contribution of lateral rooting to phosphorus acquisition efficiency in maize (Zea mays) seedlings. *Functional Plant Biology*, 31(10):949–958.

Zu, J., Yuan, B., and Du, J. (2015). Top predators induce the evolutionary diversification of intermediate predator species. *Journal of Theoretical Biology*, 387:1–12.

Appendices

Contents

Appendix A

Geometrical envelopes: Extending graphical contemporary niche theory to communities and eco-evolutionary dynamics (Article Koffel et al., JTB, 2016)

Journal of Theoretical Biology 407 (2016) 271–289

Contents lists available at ScienceDirect

Journal of Theoretical Biology

journal homepage: www.elsevier.com/locate/yjtbi

Geometrical envelopes: Extending graphical contemporary niche theory to communities and eco-evolutionary dynamics

Thomas Koffel [a,b,*], Tanguy Daufresne [a], François Massol [c], Christopher A. Klausmeier [b]

[a] UMR Eco&Sols, Campus Supagro, 2 place Viala, 34060 Montpellier, France
[b] Kellogg Biological Station, Dept. of Plant Biology, & Program in Ecology, EvolutionaryBiol. & Behavior, Michigan State University, 3700 E Gull Lake Dr, Hickory Corners, MI 49060, United States
[c] CNRS, Université de Lille – Sciences et Technologies, UMR 8198 Evo-Eco-Paleo, SPICI group, F-59655 Villeneuve d'Ascq, France

HIGHLIGHTS

- Graphical contemporary niche theory can be extended to a continuum of strategies.
- This extension is performed using geometrical envelopes of zero net growth isoclines.
- This approach provides community bifurcation diagrams along environmental gradients.
- Evolutionary singular strategies are also identified and characterized graphically.

ARTICLE INFO

Article history:
Received 29 March 2016
Received in revised form
10 July 2016
Accepted 20 July 2016
Available online 26 July 2016

Keywords:
Coexistence
Competition
Zero net growth isocline
Community ecology
Species sorting
Adaptive dynamics
Evolutionary branching

ABSTRACT

Contemporary niche theory is a powerful structuring framework in theoretical ecology. First developed in the context of resource competition, it has been extended to encompass other types of regulating factors such as shared predators, parasites or inhibitors. A central component of contemporary niche theory is a graphical approach popularized by Tilman that illustrates the different outcomes of competition along environmental gradients, like coexistence and competitive exclusion. These food web modules have been used to address species sorting in community ecology, as well as adaptation and coexistence on eco-evolutionary time scales in adaptive dynamics. Yet, the associated graphical approach has been underused so far in the evolutionary context. In this paper, we provide a rigorous approach to extend this graphical method to a continuum of interacting strategies, using the geometrical concept of the envelope. Not only does this approach provide community and eco-evolutionary bifurcation diagrams along environmental gradients, it also sheds light on the similarities and differences between those two perspectives. Adaptive dynamics naturally merges with this ecological framework, with a close correspondence between the classification of singular strategies and the geometrical properties of the envelope. Finally, this approach provides an integrative tool to study adaptation between levels of organization, from the individual to the ecosystem.

1. Introduction

Competition is a ubiquitous interaction among living organisms, and thus a major driver of community structure and evolution by natural selection. As such, it was at the core of the very first mathematical models of population dynamics and theoretical ecology (Lotka, 1925; Volterra, 1926; Gause, 1934). However, the explicit inclusion of resources for which species compete came only several decades later with the pioneering works of MacArthur and Levins (1964), MacArthur and Wilson (1967), and MacArthur (1970). Mechanistic competition models, or modules, allow a useful graphical representation introduced by MacArthur and Levins (1964), developed by León and Tumpson (1975) and largely popularized by Tilman (1980, 1982), which summarizes graphically the different outcomes of competition along environmental gradients, delimiting the coexistence regions from competitive exclusion or founder control. This method relies on the combination of three key graphical ingredients: Zero net growth isoclines (ZNGIs), consumption/impact vectors and supply points. These respectively represent a species' minimal requirements, its

* Corresponding author at: UMR Eco&Sols, Campus Supagro, 2 place Viala, 34060 Montpellier, France.
E-mail addresses: thomas.koffel@supagro.inra.fr (T. Koffel), tanguy.daufresne@inra.fr (T. Daufresne), francois.massol@univ-lille1.fr (F. Massol), klausme1@msu.edu (C.A. Klausmeier).

http://dx.doi.org/10.1016/j.jtbi.2016.07.026
0022-5193/

consumptive impacts, and the externally driven resource availability in the absence of any consumer. Supported empirically (Miller et al., 2005), the theory also brings strong conceptual results on the conditions for coexistence consistent with the competitive exclusion principle (Levin, 1970).

The concept of resource competition can be generalized to encompass any kind of regulating factors that mediate interspecific interactions. This was done by Chase and Leibold (2003) under the unifying umbrella of "contemporary niche theory", further formalized by recent developments (Meszéna et al., 2006; Barabás et al., 2014b). For example, two prey sharing one predator formally behave as if they were competing for a single resource, a situation referred to as apparent competition by Holt (1977). This allows the use of the graphical representation in this generalized framework, as was done with apparent competition plus resource competition by Holt et al. (1994), Grover (1995), Leibold (1996) and Chase and Leibold (2003). Interference competition through explicit inhibitory product emission also fits in this framework, with the inhibitor playing the role of a regulating factor (Gerla et al., 2009). Recently, several authors further extended this graphical approach to take into account several phenomena: nutrient cycling (Daufresne and Hedin, 2005), cooperation (de Mazancourt and Schwartz, 2010), niche construction (Kylafis and Loreau, 2011) and population structure, either spatial (Ryabov and Blasius, 2011; Haegeman and Loreau, 2015) or demographic (Loreau and Ebenhöh, 1994; Schellekens et al., 2010).

Popularized in the context of a couple of interacting species, these niche theoretic models can be scaled up to investigate community assembly, based on the idea that local environmental conditions are the drivers of species sorting from a large or potentially infinite number of species along a trade-off curve (Leibold et al., 2004). This approach relies on the key assumption that "everything is everywhere", namely that there is no dispersal limitation to a species' presence (Baas Becking, 1934; De Wit and Bouvier, 2006). The associated generalized graphical methods uses the concept of geometrical envelopes, the boundary of a family of curves, providing a natural way to look graphically at species sorting along an environmental gradient (Armstrong, 1979; Tilman, 1980, 1982; Leibold, 1996; Chase and Leibold, 2003; Schade et al., 2005; Danger et al., 2008). Community composition and levels of regulating factors along the gradient can thus be investigated. These mechanistic models naturally fit into trait-based approaches, which have garnered recent interest in ecology (Lavorel and Garnier, 2002; McGill et al., 2006; Westoby and Wright, 2006; Litchman and Klausmeier, 2008). Traits hold the key to linking trade-offs from the organism level to ecosystem functions and services, in both aquatic and terrestrial ecosystems (Litchman et al., 2007; Lavorel and Grigulis, 2012). Trait-based approaches also are a natural framework to study community responses to climate change (Adler et al., 2012; Thomas et al., 2012; Barabás et al., 2014b).

Simultaneously, it has long been recognized that organisms are the product of their evolutionary history (Dobzhansky, 1973) and there is growing evidence of the interplay between ecology and evolution (Thompson, 1998; Yoshida et al., 2003; Hairston et al., 2005; Grant and Grant, 2006; Stuart et al., 2014). However, the influence of this past or present evolution on food web modules remains understudied. Theoretically, those questions have been addressed during the last decades using adaptive dynamics (Hofbauer and Sigmund, 1990; Dieckmann and Law, 1996; Geritz et al., 1997, 1998). This powerful framework allows one to address evolution in arbitrarily complex ecological models. As an evolutionary game theory approach, this is done by including the density- and frequency-dependent selection arising from the feedback loop between the evolving population and its environment (Dieckmann and Metz, 2006). It clarifies the conditions under which evolution acts as an optimizing process (Dieckmann and Ferrière, 2004; Metz et al., 2008) and leads to the concept of evolutionary branching, a potential prelude to diversification (Metz et al., 1996; Geritz et al., 1997, 1998; Dieckmann and Doebeli, 1999). Unlike species sorting, adaptive dynamics considers local invasibility only. Evolution can thus get stuck on local but not global fitness maxima. When applied to food web modules, this enables one to investigate the evolutionary stability of coexistence in various ecological situations (Schreiber and Tobiason, 2003; Klausmeier et al., 2007; Shoresh et al., 2008; Zu et al., 2015). Yet the conditions that allow evolutionarily stable coexistence remain unclear, as ecological coexistence often vanishes on evolutionary time scales through convergent selection. Importantly, the graphical representation is still helpful in those adaptive competition modules to perform invasion analysis when combined with ZNGI geometrical envelopes (Meszéna and Metz, 1999).

The concept of the envelope has a long history in mathematical optimization and its applications. It has for example its own theorem in economics, the envelope theorem (Samuelson, 1947), and is related to the Pareto frontier (Pareto, 1906), a multi-objective optimization concept first introduced in economics and now commonly used in engineer and environmental sciences (Marler and Arora, 2004; Seppelt et al., 2013; Lester et al., 2013). Envelopes of environment-dependent growth rate functions have been used in ecology to identify the optimal species corresponding to given environmental conditions (Eppley, 1972; Norberg, 2013). In resource competition theory, the idea of taking the ZNGI envelope of a continuum of competing strategies can be traced back to Tilman (1982), who applied it heuristically to species sorting from a regional pool or adaptive foraging at the individual scale. It has been used more recently in the context of communities under the names "community ZNGI" (Schade et al., 2005; Danger et al., 2008) or "overall ZNGI" (Chase and Leibold, 2003). Meszéna and Metz (1999) introduced the ZNGI envelope in the eco-evolutionary context and called it "the boundary". They showed how evolution through the trait substitution process of adaptive dynamics can be pictured by ZNGIs rolling along their envelope, and how this helps identify evolutionary singularities and deduce their properties, both graphically.

The aim of the paper is to unite the theoretical approaches to community assembly processes and eco-evolutionary dynamics under the common umbrella of a graphical theory of interaction, using geometrical envelopes. This provides a promising tool to investigate adaptation, diversification and functioning along environmental gradients. We first review step-by-step how to apply the graphical method to competition modules with a few species, combining the concepts of invasion analysis and impact map. Then, we show through a rigorous mathematical framework how those ideas can be naturally extended to a continuum of competitors using geometrical envelopes. Building on the intuitions of Meszéna and Metz (1999), we demonstrate for general non-linear ZNGIs how their envelope geometry relates to local invasibility. Moreover, the use of the impact ray map allows us to identify and characterize geometrically the eco-evolutionary singularities associated with a given supply point. This provides both community and eco-evolutionary bifurcation diagrams, predicting a vast range of possible adaptive behaviors along the environmental gradients. Conditions leading to robust coexistence, evolutionary priority effects and branching points can be easily identified, as they present unambiguous graphical signatures. Conceptually, this graphical approach shows how adaptive dynamics naturally combines with mechanistic competition theory. It also emphasizes the similarities and differences between species sorting from a regional pool and evolution through small step mutations, a global versus local picture. The envelope approach provides a unified tool to navigate between scales through adaptation, from the individual

to the ecosystem level. Finally, we illustrate the method through the example of a versatile model of competition on two resources (Schreiber and Tobiason, 2003), shedding new light on the conditions leading to the evolution of resource specialization.

2. Modeling framework and analysis

2.1. Standard graphical construction for n competitors

Let us first introduce the general class of mathematical models treated in this paper. We consider a community of n species, the abundances of which are denoted $\boldsymbol{N} = (N_1, N_2, \ldots N_n)$, which interact through p regulating factors $\boldsymbol{R} = (R_1, R_2, \ldots R_p)$. The dynamics of N_j and R_i obey the following equations:

$$\frac{dN_j}{dt} = w_j(R_1, R_2, \ldots, R_p)N_j \tag{1a}$$

$$\frac{dR_i}{dt} = l_i(S_i - R_i) + \sum_{j=1}^{n} I_{ij}\big(R_1, R_2, \ldots, R_p\big)N_j \tag{1b}$$

where w_j is the net growth rate of population j and I_{ij} its per capita impact on the regulating factor i. No assumptions are made about their expression, except that they both only depend on the regulating factors $\boldsymbol{R}$. We thus follow Meszéna et al. (2006) by considering that interactions between individuals are indirect, only mediated by the regulating factors. As a particular case of Meszéna et al. (2006), Eq. (1b) assumes that the total impact of a population on a regulating factor is simply proportional to its density. Note that we have chosen the convention that resource consumption corresponds to negative impact I_{ij} but also allowed positive I_{ij}, for example with shared predators. Finally, the supply point $\boldsymbol{S} = (S_1, S_2, \ldots, S_p)$ and the leaching or mortality rates l_i parametrize the semi-chemostat intrinsic dynamics of the regulating factors, which interact only indirectly, through the species $\boldsymbol{N}$. Particularly suited for experimental setups (Novick and Szilard, 1950; Monod, 1950), this framework is classically used to describe abiotic resource dynamics in a wide range of systems (Tilman, 1982; Grover, 1997; Loreau, 1998a). For biotic resources, a well chosen change of variables can be made to map logistic growth into the chemostat dynamics of Eq. (1b) (see Appendix A). Examples of models following the particular form of Eq. (1) include resource–consumer modules (Tilman, 1980; Wolkowicz and Lu, 1992; Schreiber and Tobiason, 2003), food webs with keystone predation (Holt et al., 1994; Leibold, 1996), material-cycle models (Loreau, 1998b; Daufresne and Hedin, 2005) and interference competition through inhibitory product emissions (Gerla et al., 2009).

We will restrict our analysis of this system to its equilibria. Setting aside unrealistic fine-tuning between the demographic parameters, this implies that the maximal number of coexisting populations cannot be greater than the number p of regulating factors, a classical result known as the competitive exclusion principle (CEP) or dimension-diversity theorem (Levin, 1970; Gyllenberg and Meszéna, 2005; Meszéna et al., 2006). Because of the non-linear feedback loops between the regulating factors and the population densities, it is generally not possible to find analytical expressions for the equilibria of Eq. (1), except for some particular systems. However, it is possible to visualize those solutions graphically for up to three regulating factors, following a long tradition in theoretical ecology (León and Tumpson, 1975; Tilman, 1980, 1982; Leibold, 1996; Grover, 1997; Chase and Leibold, 2003). The aim here is to review this graphical construction in the case of the general model of Eq. (1). Doing so, we will introduce the associated basic concepts and notations needed for our generalization of this approach to the community and evolutionary frameworks in the next sections (Table 1).

Table 1
Notation.

Notation		Definition
		Regulating factor
i		Index
p		Total number
R_i		Density
S_i		External supply
l_i		Intrinsic per capita loss rate
Finite case	**Continuous case**	**Interacting population**
j	x	Index/trait value
n	$\mathcal{X}$	Total number/trait space
N_j	$N(x)$	Abundance
w_j	$w(x)$	Per capita net growth rate
I_{ij}	$I_i(x)$	Impact on regulating factor i
$\tilde{I}_{ij}$	$\tilde{I}_i(x)$	Renormalized impact on regulating factor i
	$H(x)$	Second derivative of the invasion fitness
	$J(x)$	Derivative of the fitness gradient
		Schreiber and Tobiason's model
α		Resource interaction shape parameter
m		Per capita mortality rate
g_i	$g(x)$	Per capita gross growth rate
		Acronyms
ZNGI		Zero net growth isocline
CEP		Competitive exclusion principle
ESS		Evolutionarily stable strategy
CSS		Convergence stable strategy
PIP		Pairwise invasibility plot

The method consists of two steps: invasion analysis and impact map. This decomposes the environmental feedback loop into its sensitivity and impact components following the terminology of Meszéna and Metz (1999) and Meszéna et al. (2006), which shares strong similarities with Chase and Leibold's (2003) concepts of requirement and impact niches. To help visualize our method, we will illustrate it by presenting the case of n populations $N_1, N_2, \ldots N_n$ interacting through two regulating factors R_1 and R_2. While described in general terms in the main text, we will use a flexible resource competition model introduced by Schreiber and Tobiason (2003) as a concrete example (see Box 1 and figures). The graphical construction of the ecological bifurcation diagram follows two distinct steps, that will naturally be extended later in the eco-evolutionary case.

Invasion analysis. Let us first focus our attention on the population equations, Eq. (1a). At equilibrium, they imply for every population that either (the population is absent) or $w_i = 0$ (its net growth rate is zero). There are thus three possible kinds of equilibria: "empty" or washout state with no population, one non-zero population only, or coexistence of two distinct populations with extinction of the other $n - 2$ populations. Coexistence of three or more different populations on two regulating factors is not possible due to the CEP. From Eq. (1a), the presence of a population i in the system restricts R_1 and R_2 to $w_i(R_1, R_2) = 0$. Graphically, this defines the so-called zero net growth isocline of population i or ZNGI_i (Tilman, 1980). For each competitor i, this curve delimits in the (R_1, R_2) plane the regions where net growth is positive ($w_i > 0$) from the ones where net growth is negative ($w_i < 0$) (see Fig. 1). A direct implication is that coexistence between populations at equilibrium is only possible for (R_1, R_2) where their two ZNGIs intersect. On the contrary, the "empty" equilibrium with no population exists for any set of regulating factors, as none of the populations is imposing its zero net growth constraint on the regulating factors.

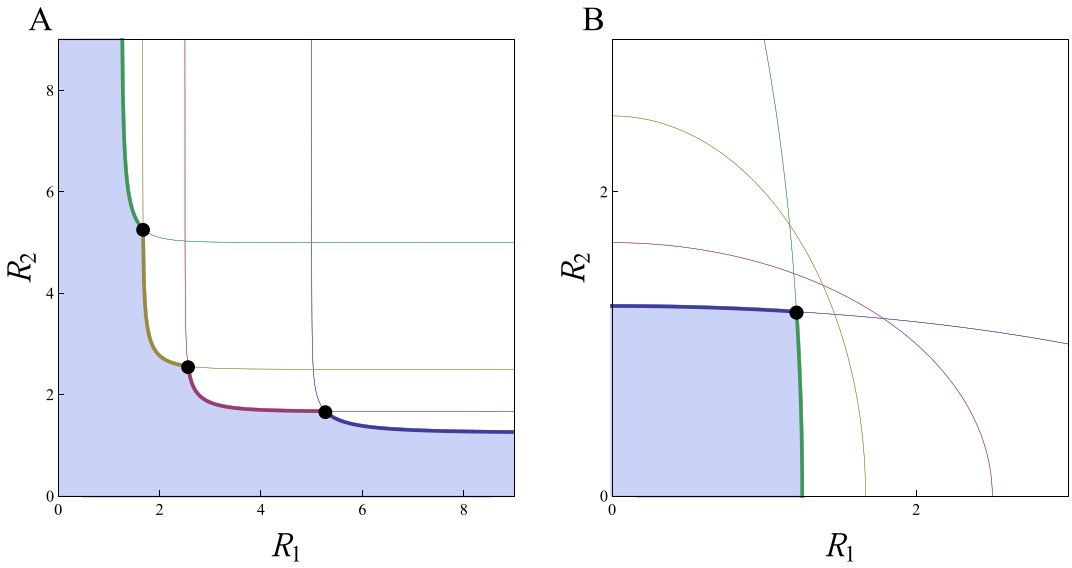

Fig. 1. Invasion analysis for a set of 4 competing populations consuming two resources R_1 and R_2. Competitors are labeled with i from 1 to 4 (respectively blue, purple, yellow, and green). They follow Schreiber and Tobiason (2003) model described in Box 1 with $x_i = 0.2i$ and $m=1$. Resources are either (A) interactive essential ($\alpha = -5$) or (B) antagonistic ($\alpha = 2$). Invasion analysis consists in drawing the set of ZNGIs (thin), selecting its outer envelope corresponding to non-invadable single population equilibria (thick) and potential coexistence points (black dots); the stable "empty" equilibria are located under the envelope (light blue). In the essential case, each strategy has a range of non-invadable equilibria and can potentially coexist with the neighboring populations. In the antagonistic case, the extreme strategies ($x_1=0.2$ and $x_4=0.8$) exclude all the other ones but can potentially coexist together. (For interpretation of the references to color in this figure caption, the reader is referred to the web version of this paper.)

More importantly, the ZNGIs also allow one to investigate the stability against invasion of those equilibria through invasion analysis. A necessary condition for any equilibrium involving either 0, 1 or 2 populations to be stable is for the point (R_1, R_2) to be located outside the positive growth regions of all the other potential invaders (Tilman, 1982; Leibold, 1996). Thus, the potentially stable "empty" equilibria are the ones for which (R_1, R_2) are simultaneously located outside (in the direction of lowered growth rate) the whole set of ZNGIs (shaded regions in Fig. 1). Population i stable equilibria can only be located on the portion of ZNGI_i that is outside all the other ZNGIs, and the same rule extends to stable coexistence points between two populations. The set of points (R_1, R_2) corresponding to non-empty potentially stable equilibria form what we can call the outer envelope of the ZNGIs (thicker

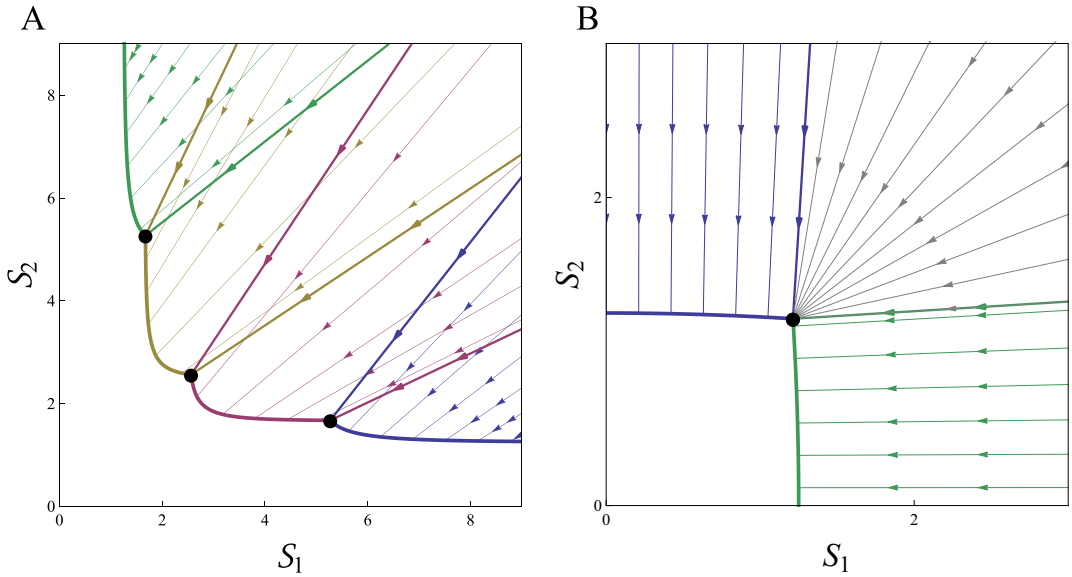

Fig. 2. Supply point map for a set of 4 competing populations consuming two resources R_1 and R_2 following the model of Box 1. Same configuration and parameters as Fig. 1. The stable ZNGI portions identified in Fig. 1 have been directly transposed into the supply point space. Starting from each non-invadable envelope portion (thick, plain), drawing a subset of the corresponding impact rays (thin, arrowed) helps visualizing the map that associates to every supply point its corresponding regulating factors at equilibrium. The boundaries of each portion map (thick, arrowed) combined with its corresponding ZNGI portion delimit zones of similar equilibria of the bifurcation diagram. (A) There are four single-population zones (green, yellow, purple and blue) plus an empty one (white). Note that some of the former overlap, accounting for priority effects. (B) There are two single-population zones (blue, green) plus an empty one (white) and a coexistence one (gray). Note that all the impact rays map to the same point in the latter case. (For interpretation of the references to color in this figure caption, the reader is referred to the web version of this paper.)

border in Fig. 1). To conclude, a ZNGI directly represents both the minimum requirements and the competitive ability of its corresponding population.

Supply point mapping. We have so far identified the candidate (R_1, R_2) values associated with the different kinds of possible equilibria using Eq. (1a) only. Yet the solutions (R_1, R_2) also have to satisfy the limiting factor equations (1b) set equal to zero. When solved together, this obviously makes them functions of the parameters of the system, including the supply point. To draw a bifurcation diagram, we would like to know for every supply point which are the corresponding (R_1, R_2) at equilibrium and thus deduce its associated characteristics ("empty", one population or coexistence). In practice, the map is performed using the supplementary constraints emerging from Eq. (1b) taken at equilibrium. First, note that this map is trivial for the regulating factors associated with the "empty" equilibrium. Indeed, having all the N_i equal to 0 leads to $\boldsymbol{S} = \boldsymbol{R}$. This means that if we now draw the ZNGI envelope in the supply plane, all the supply points situated outside of it will map to the "empty" equilibrium (white region, Fig. 2).

Where are the supply points leading to non-zero populations located? Let us first put aside the coexistence case, and focus on a single population equilibrium with $N_i \neq 0$ and $N_j = 0$ for $i \neq j$. Setting Eq. (1b) equal to zero leads to

$$\boldsymbol{S} = \boldsymbol{R} + N_i \tilde{\boldsymbol{I}}_{\boldsymbol{i}}(\boldsymbol{R}) \tag{2}$$

where $\tilde{\boldsymbol{I}}_{\boldsymbol{i}} = (I_{1i}/I_1, I_{2i}/I_2)$ is the impact vector renormalized to account for different loss rates, N_i is a positive density and $\boldsymbol{R}$ belongs to ZNGI_i stable portion of the envelope. Eq. (2) means that for a given regulating factor point on ZNGI_i, the corresponding supply points $\boldsymbol{S}$ are located along the ray that starts from the point (R_1, R_2) when $N_i = 0$ and moves away from it following the direction vector $\tilde{\boldsymbol{I}}_{\boldsymbol{i}}$ as N_i increases. This means that all the supply points along a given ray will map to the same regulating factor at equilibrium, but with different densities. Those "impact rays", as we suggest to call them, thus allow us to deduce graphically the supply points regions associated with a given single population equilibrium by moving (R_1, R_2) along its corresponding ZNGI portion along the envelope (Fig. 2). Let us note the difference between working with the limiting factors $\boldsymbol{R}$ versus their supply $\boldsymbol{S}$. While the invasion analysis takes place in a density-independent framework as we compare the growth rates of the different competitors for given $\boldsymbol{R}$ (Fig. 1), including the supply point map and thus the environmental feedback loop for given $\boldsymbol{S}$ fully captures the density and frequency dependence of the model (Fig. 2).

In the coexistence case, the method is slightly different. Eqs. (1b) now leads to $\boldsymbol{S} = \boldsymbol{R} + N_i \tilde{\boldsymbol{I}}_{\boldsymbol{i}}(\boldsymbol{R}) + N_j \tilde{\boldsymbol{I}}_{\boldsymbol{j}}(\boldsymbol{R})$ with $\boldsymbol{R}$ at the two ZNGIs' intersection. Thus, all the supply points situated in the cone originating at $\boldsymbol{R}$ and delineated by vectors $\tilde{\boldsymbol{I}}_{\boldsymbol{i}}$ and $\tilde{\boldsymbol{I}}_{\boldsymbol{j}}$ map to this coexistence equilibrium when both densities are positive (Fig. 2B). The impact vectors have to be different for this region not to be degenerate. However, this coexistence point is dynamically stable only if (see Appendix B):

$$\left(I_{1i}I_{2j} - I_{1j}I_{2i}\right)\left(\frac{\partial w_i}{\partial R_1}\frac{\partial w_j}{\partial R_2} - \frac{\partial w_i}{\partial R_2}\frac{\partial w_j}{\partial R_1}\right) > 0 \tag{3}$$

This is known as the mutual invasibility criterion and can be interpreted graphically in terms of relative position between ZNGIs and impact rays (León and Tumpson, 1975; Tilman, 1982; Leibold, 1996). Here, we simply note that it graphically translates for this region as not being an overlap between the two adjacent non-invadable single population regions (Fig. 2B). When those two regions do overlap, coexistence is unstable and replaced by a priority effect between the two single-population equilibria (Fig. 2A).

To summarize, an ecological bifurcation diagram as a function of the supply points (S_1, S_2) can be obtained by combining ZNGIs and impact rays through the following steps: (1) Draw the ZNGIs of the different populations and identify their outer envelope. (2) Locate the regulating factor points corresponding to the "empty" solutions (outside the envelope), population i only solutions (on ZNGI_i portions of the envelope) and the coexistence solutions (where the latter portions intersect, typically making a "kink" in the envelope). (3) Identify the regions of the supply point plane scanned by each population impact rays when its origin moves along its corresponding ZNGI portion (a subset of impact rays can also be represented). (4) Identify potentially stable coexistence "cones" from the kinks of the envelope.

There are two major advantages of this graphical approach. First, it delimits regions along the supply gradients for which a given species assemblage is present in the system. Historically, this allowed one to identify conditions for coexistence of two consumers (Tilman, 1982) and describe species succession along a nutrient gradient (Tilman, 1982; Leibold, 1996). Secondly, drawing the impact rays also allows one to deduce the equilibrium regulating factor levels and sometimes also population densities directly on the diagram. For consumers growing on essential resources, this is a way to identify which factor will be limiting for a given supply (Tilman, 1982). The direction of the impact vectors also enables one to assess the relative impact of a population on the regulating factors. But using impact rays has other advantages, which have been underused so far. Sometimes, a given supply point can be reached by several impact rays, which means that it maps to several distinct equilibria. In this case, the system presents alternative stable states, which is the basis of the "founder effect". There is an interesting diversity of situations that can be encountered depending on the states involved in this bistability. The most well-known case is one single population versus another one (Fig. 2A). But it is also possible to have alternative stable states inside a single population as it is often the case for structured populations (Schreiber and Rudolf, 2008; Guill, 2009; Schellekens et al., 2010), or between a community and an "empty" state as it is common in the presence of a positive feedback loop or an ecosystem engineer (Scheffer et al., 2001; Rietkerk et al., 2004; Kéfi et al., 2010). The graphical method presented here allows one to identify alternative stable states regions in the bifurcation diagram without ambiguity.

With this graphical construction, we have provided only some necessary conditions for the local stability of the different equilibria through invasion analysis, but those are not always sufficient. For example, a single population may have alternative stable states through an Allee effect. These stable states are generally separated by unstable states that would not be identified explicitly as such by the scheme presented above. However, a careful study of the envelope of the impact rays moving along the ZNGI for a single-population equilibrium can supplement this by further restricting an impact ray to its stable portion (see Appendix B). This idea will be used again in the eco-evolutionary case to identify branching points (see supply point mapping in Section 2.3). Limit cycles and other nonequilibrium attractors are also a possibility, even when criterion (3) is satisfied, as the other stability criteria cannot always be satisfied. Again, this would not be detectable on the graphical analysis. However, these two situations do not happen for simple systems like the standard two consumers on two resources (Tilman, 1982; Chase and Leibold, 2003; Schreiber and Tobiason, 2003), although they can for three or more resources (Huisman and Weissing, 1999).

2.2. Extension to a continuum of competitors: the ZNGI envelope

We now extend the previous framework from a discrete set of populations to a continuous set of strategies. The evolution of

quantitative traits and phenotypic plasticity can be considered as occurring among a continuous set of strategies, as can community assembly (Tilman, 1982, 1988; Chase and Leibold, 2003). Our motivation here is twofold. First, we aim at providing a rigorous framework to address the question of species sorting in communities and integrate this effect at the ecosystem scale. Second, this introduces the basic tools necessary to perform the eco-evolutionary analysis of the next section. This will highlight the similarities and differences between the species sorting and the adaptive dynamics approaches.

Formally, the generalization to a continuum of competitors is straightforward with the results of the previous section in mind. Omitting time-dependencies to lighten the notation, the dynamics of the system now reads:

$$\frac{\partial N(\boldsymbol{x})}{\partial t} = w(\boldsymbol{R}, \boldsymbol{x})N(\boldsymbol{x}) \tag{4a}$$

$$\frac{dR_i}{dt} = l_i(S_i - R_i) + \int_{\boldsymbol{x}\in\mathcal{X}} I_i(\boldsymbol{R}, \boldsymbol{x})N(\boldsymbol{x}) \tag{4b}$$

where the subscript j is now replaced by its continuous analog, the trait vector $\boldsymbol{x}$, which contains the functional traits that fully describe the strategy of the population with density $N(\boldsymbol{x})$. The global impact of the competitors on regulating factor i is now obtained by integrating the impact $I_i(\boldsymbol{R}, \boldsymbol{x})$ of every strategy $\boldsymbol{x}$ over the whole trait space $\mathcal{X}$. This trait space has to be seen as the collection of all the variable trait combinations that could possibly be present in the system. We assume in practice that $\mathcal{X}$ is a connected subset of a real vector space. Usually, this trait space is constrained by trade-offs inequalities which account for correlations between the traits. This usually excludes "Hutchinsonian demons" that outcompete all other species (Kneitel and Chase, 2004). In practice, those trade-offs are often taken to be saturated, i.e. as equalities instead of inequalities, in order to reduce the dimensionality of the trait space. When not, they simply add boundaries to the trait space. Note that we work at equilibrium, so the CEP still applies, which means that the $N(\boldsymbol{x})$ can only be a sum of delta functions with a number of peaks lesser or equal to the number of regulating factors p. From now, we will assume the trait space $\mathcal{X}$ to be unidimensional, i.e. an interval, to simplify the analysis and denote the trait as x (but see Appendix C and Discussion).

Global invasion analysis. Let us extend the ideas presented in the previous section to a continuum of competitors using geometrical envelopes of ZNGIs. This corresponds to species sorting, as all the strategies from the trait space are considered as potential invaders. Our aim here is to unify the different approaches and terminologies present in the literature (Meszéna and Metz, 1999; Chase and Leibold, 2003; Danger et al., 2008), provide some analytical and geometrical properties of envelopes, and combine them with impact rays to construct community/eco-evolutionary bifurcation diagrams.

The concept of the envelope is easy to understand graphically and allows an extension of the invasion analysis to a continuum of competitors. Let us superimpose a large number of ZNGIs sampled from the trait space $\mathcal{X}$ and identify their discrete outer envelope in the sense of the previous section. When the number of ZNGI sampled tends toward infinity, this discrete envelope tends toward a (generally) smooth curve called the outer geometrical envelope of the ZNGI family (Fig. 3A). Note that to every point of this envelope, there is a tangent ZNGI. Mathematically, this condition of tangency formally defines the geometrical envelope. Indeed, the points $\boldsymbol{R}$ belonging to the envelope of a set of ZNGI_x from $\mathcal{X}$ locally satisfy:

$$w(\boldsymbol{R}, x) = 0 \tag{5a}$$

$$\partial_x w(\boldsymbol{R}, x) = 0 \tag{5b}$$

where Eq. (5a) accounts for the fact that $\boldsymbol{R}$ has to belong to one of the ZNGIs and Eq. (5b) imposes the supplementary condition of tangency.

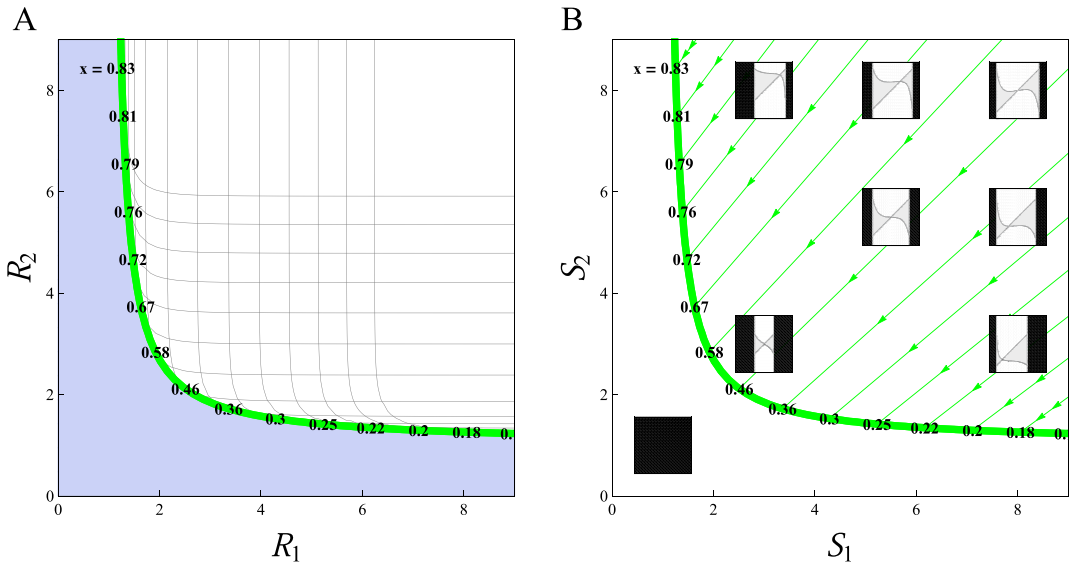

Fig. 3. Graphical representation of a continuous set of populations consuming two resources R_1 and R_2 following the model of Box 1 in the interactive essential case ($\alpha = -5$). (A) The local envelope (thick, green) of the continuum of strategies $0 \le x \le 1$ has been displayed. A discrete subsample of strategies had their ZNGIs represented (thin, gray) and the corresponding trait value displayed at the point of contact with the envelope (thick, black). This local envelope appears to be global, as all the ZNGIs are situated above it. (B) Supply point mapping through the impact rays (arrowed lined). Ecologically, there is a single strategy outcompeting all the other ones when there is enough resources (supply points above the envelope). The optimal strategy tends to be specialized on R_1 as it becomes scarcer compared to R_2, and vice-versa. Contrary to the discrete case (Fig. 2A), there is no priority effect zones between neighbor strategies. PIPs (black=resident cannot exist, gray=+, white=−) have been displayed for comparison with adaptive dynamics framework (see Section 2.3 and Fig. 5). (For interpretation of the references to color in this figure caption, the reader is referred to the web version of this paper.)

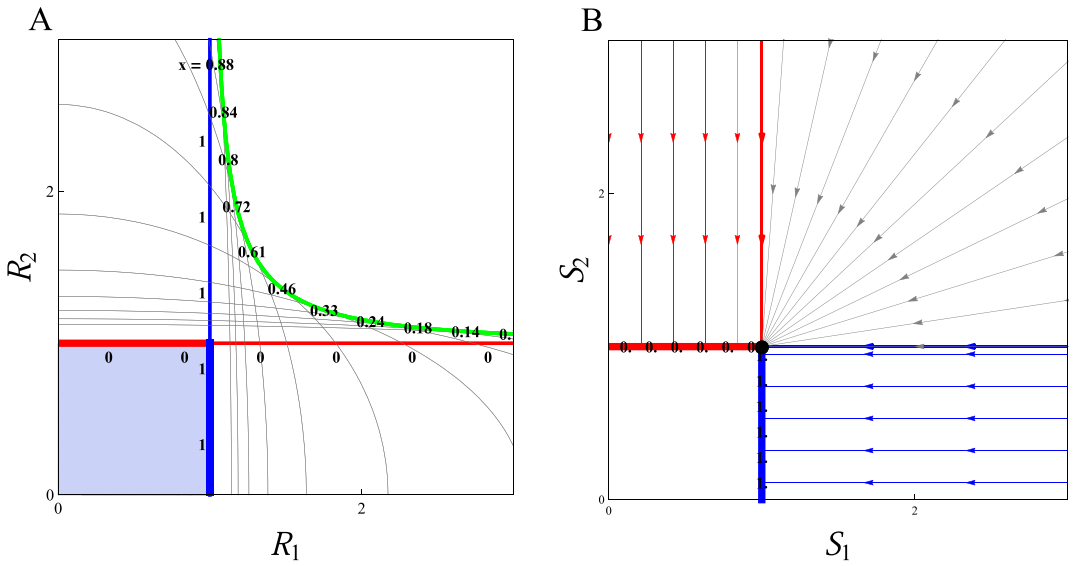

Fig. 4. (A) Local envelope (thick, green) for a continuum of strategies $0 \le x \le 1$ in the antagonistic case ($\alpha = 2$). A discrete subsample of strategies has been picked with their ZNGIs represented (thin, gray) and the corresponding trait value displayed at the point of tangency with the envelope (thick, black). The local envelope is an inner one and thus not part of the global one (thick), instead made of two portions of the boundary ZNGIs corresponding to the R_1 and R_2 specialists (resp. blue and red). (B) Supply point mapping *via* the impact rays (arrowed lined). There is room for coexistence in the "cone" (gray) originating from the kink (black dot). Those results are very similar to the ones obtained in the discrete case (Fig. 2B). (For interpretation of the references to color in this figure caption, the reader is referred to the web version of this paper.)

Note that $\boldsymbol{R}$ is a priori considered independently of x in the invasion analysis and thus not targeted by the partial derivative. In practice, an explicit equation of the envelope linking R_2 to R_1 can be obtained by eliminating x from Eqs. (5) or implicitly through a parametric equation.

Before moving on, let us emphasize the fact that Eq. (5b) is a first order, that is, local criterion. As such, this does not insure that the envelope obtained with Eq. (5b) has the global outer envelope behavior we are looking for. This situation can be understood by analogy with the problem of finding the global maximum of a differentiable function on a closed set. Setting its derivative equal to zero only locates the function's local extrema, which can be either maxima or minima. The same happens with the local envelope obtained through Eq. (5b). It can coincide with the global outer envelope we are looking for (Fig. 3A) and thus have its points $\boldsymbol{R}$ situated outside the whole ZNGI set as they satisfy $w(\boldsymbol{R}, x) \le 0$ for any x. However, some portions of this envelope could also be local but not global while others could be inner envelopes, i.e. situated inside the whole ZNGI set with $w(\boldsymbol{R}, x) \ge 0$ for any x (green segments in Fig. 4A). Those inner envelope portions have to be discarded in the global analysis as they are highly unstable, with every strategy able to invade. There is one last situation to consider. Back to our analogy of maximizing a function, the global maximum could also be situated on the boundaries of its domain and thus not be detected by setting its derivative equal to zero. In our case, it means that the global outer envelope could also be made of ZNGIs whose traits are located on the boundaries of $\mathcal{X}$ (red and blue segments in Fig. 4A). To conclude, the global invasion analysis is performed in the continuous case by putting together the local envelope defined by Eq. (5) and the boundary ZNGIs, and keeping their global outer envelope only (see Figs. 3 and 4).

When solving Eq. (5), a singular trait $x^*(\boldsymbol{R})$ is associated with every point $\boldsymbol{R}$ of the envelope (see Box 1 and Figs. 3 and 4). This trait corresponds to the ZNGI_x that contributes to the envelope at that point $\boldsymbol{R}$. In the case of a global outer envelope, it means that this strategy x is optimal for those specific regulating factor values $\boldsymbol{R}$, by outcompeting all the other strategies. Note that the global outer envelope can contain kinks where there is a discontinuity of $x^*(\boldsymbol{R})$ as $\boldsymbol{R}$ moves along the envelope. This means that two distinct ZNGIs are tangent to the envelope at that specific point. As an important consequence, those are the only values of the regulating factors where globally stable coexistence is possible. Although kinks are generally plentiful in the discrete case between neighboring strategies (Fig. 1), the majority of those kinks usually vanish when the continuous limit is taken (Fig. 3). When globally stable coexistence of two different strategies from a continuum does occur, the associated kinks in the global envelope emerge at the self-intersections of the local envelope to which has been added its boundary ZNGIs when needed (Fig. 4). This is one of the major differences with the previous discrete approaches (Leibold, 1996; Chase and Leibold, 2003) which we will discuss later. These kinks make globally stable coexistence particularly easy to find and characterize graphically.

Supply point mapping. There is virtually no difference with the discrete strategy case. We only have to remember that there is a unique non-invadable strategy $x^*(\boldsymbol{R})$ associated with every point of the global envelope that is not a kink. Plugging this relationship between the traits and the regulating factors into the renormalized impact vector components $\tilde{I}_i(\boldsymbol{R}, x) = I_i(\boldsymbol{R}, x)/l_i$ allows us to draw the impact rays originating on the envelope points, thus performing the mapping from the ZNGI envelope to the supply point. The envelope thus behaves like a community-wide ZNGI, with its associated impact rays. The functioning of the whole community can indeed be understood as a single entity that behaves like a single population. At a kink, the coexistence cone is obtained by plotting the impact rays associated with the two coexisting strategies, and the stability criterion (3) is checked as before.

To summarize, the outcome of species sorting among a continuum of strategies can be seen from the community bifurcation diagram as a function of the supply points (S_1, S_2). It is obtained by combining the envelope and impact rays through the following steps: (1) From the local envelope of the ZNGI continuum and its boundary ZNGIs, keep the global outer envelope. (2) For every

point of this envelope, identify the corresponding "optimal" strategy. (3) Locate the regulating factor points corresponding to the "empty" solutions (outside the envelope) and the potential coexistence solutions (the kinks). (4) Represent the supply point map by drawing impact rays from the envelope. (5) Identify the potentially globally stable coexistence "cones" from the kinks.

2.3. Eco-evolutionary extension: link with adaptive dynamics

The global invasion analysis presented above considered that all the possible strategies from the trait space can invade the system and compete together. This explains why we have focused on determining the global envelope and discarded local but not global envelope portions. By doing so, we adopted an "everything is everywhere" approach (Baas Becking, 1934; De Wit and Bouvier, 2006). At the opposite, the strategy space could be explored by evolving a single population through small mutation steps. In the previous section, we have presented a natural way to extend the graphical invasion analysis to a continuum of strategies by introducing the ZNGI envelope concept. As was shown by Meszéna and Metz (1999), this framework naturally allows us to address eco-evolutionary equilibria of adaptive dynamics (Hofbauer and Sigmund, 1990; Geritz et al., 1997, 1998). In fact, the idea of addressing evolution with a graphical mutant invasion analysis can be traced back as far as the early developments of resource competition theory (MacArthur and Levins, 1964; MacArthur and Wilson, 1967). Some methods based on graphical arguments in the trait space have already been developed to analyze evolutionary outcomes (Levins, 1962) and recently extended to fit in the density- and frequency-dependent context of adaptive dynamics (Rueffler et al., 2004; de Mazancourt and Dieckmann, 2004).

Here, we propose to further explore and describe the relationship between the ZNGI envelope and its geometrical properties and the evolutionary singular points and their classification. We will first provide some analytical results to support the intuition of Meszéna and Metz (1999). We will show how those results can be combined with the supply point mapping to provide a complete graphical characterization of the singular points. This approach makes it possible to draw eco-evolutionary bifurcation diagrams along the supply gradients. The whole approach relies on the observation that the growth function $w(\boldsymbol{R}, x)$, represented by ZNGI_x, is actually the invasion fitness of a mutant x in a resident-dominated environment $\boldsymbol{R}(y)$. This means that the local envelope equations (5) coupled with the supply point map given by the impact rays directly give the singular points of adaptive dynamics where the fitness gradient is zero. In the particular case of a one-dimensional trait x, we will show how the singular point classification is directly linked with the geometrical properties of the envelopes (but see Appendix C and discussion for the multidimensional case).

Local invasion analysis. The local evolutionary stability (in the sense of non-invasibility) of a singular point can be characterized using the second derivative of the invasion fitness (Geritz et al., 1998):

$$H(x) = \left[\frac{\partial^2 w(\boldsymbol{R}(y), x)}{\partial x^2}\right]_{y=x} \equiv \frac{\partial^2 w}{\partial x^2}. \tag{6}$$

Following adaptive dynamics terminology, a singular point for which H is negative is said to be a (local) evolutionarily stable strategy (ESS), uninvasible by nearby strategies. This quantity is related to the geometrical properties of the envelope through the following relationship (see Appendix C for demonstration in the multidimensional trait case):

$$H(x) = \frac{\partial w}{\partial R_2}\cdot\left(\left.\frac{\partial^2 R_2}{\partial R_1^2}\right|_E - \left.\frac{\partial^2 R_2}{\partial R_1^2}\right|_Z\right)\Big/\left(\frac{dx}{dR_1}\right)^2 \tag{7}$$

where $\partial^2 R_2/\partial R_1^2|_E$ and $\partial^2 R_2/\partial R_1^2|_Z$ are the second derivatives of respectively the envelope and the tangent ZNGI, and thus quantify their curvature. The difference between the two latter terms describes the relative curvature and thus position between the envelope and the tangent ZNGI: when negative, the envelope is located under the ZNGI set. Conversely, when this difference is positive, the envelope is located above the ZNGI set. The sign of $\partial w/\partial R_2$ translates this relative position along the y axis in terms of relative fitness: when positive (as it is the case within our example, since R_2 is a resource), "under" means "outer envelope" ($w(\boldsymbol{R}, x) \le 0$ for any nearby x) and "above" means "inner envelope" ($w(\boldsymbol{R}, x) \ge 0$ for any nearby x); conversely, when $\partial w/\partial R_2 < 0$, "under" means "inner" and "above" means "outer". Eq. (7) makes the formal link with adaptive dynamics: outer envelope portions always correspond to ESS while the inner ones, which were discarded during the global invasion analysis, are associated with non-ESS. Inner envelope portions play an important role in the eco-evolutionary case as they can be associated with branching points (see below). Eq. (7) proves and generalizes the results of Meszéna and Metz (1999) to the case of non-linear ZNGIs, as the curvature of the ZNGI comes into play. As demonstrated for ecological coexistence, evolutionarily stable coexistence can be found at the self-intersections of the local envelope. We showed that its evolutionary stability is directly linked to the ones of its two constituting strategies: coexistence is evolutionarily stable if and only if situated at the intersection of two outer ZNGI envelope portions (see Appendix C for demonstration). In any case, ESS characterization of singular points only depends on ZNGIs.

Supply point mapping. It is in fact possible to further characterize the singular points graphically. Let us introduce the Jacobian of the fitness gradient

$$\begin{aligned} J(x) &= \frac{d}{dx}\left[\frac{\partial w(\boldsymbol{R}(y), x)}{\partial x}\right]_{y=x} \equiv \left(\frac{\partial}{\partial x} + \frac{\partial \boldsymbol{R}}{\partial x}\cdot\frac{\partial}{\partial \boldsymbol{R}}\right)\frac{\partial w}{\partial x} \\ &= H(x) + \frac{\partial \boldsymbol{R}}{\partial x}\cdot\frac{\partial}{\partial \boldsymbol{R}}\frac{\partial w}{\partial x} \end{aligned} \tag{8}$$

According to the adaptive dynamics classification of singular points, this Jacobian gives information about the singular point's convergence stability, telling if it is an attractor or a repeller for the 1D adaptive dynamics (Eshel, 1983; Geritz et al., 1998). More precisely, the singular point is said to be convergence stable if J is negative. Note that this differs from the previous criterion based on the second derivative H: for example, a singular point can be convergent stable but not evolutionarily stable, which is known as a branching point and can lead a single strategy to diversify into evolutionarily stable coexistence of two different strategies (Eshel, 1983; Metz et al., 1996; Geritz et al., 1997, 1998). It is possible to show the following relationship between J and H (see Appendix C for demonstration in the multidimensional trait case):

$$J = \left(\left.\frac{\partial R_1}{\partial S_1}\right|_Z \Big/ \left.\frac{\partial R_1}{\partial S_1}\right|_E\right)H \tag{9}$$

where $\partial R_1/\partial S_1|_Z$ and $\partial R_1/\partial S_1|_E$ describe how R_1 responds to its variation in supply, when R_1 moves along respectively the tangent ZNGI (ecological case, fixed strategy) and the envelope (eco-evolutionary case, adaptive strategy). The same relationship can be obtained for R_2 simply by replacing 1 by 2 from Eq. (9). First, note that $\partial R_1/\partial S_1|_Z$ is non-negative for the usual consumer–resource or predator–prey interactions (but see Appendices B and C). This implies that J and H share the same signs when $\partial R_1/\partial S_1|_E > 0$: an ESS is a CSS and a non-ESS is a

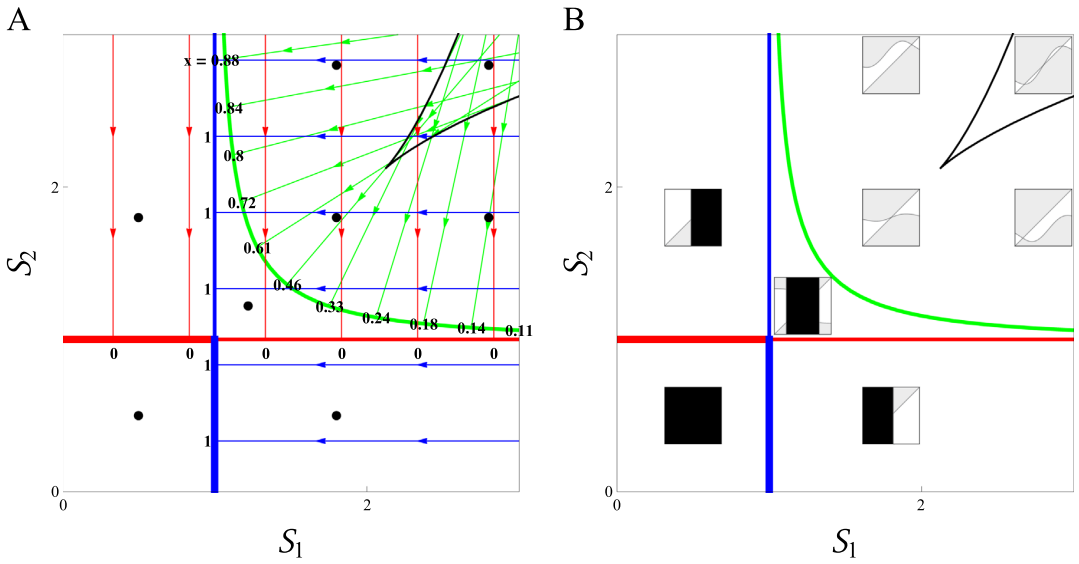

Fig. 5. Eco-evolutionary bifurcation diagram along the supply gradients for the antagonistic case ($\alpha = 2$). (A) Full envelope composed of a non-ESS local portion (green) and two boundary ZNGIs (blue, red). The impact ray map (arrows, thin) helps visualizing the number and the properties of the singular points associated with a given supply point of the diagram. For example, every supply point inside the zone delimited by the impact ray envelope (black, thin) gives two boundary CSS, two repellers and one branching point. (B) We only kept the global envelope and the skeleton of the impact ray map. Each zone delimited that way shares common properties that can be illustrated with PIPs (gray = +, white = −) being displayed at the exact location of their corresponding supply point (black dot (A)). Invasion fitness is not defined for resident traits that do not allow the resident to exist (black). (For interpretation of the references to color in this figure caption, the reader is referred to the web version of this paper.)

repeller. Conversely, J and H have opposite signs when $\partial R_1/\partial S_1|_E < 0$: an ESS is then non-convergent (Garden of Eden strategy) and a non-ESS is a branching point (Geritz et al., 1998). This last situation can be understood as follows: the eco-evolutionary feedback is so strong that the sign of the limiting factor response to supply variation, materialized by $\partial R_1/\partial S_1|_E$, is completely reversed compared to the purely ecological situation.

How can the sign of $\partial R_1/\partial S_1|_E$ be read graphically? To see this, we need to introduce the notion of envelope of impact rays, following the same definition of envelope introduced earlier in the case of ZNGIs. Indeed, the set of impact rays generated by moving the regulating factor point along the ZNGI envelope usually itself possesses an envelope (black curve, Fig. 5 and movie S1 in the Supplementary material). A given impact ray will touch and be tangent to this envelope at a unique contact point. The line portion of the impact ray situated between its origin and this point corresponds to supply points satisfying $\partial R_1/\partial s_1|_E > 0$ while the other part corresponds to $\partial R_1/\partial s_1|_E < 0$. In general, crossing this envelope in the supply point space corresponds to the appearance or the disappearance of a pair of impact rays, i.e. singular points (see Figs. 5 and 6). This whole scheme can be understood as a way to use the supply point mapping to explicitly construct how the eco-evolutionary system responds to a local trait perturbation, following the ideas presented by Meszéna and Metz (1999).

We can understand how this works in practice by looking at our example (see also movies S2 and S3 in the Supplementary Material). In the interactive essential resource case, there is no impact ray envelope (see Fig. 3). According to the previous section, this means that $\partial R_1/\partial s_1|_E > 0$ and thus all ESS are CSS. The absence of an impact ray envelope also implies that impact rays never cross each other, which explains why there is never more than one singular point per supply point. In the antagonistic resource case, there is always an impact ray envelope (see Figs. 5 and 6). Outside the impact ray envelope, the same reasoning goes as for the interacting resource case. There is thus never more than one non-ESS repeller in that region (Fig. 6A and B). In contrast, inside the impact ray envelope the impact ray map folds over on itself, leading to three singular points per supply point (Fig. 6C and D). Among them, the impact ray in the middle goes through its envelope tangency point before hitting the ZNGI envelope, which means that $\partial R_1/\partial s_1|_E < 0$ and it thus corresponds to a branching point (Fig. 6D). The two other singular points are non-ESS repellers. In our example, the impact ray envelope thus delimits the region where non-boundary impact rays intersect. The emergence of alternative stable states as we cross the impact ray envelope is a well-known phenomenon in bifurcation theory, where it is referred to as a "cusp catastrophe" (Strogatz, 2015).

As in the previous sections, evolutionary stable coexistence is only possible for supply points located between the two impact rays originating from a kink of the ZNGI envelope. Mutual invasibility, obtained by satisfying Eq. (3), is also needed to ensure that this coexistence is ecologically stable. Moreover, when polymorphism is saturated (as many distinct strategies as regulating factors) we have $J = H$ for each of the two coexisting strategies (see Appendix C). Thus, evolutionarily stable coexistence is automatically convergence stable coexistence and further evolutionary branching is impossible, in accordance with the CEP (Meszéna and Metz, 1999). This last result is consistent with a recent study of saturated polymorphism (Kisdi and Geritz, 2016).

To summarize, an eco-evolutionary bifurcation diagram along the regulating factors supply can be obtained in the unidimensional trait case through the following steps: (1) Draw the ZNGI envelope. (2) Identify the ESS and non-ESS portions (given by the envelope's relative position with ZNGIs) and add boundary ZNGIs if necessary. (3) Draw the impact ray envelope and a subset of impact rays to represent the supply point map. (4) If there is an evolutionarily stable self-intersection of the ZNGI envelope, draw the coexistence cone. (5) Identify the different regions delimited and the properties of the associated singular points (Fig. 7). Note that superimposing a pairwise invasibility plot (PIP) (Geritz et al., 1997) for every region of the diagram helps in visualizing the eco-evolutionary characteristics of the system, like the number and properties of the singular points and mutual invasibility associated with singular dimorphism (Figs. 3–6). Indeed, those conserved singular point characteristics make PIPs qualitatively similar inside a given region of the diagram.

Box 1–Schreiber and Tobiason consumer–resource model.

Schreiber and Tobiason (2003) studied the evolutionary ecology of n consumer populations feeding on two resources with densities R_1 and R_2. Their model is a particular case of model (1) from the main text, with:

$$w_i(R_1, R_2) = g_i(R_1, R_2) - m \tag{10}$$

$$g_i(R_1, R_2) = \left[(x_i R_1)^\alpha + ((1 - x_i)R_2)^\alpha \right]^{\frac{1}{\alpha}} \tag{11}$$

where x_i and $1 - x_i$ account for investment in acquisition of respectively resources 1 and 2 (note this implies a linear trade-off), m is the constant per capita mortality rate and controls the shape of the interaction between resources. Following Tilman's (1980, 1982) classification of resources relations, $\alpha < 0$ represents interactive essential resources (both necessary and slightly better in balanced proportions), $0 < \alpha < 1$ represents complementary resources (substitutable but better in balanced proportions), $\alpha = 1$ represents perfectly substitutable resources, and $\alpha > 1$ represents antagonistic resources (substitutable but worse in balanced proportions). The limiting cases $\alpha \to -\infty$ and $\alpha \to +\infty$ lead to respectively essential and switching resources (growth is limited by respectively the most limiting and the most abundant resource). The growth rate (11) is thus an elegant mathematical way to control the nutritional interaction between the resources. The intrinsic resource dynamics follows chemostat dynamics as in Eq. (1b) with $l_1 = l_2$. Finally, population N_i influences the resources dynamics in model (1) through its impact vector. For $\alpha < 1$, we retain the mass action law used by Schreiber and Tobiason (2003):

$$(I_{i1}, I_{i2}) = -[x_i R_1, (1 - x_i)R_2] \tag{12}$$

This describes purely random encounters and removal of both resources, proportionally to their densities through acquisition rates. This consumption process does not satisfy conservation of mass in general, as $I_{i1} + I_{i2} \neq g_i$ for $\alpha \neq 1$. Thus, removal of a certain resource density does not translate into an equivalent consumer growth. In the case of antagonistic resources, this situation would describe nutritional antagonism during the assimilation process, like synergistic effects of toxic compounds (Tilman, 1980). For this reason, we rather used the following impacts in the $\alpha \geq 1$ case:

$$(I_{i1}, I_{i2}) = -g_i^{1-\alpha}[(x_i R_1)^\alpha, ((1 - x_i)R_2)^\alpha] \tag{13}$$

Conservation of mass is here satisfied, and antagonism comes from the foraging strategy of the consumer itself. It describes the behavioral switching of a predator, focusing disproportionately on its most abundant prey (Murdoch, 1969). This situation can emerge when resources are spatially distributed (Murdoch et al., 1975) or through the formation of a search image (Pietrewicz and Kamil, 1979; Dukas and Kamil, 2001).

As explained in the main text, the ZNGI of a given population i is obtained by setting $g_i(R_1, R_2) - m = 0$. Its concavity is controlled by the sign of $\alpha - 1$, as can be visualized in Fig. 1: the antagonistic case ($\alpha > 1$) gives concave ZNGIs while complementary and interactive essential ($\alpha < 1$) gives convex ones. Moreover, computing the equation of the ZNGIs envelope through Eq. (5) gives the eco-evolutionary singular points of the system. Solving them in this particular case leads to the following implicit envelope equation:

$$\left(R_1^{\frac{\alpha}{1-\alpha}} + R_2^{\frac{\alpha}{1-\alpha}} \right)^{\frac{1-\alpha}{\alpha}} - m = 0 \tag{14}$$

This also gives the expression of the singular trait as a function of the resource level:

$$x(R_1) = \left(\frac{R_1}{m} \right)^{\frac{\alpha}{1-\alpha}} \tag{15}$$

When substituted into the impact vector expression, this gives the impact map linking supply points to the corresponding singular points. The resulting ZNGI envelopes and associated impact maps are represented in Figs. 3–5. In the antagonistic case, the envelope had to be supplemented with the boundary ZNGIs. Those are the horizontal and vertical lines going through the point $(1, 1)$, and correspond to the two specialist strategies $x = 0$ and $x = 1$.

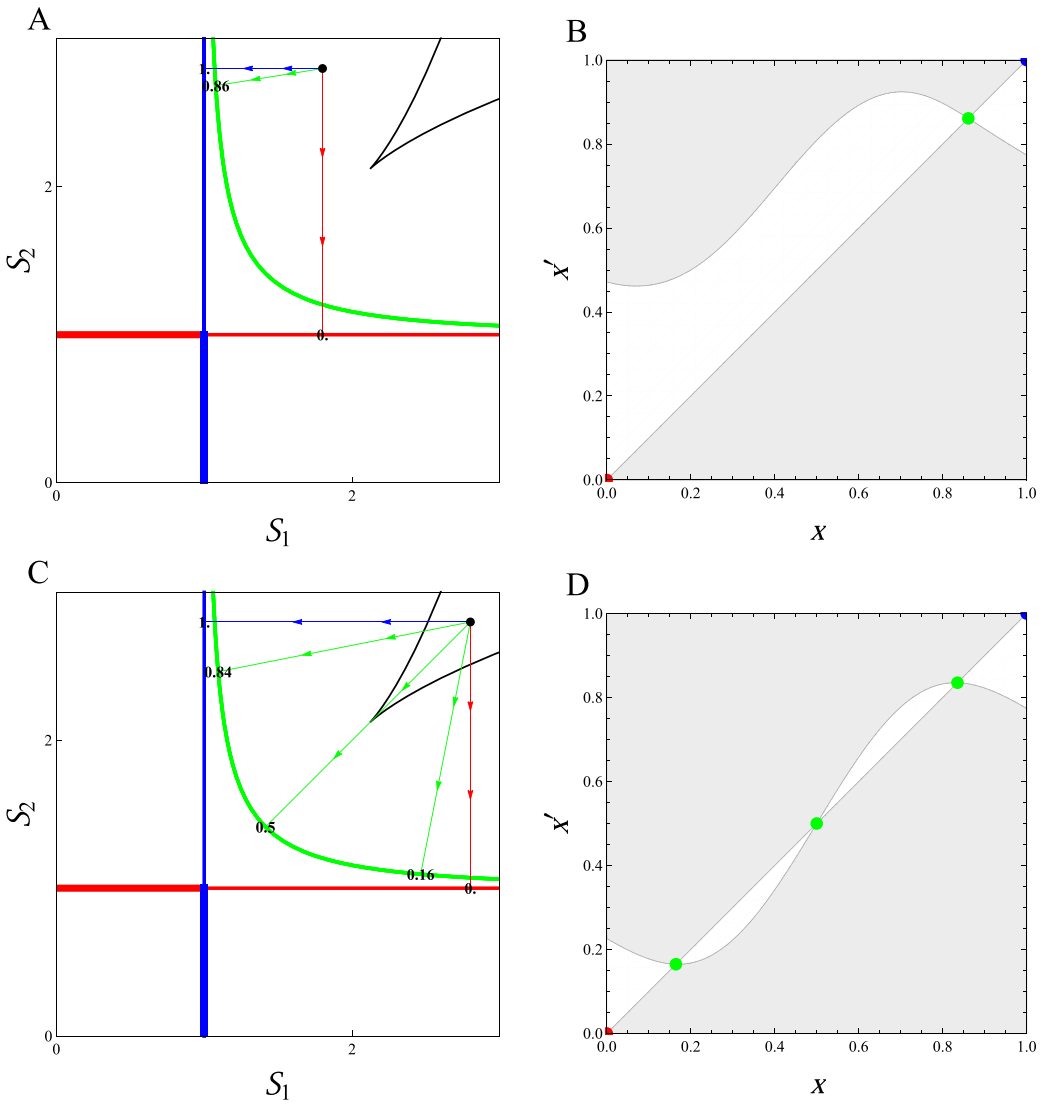

Fig. 6. Details of the supply point map and its associated pairwise invasibility plot (PIP) in the antagonistic case ($\alpha = 2$) for high but imbalanced ((A) and (B)) and balanced ((C) and (D)) resource supply, i.e. respectively $\boldsymbol{S} = (1.8, 2.8)$ and $\boldsymbol{S} = (2.8, 2.8)$. (A) The impact rays map this supply point to three different eco-evolutionary equilibria on the envelope. The associated singular trait values are also displayed. (B) PIP depicting the sign (gray = +, white = −) of the invasion fitness of a mutant with trait x' in a resident population with trait x. For a given resident strategy x, the success of the different invaders can be read along the corresponding vertical line. The limiting curves between the white and the gray regions correspond to invasion fitness equal to zero. Among them, the one-to-one line reminds us that the resident is at equilibrium. The eco-evolutionary fixed points are located at the intersection of this one-to-one line with the other contour or the boundary (colored dots). There are three of them here: one repelling singular point (green) and two boundary CSS $x=0$ (red) and $x=1$ (blue). The two latter strategies are locally non-invadable but not globally, as strategies different enough from them can invade. (C) and (D) Contrary to the imbalanced case, this supply points gets mapped to three different points on the non-ESS envelope portion (green). Note that the middle impact ray corresponding to $x=0.5$ goes through its tangency point on the impact ray envelope (black, thin) before hitting the ZNGI envelope (C). As explained in the main text, this is the signature of this singular point being a branching point, as can be visualized on the PIP (D). (For interpretation of the references to color in this figure caption, the reader is referred to the web version of this paper.)

3. Discussion

In this paper, we show how the graphical approach of contemporary niche theory can be extended to a continuum of strategies to give insights into community assembly processes and eco-evolutionary dynamics along environmental gradients. In Section 2.1, we reviewed the graphical approach by providing a general step-by-step recipe to create ecological bifurcation diagrams along environmental gradients. In Section 2.2, we adapted this recipe to the situation of a continuum of competitors using geometrical envelopes, enabling us to study community assembly from a large species pool. Finally, in Section 2.3 we demonstrated that combining this extension of the graphical approach with the adaptive dynamics framework leads to eco-evolutionary bifurcation diagrams summarizing the various possible evolutionary outcomes of the system.

3.1. Extension to structured populations

In this paper, we have restricted our attention to unstructured populations, demographically and spatially. This was done for the sake of simplicity, as there is no further complication to apply this graphical method to the case of linearly structured populations, that are defined by their dynamics satisfying $d\boldsymbol{N}_i/dt = \boldsymbol{w}_i(R_1, R_2, \ldots, R_p)\boldsymbol{N}_i$,

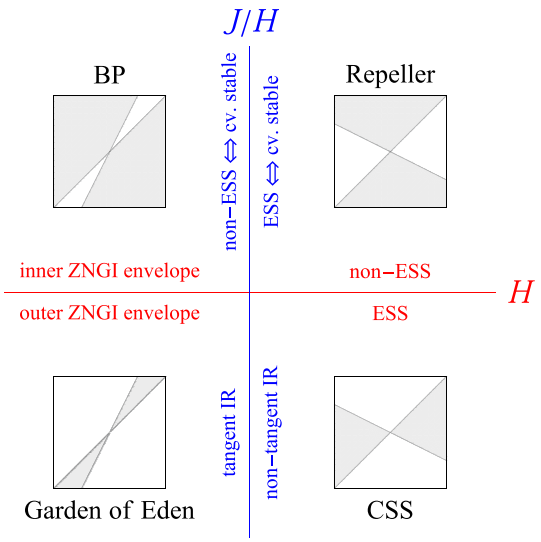

Fig. 7. Correspondence between the classification of singular strategies and their graphical characterization in the standard consumer–resource or predator–prey case where $l_2 \cdot \partial w/\partial R_2 < 0$, e.g. Schreiber and Tobiason's (2003) or Leibold's (1996). The classification has been adapted and simplified from Geritz et al. (1997). "tangent IR" and "non-tangent IR" stand for "impact ray tangent to its envelope" and "impact ray not tangent to its envelope", while "cv." stands for "convergence". The case where $l_2 \cdot \partial w/\partial R_2 > 0$ (e.g. nitrogen fixing) is obtained by permuting "tangent IR" and "non-tangent IR" from the figure.

where the $\boldsymbol{N}_i$ are vectors of abundances at the different states (ages, sizes, or patches, for example) and $\boldsymbol{w}_i$ the net growth matrix (Leslie, 1948; Caswell, 2001). In this case, the ZNGI equation is obtained by setting the largest eigenvalue of the net growth matrix equal to zero (Loreau and Ebenhöh, 1994; Schellekens et al., 2010; Haegeman and Loreau, 2015). The corresponding eigenvector determines the population structure at equilibrium, thus reducing the impact on the regulating factors to a one-dimensional problem similar to the unstructured case. Conversely, there is no such general rule in the case of non-linear population structure, e.g. two-sex models (but see Szilágyi and Meszéna, 2009; Barabás et al., 2014a). However, it may still be possible to define a ZNGI, as is the case for the Droop model after a quasi-steady state approximation (Klausmeier et al., 2004). Therefore, it is generally possible to apply the envelope method to study the eco-evolution of structured populations.

3.2. Extension to higher trait space dimensions

In this paper, we restricted the presentation of the eco-evolutionary graphical method to the case of a unidimensional trait space. However, it is still possible to define a local envelope in the general case of a trait space with dimension k by replacing the trait derivative of Eq. (5) by a k-dimensional trait gradient. This k-dimensional trait envelope can be seen as the outcome of a recursive scheme consisting of taking successively k times the envelope along every trait vector component, starting from the ZNGI multidimensional set. In any case, the ZNGI envelope keeps the property of being a unidimensional curve. This has important ecological consequences, as was pointed out by a more general result of Meszéna and Metz (1999): the singular strategies are necessarily contained in a $p-1$ sub-manifold of the trait space, where p is the number of regulating factors. This means that there is only a specific set of trait combinations that can be evolutionarily stable strategies, all the other ones being automatically discarded whatever the supply point. This introduces correlations between the traits of organisms that could ever be observed. This process can be thought as a pure "competitive filtering" as it only relies on the invasion analysis. It is thus completely independent of the details of the embedding environment and as such, a very general result. Note that Tilman's (1982) R^* rule is a special case of this result, where a single limiting factor usually leads to a unique singular strategy, or at least a countable number, whatever the supply point. Can a singular point still be characterized locally from the geometry of the envelope in the multidimensional case? Even if the relationships (7) and (9) can be extended to the k-dimensional case (see Appendix C), they do not give enough information to perform this full characterization.

To conclude, a ZNGI envelope can be obtained for any dimension of the trait space. It selects from the full trait space the strategies that are singular and represents graphically their competitive ability. Their local characteristics cannot be deduced from simple graphical properties, but global evolutionary stability remains easy to identify.

3.3. From local to global invasibility

The two perspectives presented in Sections 2.2 and 2.3 can be seen as two opposite but complementary pictures. The first, sometimes called the "everything is everywhere" picture, assumes that all the imaginable strategies from the trait space have a chance to invade the system. The details of the creation and maintenance of this diversity of invaders are simply assumed (Sauterey et al., 2015). This can be seen as the existence of a hyperdiverse regional species pool – the system being embedded in an heterogenous and connected landscape – or with mutations of arbitrary size. By contrast, the second approach focuses on the invasion of a local neighborhood of strategies around the resident, as mutations are small. In this approach, evolution can be "trapped" at a local-only ESS, and diversification from a monomorphic population only emerges from a branching point. The two approaches can lead to similar bifurcation diagrams, as it is the case for interactive essential resources in the example (Fig. 3) where all the local singular points are global CSS. However, the presence of locally non-ESS envelope portions lead to significant differences between the two pictures. In the case of antagonistic resources from our example, the local analysis identifies regions of priority effect between two locally stable specialists and a branching point (Figs. 5B and 6D). Those details do not matter in the global analysis, replaced by evolutionarily stable coexistence of the two specialists (Fig. 4B). The link between the two frameworks can be seen from the PIPs in the second picture, as shown in Fig. 5B: evolution under small mutations can be read on the diagonal neighborhood, but information about invasion of any strategy is also available away from it. Another remark clear in the previous example is that there is no reason for the evolutionarily stable coexistence region and the branching region to coincide. Evolutionarily and convergence stable dimorphism are indeed possible in the absence of branching, thus emerging through invasion or "macro-mutation" (Geritz et al., 1999) (Fig. 5B). An example of this situation was discussed by Wolf et al. (2007, 2008) and Massol and Crochet (2008). Conversely, branching can happen in a region where evolutionary stable coexistence is not possible: one of the two morphs would inevitably experience evolutionary suicide along its eco-evolutionary trajectory (Matsuda and Abrams, 1994; Rankin and López-Sepulcre, 2005; Parvinen, 2005). Local and global approaches are the two extremes of a general invasion analysis picture that can be visualized by combining local and global bifurcation diagrams and associating them with PIPs.

3.4. Up- and downscaling with ZNGI envelopes

We have explained in Section 2.2 how the envelope approach allows one to scale up from the population to the community level to sort out the best competitor from a continuum of strategies. It is also possible to scale down from the population to the individual level in the context of phenotypic plasticity (Tilman, 1982). Indeed, dynamical allocation in response to environmental cues could allow an individual to explore the trait space in search of the optimal strategy, in the sense of competition. The envelope approach gives a practical tool to do so: from all the accessible behaviors represented by the continuous set of ZNGIs, the optimization procedure only retains their envelope, which can be seen as the new integrated ZNGI of the plastic individuals. Adding the family of adaptive impact rays, a direct parallel can be drawn between populations of plastic and non-plastic individuals (Tilman, 1982; Schade et al., 2005). The only difference is that the traits of the former are optimized, thus depending on the limiting factor values. A corollary is that a variety of adaptive ZNGI shapes can arise from simple non-plastic ones. As such, the envelope method provides a practical procedure to navigate through levels of organization by taking into account adaptation and flexibility, from individuals to communities (Smith et al., 2011; Norberg, 2013).

3.5. Coevolution from distinct functional groups and discontinuous mutations

The envelope approach is easy to apply to the evolution of n independent guilds, for example from different functional groups. Those guilds must share some regulating factors to be able to interact, but can belong to completely different trait spaces, or be bound by completely distinct trade-offs. Each guild would lead to its own eco-evolutionary envelope, that can then be compared as if they were ZNGIs in the standard discrete invasion analysis (Section 2.1), as emphasized in the previous subsection. Examples could include plants and decomposers along a material cycle (Loreau, 1998a), nitrogen-fixing and non-nitrogen-fixing phytoplankton (Boushaba and Pascual, 2005; Agawin et al., 2007) or pairs of cooperators (de Mazancourt and Schwartz, 2010). This picture could also allow one to study the global eco-evolutionary outcomes of a strategy composed of a combination of continuous and discrete traits. From the previous point of view, this means allowing a jump from one functional group to another through discontinuous mutations. With a unidimensional bounded continuous trait, invasion analysis could still be accurately depicted coupling several PIPs together into a “meta-PIP”.

3.6. From discrete to continuous set of strategies

The continuous approach presented in Section 2.2 clarifies some results identified in the finite number of strategies context. Indeed, the study of species sorting along environmental gradients has usually been addressed using a large but finite number of competitors. This led some authors to conclude that “coexistence was more likely among the most similar form” (Leibold, 1996). Fig. 1A from the interactive essential case contains the signature of this phenomena, as neighboring ZNGIs cross at potential coexistence points. This does not lead to coexistence here because of our choice of impact vectors but the idea is the same. However, we argue that this pattern of coexistence of similar forms is degenerate and corresponds to some kind of nearly “neutral coexistence”, i.e. not ecologically robust sensu Meszéna et al. (2006). This can been seen when looking at the continuous limit in Fig. 3. The coexistence points identified earlier have vanished, as neighboring ZNGIs are now infinitely close. In eco-evolutionary terms, this coexistence is not evolutionarily robust as evolution tends to destroy it. Yet, this does not mean that evolutionarily stable coexistence cannot happen in the continuous limit, as we have seen in the antagonistic case (Fig. 4). It is, however, far less common as it relies on self-intersection of the local envelope, but more robust. Note that those differences depend heavily on the topology of the strategy space: disconnected in the finite case versus connected after the continuous limit. This is in practice related to the question of the existence of infinitely many intermediate forms between different strategies.

If this pattern of coexistence vanishes at the continuous limit, it still leaves a signature on the invasion dynamics. More precisely, whether the potential coexistence points lead to stable coexistence or priority effect influences the shape of the PIPs around the singular points. This can be seen in the interactive essential resource example. For high resource supplies, priority effect between neighboring strategies (Fig. 1A) translates into CSS strategies that cannot directly invade their neighborhood and are only attained monotonically through ever-decreasing evolutionary steps (see PIPs in Fig. 3B). This is one of the eight singular strategy types identified by the adaptive dynamics classification (Geritz et al., 1997). On the contrary, we predict that coexistence between neighboring strategies in the finite strategy case would lead to CSS strategies able to invade their neighborhood. Giving a mathematical proof of this is out the scope of this paper. However, those results are intuitive, as priority effects between neighboring strategies indicate that they are protected from invasion by the other strategies. To conclude, while neighboring coexistence or priority effect vanish when the continuous limit is taken, they leave their signature on the eco-evolutionary characteristics of the singular points.

3.7. Importance of the regulating factor space

For a given strategy, the corresponding ZNGI summarizes its competitive ability. This is measured in the regulating factor space, where the competitiveness of different strategies can be compared. In the case of a single regulating factor, the ZNGI reduces to one number, so all the strategies can be ordered and compared without ambiguity. This result is known as Tilman's R^* rule (Hsu et al., 1977; Tilman, 1982; Grover, 1997; Chase and Leibold, 2003) and leads to a pessimization principle in the eco-evolutionary case (Metz et al., 2008). This strict ordering is in general impossible with more regulating factors: invasion analysis with the envelope is the closest equivalent to that rule. Optimization is now multi-objective, so a Pareto front is needed to find the optimal strategies, and this role is played by the envelope. This is why the regulating factor space is so central: it controls species sorting and adaptation through this multi-objective optimization. However, the map between a strategy from the trait space and its ZNGI in the regulating factor space is non-trivial. For example, constraints on organisms encoded by trade-offs are usually inferred at the trait level. Yet, nothing ensures that they efficiently translate into a trade-off in competitive ability of the ZNGI set in the regulating factor space. Another effect of this map is to control the presence of evolutionarily stable coexistence. Indeed, it relates the geometrical characteristics of the ZNGI envelope to the ones of the trait space. For example, some trait space geometries lead to kinked global envelopes and thus potentially to evolutionarily stable coexistence while other do not.

3.8. Evolution of resource use

Applying the envelope method to Schreiber and Tobiason's (2003) resource competition model allowed us to confirm and visualize their results. Moreover, we could specify how the number of singular points and their properties depended on the

resource supplies through bifurcation diagrams. For $\alpha < 1$, there is always a single generalist CSS, under the condition that there is a sufficient supply of resources (Fig. 3). The antagonistic case ($\alpha > 1$) was further characterized with the help of the impact ray map and its envelope (Fig. 5). First, there is always a zone of supply points for which evolutionary branching is possible. This is true for both the choice of impact vector expressions used by Schreiber and Tobiason (2003) and the modification we proposed. However, this zone is pushed infinitely far away from the envelope for $\alpha \to \infty$ when using Eq. (12) while it stays close to it when using Eq. (13). The former is consistent with Tobiason's (2003) observations. The latter states that branching is still possible on highly antagonistic resources if switching is more abrupt. Note that branching demands a sufficiently large and balanced supply of the two resources to take place. Moreover, this branching point, when it exists, is always unique and separated from the boundary attracting strategies by two repellers. Also note that it is possible not to have any singular point but still one or two attractive boundaries for low enough resources.

The consumer–resource model of the example also gives some insights in the case of strictly essential resources. This corresponds to the limit obtained when $\alpha \to -\infty$, leading to a growth rate (11) following Liebig's law of the minimum and an associated L-shaped ZNGI (León and Tumpson, 1975; Tilman, 1982). It is actually in this context that the use of ZNGI envelopes first appeared (Tilman, 1988) and later spread (Schade et al., 2005; Klausmeier et al., 2007; Danger et al., 2008). The standard approach consists in getting the envelope equation simply by tracking the position of the ZNGI corner. The first order criterion (5b) is not only unnecessary in this case, it actually fails to give the envelope equation when applied directly, as the L-shaped ZNGI is non-differentiable at its corner. However, this problem can be worked around by taking the limit when $\alpha \to -\infty$ of the general envelope equation (14), leading to a consistent result. Contrary to the standard approach, our method is easy to generalize to a trait space of arbitrary dimension. It could thus be used to further investigate the evolution of consumers feeding on essential resources (Klausmeier et al., 2004; Shoresh et al., 2008).

3.9. Conclusion and perspectives

In this paper, we presented a graphical approach based on geometrical envelopes that can be used to perform invasion analysis and supply point mapping with a continuum of interacting strategies. We showed how relevant this technology is to two biological pictures, namely species sorting and adaptive dynamics, paving the way for an "evolutionary theory of the niche" (Holt, 2009). Because of its generality, this approach could be applied to investigate a variety of ecological situations: the evolution in a diamond-shaped food web (Leibold, 1996), cooperation through trading (de Mazancourt and Schwartz, 2010), informed dispersal (Haegeman and Loreau, 2015), nitrogen fixing (Agawin et al., 2007) or niche construction (Kylafis and Loreau, 2011), for example.

Acknowledgments

We thank Thomas Aubier, Géza Meszéna and an anonymous reviewer for valuable comments on the paper. This work was supported by a Grant from Simons Foundation (343149, C.A.K.). T.D., C.A.K. and F. M. were able to work together thanks to the "Stoichiometry in metaecosystems" Working Group at the National Institute for Mathematical and Biological Synthesis, sponsored by the National Science Foundation, the U.S. Department of Homeland Security, and the U.S. Department of Agriculture through NSF Award # EF-0832858, with additional support from The University of Tennessee, Knoxville. This is Kellogg Biological Station contribution #1920.

Appendix A. Transformation toward decoupled chemostat dynamics

We provide here two examples of change of variables that enable one to map more general regulating factors dynamics to a chemostat dynamics form presented in Eqs. (1b). This allows one to apply the graphical method presented in this paper to those extended situations after the change of variables.

A.1. Logistic growth

First, let us consider that a regulating factor R follows a logistic resource dynamics:

$$\frac{dR}{dt} = rR\left(1 - \frac{R}{K}\right) + \sum_{j=1}^{n} I_j(R)N_j \tag{A.1}$$

Introducing the change of variables $\rho = 1/R$, it is straightforward that:

$$\frac{d\rho}{dt} = r(\kappa - \rho) + \sum_{j=1}^{n} \chi_j(\rho)N_j \tag{A.2}$$

with $\kappa = 1/K$ and $\chi_j(\rho) = -I_j(1/\rho)\rho^2$. Thus, this change of variable maps a logistic growth in R toward a chemostat dynamics in ρ. Note that the consumer–resource relationship with N_j is reversed by the change of variable: if N_j was consuming R, it is now feeding ρ. This can be understood by looking at the dimensions of the new variable: if R is in individual per surface area, ρ is in surface area per individual. Thus, decreasing prey density by consumption conversely increases available surface area per individual.

A.2. Linear coupling through diffusion

Our second example considers two diffusion-coupled chemostats, thus following the intrinsic dynamics:

$$\frac{dR_1}{dt} = l_1(S_1 - R_1) - d_{12}R_1 + d_{21}R_2 \tag{A.3}$$

$$\frac{dR_2}{dt} = l_2(S_2 - R_2) + d_{12}R_1 - d_{21}R_2 \tag{A.4}$$

This system being linear, it can be rewritten under the general matrix form in the presence of interacting populations:

$$\frac{d\boldsymbol{R}}{dt} = \boldsymbol{T} - \boldsymbol{M}\boldsymbol{R} + \sum_{j=1}^{n} \boldsymbol{I}_j(\boldsymbol{R})N_j \tag{A.5}$$

with

$$\boldsymbol{T} = \begin{pmatrix} l_1S_1 \\ l_2S_2 \end{pmatrix} \quad \text{and} \quad \boldsymbol{M} = \begin{pmatrix} l_1 - d_{12} & d_{21} \\ d_{12} & l_1 - d_{21} \end{pmatrix} \tag{A.6}$$

Then, diagonalization gives $\boldsymbol{M} = \boldsymbol{P}\boldsymbol{D}\boldsymbol{P}^{-1}$ with $\boldsymbol{D} = \mathrm{diag}(\lambda_1, \lambda_2)$ leading to:

$$\frac{d\boldsymbol{\rho}}{dt} = \boldsymbol{D}(\boldsymbol{\sigma} - \boldsymbol{\rho}) + \sum_{j=1}^{n} \boldsymbol{\chi}_j(\boldsymbol{\rho})N_j \tag{A.7}$$

with $\boldsymbol{\rho} = \boldsymbol{P}^{-1}\boldsymbol{R}$, $\boldsymbol{\sigma} = \boldsymbol{D}^{-1}\boldsymbol{P}^{-1}\boldsymbol{T}$ and $\boldsymbol{\chi}_j(\boldsymbol{\rho}) = \boldsymbol{P}^{-1}\boldsymbol{I}_j(\boldsymbol{P}\boldsymbol{\rho})$. As $\boldsymbol{D}$ is a diagonal matrix, the regulating factor vector $\boldsymbol{\rho}$ now follows decoupled chemostat dynamics.

Appendix B. Analytical study of ecological equilibria for the two consumers on two resources system

B.1. Model

In the case of two consumers competing for two resource in a chemostat, model (1) can be rewritten as:

$$\frac{dN_i}{dt} = w_i(R_1, R_2)N_i \tag{B.1}$$

$$\frac{dR_i}{dt} = l_i(S_i - R_i) + \sum_{j=1}^{2} I_{ij}(R_1, R_2)N_j \tag{B.2}$$

Let us first classify the different equilibria of the system and characterize their local stability.

B.2. Equilibria

Those equations present different kinds of solutions at equilibrium:

Equilibrium (0): Corresponds to the case where both populations are absent, i.e. $N_1 = N_2 = 0$. Then $R_1 = S_1$ and $R_2 = S_2$.

Equilibrium (1): Corresponds to the case where only population 2 is absent, i.e. $N_1 \neq 0$ and $N_2 = 0$. The system can be rewritten as:

$$w_1(R_1, R_2) = 0 \tilde{I}_{12}(R_1, R_2)(S_1 - R_1) = \tilde{I}_{11}(R_1, R_2)(S_2 - R_2)N_1 = \frac{(R_1 - S_1)}{\tilde{I}_{11}(R_1, R_2)} \tag{B.3}$$

where we have used the simplifying notation $\tilde{I}_{ij} = I_{ij}/l_i$. The regulating factor values at equilibrium (R_1, R_2) are obtained by solving the first two equations together. N_1 is then deduced from the result using the third equation.

Equilibrium (2): Corresponds to the case where only population 1 is absent, i.e. $N_2 \neq 0$ and $N_1 = 0$. The equilibrium values can be deduced from the previous paragraph by switching subscripts.

Equilibrium (1+2): Corresponds to the case where the two populations coexist, i.e. $N_2 \neq 0$ and $N_1 \neq 0$. Then (R_1, R_2) are given after solving:

$$w_1(R_1, R_2) = 0 \quad w_2(R_1, R_2) = 0$$

The density values at equilibrium follow with:

$$\boldsymbol{N} = \tilde{\boldsymbol{I}}^{-1}(\boldsymbol{S} - \boldsymbol{R}) \tag{B.4}$$

where $\boldsymbol{N} = (N_1, N_2)^T$, $\boldsymbol{S} = (S_1, S_2)^T$, $\boldsymbol{R} = (R_1, R_2)^T$ and $\tilde{\boldsymbol{I}}$ is a 2 by 2 matrix with coefficients $\tilde{I}_{ij} = I_{ij}/l_i$. Note that $\tilde{\boldsymbol{I}}$ is invertible if and only if the renormalized impacts vectors of the two populations are not collinear, which is improbable in the absence of fine-tuning.

B.3. Stability

The stability of those different types of equilibria can be assessed introducing the Jacobian of the system:

$$\boldsymbol{J}(N_1, N_2, R_1, R_2) = \begin{pmatrix} w_1 & 0 & \partial_1 w_1 N_1 & \partial_2 w_1 N_1 \\ 0 & w_2 & \partial_1 w_2 N_2 & \partial_2 w_2 N_2 \\ I_{11} & I_{12} & -l_1 + \sum_{j=1}^{2} \partial_1 I_{1j} N_j & \sum_{j=1}^{2} \partial_2 I_{1j} N_j \\ I_{21} & I_{22} & \sum_{j=1}^{2} \partial_1 I_{2j} N_j & -l_2 + \sum_{j=1}^{2} \partial_2 I_{2j} N_j \end{pmatrix} \tag{B.5}$$

where we have omitted the explicit dependencies in (R_1, R_2) and the notation ∂_i stands for $\partial/\partial R_i$. This Jacobian can be evaluated for the different kinds of equilibria we have identified. It is not to be confused with the Jacobian of the fitness gradient J of Eq. (8).

Equilibrium (0): The Jacobian can be rewritten as:

$$\boldsymbol{J} = \begin{pmatrix} w_1 & 0 & 0 & 0 \\ 0 & w_2 & 0 & 0 \\ I_{11} & I_{12} & -l_1 & 0 \\ I_{21} & I_{22} & 0 & -l_2 \end{pmatrix} \tag{B.6}$$

As $(R_1, R_2) = (S_1, S_2)$, the empty equilibrium is stable if both $w_1(S_1, S_2) < 0$ and $w_2(S_1, S_2) < 0$, which means that none of the two populations can invade. There is no other constraint as the chemostat dynamics are "intrinsically" stable.

Equilibrium (1): After permutation, the Jacobian can be rewritten as a block-diagonal matrix:

$$\boldsymbol{J} = \begin{pmatrix} w_2 & \boldsymbol{0} \\ \boldsymbol{0} & \boldsymbol{K} \end{pmatrix} \tag{B.7}$$

with

$$\boldsymbol{K} = \begin{pmatrix} 0 & \partial_1 w_1 N_1 & \partial_2 w_1 N_1 \\ I_{11} & -l_1 + \partial_1 I_{11} N_1 & \partial_2 I_{11} N_1 \\ I_{21} & \partial_1 I_{21} N_1 & -l_2 + \partial_2 I_{21} N_1 \end{pmatrix} \tag{B.8}$$

Thus, a first necessary condition is non-invasibility by population 2 through $w_2(R_1, R_2) < 0$. Routh–Hurwitz criteria applied on $\boldsymbol{K}$ gives a second necessary condition $\det \boldsymbol{K} < 0$. It is actually possible to show that:

$$\det \boldsymbol{K} = l_2 N_1 I_{11} \frac{\partial w_1}{\partial R_1} \Big/ \frac{\partial R_2}{\partial S_2} \tag{B.9}$$

The object $\partial R_2/\partial S_2$ has an intuitive geometrical interpretation linked to the envelope of the impact rays. The scheme is similar to the one developed in the main text in the eco-evolutionary context (see supply point map in Section 2.3). Indeed, the family of impact rays associated with a given ZNGI can possess an envelope. When it is the case, a given impact ray is tangent to its envelope at a particular point. The line portion of the impact ray situated between its origin and this point corresponds to supply points satisfying $\partial R_2/\partial S_2 > 0$ while the other part corresponds to $\partial R_2/\partial S_2 < 0$. In the classical consumer–resource situation where $I_{11}\partial w_1/\partial R_1 < 0$, this means that only the supply points situated before the envelope on the impact ray map to stable equilibria, the other ones being unstable. This graphical criterion shares strong similarities with the eco-evolutionary case presented in the main text. Note that the condition $\det \boldsymbol{K} < 0$ is necessary but not sufficient to ensure stability.

Equilibrium (2): Can be deduced from the previous paragraph by switching subscripts. Note that we get the necessary condition $\det \boldsymbol{K}' < 0$ for stability with:

$$\det \boldsymbol{K}' = l_1 N_2 I_{22} \frac{\partial w_2}{\partial R_2} \Big/ \frac{\partial R_1}{\partial S_1} \tag{B.10}$$

Equilibrium (1 + 2): The Jacobian can be rewritten as:

$$\boldsymbol{J}=\begin{pmatrix} 0 & 0 & \partial_1 w_1 N_1 & \partial_2 w_1 N_1 \\ 0 & 0 & \partial_1 w_2 N_2 & \partial_2 w_2 N_2 \\ I_{11} & I_{12} & -l_1+\sum_{j=1}^{2}\partial_1 l_{1j} N_j & \sum_{j=1}^{2}\partial_2 l_{1j} N_j \\ I_{21} & I_{22} & \sum_{j=1}^{2}\partial_1 l_{2j} N_j & -l_2+\sum_{j=1}^{2}\partial_2 l_{2j} N_j \end{pmatrix} \tag{B.11}$$

The necessary condition for stability $\det \boldsymbol{J}>0$ can be obtained where:

$$\det \boldsymbol{J}=\left(I_{11}I_{22}-I_{12}I_{21}\right)\left(\frac{\partial w_1}{\partial R_1}\frac{\partial w_2}{\partial R_2}-\frac{\partial w_1}{\partial R_2}\frac{\partial w_2}{\partial R_1}\right)N_1N_2 \tag{B.12}$$

this is the mutual invasibility criterion of Eq. (3) in the main text. We recognize in Eq. (B.12) the general decomposition of $\det \boldsymbol{J}$ as the product of the impact and sensitivity map volumes (Meszéna et al., 2006).

Appendix C. Demonstration of the geometrical relationships in the *k*-dimensional traitspace case

The aim of this section is to link the ZNGI and impact ray envelope properties to the eco-evolutionary properties of the corresponding singular points. We restrict our attention to the case of two regulating factors R_1 and R_2, for a completely general k-dimensional trait $\boldsymbol{x}$.

C.1. Monomorphic singular point

When there is only one singular population in the system, the eco-evolutionary invasion analysis of Eq. (5) can be generalized to the k-dimensional case as:

$$w(\boldsymbol{R},\boldsymbol{x})=0 \tag{C.1}$$

$$\partial_{\boldsymbol{x}} w(\boldsymbol{R},\boldsymbol{x})=\boldsymbol{0} \tag{C.2}$$

where we have used the simplifying notation for the fitness gradient:

$$\partial_{\boldsymbol{x}} w(\boldsymbol{R},\boldsymbol{x})\equiv\left[\frac{\partial w(\boldsymbol{R}(\boldsymbol{y}),\boldsymbol{x})}{\partial \boldsymbol{x}}\right]_{y=x} \tag{C.3}$$

the notation $\partial/\partial_{\boldsymbol{x}}$ standing for a nabla operator along $\boldsymbol{x}$. Graphically, we recognized in the main text that this set of equations parametrizes the ZNGI envelope. This particular expression of the fitness gradient as a partial derivative along its second coordinate is specific to the fact that mutant and resident only interact indirectly through the regulating factors. This has to be combined with the supply point map:

$$v(\boldsymbol{S},\boldsymbol{R},\boldsymbol{x})=0 \tag{C.4}$$

with $v(\boldsymbol{S},\boldsymbol{R},\boldsymbol{x})=(S_1-R_1)\tilde{I}_2(\boldsymbol{R},\boldsymbol{x})-(S_2-R_2)\tilde{I}_1(\boldsymbol{R},\boldsymbol{x})$. Jointly solving this system gives the singular point trait values.

How can we link the tangent ZNGI and ZNGI envelope relative curvature to the properties of its corresponding singular points? As was done in the main text in the unidimensional case, we need to introduce the Hessian matrix of the invasion fitness $\boldsymbol{H}$:

$$\boldsymbol{H}(\boldsymbol{x})=\left[\frac{\partial}{\partial \boldsymbol{x}}\frac{\partial}{\partial \boldsymbol{x}^T}w(\boldsymbol{R}(\boldsymbol{y}),\boldsymbol{x})\right]_{y=x}\equiv\partial_{\boldsymbol{x}}\partial_{\boldsymbol{x}}^T w \tag{C.5}$$

The ZNGI and envelope curvatures at the singular point are both given by second derivatives. The ZNGI curvature can be obtained differentiating $w(R_1,R_2,\boldsymbol{x})=0$ twice with respect to R_1, where $R_2=f(R_1)$:

$$-\partial_{R_2}w\cdot\left.\frac{\partial R_2}{\partial R_1}\right|_{Z}=\partial_{R_1}w \tag{C.6}$$

$$-\partial_{R_2}w\cdot\left.\frac{\partial^2 R_2}{\partial R_1^2}\right|_{Z}=\partial_{R_1}^2 w+2\frac{\partial R_2}{\partial R_1}\partial_{R_2}\partial_{R_1}w+\left(\frac{\partial R_2}{\partial R_1}\right)^2\partial_{R_2}^2 w \tag{C.7}$$

where $\boldsymbol{x}$ has been kept fixed for this calculation as we are interested by the properties of the tangent ZNGI. This is not the case for the ZNGI envelope. The envelope curvature is obtained differentiating $w(R_1,R_2,\boldsymbol{x})=0$ twice with respect to R_1 and using $\partial_{\boldsymbol{x}}w(R_1,R_2,\boldsymbol{x})=\boldsymbol{0}$, where $R_2=g(R_1)$ and $\boldsymbol{x}=\boldsymbol{h}(R_1)$:

$$-\partial_{R_2}w\cdot\left.\frac{\partial R_2}{\partial R_1}\right|_{E}=\partial_{R_1}w \tag{C.8}$$

$$-\partial_{R_2}w\cdot\left.\frac{\partial^2 R_2}{\partial R_1^2}\right|_{E}=\partial_{R_1}^2 w+2\frac{\partial R_2}{\partial R_1}\partial_{R_2}\partial_{R_1}w+\left(\frac{\partial R_2}{\partial R_1}\right)^2\partial_{R_2}^2 w+\frac{\partial \boldsymbol{x}^T}{\partial R_1}\left(\partial_{R_1}\partial_{\boldsymbol{x}}w+\frac{\partial R_2}{\partial R_1}\partial_{R_2}\partial_{\boldsymbol{x}}w\right) \tag{C.9}$$

Note that the first order derivatives are the same for the ZNGI and the envelope, which is a result of their tangency and is known in economics as the envelope theorem (Samuelson, 1947). However, the second derivatives differ by a term that accounts for the fact that $\boldsymbol{x}$ also varies along the envelope. Differentiating $\partial_{\boldsymbol{x}}w(R_1,R_2,\boldsymbol{x})=\boldsymbol{0}$ once with respect to R_1 shows how the last term of (C.9) is actually related to the Hessian:

$$\frac{\partial \boldsymbol{x}^T}{\partial R_1}\left(\partial_{R_1}\partial_{\boldsymbol{x}}w+\frac{\partial R_2}{\partial R_1}\partial_{R_2}\partial_{\boldsymbol{x}}w\right)=-\frac{\partial \boldsymbol{x}^T}{\partial R_1}\boldsymbol{H}\frac{\partial \boldsymbol{x}}{\partial R_1} \tag{C.10}$$

In conclusion, combining all the previous results as the sum $-$(C.9)$+$(C.7)$-$(C.10) and using the fact that $\partial R_2/\partial R_1$ coincides for both ZNGI and envelope leads to the final result:

$$\frac{\partial w}{\partial R_2}\left(\left.\frac{\partial^2 R_2}{\partial R_1^2}\right|_{E}-\left.\frac{\partial^2 R_2}{\partial R_1^2}\right|_{Z}\right)=\frac{d\boldsymbol{x}^T}{dR_1}\cdot\boldsymbol{H}\cdot\frac{d\boldsymbol{x}}{dR_1} \tag{C.11}$$

When $\boldsymbol{x}$ is a scalar, the latter expression directly rewrites as Eq. (7), which concludes the proof.

The second result presented in the main text relates the convergence properties of a singular point to the impact ray envelope. Let us introduce the Jacobian of the fitness gradient $\boldsymbol{J}$:

$$\boldsymbol{J}(\boldsymbol{x})=\frac{\partial}{\partial \boldsymbol{x}}\left[\frac{\partial}{\partial \boldsymbol{x}^T}w(\boldsymbol{R}(\boldsymbol{y}),\boldsymbol{x})\right]_{y=x}\equiv\left(\partial_{\boldsymbol{x}}+\partial_{\boldsymbol{x}}\boldsymbol{R}^T\cdot\partial_{\boldsymbol{R}}\right)\partial_{\boldsymbol{x}}^T w \tag{C.12}$$

We thus have:

$$\boldsymbol{J}(\boldsymbol{x})=\boldsymbol{H}(\boldsymbol{x})+\partial_{\boldsymbol{x}}\boldsymbol{R}^T\cdot\partial_{\boldsymbol{R}}\partial_{\boldsymbol{x}}^T w \tag{C.13}$$

It is very important to understand that the dependency of $\boldsymbol{R}$ in $\boldsymbol{x}$ depicted by the term $\partial_{\boldsymbol{x}}\boldsymbol{R}^T$ comes from solving completely the ecological system by combining ZNGI and impact ray equations (C.1) and (C.4) for $\boldsymbol{S}$ fixed. This has to be done for any strategy, singular or not. Note that this object is not directly related to the expression $d\boldsymbol{x}/dR_1$ manipulated above, which tracks how a singular strategy varies along the envelope. Differentiating $w(\boldsymbol{R},\boldsymbol{x})=0$ and $v(\boldsymbol{S},\boldsymbol{R},\boldsymbol{x})=0$ with respect to $\boldsymbol{x}$ and evaluating it at a singular point gives the following relationships:

$$\partial_{\boldsymbol{x}} R_1 = -\partial_{\boldsymbol{x}} v \Big/ \left(\partial_{R_1} v + \frac{\partial R_2}{\partial R_1} \partial_{R_2} v \right) \tag{C.14}$$

$$\partial_{\boldsymbol{x}} R_2 = \frac{\partial R_2}{\partial R_1} \partial_{\boldsymbol{x}} R_1 \tag{C.15}$$

Let us first use Eq. (C.15) only to rewrite:

$$\boldsymbol{J} - \boldsymbol{H} = \partial_{\boldsymbol{x}} R_1 \left(\partial_{R_1} \partial_{\boldsymbol{x}}^T w + \frac{\partial R_2}{\partial R_1} \partial_{R_2} \partial_{\boldsymbol{x}}^T w \right) \tag{C.16}$$

after multiplying Eq. (C.16) on the right by $d\boldsymbol{x}/dR_1$, the RHS reads as the transpose of the LHS of Eq. (C.10). When also multiplied by $d\boldsymbol{x}^T/dR_1$ on the left, it leads to:

$$\frac{d\boldsymbol{x}^T}{dR_1} \boldsymbol{J} \frac{d\boldsymbol{x}}{dR_1} = \left(1 - \frac{d\boldsymbol{x}^T}{dR_1} \cdot \partial_{\boldsymbol{x}} R_1 \right) \frac{d\boldsymbol{x}^T}{dR_1} \boldsymbol{H} \frac{d\boldsymbol{x}}{dR_1} \tag{C.17}$$

Finally, coming back to the expression of $\partial_{\boldsymbol{x}} R_1$ given by Eq. (C.15):

$$1 - \frac{d\boldsymbol{x}^T}{dR_1} \cdot \partial_{\boldsymbol{x}} R_1 = \left(\partial_{R_1} v + \frac{\partial R_2}{\partial R_1} \partial_{R_2} v + \frac{d\boldsymbol{x}^T}{dR_1} \cdot \partial_{\boldsymbol{x}} v \right) \Big/ \left(\partial_{R_1} v + \frac{\partial R_2}{\partial R_1} \partial_{R_2} v \right) \tag{C.18}$$

$$\equiv \left. \frac{dv}{dR_1} \right|_{\mathrm{E}} \Big/ \left. \frac{dv}{dR_1} \right|_{\mathrm{Z}} \tag{C.19}$$

Now, there is a last step to make the link with the supply point map. Differentiating (C.4) once with respect to S_1, along a ZNGI and the envelope respectively leads to:

$$\left. \frac{\partial R_1}{\partial S_1} \right|_{\mathrm{Z}} = -\tilde{I}_2 \Big/ \left. \frac{dv}{dR_1} \right|_{\mathrm{Z}} \tag{C.20}$$

$$\left. \frac{\partial R_1}{\partial S_1} \right|_{\mathrm{E}} = -\tilde{I}_2 \Big/ \left. \frac{dv}{dR_1} \right|_{\mathrm{E}} \tag{C.21}$$

Putting the pieces together, we finally get the result:

$$\left. \frac{\partial R_1}{\partial s_1} \right|_{\mathrm{E}} \frac{d\boldsymbol{x}^T}{dR_1} \boldsymbol{J} \frac{d\boldsymbol{x}}{dR_1} = \left. \frac{\partial R_1}{\partial s_1} \right|_{\mathrm{Z}} \frac{d\boldsymbol{x}^T}{dR_1} \boldsymbol{H} \frac{d\boldsymbol{x}}{dR_1} \tag{C.22}$$

When $\boldsymbol{x}$ is a scalar and $dx/dR_1 \neq 0$, the latter expression directly rewrites as Eq. (9), which concludes the proof.

Using the ecological stability criteria (B.10) obtained in the previous section for a single-population, we have:

$$\left. \frac{\partial R_1}{\partial s_1} \right|_{\mathrm{Z}} = -\beta \tilde{I}_2 \frac{\partial w}{\partial R_2} \tag{C.23}$$

where β is a positive function when the ecological equilibrium is stable and the two other terms of the RHS are related to the relationship between the population and the regulating factor R_2. For the usual consumer–resource and predator–prey interactions, this thus leads to $\partial R_1/\partial s_1 > 0$.

Note that the two main relationships obtained here in the case of a general k-dimensional trait $\boldsymbol{x}$ only give information on the Hessian and Jacobian of the eco-evolutionary system along the envelope, i.e. the direction $d\boldsymbol{x}/dR_1$. In the one dimensional case, this is not a problem as soon as this direction exists (is non-zero): it leads to a squared term with thus no effect of its sign for the first result or can be simplified in the second result. For dimensions greater than one, this projection leads to insufficient information on the multiple eigenvalues of both the Hessian and Jacobian matrices, not allowing to conclude on the ESS and convergent properties of the singular points based only on the relative position between the ZNGI and its envelope. Also note that contrary to the one dimensional case, eco-evolutionary stability in the k-dimensional case may also depend on the specific shape of the mutation process (Leimar, 2009).

C.2. Dimorphic singular point

When there are two coexisting singular populations in the system with traits $\boldsymbol{x_1} \neq \boldsymbol{x_2}$, the eco-evolutionary invasion analysis reads:

$$w(\boldsymbol{R}, \boldsymbol{x_i}) = 0 \tag{C.24}$$

$$\partial_{\boldsymbol{x}} w(\boldsymbol{R}, \boldsymbol{x_i}) = \boldsymbol{0} \tag{C.25}$$

with $i=1,2$. As in the ecological case, this is enough to fully determine the regulating factors at the eco-evolutionary equilibrium, thus the supply point map is not needed here. According to the adaptive dynamics picture, the eco-evolutionary properties of this singular coalition directly emerges from those of its constituents. Thus, we still have:

$$\frac{\partial w}{\partial R_2} \left(\left. \frac{\partial^2 R_2}{\partial R_1^2} \right|_{\mathrm{E}} - \left. \frac{\partial^2 R_2}{\partial R_1^2} \right|_{\mathrm{Z}} \right) = \frac{d\boldsymbol{x_i}^T}{dR_1} \cdot \boldsymbol{H} \cdot \frac{d\boldsymbol{x_i}}{dR_1} \tag{C.26}$$

and thus this coalition is evolutionarily stable if and only if both coexisting strategies satisfy the geometrical condition relatively to their local envelope. The situation is a bit different for the convergence characteristics as $\boldsymbol{R}$ is obtained without the supply point map (and is thus independent of it) in the dimorphic case. Differentiating $w(\boldsymbol{R}, \boldsymbol{x_1}) = 0$ and $w(\boldsymbol{R}, \boldsymbol{x_2}) = 0$ with respect to $\boldsymbol{x_i}$ and evaluating it at the singular point where $R_2 = g(\boldsymbol{x_1}, \boldsymbol{x_2})$ gives the trivial result:

$$\partial_{\boldsymbol{x_i}} R_1 = \partial_{\boldsymbol{x_i}} R_2 = \boldsymbol{0} \tag{C.27}$$

Thus, the regulating factors at equilibrium around a singular coalition are linearly independent from the traits of this coalition. As a result, $\boldsymbol{J} = \boldsymbol{H}$ for each of the two coexisting strategies, so the convergence properties are automatically linked to the invasion one. This means that ESS coalitions are automatically CSS ones and further branching is excluded. This result obtained here in the case of a saturated dimorphism (two populations on two regulating factors) strongly echoes to the situation of a single population evolving on a single resource, and can be generalized to any number of regulating factors (Kisdi and Geritz, 2016).

Appendix D. Supplementary material

Supplementary material associated with this paper can be found in the online version at http://dx.doi.org/10.1016/j.jtbi.2016.07.026.

References

Adler, P.B., Dalgleish, H.J., Ellner, S.P., 2012. Forecasting plant community impacts of climate variability and change: when do competitive interactions matter?. J. Ecol. 100 (2), 478–487.

Agawin, N.S.R., Rabouille, S., Veldhuis, M.J.W., Servatius, L., Hol, S., van Overzee, H. M.J., Huisman, J., 2007. Competition and facilitation between unicellular nitrogen-fixing cyanobacteria and non-nitrogen-fixing phytoplankton species. Limnol. Oceanogr. 52 (5), 2233–2248.

Armstrong, R.A., 1979. Prey species replacement along a gradient of nutrient enrichment: a graphical approach. Ecology 60 (1), 76–84.

Baas Becking, L.G.M., 1934. Geobiologie of Inleiding Tot de Milieukunde. Van

Stockum, Den Haag.
Barabás, G., Meszéna, G., Ostling, A., 2014a. Fixed point sensitivity analysis of interacting structured populations. Theor. Popul. Biol. 92, 97–106.
Barabás, G., Pásztor, L., Meszéna, G., Ostling, A., 2014b. Sensitivity analysis of coexistence in ecological communities: theory and application. Ecol. Lett. 17 (12), 1479–1494.
Boushaba, K., Pascual, M., 2005. Dynamics of the 'echo' effect in a phytoplankton system with nitrogen fixation. Bull. Math. Biol. 67 (3), 487–507.
Caswell, H., 2001. Matrix Population Models: Construction, Analysis, and Interpretation. Sinauer Associates, Sunderland, MA.
Chase, J.M., Leibold, M.A., 2003. Ecological Niches: Linking Classical and Contemporary Approaches. University of Chicago Press, Chicago.
Danger, M., Daufresne, T., Lucas, F., Pissard, S., Lacroix, G., 2008. Does Liebig's law of the minimum scale up from species to communities? Oikos 117 (11), 1741–1751.
Daufresne, T., Hedin, L.O., 2005. Plant coexistence depends on ecosystem nutrient cycles: extension of the resource-ratio theory. Proc. Natl. Acad. Sci. 102 (26), 9212–9217.
de Mazancourt, C., Dieckmann, U., 2004. Trade-off geometries and frequency-dependent selection. Am. Nat. 164 (6), 765–778.
de Mazancourt, C., Schwartz, M.W., 2010. A resource ratio theory of cooperation. Ecol. Lett. 13 (3), 349–359.
De Wit, R., Bouvier, T., 2006. 'Everything is everywhere, but, the environment selects'; what did Baas Becking and Beijerinck really say? Environ. Microbiol. 8 (4), 755–758.
Dieckmann, U., Doebeli, M., 1999. On the origin of species by sympatric speciation. Nature 400 (6742), 354–357.
Dieckmann, U., Ferrière, R., 2004. Adaptive dynamics and evolving biodiversity. In: Evolutionary Conservation Biology. Cambridge University Press, Cambridge, UK, pp. 188–224.
Dieckmann, U., Law, R., 1996. The dynamical theory of coevolution: a derivation from stochastic ecological processes. J. Math. Biol. 34 (5-6), 579–612.
Dieckmann, U., Metz, J.A.J., 2006. Surprising evolutionary predictions from enhanced ecological realism. Theor. Popul. Biol. 69 (3), 263–281.
Dobzhansky, T., 1973. Nothing in biology makes sense except in the light of evolution. Am. Biol. Teach. 35 (3), 125–129.
Dukas, R., Kamil, A.C., 2001. Limited attention: the constraint underlying search image. Behav. Ecol. 12 (2), 192–199.
Eppley, R.W., 1972. Temperature and phytoplankton growth in the sea. Fish. Bull. 70 (4), 1063–1085.
Eshel, I., 1983. Evolutionary and continuous stability. J. Theor. Biol. 103, 99–111.
Gause, G.F., 1934. The Struggle for Existence. Williams & Wilkins Company, Baltimore, MD.
Geritz, S., Metz, J.A.J., Kisdi, É., Meszéna, G., 1997. Dynamics of adaptation and evolutionary branching. Phys. Rev. Lett. 78 (10), 2024–2027.
Geritz, S.A., van der Meijden, E., Metz, J.A., 1999. Evolutionary dynamics of seed size and seedling competitive ability. Theor. Popul. Biol. 55 (3), 324–343.
Geritz, S.A.H., Kisdi, É., Meszéna, G., Metz, J.A.J., 1998. Evolutionarily singular strategies and the adaptive growth and branching of the evolutionary tree. Evol. Ecol. 12 (1), 35–57.
Gerla, D.J., Vos, M., Kooi, B.W., Mooij, W.M., 2009. Effects of resources and predation on the predictability of community composition. Oikos 118 (7), 1044–1052.
Grant, P.R., Grant, B.R., 2006. Evolution of character displacement in Darwin's finches. Science (New York, N.Y.) 313 (5784), 224–226.
Grover, J.P., 1995. Competition, herbivory and enrichment: nutrient-based models for edible and inedible plants. Am. Nat. 145 (5), 746–774.
Grover, J.P., 1997. Resource Competition. Chapman & Hall, London.
Guill, C., 2009. Alternative dynamical states in stage-structured consumer populations. Theor. Popul. Biol. 76 (3), 168–178.
Gyllenberg, M., Meszéna, G., 2005. On the impossibility of coexistence of infinitely many strategies. J. Math. Biol. 50, 133–160.
Haegeman, B., Loreau, M., 2015. A graphical-mechanistic approach to spatial resource competition. Am. Nat. 185 (1), 1–13.
Hairston, N.G., Ellner, S.P., Geber, M.A., Yoshida, T., Fox, J.A., 2005. Rapid evolution and the convergence of ecological and evolutionary time. Ecol. Lett. 8 (10), 1114–1127.
Hofbauer, J., Sigmund, K., 1990. Adaptive dynamics and evolutionary stability. Appl. Math. Lett. 3 (4), 75–79.
Holt, R.D., 1977. Predation, apparent competition, and the structure of prey communities. Theor. Popul. Biol. 12 (2), 197–229.
Holt, R.D., 2009. Bringing the Hutchinsonian niche into the 21st century: ecological and evolutionary perspectives. Proc. Natl. Acad. Sci. 106, 19659–19665.
Holt, R.D., Grover, J.P., Tilman, D., 1994. Simple rules for interspecific dominance in systems with exploitative and apparent competition. Am. Nat. 144 (5), 741–771.
Hsu, S.B., Hubbell, S., Waltman, P., 1977. A mathematical theory for single-nutrient competition in continuous cultures of micro-organisms. SIAM J. Appl. Math. 32 (2), 366–383.
Huisman, J., Weissing, F.J., 1999. Biodiversity of plankton by species oscillations and chaos. Nature 402 (6760), 407–410.
Kéfi, S., Eppinga, M.B., de Ruiter, P.C., Rietkerk, M., 2010. Bistability and regular spatial patterns in arid ecosystems. Theor. Ecol. 3 (4), 257–269.
Kisdi, É, Geritz, S.A.H., 2016. Adaptive dynamics of saturated polymorphisms. J. Math. Biol. 72 (4), 1039–1079.
Klausmeier, C.A., Litchman, E., Daufresne, T., Levin, S.A., 2004. Optimal nitrogen-to-phosphorus stoichiometry of phytoplankton. Nature 429 (6988), 171–174.
Klausmeier, C.A., Litchman, E., Levin, S.A., 2007. A model of flexible uptake of two essential resources. J. Theor. Biol. 246 (2), 278–289.
Kneitel, J.M., Chase, J.M., 2004. Trade-offs in community ecology: linking spatial scales and species coexistence. Ecol. Lett. 7 (1), 69–80.
Kylafis, G., Loreau, M., 2011. Niche construction in the light of niche theory. Ecol. Lett. 14 (2), 82–90.
Lavorel, S., Garnier, E., 2002. Predicting changes in community composition and ecosystem functioning from plant traits: revisting the Holy Grail. Funct. Ecol. 16 (5), 545–556.
Lavorel, S., Grigulis, K., 2012. How fundamental plant functional trait relationships scale-up to trade-offs and synergies in ecosystem services. J. Ecol. 100 (1), 128–140.
Leibold, M.A., 1996. A graphical model of keystone predators in food webs: trophic regulation of abundance, incidence, and diversity patterns in communities. Am. Nat. 147 (5), 784–812.
Leibold, M.A., Holyoak, M., Mouquet, N., Amarasekare, P., Chase, J.M., Hoopes, M.F., Holt, R.D., Shurin, J.B., Law, R., Tilman, D., Loreau, M., Gonzalez, A., 2004. The metacommunity concept: a framework for multi-scale community ecology. Ecol. Lett. 7 (7), 601–613.
Leimar, O., 2009. Multidimensional convergence stability. Evol. Ecol. Res. 11 (2), 191–208.
León, J.A., Tumpson, D.B., 1975. Competition between two species for two complementary or substitutable resources. J. Theor. Biol. 50 (1), 185–201.
Leslie, P.H., 1948. Further notes on the use of matrices in population mathematics. Biometrika 35, 213–245.
Lester, S.E., Costello, C., Halpern, B.S., Gaines, S.D., White, C., Barth, J.A., 2013. Evaluating tradeoffs among ecosystem services to inform marine spatial planning. Marine Policy 38, 80–89.
Levin, S.A., 1970. Community equilibria and stability, and an extension of the competitive exclusion principle. Am. Nat. 104 (939), 413–423.
Levins, R., 1962. Theory of fitness in a heterogeneous environment. I. The fitness set and adaptive function. Am. Nat. 96 (891), 361–373.
Litchman, E., Klausmeier, C.A., 2008. Trait-based community ecology of phytoplankton. Ann. Rev. Ecol. Evol. Syst. 39 (1), 615–639.
Litchman, E., Klausmeier, C.A., Schofield, O.M., Falkowski, P.G., 2007. The role of functional traits and trade-offs in structuring phytoplankton communities: scaling from cellular to ecosystem level. Ecol. Lett. 10 (12), 1170–1181.
Loreau, M., 1998a. Biodiversity and ecosystem functioning: a mechanistic model. Proc. Natl. Acad. Sci. U. S. A. 95 (10), 5632–5636.
Loreau, M., 1998b. Ecosystem development explained by competition within and between material cycles. Proc. R. Soc. B: Biol. Sci. 265 (1390), 33–38.
Loreau, M., Ebenhöh, W., 1994. Competitive exclusion and coexistence of species with complex life cycles. Theor. Popul. Biol. 46 (1), 58–77.
Lotka, A.J., 1925. The empirical element in population forecasts. J. Am. Stat. Assoc. 20, 569–570.
MacArthur, R.H., 1970. Species packing and competitive equilibrium for many species. Theor. Popul. Biol. 1, 1–11.
MacArthur, R.H., Levins, R., 1964. Competition, habitat selection and character displacement in a patchy environment. Proc. Natl. Acad. Sci. U. S. A. 51 (6), 1207–1210.
MacArthur, R.H., Wilson, E.O., 1967. The Theory of Island Biogeography. Princeton University Press, Princeton, NJ.
Marler, R.T., Arora, J.S., 2004. Survey of multi-objective optimization methods for engineering. Struct. Multidiscip. Optim. 26 (6), 369–395.
Massol, F., Crochet, P.A., 2008. Do animal personalities emerge? Nature 451 (7182), E8–E9.
Matsuda, H., Abrams, P.A., 1994. Runaway evolution to self-extinction under asymmetrical competition. Evolution 48 (6), 1764–1772.
McGill, B.J., Enquist, B.J., Weiher, E., Westoby, M., 2006. Rebuilding community ecology from functional traits. Trends Ecol. Evol. 21 (4), 178–185.
Meszéna, G., Gyllenberg, M., Pásztor, L., Metz, J.A.J., 2006. Competitive exclusion and limiting similarity: a unified theory. Theor. Popul. Biol. 69 (1), 68–87.
Meszéna, G., Metz, J.A.J., 1999. Species Diversity and Population Regulation: The Importance of Environmental Feedback Dimensionality. IIASA Working Paper WP-99-045.
Metz, J.A.J., Geritz, S.A.H., Meszéna, G., Jacobs, F.J.A., van Heerwaarden, J.S., 1996. Adaptive dynamics, a geometrical study of the consequences of nearly faithful reproduction. In: Stochastic and Spatial Structures of Dynamical Systems. Proceedings of the Royal Dutch Academy of Science, pp. 183–231.
Metz, J.A.J., Mylius, S.D., Diekmann, O., 2008. When does evolution optimize? Evol. Ecol. Res. 10, 629–654.
Miller, T.E., Burns, J.H., Munguia, P., Walters, E.L., Kneitel, J.M., Richards, P.M., Mouquet, N., Buckley, H.L., 2005. A critical review of twenty years' use of the resource-ratio theory. Am. Nat. 165 (4), 439–448.
Monod, J., 1950. Theory and application of the technique of continuous culture. Ann. Pasteur Inst. 79, 410–590.
Murdoch, W.W., 1969. Switching in general predators: experiments on predator specificity and stability of prey populations. Ecol. Monogr. 39 (4), 335–354.
Murdoch, W.W., Avery, S., Smyth, M.E.B., 1975. Switching in predatory fish. Ecology 56 (5), 1094–1105.
Norberg, J., 2013. Biodiversity and ecosystem functioning: a complex adaptive systems approach. Limnol. Oceanogr. 49 (4), 1269–1277.
Novick, A., Szilard, L., 1950. Description of the chemostat. Science 112, 715–716.
Pareto, V., 1906. Manuale di Economia Politica con una Introduzione alla Scienza Sociale. Societa Editrice Libraria, Milano.
Parvinen, K., 2005. Evolutionary suicide. Acta Biotheor. 53 (3), 241–264.
Pietrewicz, A.T., Kamil, A.C., 1979. Search image formation in the blue jay (*Cyanocitta cristata*). Science (New York, N.Y.) 204 (4399), 1332–1333.

Rankin, D.J., López-Sepulcre, A., 2005. Can adaptation lead to extinction? Oikos 111 (3), 616–619.
Rietkerk, M., Dekker, S.C., de Ruiter, P.C., van de Koppel, J., 2004. Self-organized patchiness and catastrophic shifts in ecosystems. Science 305 (5692), 1926–1929.
Rueffler, C., Van Dooren, T.J.M., Metz, J.A.J., 2004. Adaptive walks on changing landscapes: Levins' approach extended. Theor. Popul. Biol. 65 (2), 165–178.
Ryabov, A.B., Blasius, B., 2011. A graphical theory of competition on spatial resource gradients. Ecol. Lett. 14 (3), 220–228.
Samuelson, P.A., 1947. Foundations of Economic Analysis. Harvard University Press, Cambridge.
Sauterey, B., Ward, B.A., Follows, M.J., Bowler, C., Claessen, D., 2015. When everything is not everywhere but species evolve: an alternative method to model adaptive properties of marine ecosystems. J. Plankton Res. 37 (1), 28–47.
Schade, J.D., Espeleta, J.F., Klausmeier, C.A., McGroddy, M.E., Thomas, S.A., Zhang, L., 2005. A conceptual framework for ecosystem stoichiometry: balancing resource supply and demand. Oikos 109 (1), 40–51.
Scheffer, M., Carpenter, S., Foley, J.A., Folke, C., Walker, B., 2001. Catastrophic shifts in ecosystems. Nature 413, 591–596.
Schellekens, T., de Roos, A.M., Persson, L., 2010. Ontogenetic diet shifts result in niche partitioning between two consumer species irrespective of competitive abilities. Am. Nat. 176 (5), 625–637.
Schreiber, S.J., Rudolf, V.H.W., 2008. Crossing habitat boundaries: coupling dynamics of ecosystems through complex life cycles. Ecol. Lett. 11 (6), 576–587.
Schreiber, S.J., Tobiason, G.A., 2003. The evolution of resource use. J. Math. Biol. 47, 56–78.
Seppelt, R., Lautenbach, S., Volk, M., 2013. Identifying trade-offs between ecosystem services, land use, and biodiversity: a plea for combining scenario analysis and optimization on different spatial scales. Curr. Opin. Environ. Sustain. 5 (5), 458–463.
Shoresh, N., Hegreness, M., Kishony, R., 2008. Evolution exacerbates the paradox of the plankton. Proc. Natl. Acad. Sci. U. S. A. 105 (34), 12365–12369.
Smith, S.L., Pahlow, M., Merico, A., Wirtz, K.W., 2011. Optimality-based modeling of planktonic organisms. Limnol. Oceanogr. 56 (6), 2080–2094.
Strogatz, S.H., 2015. Nonlinear Dynamics and Chaos: With Applications to Physics, Biology, Chemistry, and Engineering. Westview Press, Boulder, CO.
Stuart, Y.E., Campbell, T.S., Hohenlohe, P.A., Reynolds, R.G., Revell, L.J., Losos, J.B., 2014. Rapid evolution of a native species following invasion by a congener. Science 346 (6208), 463–466.
Szilágyi, A., Meszéna, G., 2009. Limiting similarity and niche theory for structured populations. J. Theor. Biol. 258, 27–37.
Thomas, M.K., Kremer, C.T., Klausmeier, C.A., Litchman, E., 2012. A global pattern of thermal adaptation in marine phytoplankton. Science 338, 1085–1089.
Thompson, J.N., 1998. Rapid evolution as an ecological process. Trends Ecol. Evol. 13 (8), 329–332.
Tilman, D., 1980. Resources: a graphical-mechanistic approach to competition and predation. Am. Nat. 116 (3), 362–393.
Tilman, D., 1982. Resource Competition and Community Structure. Princeton University Press, Princeton, NJ.
Tilman, D., 1988. Plant Strategies and the Dynamics and Structure of Plant Communities. Princeton University Press, Princeton, NJ.
Volterra, V., 1926. Fluctuations in the abundance of a species considered mathematically. Nature 118 (2972), 558–560.
Westoby, M., Wright, I.J., 2006. Land–plant ecology on the basis of functional traits. Trends Ecol. Evol. 21 (5), 261–268.
Wolf, M., van Doorn, G.S., Leimar, O., Weissing, F.J., 2007. Life-history trade-offs favour the evolution of animal personalities. Nature 447 (7144), 581–584.
Wolf, M., van Doorn, G.S., Leimar, O., Weissing, F.J., 2008. Wolf et al. reply. Nature 451 (7182), E9–E10.
Wolkowicz, G.S.K., Lu, Z., 1992. Global dynamics of a mathematical model of competition in the chemostat: general response functions and differential death rates. SIAM J. Appl. Math. 52 (1), 222–233.
Yoshida, T., Jones, L.E., Ellner, S.P., Fussmann, G.F., Hairston, N.G., 2003. Rapid evolution drives ecological dynamics in a predator–prey system. Nature 424 (6946), 303–306.
Zu, J., Yuan, B., Du, J., 2015. Top predators induce the evolutionary diversification of intermediate predator species. J. Theor. Biol. 387, 1–12.

Appendix B

Résumé détaillé

Les plantes sont présentes partout à la surface de la Terre où l'on peut trouver de l'eau liquide, et présentent une grande diversité de tailles, de formes et d'adaptations à leur environnement. Malgré cela, les plantes sont aussi caractérisées par une unité en termes de fonctionnement. En effet, la photosynthèse leur permet de convertir la lumière du soleil, le CO_2 de l'atmosphère et les nutriments du sol en énergie et matière disponible pour leur croissance. Cela les place à la base des réseaux trophiques terrestres et aquatiques, des cycles biogéochimiques des éléments et des activités économiques humaines. Qu'est ce qui détermine les différentes formes et la diversité des plantes rencontrées à la surface de la Terre ? Comment les plantes interagissent-elles avec leur environnement physique, et l'influencent-elles au travers de leurs activités ?

Pour répondre à ces questions, un cadre conceptuel décrivant les interactions réciproques entre les plantes et leur environnement est nécessaire. En effet, les plantes doivent pouvoir faire face aux contraintes imposées par leur environnement pour s'établir et persister (via leurs besoins), mais leur présence et activité modifient en retour leur environnement (via leurs impacts). Cette dualité entre besoins et impacts est au centre de la théorie contemporaine de la niche, et donne lieu à la boucle de rétroaction environnementale, le moteur principal des dynamiques éco-évolutives. Pourtant, les perspectives évolutives sur la théorie de la niche restent à développer, et la dynamique adaptative pourrait tirer profit de l'aspect dual de la niche ainsi que de son approche graphique. L'objectif de cette thèse est d'entreprendre une telle unification, en vue d'élaborer un cadre conceptuel général des interactions plantes-environnement. Seul un tel cadre peut nous permettre de comprendre comment l'environnement détermine les plantes et leurs adaptations, et comment ces plantes déterminent la structure et le fonctionnement des écosystèmes en retour.

Pour décrire les plantes, nous nous appuierons sur les traits fonctionnels, ces caractéristiques des plantes qui peuvent être mesurées et qui permettent des comparaisons quantitatives entre individus, de la même ou d'une autre espèce. Ces traits sont liés aux composantes principales du succès reproducteur de la plante, telles que croissance, survie et reproduction. Ils décrivent les interactions fondamentales des plantes avec leur environnement, et caractérisent collectivement

la stratégie d'une plante. Ces traits variant d'un individu à l'autre et d'une espèce à l'autre, ils permettent lorsqu'ils sont appréhendés dans leur ensemble de décrire un ensemble des stratégies possibles des plantes. Cet ensemble des possibles constitue alors la variabilité sur laquelle la sélection naturelle peut agir.

La croissance et la reproduction des plantes sont conditionnées par la disponibilité d'une diversité de facteurs environnementaux, tels que l'espace, la lumière, l'eau et les nutriments. Cette disponibilité est très variable à la surface de la Terre pour des raisons de climat, de types de sols et d'activités humaines, et forme ce que l'on appelle les gradients environnementaux. Plus précisément, les nutriments comme l'azote et le phosphore limitent parfois fortement la croissance des plantes dans certains écosystèmes naturels, mais peuvent aussi être à l'origine de pollutions aux conséquences importantes lorsqu'ils sont apportés en excès par l'Homme. Une question centrale est de savoir comment ces gradients environnementaux influencent les adaptations des plantes et le fonctionnement des écosystèmes.

Lorsque les conditions environnementales nécessaires à la croissance d'une population d'une plante donnée sont réunies, celle-ci colonise cet environnement et l'influence en retour, le plus souvent en épuisant ces mêmes ressources qui ont rendu sa croissance possible. Un tel mécanisme de rétroaction environnementale donne lieu à des interactions négatives entre les individus médiées par l'environnement, la compétition. A l'échelle de la population, cette compétition donne lieu à la régulation de la population qui se stabilise à sa capacité de charge. Le même principe s'applique entre individus d'espèces différentes, et la compétition qui en résulte est centrale pour comprendre la coexistence de plusieurs espèces au sein d'un même environnement. De même, cette boucle de rétroaction environnementale est au cœur de l'évolution par sélection naturelle, puisqu'elle est à l'origine des remplacements successifs de stratégies résidentes par des stratégies mutantes plus compétitives et donc plus adaptées.

Ces approches basées sur la sélection médiée par la boucle de rétroaction environnementale peuvent être utilisées pour comprendre comment le vivant influence le fonctionnement des écosystèmes et la régulation des cycles biogéochimiques. Les cycles biogéochimiques décrivent comment les éléments chimiques transitent de manière cyclique entre les différents compartiments de l'écosphère, i.e. la lithosphère, l'atmosphère, l'hydrosphère et la biosphère. Contrôlés par les lois de la physique et de la chimie, ces cycles sont aussi influencés par les organismes vivants, qui acquièrent cette matière proportionnellement à leurs besoins, la transforment, et la libèrent à leur mort. Selon cette perspective biogéochimique, l'abondance et la diversité des organismes vivants ne sont pas une finalité en soi, mais le moyen par lequel ces cycles sont mis en mouvement, régulés et couplés entre eux à la surface de la Terre.

Longtemps réduite à des approches phénoménologiques et holistiques, la théorie des écosystèmes vue comme une théorie des systèmes complexes émergents peut nous aider dans notre recherche de lois générales du fonctionnement des écosystèmes et des cycles biogéochimiques. Une telle approche est basée sur les lois régissant les interactions entre ses constituants élémen-

taires, d'un côté le vivant soumis à la sélection naturelle et de l'autre la matière soumise aux lois de la physique et de la chimie. En naviguant entre les échelles de l'individu à l'écosystème, une telle théorie permet de faire le pont entre l'écologie des communautés, l'écologie évolutive et l'écologie fonctionnelle, vers une théorie générale des écosystèmes.

Dans cette thèse, nous nous basons sur la perspective duale des relations entre les plantes et leur environnement pour répondre aux deux questions suivantes : comment la sélection issue de la boucle de rétroaction environnementale détermine-t-elle les adaptations des plantes et leur diversification le long des gradients environnementaux ? Comment le remplacement adaptatif de plante contrôle-t-il le développement, la régulation et le fonctionnement des écosystèmes le long des gradients environnementaux ?

Dans le premier chapitre de cette thèse, je développe un cadre mathématique général et rigoureux de la théorie contemporaine de la niche et l'adapte pour prendre en compte le remplacement adaptatif d'espèces le long de gradients environnementaux. La théorie de la niche est un cadre conceptuel puissant autour duquel l'écologie théorique est depuis longtemps structurée. Initialement, la théorie de la niche a été restreinte à la compétition pour les ressources, plus particulièrement au cas de deux consommateurs et de deux ressources. Plus tard, cette théorie a été étendue pour prendre en compte d'autres facteurs régulateurs, tels que les prédateurs, les parasites et les inhibiteurs. Un élément essentiel de la théorie de la niche est la méthode graphique popularisée par Tilman. Celle-ci permet de représenter graphiquement les différentes situations résultant de la compétition de deux consommateurs le long de gradients environnementaux, par exemple la coexistence, l'exclusion compétitive et les effets de priorité. D'un autre côté, des petits modules trophiques composés de quelques consommateurs en interaction avec un faible nombre de facteurs régulateurs ont été utilisés pour étudier l'effet du remplacement d'espèces le long de gradients en écologie des communautés, ainsi que l'adaptation et la coexistence sur des échelles de temps évolutives dans des approches éco-évolutives. Pourtant, la méthode graphique associée a jusqu'à maintenant été sous-utilisée dans ce contexte d'assemblage des communautés et d'évolution.

Dans ce chapitre, nous étendons formellement et graphiquement la théorie contemporaine de la niche pour prendre en compte le remplacement adaptatif d'espèces le long de gradients environnementaux, en utilisant la notion d'enveloppe géométrique. Cette approche graphique permet de dessiner des diagrammes de phase éco-évolutifs le long de gradients environnementaux, en identifiant les stratégies évolutivement stables correspondant à des conditions données, ainsi que les régions de coexistence évolutivement stable, les points de branchements et les états stables alternatifs évolutifs. Similairement, cette approche permet d'identifier les stratégies évolutivement stables dans un contexte d'assemblage des communautés par un continuum de stratégies issues du réservoir régional d'espèces. Cette approche nous permet au passage de comparer ces deux perspectives, éco-évolutive et assemblage des communautés, qui sont essentiellement les

mêmes, différant uniquement par la gamme d'envahisseurs considérée, allant respectivement de mutants infiniment similaires à des stratégies quelconques issues du réservoir d'espèce. Les concepts issus de la dynamique adaptative s'intègrent naturellement au sein de la théorie de la niche, via une correspondance rigoureuse entre la classification des stratégies singulières de la dynamique adaptative et les propriétés graphiques des courbes enveloppes. Ce chapitre met aussi en lumière le fait que seule la niche de besoin est soumise à la sélection naturelle, l'évolution de la niche d'impact n'étant qu'un effet secondaire de l'évolution de cette dernière. Enfin, cette approche fournit un outil intégratif pour étudier l'adaptation du vivant le long de gradients environnementaux et ses conséquences sur le fonctionnement de l'écosystème, de l'échelle individuelle aux échelles des communautés ou de l'évolution.

Dans le deuxième chapitre de cette thèse, j'applique l'approche éco-évolutive développée au chapitre précédent à l'étude de l'évolution des défenses des plantes contre les herbivores le long de gradients de nutriments, en considérant l'évolution couplée des traits d'acquisition de la ressource, de tolérance et de résistance aux herbivores. En effet, les plantes sont confrontées à une importante pression de sélection issue de leur consommation par les herbivores. Les plantes ont donc développé des adaptations spécifiques appelées défenses pour faire face à leurs herbivores, classifiées en deux grandes catégories par la biologie évolutive : la résistance, qui consiste à réduire la quantité de dommages reçue, et la tolérance, qui ne réduit pas la quantité de dommages reçue mais réduit leur effet sur le succès reproducteur de la plante, par des mécanismes de croissance compensatoire. La disponibilité en ressources, telles que l'eau, les nutriments ou la lumière, étant aussi un facteur limitant la croissance des plantes, on peut s'attendre à des différences le long de gradients environnementaux en matière d'allocation entre (i) compétitivité pour l'acquisition de ces ressources et (ii) défense. Pourtant, les conditions environnementales et les mécanismes allocatifs favorisant un type de défense par rapport à un autre sont toujours mal compris.

Dans ce chapitre, nous étudions les patrons adaptatifs d'allocation entre l'acquisition des ressources, la résistance et la tolérance le long d'un gradient de disponibilité en ressources au sein d'un petit module trophique où les plantes sont en compétition pour un nutriment et sont consommées par un herbivore généraliste. L'évolution de la plante par dynamique adaptative est implémentée en utilisant la méthode graphique des enveloppes développée dans le premier chapitre. Nous montrons que la prise en compte des transferts trophiques conduit à la sélection de stratégies très compétitives mais non défendues dans les environnements pauvres en nutriments, alors que ce sont toujours des stratégies défendues (résistantes, tolérantes, ou la coexistence des deux) qui dominent dans les environnements riches en nutriments. Le caractère croissant ou décroissant du rendement marginal de ces allocations joue un rôle important dans ces prévisions : les rendements croissants tendent à favoriser la coexistence de stratégies spécialistes, plus précisément une stratégie à croissance rapide non résistante et une stratégie à croissance lente mais non comestible, alors que les rendements décroissants mènent à l'émergence d'une stratégie

généraliste unique. Nous explorons aussi les conséquences de ces patrons d'allocations sur le fonctionnement de la chaîne trophique, en mettant par exemple en évidence l'émergence d'un cul-de-sac trophique associé à l'évolution de la résistance. Nos résultats mettent en évidence le rôle souvent sous-estimé des transferts trophiques sur l'évolution des défenses des plantes, via la prise en compte de la boucle de rétroaction environnementale. Dans ce contexte, notre modèle théorique est le premier à étudier en détail l'évolution de la tolérance et de la résistance des plantes le long d'un gradient de ressources au sein d'un petit module trophique, en utilisant un compromis d'allocation entre trois traits quantitatifs.

Dans le troisième chapitre de cette thèse, j'étends la théorie de la niche contemporaine à la facilitation pour montrer comment la colonisation d'un substrat nu par une communauté de plantes fixatrices d'azote couplée au recyclage des nutriments peut donner naissance à de la succession par facilitation. En effet, les plantes fixatrices d'azote par symbiose telles que les plantes actinorhiziennes et les légumineuses sont connues pour prospérer pendant la succession primaire, les substrats typiques étant très pauvres en azote. L'azote ainsi fixé s'accumule ensuite dans les sols grâce aux dépôts de litière et à leur recyclage, et devient disponible à l'ensemble de la communauté. Ce mécanisme de facilitation par les fixateurs d'azote est considéré comme un des principaux moteurs de la succession primaire sur certains substrats. Cependant, ces plantes sont aussi en compétition pour l'accès à d'autres ressources, comme le phosphore. Comment compétition pour le phosphore et facilitation pour l'azote interagissent-elles, et sous quelles conditions la succession par facilitation a-t-elle lieu ? Sous quelles conditions la succession est-elle directionnelle et relativement ordonnée, et comment évolue la stabilité de l'écosystème au cours de la succession ?

Dans ce chapitre, nous répondons à ces questions en utilisant un modèle à ressources explicites pour simuler l'assemblage des communautés par des espèces de plantes fixatrices d'azote en compétition pour l'azote et le phosphore. Ces différentes espèces diffèrent dans leur allocation relative entre acquisition du phosphore et fixation de l'azote, avec certaines espèces très compétitives pour le phosphore mais fixant faiblement, et d'autres mauvaises acquisitrices du phosphore mais étant capables de fixer la totalité de leurs besoins en azote. Ce modèle est analysé en utilisant notre extension de la théorie contemporaine de la niche à la facilitation et à l'assemblage des communautés. Nous étudions et caractérisons l'allure des différentes trajectoires de succession le long des deux gradients de disponibilité en azote et phosphore. Nous montrons que la succession par facilitation a seulement lieu lorsque l'azote est très peu disponible dans le milieu. Ce type de succession est conditionné par l'invasion initiale du substrat vierge par une espèce pionnière très bonne fixatrice, puis leur remplacement successif par des plantes de plus en plus compétitives pour le phosphore mais dont l'établissement est uniquement rendu possible par l'azote accumulé par les espèces précédentes. Cette succession est à l'origine d'un développement autogène de l'écosystème, avec augmentation de la biomasse totale et de l'azote

présent dans le sol au cours du temps. La succession par facilitation est associée à deux signatures caractéristiques. Tout d'abord, l'ordre très strict suivant lequel les espèces peuvent se remplacer les unes et les autres filtre fortement le processus de colonisation, intrinsèquement très aléatoire, ce qui donne lieu à des trajectoires de succession relativement ordonnées. Ensuite, la fin de succession est caractérisée par des états stables alternatifs, ce qui veut dire que l'écosystème en fin de succession est très sensible à des transitions abruptes vers un état très fortement dégradé. A l'inverse, une forte disponibilité en azote inhibe la fixation, ce qui a pour conséquence de faire disparaître l'effet de facilitation et donne lieu à de la succession purement dirigée par la compétition. Dans ce cas, les trajectoires de succession sont plus aléatoires, mais ne présentent pas d'états alternatifs en fin de succession. En synthétisant ces différents scénarios de succession le long de gradients de disponibilité en azote et en phosphore, nos résultats donnent lieu à une version enrichie de la théorie du ratio de ressource de la succession de Tilman.

Dans cette thèse, nous avons développé un cadre général basé sur la théorie contemporaine de la niche pour étudier le couplage entre l'adaptation des plantes et le fonctionnement des écosystèmes le long de gradients de nutriments, et l'avons appliqué à deux exemples particulièrement importants en écologie, à savoir l'évolution des défenses des plantes et la succession par des plantes fixatrices d'azote. Nous avons montré comment la sélection médiée par la boucle de rétroaction environnementale détermine les traits des stratégies dominantes et influence en retour le fonctionnement des écosystèmes. Notre approche basée sur les enveloppes s'avère être un outil efficace pour passer de l'échelle individuelle aux échelles de la population puis de l'écosystème, en assimilant le remplacement adaptatif d'espèces le long de gradients à une plasticité des propriétés écosystémiques. Cette approche nous a alors permis de décrire l'émergence des boucles de régulation à l'échelle écosystémique qui contrôlent la dynamique et le fonctionnement des écosystèmes, comme l'illustrent nos résultats le long de gradients de nutriments sur la transition entre régimes de succession ou encore l'émergence de culs-de-sac trophiques.

Pour obtenir ces résultats, nous nous sommes largement appuyés sur la théorie contemporaine de la niche, un cadre conceptuel particulièrement adapté à l'étude des interactions réciproques entre les plantes et leur environnement. Ce faisant, nous avons développé de nouveaux outils à la théorie contemporaine de la niche et solidifié ses fondations mathématiques. Par exemple, nous présentons dans le chapitre 1 la méthode graphique dans un cadre très général où les niches de besoin et d'impact peuvent prendre une forme quelconque. Cela permet notamment de traiter graphiquement les boucles de rétroaction positive, qui peuvent émerger lorsqu'une ressource inhibe la croissance d'une population à haute densité, ou lorsque de l'azote fixé est réinjecté dans le sol par recyclage stimulant ainsi la croissance d'une plante fixatrice (Chapitre 3). Ces boucles de rétroaction positive sont souvent à l'origine d'états stables alternatifs, et nous avons montré comment ceux-ci peuvent être identifiés graphiquement en combinant isoclines et rayons d'impact. Notre méthode graphique permet en fait d'identifier sans ambiguïté toute

une variété d'états stables alternatifs : entre deux espèces (les classiques effets de priorité), entre deux états d'une même population (dans certains modèles structurés, ou les effets Allee), entre une paire d'espèces en coexistence et une troisième espèce, etc. La prise en compte des boucles de rétroaction positive permet aussi d'étendre la théorie contemporaine de la niche à la facilitation, comme nous l'avons vu au Chapitre 3. Dans ce contexte, nous donnons vie aux concepts de niche d'invasion et niche de persistance de Holt, et d'extension de la niche réalisée par une espèce facilitatrice. Enfin, l'approche basée sur les enveloppes développée au Chapitre 1 et appliquée aux Chapitres 2 et 3 fournit un outil rigoureux pour étudier l'émergence des niches évolutives ou de niche à l'échelle de la communauté.

Cette thèse met aussi en lumière certaines limitations de notre approche lorsqu'il s'agit d'étudier l'évolution de la niche d'impact et la construction de niche. En effet, le chapitre 1 montre que seule la niche de besoin est sous l'influence directe de la sélection, la niche d'impact n'intervenant pas dans la valeur sélective. Comment l'évolution peut-elle alors amener les organismes à modifier leur environnement, notamment d'une manière positive ? Il est important de noter que pour des raisons de conservation de la matière, besoins et impacts sont souvent contrôlés par les mêmes traits. La sélection directe sur les besoins peut donc amener à l'évolution indirecte des impacts. Cette évolution reste néanmoins indirecte, et ne garantit pas le maintien d'impacts positifs nécessaires à la population, comme le montre la sensibilité à une transition catastrophique de la population de fixateurs d'azote en fin de fixation au Chapitre 3. En réalité, cette tragédie des biens communs est souvent évitée par la spatialisation des populations de plantes, qui ont un accès privilégié aux ressources présentes dans leur voisinage et interagissent préférentiellement avec leurs voisins. D'un point de vue théorique, il est connu que la prise en compte explicite de cette spatialisation permet l'évolution locale d'impacts positifs et peut stabiliser la facilitation. Inclure l'espace dans les modèles de niche devrait donc permettre d'expliquer comment la sélection sur les impacts, la facilitation et la construction de niche peuvent émerger. Ces impacts locaux ayant une influence diffuse à plus large échelle, on peut s'attendre à des conséquences importantes de leur évolution sur le fonctionnement global des écosystèmes.

Summary

As living organisms, plants present a dual relationship with their biotic and abiotic environment. The environment selects plant strategies that can establish, and selected strategies in turn impact and shape the environment as they spread. This environmental feedback loop – when fueled by variation, through mutation or immigration from a local species pool – drives evolution, community assembly and ecosystem development, and eventually determines the emergent properties of ecosystems.

Theoretical ecology approaches have long recognized this duality, as it is at the core of contemporary niche theory through the concepts of requirement and impact niche. Similarly, game-theoretical approaches such as adaptive dynamics have emphasized the role played by the environmental feedback loop in driving eco-evolutionary dynamics. However, niche theory could benefit from a more individualistic, selection based perspective, while adaptive dynamics could benefit from niche theory's duality and graphical approach.

In my dissertation, I unify these theoretical perspectives and apply them to various ecological situations in an attempt to understand how the reciprocal interaction between plants and their environment determines plant adaptive traits and emergent ecosystem functions.

First, I introduce a general and rigorous mathematical framework to contemporary niche theory and the associated graphical approach. By extending these ideas to a continuum of interacting strategies using geometrical envelopes, I show how contemporary niche theory enables the study of both eco-evolutionary dynamics and community assembly through species sorting. I show how these two perspectives only differ by the range of invaders considered, from infinitesimally similar mutants to any strategy from the species pool. My results also emphasize the fact that selection only acts on the requirement niche, evolution of the impact niche being just an indirect consequence of the former.

Second, I use this approach to study the evolution of plant defenses against herbivores along a nutrient gradient, by considering the joint evolution of resource acquisition, tolerance and resistance to herbivores. I show that trophic transfers lead to the selection of very competitive, undefended strategies in nutrient-poor environments, while defended strategies – either resistant, tolerant or the coexistence of both – always dominate in nutrient-rich environments. My results highlight the central, and often underestimated, role played by plant-environment feedbacks and allocation trade-offs in shaping plant defense patterns.

Third, I extend contemporary niche theory to facilitation originating from positive environmental feedback loops. I use these new tools to show how colonization of a bare substrate by a community of nitrogen-fixing plants coupled with nutrient recycling can lead to facilitative succession. Contrarily to previous competition-based succession models, I point out that facilitative succession leads to autogenic ecosystem development, relatively ordered trajectories and late succession bistability between the vegetated ecosystem and the bare substrate. By showing how facilitative succession can turn into competition-based succession along an increasing

nitrogen gradient, I derive a new resource-ratio theory of succession.

Overall, these new theoretical developments demonstrate that niche theory can be adapted to study a broad range of ecological situations, from facilitation to eco-evolutionary dynamics and community assembly. Within this framework, my envelope-based approach provides a powerful tool to scale from the individual and population levels to the ecosystem level, lumping selection-driven species turnover into plastic ecosystem properties. This, is turn, helps describing the emergence at the ecosystem scale of regulation feedback loops that drive ecosystem dynamics and functioning, as exemplified by my results along increasing resource gradients showing a transition from facilitation- to competition-based succession or the emergence of trophic dead-ends.

Keywords: Contemporary niche theory, ecosystem functioning, adaptive dynamics, plant defenses, nutrient gradients, facilitation, primary succession